T-3506

FORMATION OF HYDRATES IN WATER-BASED DRILLING MUDS AND MUD-LIKE FLUIDS

by

S.B. CHA

A thesis submitted to the Faculty and the Board of Trustees of the Colorado School of Mines in partial fulfillment of the requirements for the degree of Master of Science in Chemical Engineering and Petroleum-Refining.

Golden, Colorado

Date Feb. 2 / 1988

Signed: Suk-Bae Cha

Suk-Bae Cha

Approved: E.D. Sloan

E.D. Sloan

Thesis Advisor

Golden, Colorado

Date 2/2/88

A.J. Kidnay

A.J. Kidnay

Professor and Head of

Chemical Engineering

and Petroleum Refining

Department

ABSTRACT

The formation of natural gas hydrates in drilling muds and mud-like systems was studied. This involved determining the effect of individual water-based drilling mud components on hydrate formation in drilling muds. The water-based mud components examined by this work were: water, barite, LVT oil, bentonite, thinner, caustic, PHPA polymer, XCD polymer, simulated drill cuttings, NaCl, and MEOH.

Hydrate formation tests were also done with additional fluids in order to reaffirm some of the major hypotheses resulting from the drilling mud work, and to gain some insight into the fundamental interactions which may govern hydrate formation in water-based drilling muds and mud-like fluids.

A personal computer based data acquisition system was also built. The system was used to obtain data during hydrate formation experiments, some of which lasted 70 hours.

Bentonite and PHPA polymer were found to promote the formation of hydrates in drilling muds while NaCl, MEOH, XCD polymer, and LVT oil were found to inhibit hydrate formation.

A physical model of hydrate formation in mud-like systems was also proposed. The model was thermodynamically and experimentally consistent.

TABLE OF CONTENTS

LIST OF FIGURES

LIST OF TABLES

ACKNOWLEDGMENTS

The author wishes to extend his thanks and sincere appreciation to Dr. E.D. Sloan, for acting as thesis advisor and for his continuous support and guidance during this research. Also many thanks are due to Dr. T.R. Wildeman for his contributions and patience during the course of this work.

The author would also like to recognize, and express sincere gratitude to, Mr. Hamid Ouar and Mr. Tony Inserni for their contributions to the experimental work. Together with the author, Mr. Ouar and Mr. Inserni spent many hours in the laboratory inorder to gather the large amount of data required for this study.

Appreciation is also extended to, Dr. M. Sami Selim and Dr. F. Poettmann for contributions as members of the author's thesis committee, and the five consortium member Companies (Arco, Amoco, Conoco, Shell, and Sohio) for their support of this work.

Chapter 1

INTRODUCTION

Natural gas hydrates are solid non-stochiometric compounds formed by the inclusion of gas molecule into crystalline cages formed by hydrogen bonded water molecules. The gas molecules are not chemically bonded to any water molecules but are physically constrained within a crystalline structure of water molecules by van der Waals forces. Natural gas hydrates are not stable without the presence of the gas molecules but can form at temperatures well above the ice point

The past problems that hydrates have caused in the hydrocarbon industry have been well documented. Hydrates can form in gas pipelines, valves, and even in producing gas wells, and they present many safety and economic problems. Accordingly, much work has been done in the prevention and control of hydrates in systems where water can come in contact with natural gas at high pressures and low temperatures.

Recently, a new hydrate related problem has been identified. In at least two cases, hydrates have formed in the water-based drilling mud of a deepwater oil well leading to costly delays and remedial procedures (Jones & Sherman, 1986; Barker & Gomez, 1987). As the petroleum industry continues to extend and expand drilling efforts into deeper waters, where increased hydrostatic pressure and lower environmental temperatures favor hydrate formation, the problems are bound to continue.

Since there is no data base for combatting hydrates in drilling operations, operators have been forced to apply inhibition methods that have worked for the natural gas industry in the past, such as salt or methanol addition, without any knowledge of how effective these techniques will be in a drilling environment.

The purpose of this work was to study the formation of natural gas hydrates in water-based drilling muds and mud-like fluids. This involved a statistically designed screening program, consisting of hydrate formation experiments with 17 unique fluids, which helped determine the effect of individual water-based drilling mud components on hydrate formation. The water-based drilling mud components examined by this work were: water, barite, LVT oil, bentonite/thinner/caustic, XCD polymer, PHPA polymer, and drill solids (all components are discussed in chapter 3). In addition, two possible inhibitors, NaCl and

MEOH, were also examined.

Hydrate formation tests were also done with four additional fluids not involved in the screening program. The purpose of these experiments were to reaffirm some of the major hypotheses resulting from the screening work, and to gain some insight into the fundamental interactions which may govern hydrate formation in water-based drilling muds and systems similar to water-based muds.

Because of the nature of hydrate formation experiments, which can involve as much as 70 hrs of continuous monitoring, a personal computer based data acquisition system was designed and built to help expedite the experimental work.

1.1 NATURE OF NATURAL GAS HYDRATES

Gas hydrates are formed when certain pure gases or mixture of gases come into contact with water at elevated pressures. These compounds can form at temperatures significantly above the freezing point of water and can plug wells, valves, and transmission lines.

Hydrates belong to a class of substances known as clathrates. Clathrates are physical, non-stochiometric, combinations of components in which a guest compound fits into a cavity formed by the molecules of a host crystalline compound. In the case of gas hydrates, the guest compounds are the encaged gas molecules while the host compound is water. The water molecules that form the crystalline lattice are strongly hydrogen-bonded to each other and do not interact chemically with the gas molecule that is in close proximity. Rather, the gas molecule stabilizes the cage structure, which cannot exist without the presence of a guest, through van der Waals type forces of interaction.

Methane, ethane, propane, isobutane, hydrogen sulfide, nitrogen, and carbon dioxide are among the natural gas components known to form hydrates with water. N-butane cannot form hydrates as a pure compound but requires a 'helper' compound such as methane. Hydrocarbons larger than n-butane cannot form hydrates because of size limitations.

Hydrates are known to exist in several distinct crystalline structures (Jefferey & McMullen, 1967) including a recently discovered H hydrate (Ripmeester, 1987). However, most nonpolar gases and some weakly polar gases will form one of two types of hydrates, known as structure I and structure II, depending on the shape and size of the guest molecule. The major difference between the two structures is the basic unit cell type that forms each structure. Physical properties for each structural type are listed in Table 1.

The unit structure makeup of a structure I hydrate is a body centered cubic, shown in Figure 1. Each hydrate type has a small and large cavity. In the structure I hydrate, there are 2 small (3.94 A diameter) and 6 large (4.3 A diameter) cavities, for a total of 8 cavities per unit cell. Each small cavity is formed by a pentagonal dodecahedral lattice of 20 water molecules while the large cavities are formed by 6 additional water molecules that bridge between the small cavity structures to form a tetrakaidecahedron. A total of 46 water molecules are needed to form the structure I unit cell. Since each cavity can hold only one gas molecule, this results in an ideal hydration number (the ratio of water molecule to gas molecules, similar to the stochiometric coefficient for a chemical reaction) of 5.75. This number is 'ideal' because it corresponds to the filling of all cavities in the hydrate structure by a molecule small enough to fit into both small and large cavities. Typical filling is around 90%. A result of this type of filling is the amount of gas that can be trapped in a volume of hydrate. A cubic foot of hydrate can contain as much as 170 SCF of gas.

TABLE 1

PROPERTIES OF HYDRATE LATTICES

PROPERTY	STRUC I	STRUC II
UNIT CELL SIZE Å	12.03	17.31
NUMBER OF SMALL CAVITIES	2	16
NUMBER OF LARGE CAVITIES	6	8
COORDINATION NUMBER, SMALL CAVITY	20	20
COORDINATION NUMBER, LARGE CAVITY	24	28
NUMBER OF WATER MOLECULES/UNIT CELL	46	136
SMALL CAVITIES/UNIT CELL	2	16
LARGE CAVITIES/UNIT CELL	6	8
SMALL CAVITIES/WATER MOLECULE	1/23	2/17
LARGE CAVITIES/WATER MOLECULE	3/23	1/17

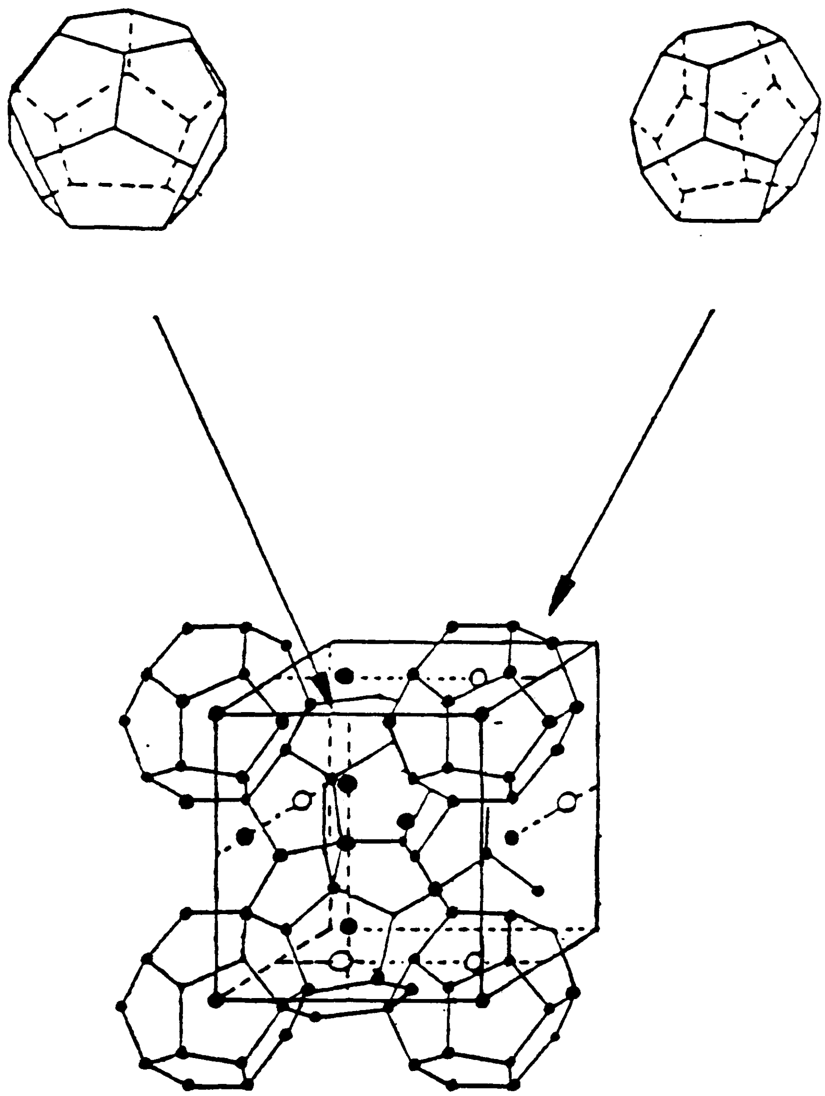

Figure 1 HYDRATE LATTICE OF STRUCTURE I

(Reproduced from Makogon,1981)

The unit crystal of structure II hydrate is a diamond lattice, shown in Figure 2. There are 16 small (3.91 A diameter) and 8 large (4.73 A diameter) cavities, for a total of 24 cavities available for filling. The small cavities are formed by distorted pentagon dodecahedra while the large cavities are formed by a hexadecahedron structure. A total of 136 water molecules are needed to form one unit cell which results in an ideal hydration number of 5.6 for molecules that can occupy both cavities.

Since there are size differences between structure I and structure II, the size of the guest molecule will strongly influence which structure is formed. For years it was thought that small molecules would favor structure I while larger molecules would only form structure II. However, recent studies (Davidson et al, 1984) have shown that some of the smallest molecules (Kr, Ar, N_2, O_2) will form structure II hydrate because there are many more small cavities available for occupation. Among pure hydrocarbon gases, methane and ethane will form structure I while propane and butane form structure II hydrate. Table 2 lists some common hydrate forming gases and the structure in which they exist.

The ability of a gas to form hydrate is not solely

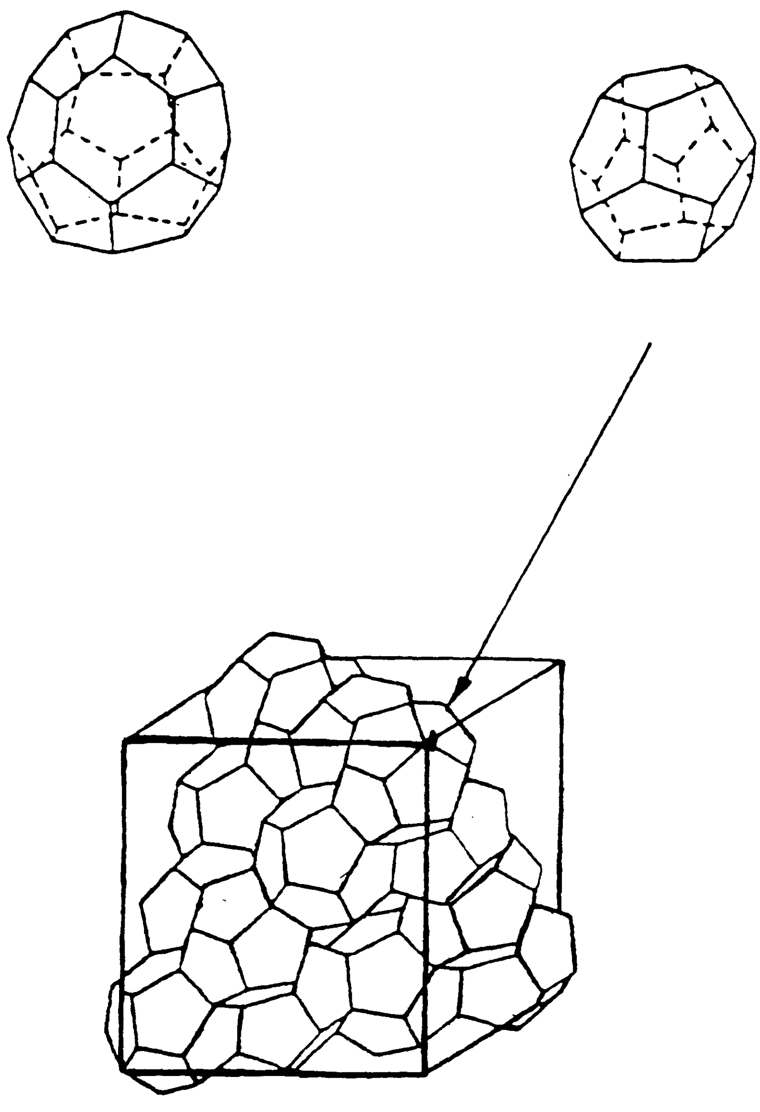

Figure 2 HYDRATE LATTICE OF STRUCTURE II

(Reproduced from Makogon, 1981)

TABLE 2

HYDRATE STRUCTURES OF VARIOUS GASES

GAS	HYDRATE STRUCTURE	CAVITIES ENTERED
Ar	II	All
Kr	II	All
Xe	I	All
N_2	II	All
O_2	II	All
CO_2	II	All
H_2S	I	All
CH_4	I	All
C_2H_4	I	All
C_2H_6	I	Large
C_3H_6	II	large
C_3H_8*	II	Large
Cyclo-C_3H_6	I,II	Large
i-C_4H_{10}*	II	Large
n-C_4H_{10}**	II	Large
cis-2-butene**	II	Large
trans-2-butene	none	none

* will not fit into large cavity of structure I

** will only form hydrates from a vapor if a small molecule such as CH_4 is also present. No pure hydrates can from this gas.

determined by mass (molecular weight) considerations alone. Another important factor is the configuration of the molecule. The molecule must also be properly shaped in order to fit into a cavity. Thus several molecules are non-hydrate formers even though their molecular weight may be the same or smaller than that of some hydrate formers. For example, iso-butane will form hydrates, while trans-2-butene will not, even thought the molecular weight of iso-butane is greater than that of the butene.

Natural gas mixtures can form either structure depending on the composition of the gas. Methane and ethane mixtures will form structure I hydrate but the addition of less than 1% propane, or heavier gas, will normally result in the formation of structure II hydrate. The largest hydrocarbon hydrate formers are n-butane and cis-2-butene (Kamath & Holder, 1982) which cannot form as pure gases but require the presence of a lighter, 'helper' gas.

Structure II is more stable than structure I due to the approximately tetrahedral angle found in structure II hydrate. The stability of structure II hydrates allows them to exist in a wider range of environmental conditions. Davidson (1973) provides an excellent review of the physical and chemical nature of hydrates.

1.2 HYDRATE PHASE EQUILIBRIA

Gas hydrate phase equilibria is controlled by phase composition as well as temperature and pressure. The temperature, pressure, and composition will determine the phase nature (gas, liquid, solid, hydrate) of a system. Figure 3 is a phase diagram which represents some of the possible phases for a gas/water/hydrate system. The diagram shows that hydrate formation is favored by low temperature and high pressure.

Figure 3 illustrates the regions of specific interest for hydrate formation when water is in contact with a pure hydrate forming gas, such as ethane or carbon dioxide. The line ABCD represents the locus of pressures and temperatures which separate the hydrated zone from the non-hydrated zone. Any pressure and temperature combination to the left of this line would result in hydrate formation while hydrates could not form when temperature and pressure conditions lie to the right of the line. The line AB represents the conditions at which hydrate (H) exist in equilibrium with ice (I) and vapor (V). Similarly, the line BC represents the univarent locus along which hydrates would exist in equilibrium with liquid water (L_1) and vapor. The point C represents the intersection of the vapor pressure curve of the gas with the three phase, HL_1V,

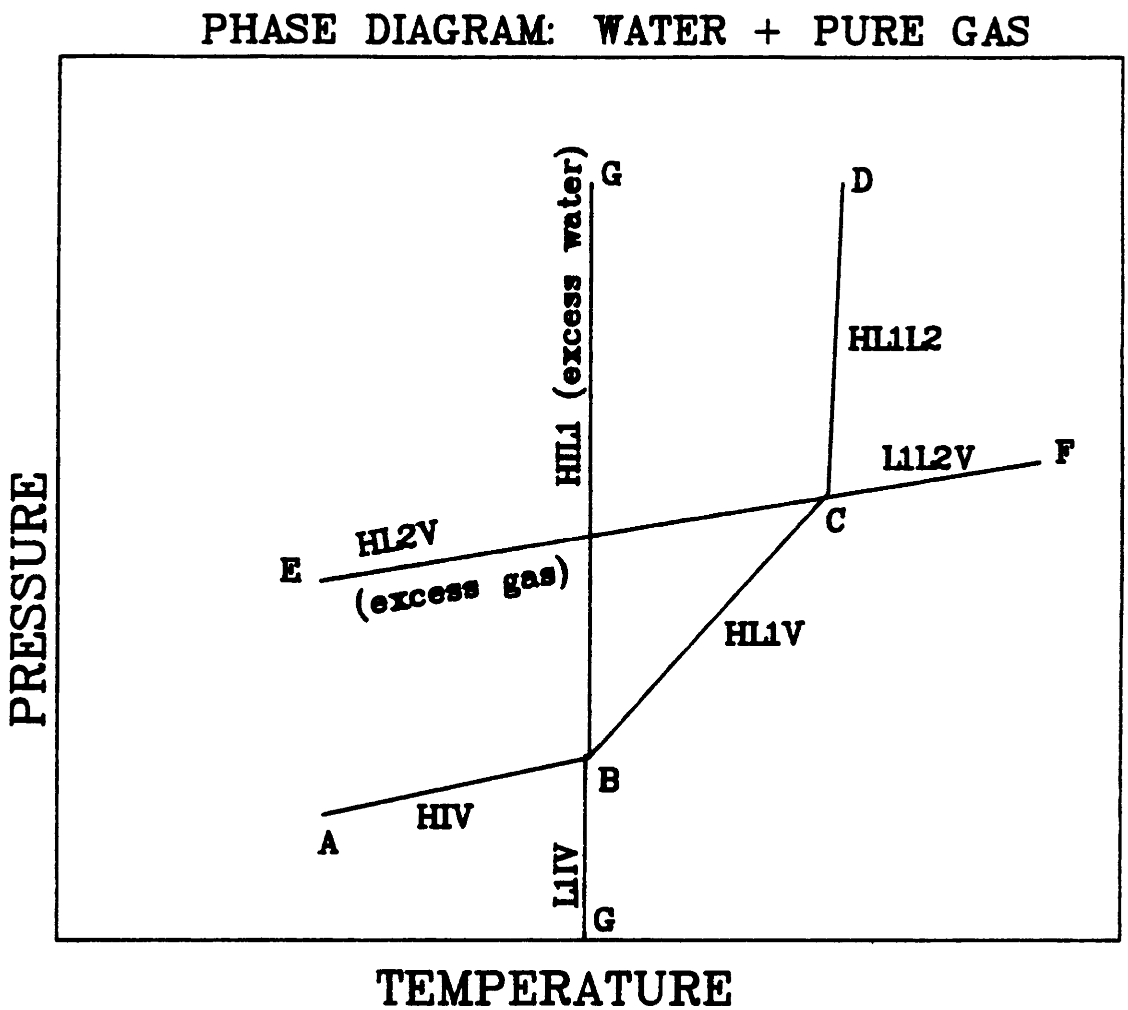

Figure 3 PURE GAS HYDRATE PHASE DIAGRAM

line. At this point the HL_1V line terminates, and a four phase point commences, as the gas condenses and a second liquid phase (L_2) is formed. The line CD represents the conditions at which hydrate would exist in equilibrium with L_1 and L_2. Line BG separates the H-I region from the L_1-H region when water is in excess. Similarly, line EC separates the H-L_2 region from the H-V region when gas is in excess. The line BH separates the I-V region from the L_1-V region. The points B and C both represent four phase conditions, HIL_1V and HL_1L_2V, respectively. Most experimental work, including this investigation, is carried out along BC, the three phase (HL_1V) line.

A similar diagram for a gas mixture of more than 2 hydrocarbons, where at least one component is a hydrate former, is shown in Figure 4. The line of interest, with respect to hydrate formation, is now ABKCD. The line ABKCD in Figure 4 is the same in principle as the line ABCD in Figure 3, except that KC is a four phase line rather than a three phase line. The points K and C represent the superposition of the dew point/bubble point curve for the gas upon the hydrate equilibrium line (point F denotes the critical point of the gas). The three phase line of interest, HL_1V, is now BK.

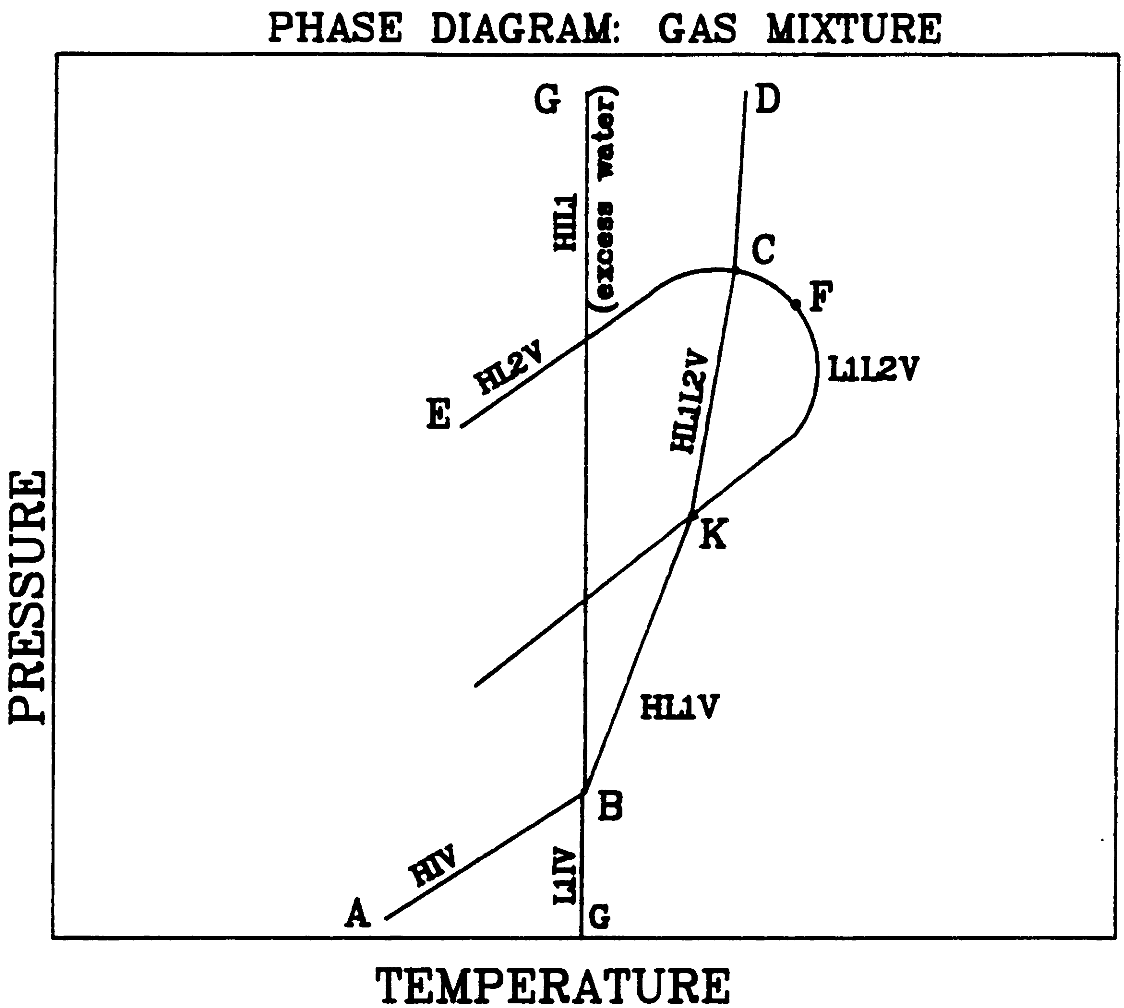

Figure 4 GAS MIXTURE HYDRATE PHASE DIAGRAM

The effect of gas phase compositions is, in general, that larger hydrate forming molecules, such as propane, will form hydrates with lower dissociation pressures than smaller molecules, such as methane. Thus heavy gas molecule hydrates are stable at higher temperatures than smaller molecule hydrates, at the same pressure.

Hydrates from gas mixtures of small and large molecules will usually have equilibrium conditions nearer to those of the larger molecule than the smaller molecule. For example, for a 99% methane-1% propane mixture, the dissociation pressure is less than half the dissociation pressure of pure methane. A few studies have shown that a gas mixture can have dissociation pressures lower than those of the pure components. For example, at 278 K, a 75% CH_4-25% C_3H_8 mixture forms hydrates at a pressure that is 10% lower than that of pure propane (Holder & Grigoriou, 1980).

Liquid phase composition is also important in hydrate equilibria. It is in the aqueous liquid phase that most traditional attempts of inhibition have taken place. Basically, inhibitors such as salts and alcohols have the same effect on hydrate formation as they have on ice formation. A general heuristic is that an inhibitor will depress hydrate formation temperatures to about the same extent as they would the freezing point of water. The effect will be slightly different because of the presence of dissolved gas and elevated pressure. Figure 5 illustrates how an inhibitor shifts the three phase, HL_1V, line and four phase point.

It is interesting to note that larger hydrocarbon molecules can also act as hydrate inhibitors. Pentane, for example, is too large to form hydrates and the presence of pentane in a gas or liquid phase containing hydrate formers, will make it more difficult to form hydrates by diluting the fugacity of the hydrate forming gases. Consequently, it is more difficult to form hydrates from dissolved gases in petroleum than from pure natural gas (Ng & Robinson, 1976).

1.3 RESEARCH HISTORY

The existence of hydrates was first shown by Sir Humphery Davy, in 1810, who precipitated a chlorine hydrate. His results were confirmed by Faraday some 13 years later in 1823. The first researchers to do significant work on hydrates were Villard (1879, 1888, 1896) and De Forcrand (1902, 1925) who, in the last half of

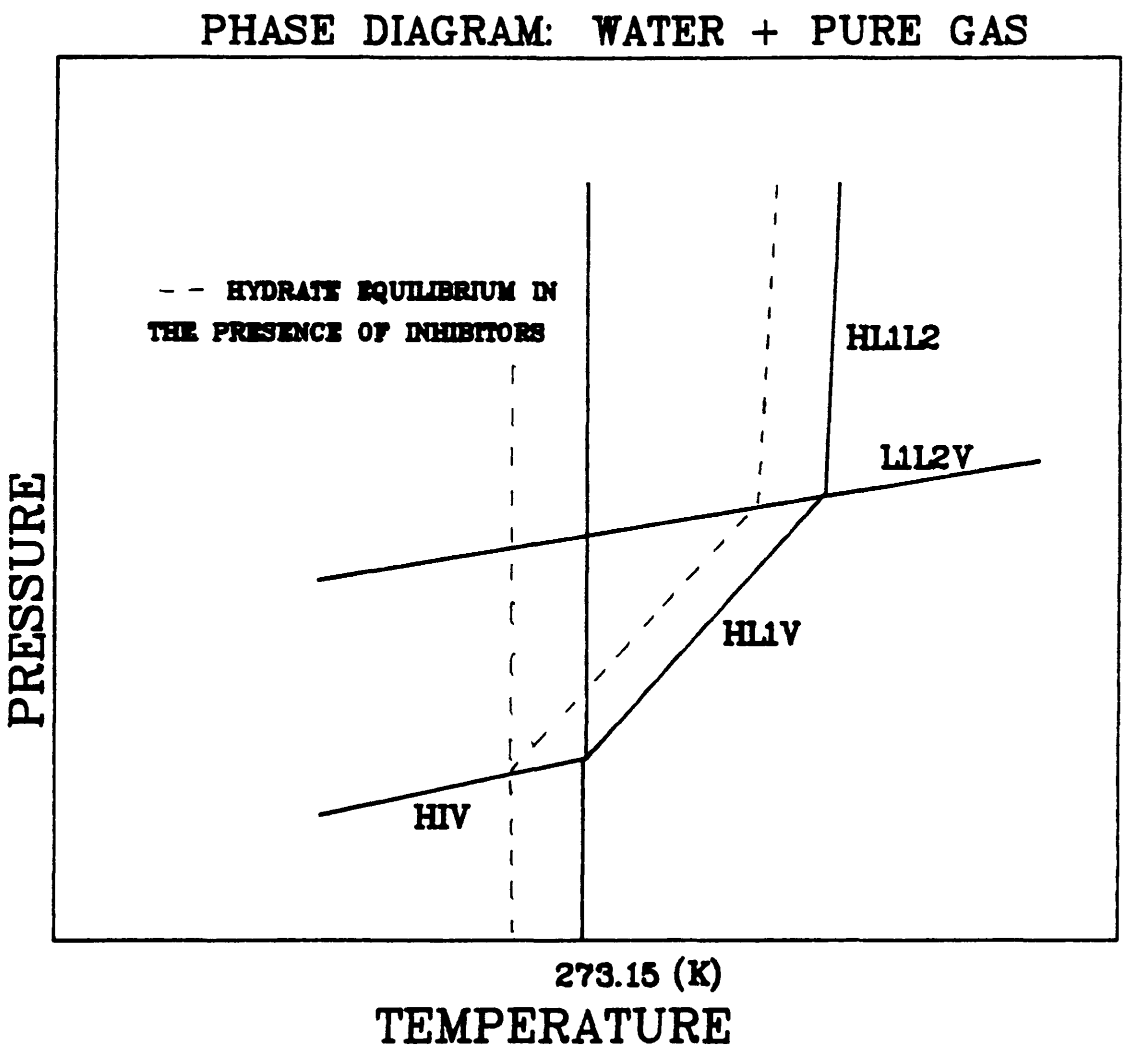

Figure 5 EFFECT OF INHIBITOR ON HYDRATE EQUILIBRIUM

the nineteenth century and early part of the twentieth century, formed hydrates of many important gases, including CO_2, CS_2, C_2H_2, NH_3, CH_4, C_2H_6, C_3H_8, Ar, Kr, and Xe.

Interest in hydrates was purely academic until the 1930's when Hammerschmidt (1934, 1936) showed that hydrates were responsible for plugging natural gas pipelines. Hammerschmidt provided the first detailed studies of hydrate formation in gas pipelines along with possible ways to control and prevent hydrate formation. He also developed the first model to predict formation conditions.

As is the case with most research areas, the first model was an empirical fit. The relationship Hammerschmidt proposed between the temperature and pressure that hydrates would form was:

$$T = 8.9\ P^{.285}$$

T= temperature, ^{o}F

P= pressure, PSIA

The main drawback of this method was a lack of parameters which would take into account the composition of the gas phase.

Hammerschmidt's work led to a detailed investigation of hydrates by the U.S. Bureau of Mines under the supervision of Deaton and Frost (1946). Their work into natural gas hydrates led to a modification of Hammerschmidt's equation which was re-expressed as:

$$T = a + 33.5 \text{ Log } P$$

a= experimentally determined constant depending on the type of gas used to form hydrates.

The modifications by Deaton and Frost corrected some of the problems associated with the Hammerschmidt equation. However, both methods were not general relations but applied only to natural gases and light hydrocarbons.

About the same time as Deaton and Frost, several other investigators, such as Bechtold (1942), Wilcox et al (1941), Carson et al (1942), and Katz et al (1945, 1946), studied the formation of hydrates under laboratory conditions in order to obtain a better understanding of hydrates and to develop a general predictive scheme. Wilson, Carson, and Katz found an empirical method which was based on the use of vapor/solid equilibrium constants, K_{v-s} which were similar to the equilibrium constants in vapor/liquid equilibria. The hydrate formation conditions for a multicomponent gas were calculated by using the K-values in a method similar to that of a dew point calculation:

$$\Sigma Z_i = 1.0 = \sum_i Y_i/K_{vs,i}$$

Y_i = mole fraction of species i in gas phase

Z_i = mole fraction of species i in solid phase

Even though this method has some fundamental flaws, such as the inability to predict or account for structurally different hydrates, it is still widely used.

The 1950's saw the first investigations into the molecular structure of hydrates by workers such as Von Stackelberg (1947, 1951), Claussen (1951), Mueller (1951), Marsh and Pauling (1952). It was the X-ray diffraction studies of Von Stackelberg and Mueller which first suggested that the molecules comprising the water lattice were hydrogen bonded to each other. It was the same studies that also showed the existence of structure I and structure II hydrates. Van der Waals and Platteeuw (1959) were able to take advantage of these structural results and apply statistical thermodynamics to develop the first fundamental equations to describe hydrate equilibria.

In the 1960's, McKoy and Sinanoglu (1963) modified the techniques of van der Waals and Platteeuw by using different potential models. Their investigations suggested that the Kihara model gave the best results. Also during this time, researchers such as Kobayashi (1964, 1965, 1966) investigated the behavior of hydrates at high pressures and temperatures. The results from this type of work led to the development of many parameters necessary for the statistical models.

The 1970's saw the development of the Parrish and Prausnitz (1972) model of hydrate equilibria, probably the first successful and comprehensive predictive method for gas mixtures. This decade also saw a new field of hydrate research open as hydrates were found to exist in natural reservoirs located in permafrost regions and in ocean sediments, leading to the consideration of hydrates as a possible energy source. Investigators such as Katz (1971, 1972), Stoll & Bryan (1979), Billy & Dick (1974), and Franklin (1980) studied the formation of hydrates in nature and the feasibility of recovery.

Recently, the first comprehensive studies of the kinetics of hydrate formation have been done by Makogan (1981) and Bishnoi (1983). Researchers, such as Holder (1984), Robinson (1987), and Sloan (1985), are continuing study of hydrate formation, possible inhibitors, and thermodynamic parameters for predictive models. There are also many researchers investigating the molecular dynamics of hydrate formation.

1.4 HYDRATES IN OIL WELL DRILLING

In recent years, the petroleum industry has expanded operations in deepwater areas of the world. As drilling depths increase, the potential for formation of natural gas hydrate during drilling operations also increases due to the higher seafloor hydrostatic pressure and lower environmental temperatures. Actual instances of hydrate related problems have been well documented (Jones & Sherman, 1986; Barker & Gomez, 1987).

Unlike the traditional problems that the petroleum industry has had with hydrates, where formation took place at some juncture of free water and natural gas, such as a gas pipeline, the present problems involve formation within the drilling fluid of an operating oil well. This can result in several safety and economic problems (Barker & Gomez, 1987), including:

1. Plugging of choke and kill lines preventing their use in well circulation

2. Formation of a plug at or below the blow out preventors (BOP's), preventing the monitoring of pressure below the BOP's

3. Formation of a plug around the drillstring in the riser, BOP's, or casings which can hinder or prevent drillstring movement.

4. Formation of a plug between the drillstring and the BOP's which may prevent full closure of the BOP's

5. Formation of a plug in the ram cavity of a closed BOP preventing it from opening fully.

A diagram of an oil well is shown in Figure 6.

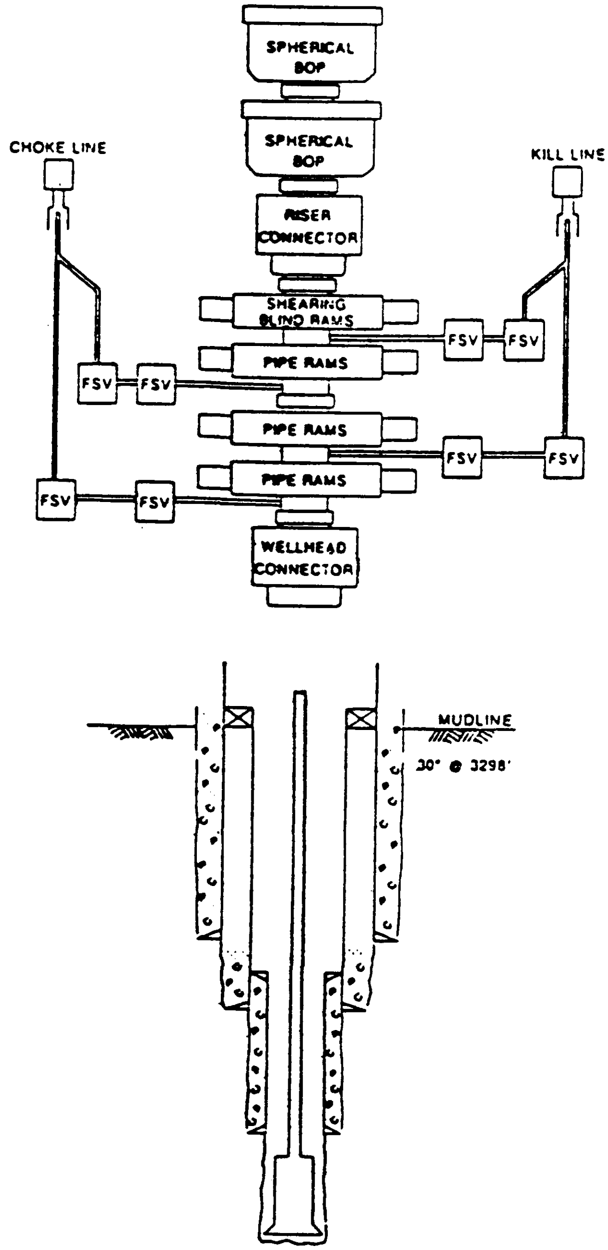

Figure 6 DIAGRAM OF TYPICAL DEEPSEA OIL WELL AND BOP STACK

The problem facing operators is that no detailed studies have been done examining hydrate formation in drilling muds or fluids that resemble drilling muds. Therefore, there is no way to predict the conditions of hydrate formation in drilling muds nor to determine, apriori, the effectiveness of inhibitors.

Traditionally, the hydrocarbon industry has used many predictive schemes (Parrish and Prausnitz, 1972; Ng and Robinson, 1977) to determine and avoid conditions (temperature and pressure) which may lead to hydrate formation. However, for these predictive schemes to be accurate, the composition of both liquid and gas phases must be known. Further, they also require the knowledge of how any impurities in the liquid phase may affect the activity of water molecules in the aqueous liquid phase. Since a drilling mud is a very complex system with many possible interactions, this information does not yet exist, and may be quite difficult to obtain. Therefore, existing predictive methods cannot be relied upon to accurately predict conditions at which hydrates will form in drilling muds and mud-like fluids.

Predictive methods also exist (Menten, Parrish, and

Sloan, 1980) which can predetermine the effectiveness of certain inhibtors, such as methanol or salt. However, these methods are faced with the same difficulties which undermine the accuracy of the general predictive schemes. Thus, it is almost impossible to accurately predict apriori the effect an inhibitor will have in preventing hydrate formation in drilling muds. Many companies have resorted to applying the traditional methods of hydrate inhibition without any real knowledge of how effective the techniques are. In one instance, a company recognized that a plug of hydrates had formed in the kill and choke lines and tried to remove the obstruction by applying pressure surges, without realizing that increasing pressure would lead to even further formation of hydrates (Barker & Gomez, 1987).

The documented cases seem to indicate that salt addition, either NaCl or KCl, is the most effective way of combatting hydrates (Jones & Sherman, 1986). Another alternative has been to switch from water-based drilling fluids to oil-based drilling muds. However, there are many barriers, such as cost and environmental considerations which make this a difficult alternative.

Chapter 2

EXPERIMENTAL APPARATUS AND PROCEDURE

2.1 EXPERIMENTAL APPARATUS

The apparatus used by this investigation consisted of two primary parts: (1) an existing high pressure equilibrium system and (2) a personal computer-based data acquisition system.

The original experimental equipment, shown in Figures 7 and 8, was constructed by Giussani (M.Sc. C.S.M.,1981). The heart of the system is a Jerguson sight glass, where the mud sample is loaded and contacted with natural gas. The fluid in the cell is pressurized via the gas mixture in a high pressure tank and if necessary, a piston pump is used to add additional pressure. To keep the fluid mixed during an experiment, a motor is used to continually rock the cell.

The cell is immersed in a large water/glycol bath to provide temperature control, which is achieved by balancing a Bayley heater control against a refrigeration unit. The thermal mass of the water/glycol bath is large enough to ensure slow cooling and heating rates so that the cell and bath temperature are on average, within 1 ^{o}F of each other.

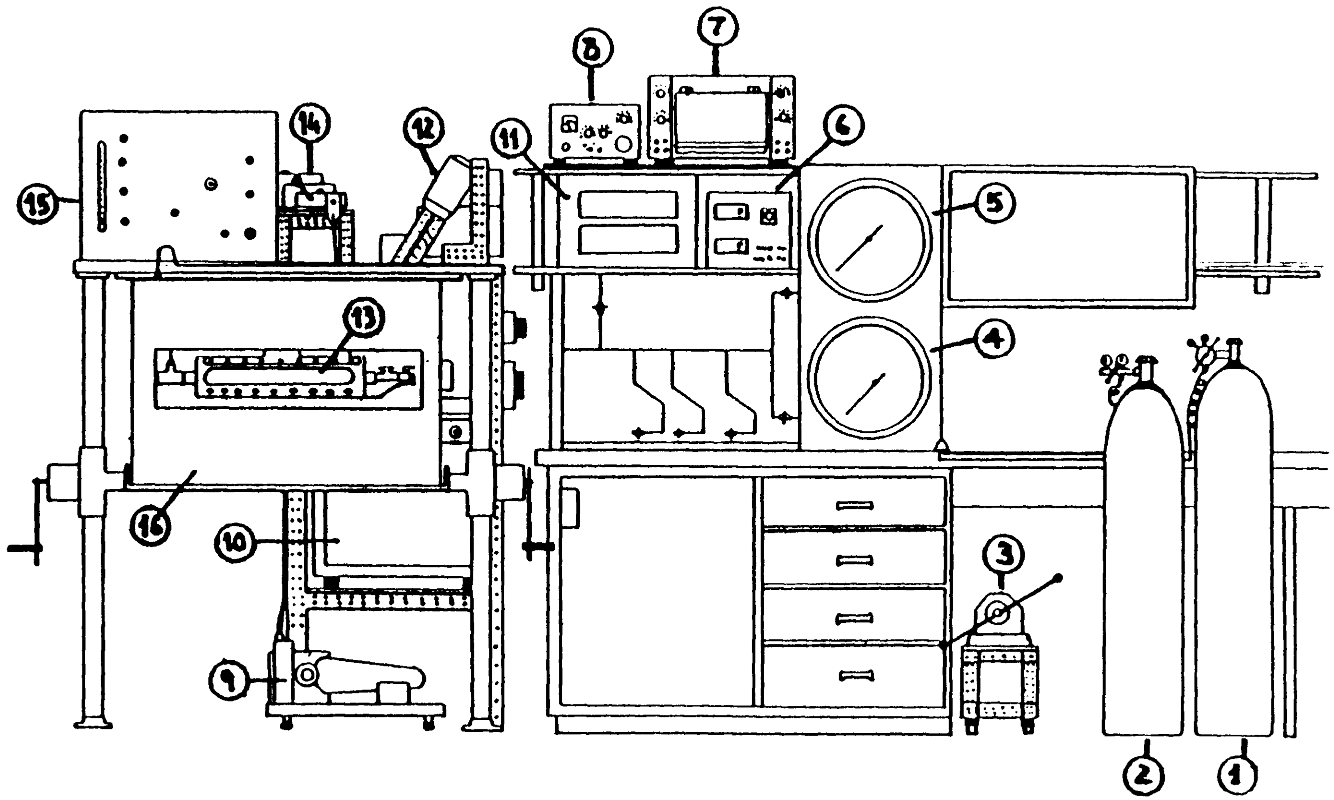

1 - GAS TANK	5 - HEISE GAUGE	9 - VACUUM PUMP	13 - CELL
2 - GAS TANK	6 - CONTROL PANEL	10 - COOLER	14 - MOTOR
3 - RUSKA PUMP	7 - CHART RECORDER	11 - TEMP DISPLAY	15 - BURET
4 - HEISE GAUGE	8 - HEATER CONTROL	12 - MIXER	16 - BATH

Figure 7 ORIGINAL APPARATUS (Giussani, 1981)

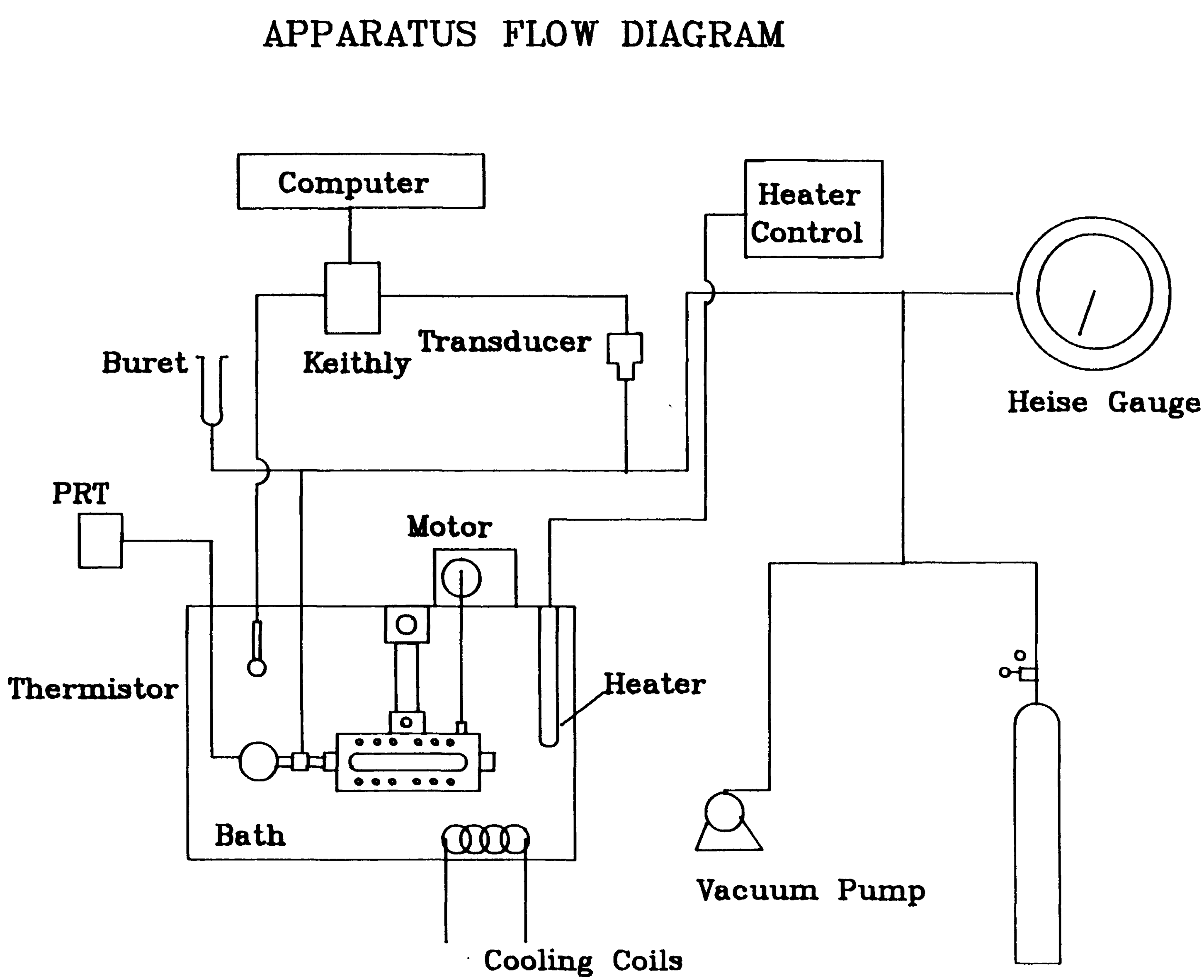

Figure 8 EXPERIMENTAL APPARATUS FLOW DIAGRAM

Pressure and temperature are monitored by external gauges and recorded by a computerized data acquisition system. Pressure is measured using a Omega pressure transducer, accurate to 0.15% of full scale (3000 psig), and backed up by a 0-2000 psig Heise gauge, accurate to 2 psi. Both devices are linked directly to the cell by stainless steel lines. The transducer sends an analog signal that is recorded by the computer. Maximum deviation between the two gauges was experimentally observed to be 8 psi but usually less than 4 psi. These values are within the accuracy of both gauges.

The temperature of the glycol bath is measured by a thermistor, accurate to 0.1 ^{o}F, and recorded by the computer. The cell temperature is additionally monitored by a RTD probe, accurate to +/- 0.3 ^{o}F. This allows the temperature difference to be maintained and minimized. The error induced by recording the bath temperature rather than the cell temperature was observed to be usually less than 0.8 ^{o}F.

The analog input system that receives the electronic signals from the gauges is a Keithly series 500 . The system consists of an analog input module, an analog-to-digital converter board, a digital-to-analog converter, and a system board which allows easy interfacing into a IBM XT computer. The system uses the analog input board to acquire the analog signal from a gauge, the A/D converter to condition the signal for processing, and the system board to send the signal to the computer. Once inside the computer, a data acquisition computer program uses calibration equations to convert the signal into a pressure or temperature reading. The computer program takes a reading every three minutes then displays, stores, and plots the data. The data file records the time,pressure, and temperature of every data point.

A detailed discussion of the computerized data acquisition system is available in Appendix B. The reader is referred to Giussani (1981) for details concerning the equilibrium system.

2.2 EXPERIMENTAL PROCEDURE

The experimental procedure that was utilized for this work consisted of two major sections: (1) mixing of the test fluids and (2) hydrate formation experiments on the test fluid. The compositions for all hydrate formation tests are listed in table 3.

TABLE 3

COMPOSITION OF EXPERIMENTAL FLUIDS

FLUID	COMPOSITION
2	Lig/S/XC/PHPA/DS/MEOH
3	Lig/XC/PHPA/O
4	B/S/XC/PHPA/DS
5	Lig/B/S/XC/O
6	LIG/B/S/PHPA/O
7	LIG/B/DS/MEOH
8	B/XC/PHPA/MEOH
9	S/O/DS/MEOH
10	Lig/S/XC/MEOH
11	B/XC/O/DS
12	B/S/PHPA/O/MEOH
13	LIG/PHPA/DS
14	XC/PHPA/O/MEOH
15	Lig/B/O/DS/MEOH
16	S
17	Lig/S/XC/PHPA/O/DS
F1	BENTONITE
F2	Lig
F3	PHPA
F4	Lig/PHPA

* Lig = Bentonite/thinner/caustic
B = Barite
S = Salt
XC = XCD Polymer (Polymer A)
PHPA = New Drill (Polymer B)
O = LVT Oil
DS = Drill SOlids
MEOH = Methyl Alcohol

Mixing Procedure: A mixing procedure for all screening tests is listed in Table 4. The important point is that components were added in the same order, and mixed for the same amount of time, for all screening tests. After all components were added, each fluid was mixed an additional time to insure that total mixing time was at least 70 minutes.

The mixing procedure for the fundamental tests was similar to that of the screening program. Components were added in the same order and mixed for the same time interval as the screening mixing procedure. Total mixing time was also at least 70 minutes

The fluids were mixed from the same component stocks and allowed to sit for approximately 24 hours. Before being loaded into the equilibrium cell, the fluids were remixed for approximately one minute.

Hydrate Formation Experimental Procedure: The procedure for hydrate formation experiments began with the complete evacuation of the equilibrium cell by means of a vacuum pump. The cell was then loaded with 80 ml of the test fluid, and 'swept', by means of pressurizing and releasing gas from the cell. This was done to insure that

TABLE 4

MIXING PROCEDURE

Equipment: -Multimixer or Malt Mixer set at 11,000 rpm
-A balance that can weight to 0.01 gms
-Metal mixing cups

ORDER OF ADDITION	MIXING TIME, MIN.
Water	Start
Bent/Thin/Caus Drill solids	25 min. total
Polymer A	10
Polymer B	10
Nacl	5
Barite	5
Oil	5
MEOH (last)	5
	65 minutes

Note: All samples mixed a total of 70 minutes even if only a few variable were used.

the gas in contact with the sample was "clean", consisting of only the components that were desired. The sample was then pressurized to the desired value and allowed to equilibrate for approximately one hour. The starting temperature was always between 70 and 80 ^{o}F, depending on the pressure.

Once the sample was stable, no more gas or mud were input into the cell and the temperature of the bath was slowly lowered until hydrate formation commenced. Hydrate formation was easily detected by a sudden pressure drop which resulted from gas being encapsulated into hydrates. If hydrate formation occurred before the temperature reached 30 ^{o}F, the temperature was held constant at the point of formation. This temperature was then maintained until the pressure stabilized which signalled that the hydrate formation had effectively stopped. If formation did not take place before the temperature reached 30 ^{o}F, the temperature is maintained around 30 ^{o}F for about four hours or until formation took place.

Once hydrate formation was complete, or determined as unlikely, the temperature was slowly increased and the hydrates dissociated. The heating rate was very important, and had to be extremely slow in order to allow the hydrate/water/gas system to stay in equilibrium. Our experience indicated that 3 ^{o}F/hr was the maximum value. The actual value was approximately 2 ^{o}F/hr. Because of the slow cooling and heating rates, along with the time required for hydrate formation, a single experimental run could last from 20-40 hours.

Hydrate dissociation was complete at the point where the dissociation curve joined the cooling curve. This can be seen graphically in Figure 9, which displays a typical pressure-temperature trace generated during an experimental run. Because of the highly metastable nature of hydrate formation, the dissociation point (point A, on Figure 9) represented the equilibria condition between hydrate, water, and the gas sample. This point could be visually confirmed for clear fluids, such as water or water/salt, but not for most of the test fluids, which were too cloudy to observe. If the dissociation curve failed to join the cooling curve, the experiment was repeated until an intersection was achieved. This procedure was repeated for four different pressures (two end points, 1300 psi and 400 psi, and two intermediate points, approximately 600 psi and 900 psi). A test was then rerun to insure the reproducibility of the data.

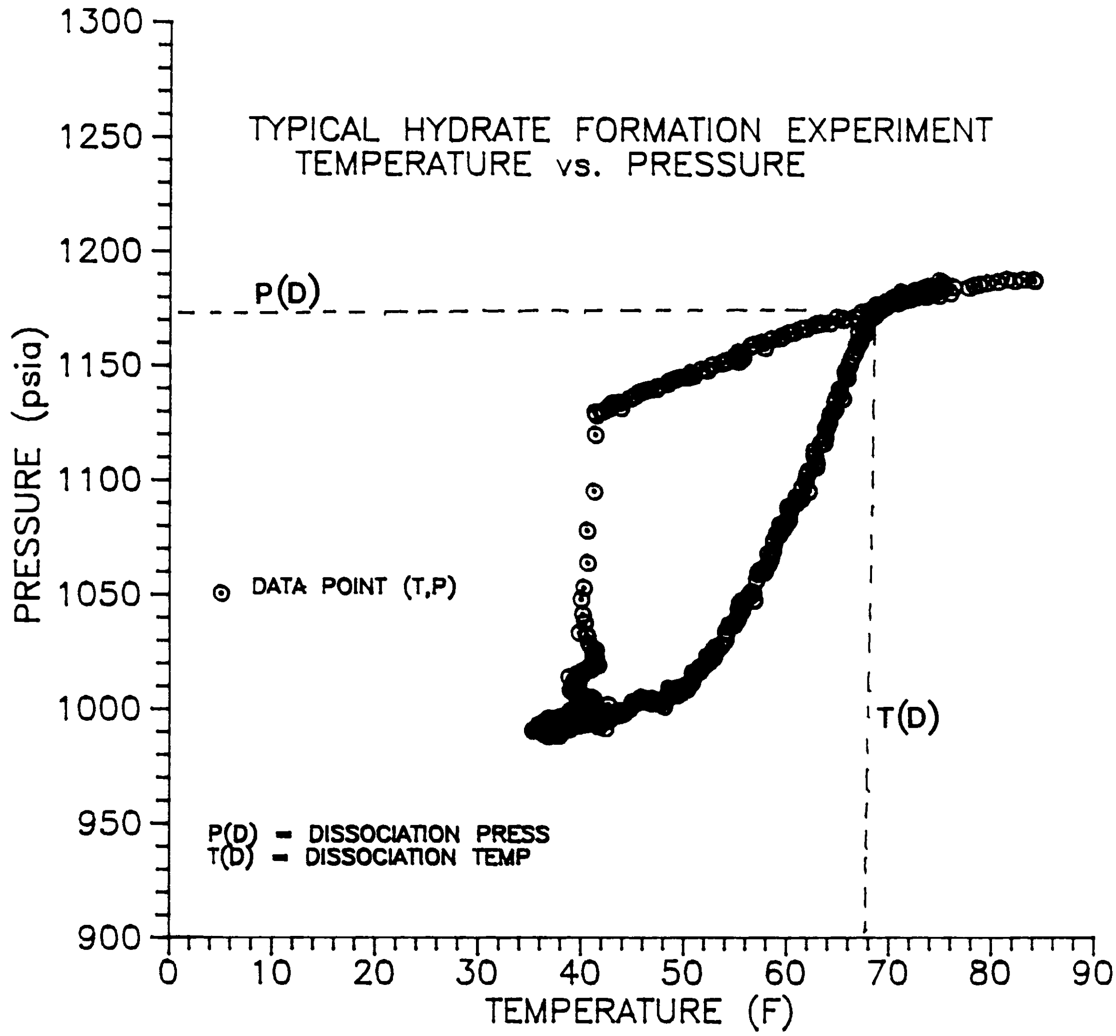

Figure 9 SAMPLE TEMP-PRESS TRACE

The fluid was continually rocked in order to maintain a homogenous mixture. In some cases, hydrate formation was severe enough to cause separation of water and oil from the fluid. When this was the case, the gas was rapidly vented in order to cause extreme turbulence within the cell, as the pressure was released. This turbulence remixed the fluid in most cases. If this was unsuccessful, the fluid was cleaned out of the cell and a new sample was loaded.

Chapter 3

SAMPLE CHARACTERIZATION

3.1 NATURAL GAS

The gas used for the hydrate formation experiments was a simulated, Gulf of Mexico natural gas recommended by CONOCO and supplied by Matheson Gas products Company. The volumetric composition of the gas was:

87.2% Methane, CH_4
7.6% Ethane, C_2H_6
3.1% Propane, C_3H_8
0.5% i-Butane, C_4H_{10}
0.8% n-Butane, C_4H_{10}
0.2% i-Pentane, C_5H_{12}
0.2% n-Pentane, C_5H_{12}
0.4% Nitrogen, N_2

The gas mixture was made gravimetrically and checked chromatographically. A phase diagram, Figure 10, was generated using the Peng-Robinson Equation of State and indicates that the natural gas will not condense over the experimental range of temperatures and pressures.

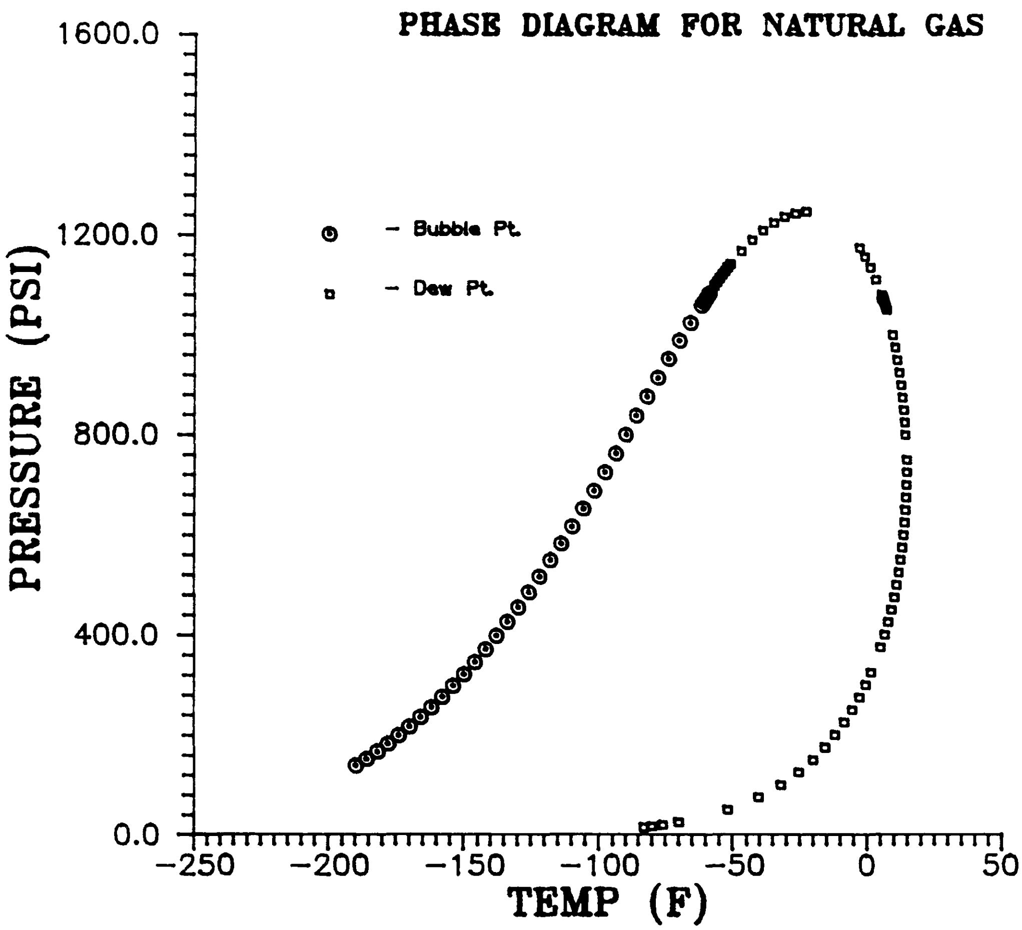

Figure 10 PHASE DIAGRAM of NATURAL GAS MIXTURE GENERATED USING THE PENG-ROBINSON EQ.

3.2 DRILLING MUD COMPONENTS

The test fluids were made-up using typical water-based mud components. These were:

Water	
Bentonite/thinner/caustic	Barite
NaCl	XCD Polymer
PHPA Polymer	LVT Oil
Drill Solids	MEOH

Table 5 lists a brief properties summary for all water-based mud components used for this investigation. A brief description of each component is provided below.

Water: The water for this study was obtained from the U.S. Geological Survey, and was deionized and quadruply distilled. Eight liters were obtained and stored in 500 ml polyethylene bottles to ensure that all test fluids were made-up with the same water.

Bentonite/Thinner/Caustic: Both the bentonite and the thinner, which is lignosulfonate, are from Baroid. The Wyoming bentonite is Baroid's Aquagel brand, while the lignosulfonate is Baroid's Q-Broxin brand. The bentonite and thinner were always added together in the ratio of 12

TABLE 5

SOME PROPERTIES OF TEST COMPONENTS

COMPONENT	SPECIFIC GRAVITY, (APPROX.)	POUNDS OF MATERIAL PER BARREL	TESTING RANGE VOLUME PERCENT
BENT/THIN/CAUS	2.5	14	0-1.6
BARITE	4.2	150	0-10.2
NaCL	--	50.3	0-5.2
POLYMER A (XCD)	1.5	1.0	0-.2
POLYMER B (PHPA)	1.5	1.0	0-.2
OIL (CONOCO LVT)	0.815	29.0	0-10
DRILL SOLIDS	2.5	20	0-2.3
MEOH	0.79	28	0-10
WATER	1.0	--	57-100

gms bentonite/ 2 gms thinner. Approximately 0.5 to 1.0 gms of caustic, NaOH, is added to achieve a pH of 9.0-10.5 once the fluid was completely mixed. The NaOH and lignosulfonate were used to keep the clay dispersed in solution to avoid viscosity and gelling problems. The NaOH acts to convert the acidic lignosulfonate to the more water soluble sodium salt. In its solution state, the negatively charged lignosulfonate ion adsorbs onto the surface of clay particles. This negatively charged coating accomplishes two purposes:

1. It keeps clays (and other coated solid particles) dispersed through the repulsion of like charges.

2. It helps maintain the clay in the same state of hydration thus preventing further dispersion of clay platelets.

Barite: The barite is mostly Barium Sulfate ($BaSO_4$), with smaller portions of various minerals, such as quartz, calcite, and silicates. The size of the barite particles should be between 2 and 100 micrometers. Barite is chemically neutral towards most components and virtually insoluble in water.

NaCl: The NaCl is a commercial grade salt made by Morton Salt Company. The concentration of salt in water ranges between 0-19% by weight.

Polymer A: Polymer A, a biopolymer, is Kelzan's XCD polymer, which is xanthan gum. Xanthan gum consists of a linear backbone of glucose residues alternately linked to a three-unit-long side chain. Molecular weight is estimated to be about 5,000,000. A diagram of the polymer's structure is shown in Figure 11.

Polymer B: Polymer B, a synthetic polymer, is a partially hydrolyzed polyacrylamide (PHPA) made by Nalco Chemical Company. The commercial brand, which is sold by Milpark under the brand name 'New Drill', contains KCl which is absent from our sample. Figure 12 displays the structure of polymer B.

LVT Oil: The LVT oil was supplied by CONOCO and has the following characteristics:

API gravity - 42.2

Ave. Mol. Wt. - 164 g/mol

Composition: n-paraffins - 3.2%

branched paraffins - 41.5%

cycloparaffins - 40.2%

aromatics - 15.1%

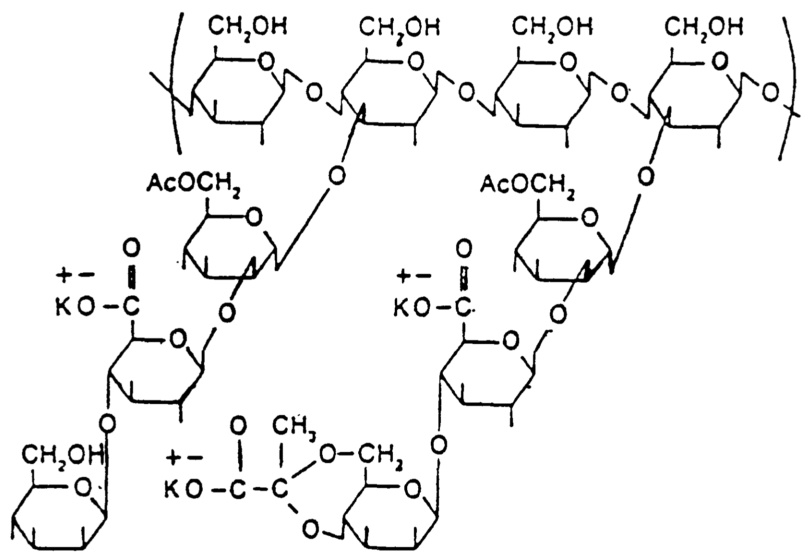

Figure 11, STRUCTURE OF POLYMER A (XCD POLYMER)

(Reproduced from Grey & Darcy, 1980)

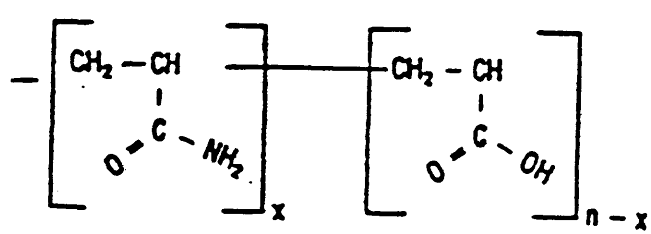

Figure 12, STRUCTURE OF POLYMER B (PHPA POLYMER)

(Reproduced from Malachosky, 1987)

Drill Solids: The drill solids, or rev dust, are intended to simulate well hole cuttings. The rev dust is generally much finer than barite, between 10 and 30 microns, and consists of a mixture of components. X-ray diffraction (Malachosky, 1988) identifies the following:

1. Kaolinite 45-50%
2. Calcium Smectite 25-30%
3. Quartz 15-20%
4. Crystalline 5-10%

The calcium smectite is structurally similar to the bentonite.

MEOH: The methanol is added as a possible inhibitor. It is chromatically pure material and is present in concentrations of 8%-14% by weight.

Chapter 4

EXPERIMENTAL RESULTS

The experimental work consisted of two major sections: (1) the screening program of water-based drilling mud components and (2) fundamental tests designed to confirm the major hypotheses of the screening work.

The screening program consisted of 17 tests designed to determine the effect of each component on the formation of natural gas hydrates in drilling muds. A complete discussion of the statistical approach is located in Appendix A. Some of the major ideas behind the statistical design were:

1. The system (formation of hydrates in drilling muds) was reduced to two groups of variables: dependent and independent. The dependent variable was the hydrate formation temperature at a given pressure for a given mud composition. The independent variables were the volumetric concentrations of the drilling mud components.

2. Once the variables were defined, a function relating the independent and dependent variables

had to be decided upon. Some possible functions were: quadratic, where the formation temperature is a function of the (composition)^2, an exponential function, where the formation temperature is a function of the exponential of composition, or linear, where the formation temperature is a function of concentration multiplied against a constant. The linear model was chosen.

3. A linear model assumes that there are no interactions between components that will effect the formation temperature. Therefore, the effect a component has, on the formation temperature of hydrates in a drilling mud, should be independent of the other constituents of the fluid.

4. 17 experimental fluids (or muds) were designed, by a computer program, to test the model. Each fluid was a unique combination of drilling mud components. The composition of all 17 test fluids is located in Tables 6 and 7.

Natural gas hydrates were successfully formed in 14 of

TABLE 6

COMPOSITION OF TEST FLUIDS
FOR SCREENING PROGRAM

TRIAL NO.	BENT/THIN/CAUS	BARTIE	SALT	POLYMER A	POLYMER B	OIL	DRILL SOLID	MEOH	WATER
1	0	0	0	0	0	0	0	0	100.0
7	14.0	150.0	0	0	0	0	20.0	28.0	256.6
15	14.0	150.0	0	0	0	29.0	20.0	28.0	230.6
4	0	150.0	50.3	1.0	1.0	0	20.0	0	287.3
14	0	0	0	1.0	1.0	29.0	0	28.0	278.6
2	14.0	0	50.3	1.0	1.0	0	20.0	28.0	282.2
5	14.0	150.0	50.3	1.0	0	29.0	0	0	254.3
6	14.0	150.0	50.3	0	1.0	29.0	0	0	254.3
12	0	150.0	50.3	0	1.0	29.0	0	28.0	223.8
10	14.0	0	50.3	1.0	0	0	0	28.0	291.3
13	14.0	0	0	0	1.0	0	20.0	0	335.6
16	0	0	50.3	0	0	0	0	0	334.2
8	0	150.0	0	1.0	1.0	0	0	28.0	277.9
11	0	150.0	0	1.0	0	29.0	20.0	0	270.5
3	14.0	0	0	1.0	1.0	29.0	0	0	308.0
7	14.0	0	50.3	1.0	1.0	29.0	20.0	0	282.2
9	0	0	50.3	0	0	29.0	20.0	28.0	253.2

Compositions given in units of [grams]

TABLE 7

RESULTING TEST FLUIDS FOR SCREENING PROGRAM IN VOL%

TRIAL NO.	BENT/THIN/CAUS	BARITE	SALT	POLYMER A	POLYMER B	OIL	DRILL SOLID	MEOH	WATER
1	0	0	0	0	0	0	0	0	100.0
7	1.6	10.2	0	0	0	0	2.3	10.0	75.9
15	1.6	10.2	0	0	0	10.0	2.3	10.0	65.9
4	0	10.2	5.0	0.2	0.2	0	2.3	0	82.1
14	0	0	0	0.2	0.2	10.0	0	10.0	79.6
2	1.6	0	5.0	0.2	0.2	0	2.3	10.0	80.7
5	1.6	10.2	5.0	0.2	0	10.0	0	0	73.0
6	1.6	10.2	5.0	0	0.2	10.0	0	0	73.2
12	0	10.2	5.0	0	0.2	10.0	0	10.0	64.6
10	1.6	0	5.0	0.2	0	0	0	10.0	83.2
13	1.6	0	0	0	0.2	0	2.3	0	95.9
16	0	0	5.0	0	0	0	0	0	95.0
8	0	10.2	0	0.2	0.2	0	0	10.0	79.4
11	0	10.2	0	0.2	0	10.0	2.3	0	77.3
3	1.6	0	0	0.2	0.2	10.0	0	0	88.0
7	1.6	0	5.0	0.2	0.2	10.0	2.3	0	80.7
9	0	0	5.0	0	0	10.0	2.3	10.0	72.7

Compositions given in volume %

the 17 test fluids.

The fundamental work consisted of hydrate formation experiments with 4 additional test fluids, all of which formed hydrates. The composition of each fluid is shown in Table 8.

The results for hydrate formation tests with the simulated natural gas consist of equilibrium temperature and pressure pairs. A single data point is generated during an experimental run which can last 20-40 hours. At least four data points were obtained for all hydrate forming fluids.

The point of thermodynamic equilibrium was taken as the point of hydrate dissociation rather than the point of initial hydrate formation because of the extreme metastability of hydrate formation. The dissociation point, which is not metastable, represents the highest possible temperature for hydrate formation. If the metastability were removed, the formation point would be identical to the dissociation point. The dissociation point was taken as the point where the reheat curve rejoined the cooling isochore (discussed further in the procedure section).

TABLE 8

COMPOSITION OF FUNDAMENTAL TESTS

TEST	COMPOSITION			
	BENTONITE	THINNER	CAUSTIC	PHPA
1	12 gms	---	---	---
2	12 gms	2 gms	.5 gms	---
3	---	---	---	1 gm
4	12 gms	2 oms	.5 gms	1 gm

H2O was added to each test so that final weight was always 350 gms

Hydrate dissociation points were determined from plots of raw data, which are listed in the appendix. The visually obtained point was then confirmed by a best fit method which involved fitting, both the cooling portion and the reheat portion of the hysteresis loop, to separate mathematical expressions. The hydrate equilibrium point could be determined by the intersection of curves generated by equations which represented the reheat and cooling portions of the curve.

4.1 DRILLING MUD RESULTS

The results of formation tests on all drilling-mud fluids are summarized in Table 9, and depicted graphically in Figures 13, 14. The X-axis of Figures 13 and 14 plots reciprocal absolute temperature, in units of inverse degrees Rankine, increasing to the left so that real absolute temperature increases to the right. The Y-axis of Figures 13 and 14 plots the natural logarithm of pressure, in psi. The graphs also display best-fit lines of the data which are identical to those used for the statistical analysis. The slope of the best-fit line is listed in Table 9 for every hydrate forming test. Table 10 also displays the corresponding values of the heat of hydrate formation,

TABLE 9

SUMMARY OF HYDRATE POINTS

		INITIAL CONDITIONS		HYDRATE CONDITIONS	
MUD#	RUN#	TEMP(F)	PRESS(PSI)	TEMP(F)	PRESS(PSI)
7	1	70	330	50	318
	1b	70	330	47	295
	2	70	500	58	492
	3	70	800	62	785
	4	80	1200	69	1160
	5	80	1200	68	1175
15	1	70	300	DID NOT FORM	
	2	70	600	DID NOT FORM	
	3	70	900	61	880
	4	70	1200	63	1090
	2B	70	600	53	598
	1B	70	410	53	404
	5	70	1200	63	1100
	6	70	800	60	770
5	1	70	1200	DID NOT FORM	
	2	70	1200	DID NOT FORM	
	3	70	1200	DID NOT FORM	
4	1	70	1200	DID NOT FORM	
	2	70	1200	DID NOT FORM	
	3	70	1200	DID NOT FORM	
14	1	70	1200	69	1148
	2	70	900	66	880
	2B	70	900	66	885
	3	70	600	60	592
	4	70	300	51	292
2	1	70	1200	55	1132
	1B	70	1200	54	1112
	2	70	900	49	904
	3	70	600	45	588
	4	70	400	DID NOT FORM	

(Continued)

TABLE 9 (CONT.)

		INITIAL CONDITIONS		HYDRATE CONDITIONS	
MUD#	RUN#	TEMP(F)	PRESS(PSI)	TEMP(F)	PRESS(PSI)
6	1	70	1100	59	1006
	2	70	900	57	884
	3	70	400	DID NOT FORM	
	4	70	600	54	596
	5	70	1100	59	1006
12	1	70	1100	DID NOT FORM	
	1B	70	1100	DID NOT FORM	
	1C	70	1100	DID NOT FORM	
10	1	70	1100	58	1060
	1B	70	1100	58	1060
	2	70	900	54	880
	3	70	610	51	600
	4	70	400	DID NOT FORM	
	5	70	450	DID NOT FORM	
13	1	80	1050	72	1030
	1B	80	1050	71	1030
	1C	80	1050	71	1030
	2	78	810	69	800
	3	78	610	68	600
	4	78	400	64	394
16	1	75	1050	65	1048
	2	70	800	58	800
	2B	70	800	59	790
	3	70	600	55	582
	3B	70	600	56	584
	4	70	400	49	385
8	1	70	1000	66	985
	2	70	800	65	790
	3	70	600	62	590
	3b	70	600	63	600
	4	70	415	60	410

(Continued)

TABLE 9(CONT.)

		INITIAL CONDITIONS		HYDRATE CONDITIONS	
MUD#	RUN#	TEMP(F)	PRESS(PSI)	TEMP(F)	PRESS(PSI)
3	1	80	1000	70	940
	1B	80	1000	71	925
	2	70	600	64	594
	2B	70	600	63	596
	3	70	400	56	390
	4	80	1200	73	1145
17	1	80	1350	60	1300
	1B	80	1350	61	1310
	2	70	1050	58	1000
	3	70	650	54	644
	4	70	420	48	400
9	1	70	1300	43	1275
	1B	70	1300	44	1280
	2	70	1000	DID NOT FORM	
	3	70	800	DID NOT FORM	
BENT	1	70	400	DID NOT FORM	
	2	80	820	73	800
	2b	80	810	72	800
	3	85	1200	75	1180
	3b	85	1300	76	1260
BE/TH/CA	1	80	1350	74	1300
	2	80	440	60	420
	2B	80	440	59	420
	3	85	825	68	800
PHPA	1	85	1355	75	1300
	2	80	810	71	800
	3	70	445	64	435
BE/TH/CA +PHPA	1	85	420	61	400
	1B	80	420	59	408
	2	85	600	65	580
	2B	80	640	65	612
	3	80	1310	74	1300

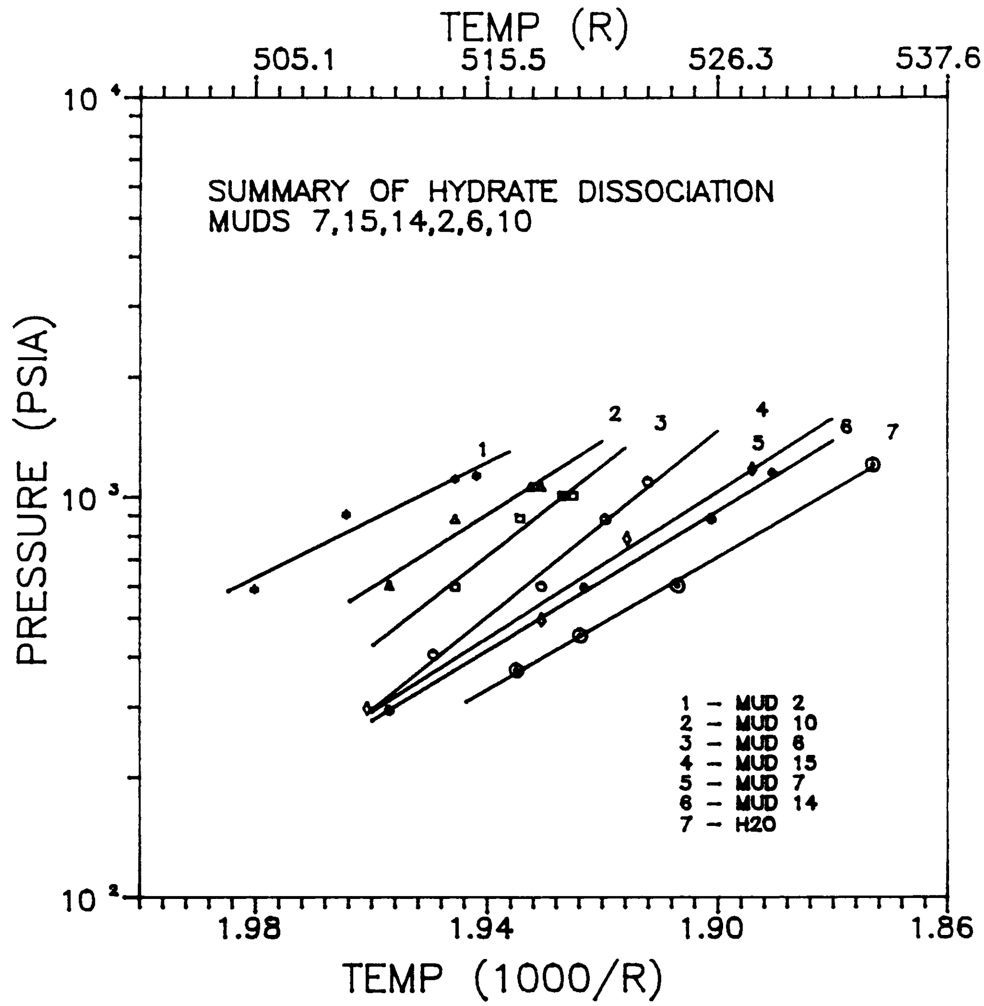

Figure 13 HYDRATE EQUILIBRIUM CONDITIONS FOR TEST FLUIDS 2, 10, 6, 15, 7, 14

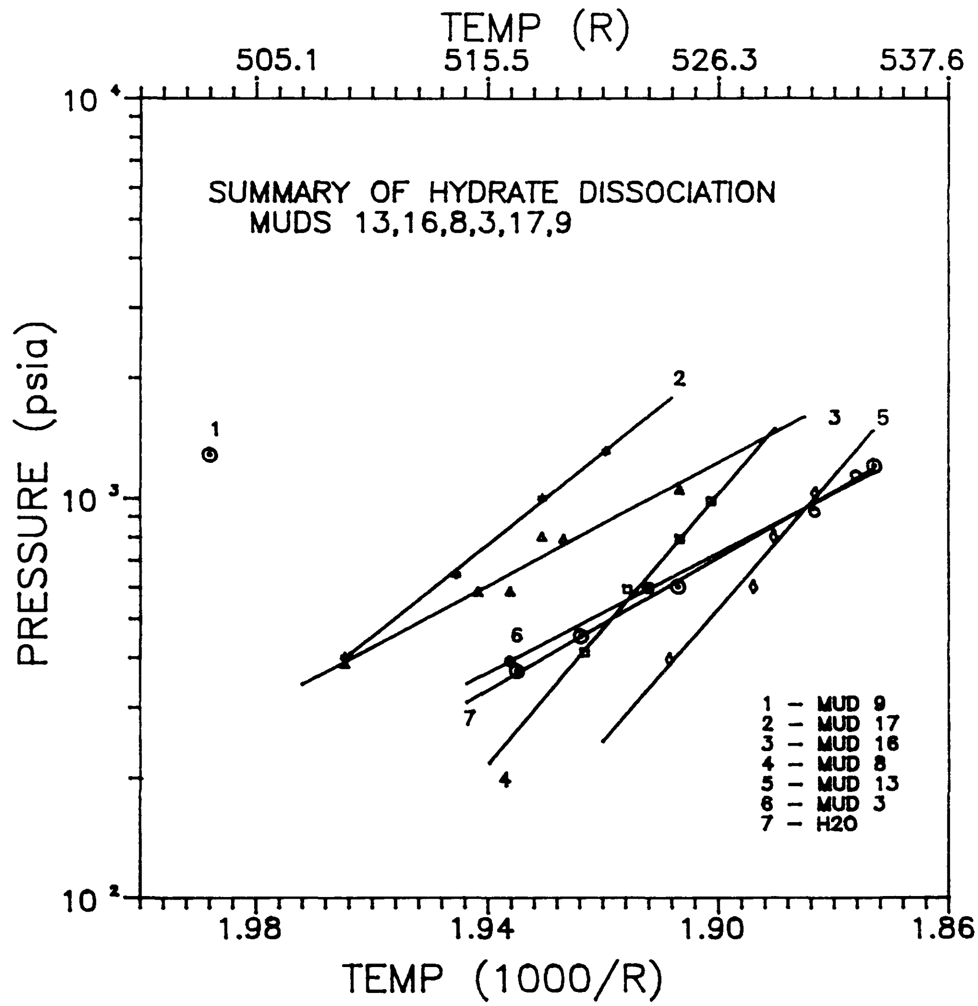

Figure 14 HYDRATE EQUILIBRIUM CONDITIONS FOR

TEST FLUIDS 9, 17, 16, 8, 13, 3

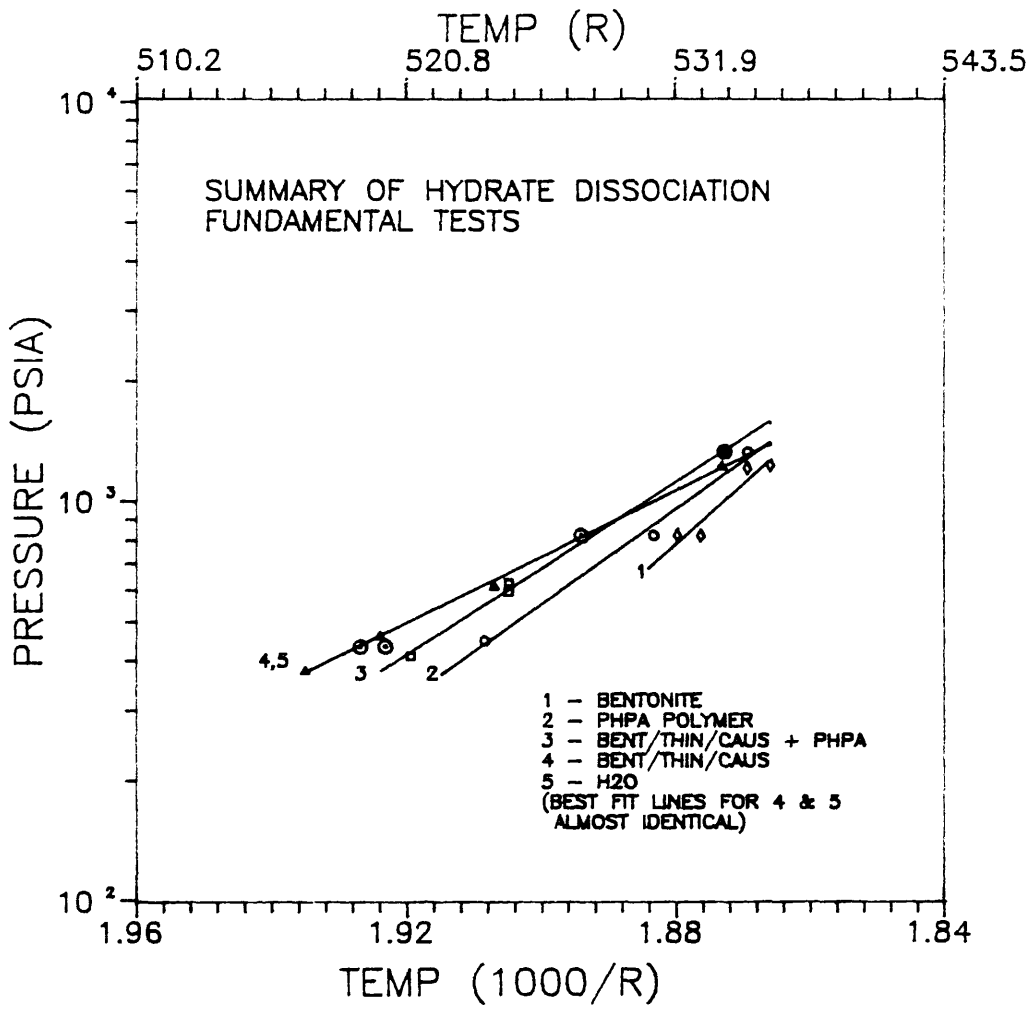

Figure 15 HYDRATE EQUILIBRIUM CONDITIONS FOR FUNDAMENTAL TEST FLUIDS

TABLE 10

HEAT OF HYDRATION FROM THE SLOPE
OF EQUILBRIUM LINE

TEST	SLOPE (x 1000)	DEL H (KBTU/LBM)	DEL H (KCAL/MOL)	DEL H (KJ/MOL)
H2O	-19.132	-38.015	-21.129	-88.370
7	-20.249	-40.235	-22.353	-93.530
15	-26.759	-53.243	-29.579	-123.767
14	-20.134	-40.007	-22.226	-92.999
2	-16.503	-32.791	-18.217	-76.225
6	-30.896	-61.390	-34.106	-142.700
10	-20.230	-40.196	-22.332	-93.440
13	-36.683	-72.890	-40.495	-169.437
16	-17.325	-34.424	-19.215	-80.020
8	-37.457	-74.426	-41.358	-173.100
3	-17.157	-34.089	-18.939	-79.244
17	-27.344	-54.333	-30.185	-126.300
BENTONITE	-34.313	-68.180	-37.878	-158.482
BENT/THIN/CAU	-21.408	-54.579	-30.322	-126.867
PHPA	-27.468	-54.579	-30.322	-126.867
BENT/TH/CAU + PHPA	-25.003	-49.681	-27.601	-115.483

which are derived from the slope and the Clausius-Clapeyron relation, in various units. The symbols on Figures 13 and 14 indicate actual data points of hydrate dissociation.

Additional data from the experiments include total pressure drop measurements for all hydrate forming fluids. Since the data is widely distributed, Figure 16 displays regions where a best fit line, of pressure drop versus formation pressure, would be. This approach can distinguish general trends but cannot provide absolute comparisons.

Table 11 provides a summary of single additive and mixture behaviors. The results presented in Table 11 are discussed in the discussion of results.

4.2 FUNDAMENTAL TEST RESULTS

The results of hydrate formation experiments on the fundamental tests are located in Table 9, and graphically presented in Figure 15, which, like Figures 13 and 14, plots logarithm of formation pressure versus the reciprocal of absolute formation temperature. The heat of hydrate formation is located in Table 10. Pressure drop measurements for the fundamental tests are shown in Figure

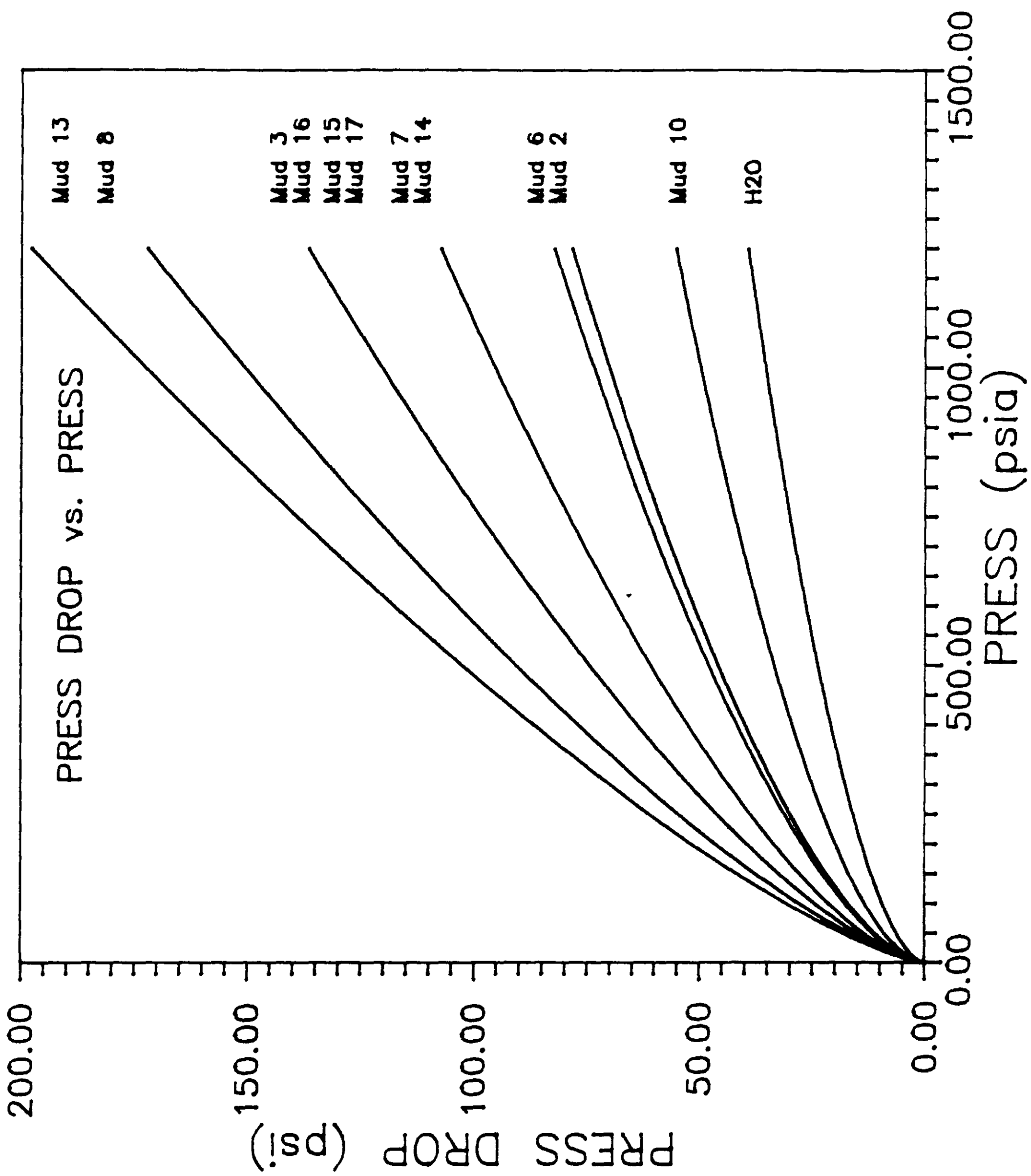

Figure 16 PRESSURE DROP DATA FOR DRILLING MUD TEST

TABLE 11

PURE COMPONENT AND MIXTURE RESULTS

COMPONENT	THERMO EFFECT	KINETIC EFFECT
Bent/thin/caustic	++	++
Barite	00	++
Salt	--	--
Poly A	--	--
Poly B	++	00
Oil	--	--
Drill Solids	00	++
MEOH	--	00
Bent + Poly B	++	++
Barite + Poly B	++	++
Oil + Poly A	--	00
Barite + Oil + Poly A	--	--

key: ++ promoter, -- inhibitor, 00 no effect

17, which is patterned after Figure 16.

The results of the fundamental tests are analyzed in the discussion of results.

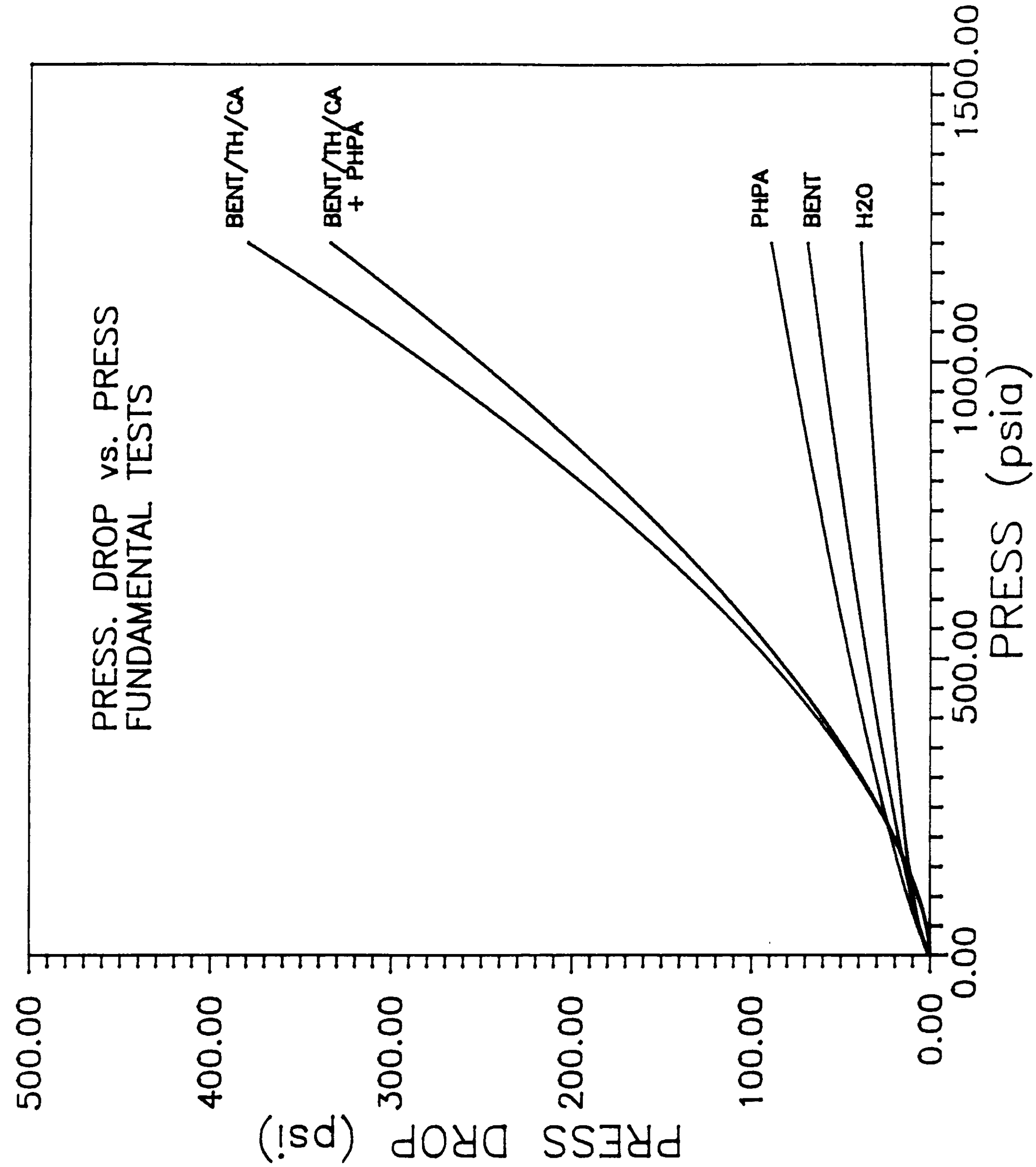

Figure 17 PRESSURE DROP DATA FOR FUNDAMENTAL TESTS

Chapter 5

DISCUSSION OF RESULTS

The experimental program consisted of two major sections. The first portion was the screening program of water-based mud components while the second portion was a series of fundamental tests. The fundamental tests were experiments designed to confirm the hypotheses that arose from the screening test concerning the effect of certain components on the formation of natural gas hydrates

5.1 DISCUSSION OF HYDRATE FORMATION IN DRILLING MUDS

The hydrate formation experiments with water-based drilling mud components consisted of 17 tests, statistically designed to determine the effect of each component on the formation of hydrates in water-based drilling muds. A complete discussion of the statistical approach is located in Appendix A. The design of the experiments permitted the use of statistical analysis on the experimental results in addition to the conventional analysis of the researchers. The advantage of the statistical analysis is that the interpretation of results is completely objective and will yield well supported conclusions. However, this type of approach is not flawless. The analysis cannot extend beyond the limitations of the experimental design, which included the assumption that components do not interact with other components. Therefore, the effect a component has on hydrate formation in a drilling mud will be same regardless of the overall composition of the drilling mud. However, in fluids as complex as drilling muds, some interaction of components (mixture effects) must be expected. .

The major conclusion of the analysis is that mixture affects are present and are stronger at lower pressures. The statistical analysis also identified water and the bentonite group as thermodynamic promoters and NaCl as a thermodynamic inhibitor. Since water is essential for hydrate formation, it may be incorrect to classify water as a promoter.

Even though the statistical analysis is weakened by the presence of mixture effects, the conclusions do not seem to contradict any experimental observations or results. However, more information can be obtained from the experimental results by closely examining the role of each component and by considering mixture effects.

Natural gas hydrates were formed in 13 of the 17 test fluids. The nonforming fluids were 4, 5, 12, and 11. Additionally, only one formation point, at high pressure, was found for test fluid 9. The experimental results indicate that most hydrate forming test fluids will exhibit different formation characteristics when compared to pure water. The differentiating characteristics were promotion or inhibition of: (1) thermodynamic equilibria and (2) formation kinetics.

Thermodynamic promotion indicates that the hydrate structure is stable at higher temperatures than pure water hydrates, at the same pressure. Conversely, thermodynamic inhibition indicates that a hydrate is stable at lower temperatures than pure water hydrates, at the same pressure. The kinetics of formation involve two effects: the rate of reaction and the extent of formation. Thus a kinetic promotion involves an increase in both the rate and the extent of formation over pure water hydrates while a kinetic inhibition denotes a decrease in both the rate and extent of formation when compared to pure water hydrates.

With in the experimental scheme, the thermodynamics can be well observed, the extent of reaction can be reasonably approximated, but only an educated guess can be made about the rate of formation. The rate is difficult to analyze because the speed at which hydrates form is a strong, perhaps stronger, function of variables besides liquid phase composition, many of which are outside of experimental control. An example of such a variable is the subcooling required before formation of hydrates will commence. The degree of subcooling was different for almost every test. Evidence exists (Makogon, 1981) which suggests that the rate of formation is a very strong function of subcooling. The net result is that the effect of liquid composition on the rate of formation cannot be explicitly defined, only subjectively observed. A general heuristic is that the greater the extent of formation, the faster the rate.

The extent of reaction was measured by the total pressure drop during hydrate formation. Since hydration involves encapsulation of gas, loss of pressure should indicate the relative amount of hydrates formed. A comparative analysis of test fluids based upon pressure loss as an indication of formation extent is very approximate, since the assumption is made that similar ratios of gas to water exist within the hydrate structure of each fluid and that liquid phase composition is the only variable. The analysis also includes the assumption that each fluid has the same amount of water (hydrate forming potential) present, which is not true. Table 12 lists the test fluids in order of decreasing amount water present.

TABLE 12 FLUIDS IN ORDER OF AMOUNT WATER

RANK	FLUID #	AMOUNT WATER (gms)
1.	13	335.6
2.	16	334.2
3.	3	308.0
4.	10	291.3
5.	4	287.3
6.	17	282.2
7.	2	282.2
8.	14	278.6
9.	8	277.9
10	11	270.5
11	7	256.6
12	5	254.3
13	6	254.3
14	9	253.2
15	15	230.6
16	12	223.8

Therefore, Figure 16, which displays best fit lines of pressure drop versus the formation pressure, should be considered as a good first order indication of relative kinetic behaviors.

Within the accuracy of Figure 16, certain groups can be identified. Test fluids 8 and 13 formed more hydrates than fluids 3,10,15,17,7, and 14, which formed more hydrates than fluids 6,2 and 10 formed. Compositional effects can be seen since the extent of hydrate formation does not correlate to the amount of water in the fluid. In particular, fluid 8, which had an average amount of water, had the second largest pressure drops, while fluid 10, which had a high amount of water, had the smallest pressure drops. In general, components which provide large amounts of surface area will increase the amount of hydrates formed. This hypothesis was observed experimentally, and confirmed past research which determined that hydrates have an affinity for surfaces. Hydrates form easier on a surface, therefore, the larger the available surface area, the greater the amount of hydrates formed. However, compounds which decrease the activity of water molecules, preventing them from rearranging into hydrates, will decrease the extent of hydrate formation.

The experimental results indicated a wide range of temperatures and pressures at which hydrates would form. Most fluids formed at temperatures below that of pure water, at a given pressure. Only two tests, 8 and 13, resulted in equilibrium temperatures above pure water, while one fluid, test 3, was almost identical to water.

A hypothesis also exists for the thermodynamic effects. Phase equilibria depend on both gas phase and liquid phase compositions. Since the gas phase composition was constant for all experiments, deviations must be the result of liquid phase composition. The controlling thermodynamic variable is the chemical potential of water in the liquid phase. Compounds which decrease the activity of water, by competing for available water molecules, will act as thermodynamic inhibitors. We hypothesize that compounds which set up water structures more favorable to the formation of hydrate crystals, as in certain types of adsorption, will act as thermodynamic promoters.

Two thermodynamic differences were observed when hydrate formation in drilling muds was compared to pure water hydrate formation. Both differences involved the three phase line (hydrate/fluid/gas) on a ln (pressure) vs. 1/temperature plot, like those shown in figures 12 and 13. The slope of the equilibrium line is related to the heat of hydrate formation by the Clapeyron equation:

$$d(\ln P)/d(1/T) = - \Delta H/R$$

The first difference was a uniform displacement of the three phase line without a slope change. This indicated that while the hydrate formation temperature in a test fluid was different when compared to that of pure water hydrates, the temperature difference was the same at any given pressure, and that the heat of formation was unchanged. The second difference was a displacement of the three phase equilibrium line with a slope change. This indicated that not only were the formation conditions, temperature and pressure, different, but that the heat of formation had also changed. The test fluids seemed to fall into three groups of slope types. These were:

1. Slopes similar to pure water: fluids 7,2,14,10, 16,3,17

2. Slopes steeper than water: fluids 15,6,17

3. Slopes much steeper than water: fluids 8,13

The heat of formation (slope) is a function of two possible variables: the type of hydrate formed, either structure I or II, or the phase composition of the liquid. Since the type of hydrate formed is controlled mostly by the gas composition, which was the same for all tests, the second possibility seems most reasonable. Thus, fluids with slopes similar to pure water must have water as the major phase, while the fluids with slopes differing from that of water must have other phases present. We hypothesize that the behavior of group 2 fluids resulted from the presence of a free oil phase or a small adsorbed phase while the behavior of group 3 fluids resulted from the presence of a large adsorbed phase.

The free oil phase, which may have existed in fluids 15 and 6, may have been caused by the presence of LVT oil without polymer A, which seemed to act as an emulsifying agent. Free oil was experimentally observed in fluid 6 but not in fluid 15. However, we suspect that a free oil phase did exist in fluid 15 simply because there were no emulsifying agents present. An emulsion would disperse the oil and prevent it from forming a separate phase. The behavior of fluid 17 may have been caused by a small adsorbed phase, setup by the competition of polymer B and polymer A for water molecules, or by a component, perhaps salt or the bentonite, interfering with the polymer A, preventing an emulsion of the oil.

The adsorbed phase in fluids 8 and 13 may have been formed by the combination of polymer B and surface, either bentonite or barite, without the presence of salt, oil, or polymer A. It is possible that these compounds disrupted the adsorbed phase by changing either the surface, polymer B, or the water structure itself. It is also interesting to note that hydrate formation was thermodynamically and kinetically promoted in both tests. This may give some indication of how a strong adsorption of water molecules will affect hydrate formation.

5.1.1 SINGLE ADDITIVE EFFECTS

Analysis of the experimental data has identified pure component effects and some important mixture effects. Table 11 provides a summary of each component and its effect on phase equilibrium, extent of reaction, and rate of formation. The rate of formation effect is a subjective determination and cannot be verified with substantial experimental data. Table 11 also lists some major mixture effects. There is some indication, discussed later in the text, that mixture effects maybe stronger than pure component effects.

BENTONITE/THINNER/CAUSTIC: The bentonite/thinner/caustic group of compounds was identified as a strong kinetic promoter and a slight thermodynamic promoter. Experimental results indicated that the addition of this group to water will result in greater amounts of hydrates being formed at temperatures equal to or higher than those at which pure water hydrates would form. This group can also act as a counter against some inhibitors, decreasing the strength of the inhibitor. This type of behavior can be seen when tests 10 and 9 are compared. Test 9 contained three inhibitors: salt, oil, and MEOH. It did not form hydrates except at the highest pressure (1300 psi). Like test 9, fluid 10 also contained three inhibitors, salt, polymer A, MEOH, but also contained the bentonite group. This test formed hydrates at all pressures (1100,900,600 psi) except the lowest (400 psi). The different behavior might be attributed to the presence of oil in test 9 and polymer A in test 10, but since polymer A seems to be a stronger inhibitor than the oil, the bentonite group must be responsible for the promotional effects.

A possible hypothesis for the behavior of the bentonite/thinner/caustic is that layered bentonite might reorganize water into an adsorbed state which is very close in structure to that of a hydrate cage. The water molecules could then rearrange into hydrates much easier, leading to a possible thermodynamic promotion. Further, the thinner probably disperses the clay so that this adsorption of water, which might hinder the kinetics of formation by shielding the water from the gas does not take place. This would lead to large amounts of surface being available for hydrates to form around, which might explain the strong kinetic promotion. By reducing the amount of adsorption present, the thinner is probably reducing the thermodynamic enhancement but strongly encouraging the kinetic promotion.

BARITE: Experimental results indicate that the barite, by itself, is probably a thermodynamic neutral, perhaps a very slight inhibitor, and a strong kinetic promoter. This behavior may arise from the structure of the barite, which, like bentonite, does have strong ionic sites to bond water, but does not seem able to properly order the water molecules for thermodynamic promotion. However, since the structure of barite has large amounts of surface, it seems to act as a kinetic promoter.

NACL: Salt is a strong thermodynamic inhibitor whose behavior in pure water has been well documented. Salt inhibits formation by hydrating water molecules in direct competition with dissolved gas. This makes the formation of the first hydrate cage much more difficult, and the dissociation of the last hydrate cage, much easier. Although there is no proof from these experiments, there is some documentation present to suggest that the salt can also interact with the clay (Van Olphen, 1974), possibly diminishing the promotional capacity of the clay by adsorbing onto the surface and disrupting the adsorbed water structure.

There is some evidence to suggest that salt will also inhibit the extent of hydrate formation. Fluid 16, which contained only salt and water, formed only an average amount of hydrates (Figure 12) although containing the most water (by volume %).

POLYMER A: The experimental results indicate that polymer A is a pure component inhibitor whose strength can vary according to its surroundings. This type of behavior probably arises from the structure of polymer A, shown in Figure 11. The polymer has ionic sites which can bond water, but the adsorption may be structurally unfavorable towards hydrate formation, much like the rearrangement of water molecules around NaCl.

POLYMER B: Polymer B is structurally similar to polymer A, but behaves in the opposite manner. The polymer seems to act as a thermodynamic promoter, both as a pure component and within a mixture of compounds. The promotion is probably stronger thermodynamically than kinetically.

A possible hypothesis begins again with the structure of the polymer, which is shown in Figure 12. Like polymer A, the structure has ionic sites which can bond water. However, polymer B has a stronger tendency to adsorb onto solid surfaces, particularly clays (Malachosky, 1988), than polymer A. This may result in a further ordering of clay particles and the water molecules adsorbed onto the clay particles, which may contribute to the formation of hydrates.

LVT OIL: The LVT oil is a thermodynamic inhibitor which is effective as a pure component or in a mixture. The experimental results do not show a strong indication of kinetic inhibition. The oil inhibits by acting as a barrier to gas/water contact and by affecting the activity of water molecules in liquid phase. This action results in a shift in equilibrium and a change in the heat of reaction (slope of the equilibrium line). This is evident in fluids 15 and 6, which contained oil without polymer A to act as an emulsifying agent, and whose slopes are similar.

DRILL SOLIDS: The drill solids are a combination of certain minerals and clays (the precise composition is list on page 47 of the sample characterization section). There is no strong experimental evidence to suggest that drill solids can act as thermodynamic promoters, but the presence of clays suggests that some effect may exist. The clays are are somewhat structurally different from bentonite. Since this work cannot distinguish the effect of different clays, future work should study how structurally different clays can perturb hydrate formation.

MEOH: The MEOH was observed to be an inhibitor. The nature of MEOH inhibition has been well documented (Makogon, 1981). There is no experimental evidence to suggest that MEOH can inhibit the kinetics of hydrate formation.

5.1.2 MIXTURE EFFECTS

The experimental results indicate the presence of strong mixture effects, some of which may be stronger than pure component effects. For example, tests which contained many pure component inhibitors, such as salt or MEOH, still formed hydrates. Yet tests with polymer A, Barite, and oil never formed hydrates. Therefore, inhibition caused by the combination of oil, polymer A, and Barite must be stronger than the that of salt, MEOH, and oil.

SURFACE + POLYMER B: This group of compounds is thought to be the strongest promotional group, both thermodynamically and kinetically. The mixture is the common link between test 8 and 13, which formed the most hydrates at the highest equilibrium temperatures. The promotion is probably stronger than any pure component inhibitors, but not stronger than some mixture inhibitors.

The strong mixture behavior may arise from the polymer-surface interaction. It may be possible for the polymer to attach onto the surface, reorganizing into a more open structure which can bond large amounts of water into a hydrate favoring structure.

POLYMER A + OIL: This group of components inhibits the formation of hydrates. The polymer acts as an emulsifying agent, keeping the oil dispersed. The emulsion globules may inhibit the movement of water molecules which may cause the inhibitory behavior.

POLYMER A + OIL + BARITE: This mixture is the strongest inhibition group. Hydrates could not be formed in any liquid when this combination was present (tests 4, 5, 11). The behavior may arise from the polymer using the both the oil and the Barite to organize into a structure than is open enough to strongly bond a substantial amount of water into a structure much too stable to form hydrates.

All hypotheses of pure component and mixture behavior are subject to further experimental verification. Specifically, the results may change for higher pressure studies and studies with differing concentrations and components.

The experimental data suggests that mixture effects will change with pressure. It is important to note that all thermodynamic promotion was observed at pressures below 1100 psi. It is also important to notice that the statistical test, which assumes no mixture effects, seems to work better at high pressures. This indicates that pressure is a variable when considering compound behavior. The results should not be extrapolated directly to higher pressures.

Another important limitation of the experimental results is that, except for water, only extreme concentrations were tested. That is, a component was present either in full concentration or absent all together. By not varying the concentration, the analysis of mixture effects is weakened and should not be considered as more than a first approximation.

5.2 DISCUSSION OF FUNDAMENTAL TESTS

The analysis of hydrate formation tests with water-based drilling mud components indicated two important results (1) Thermodynamic promotion of hydrate formation is possible (2) Enhancement of formation kinetics is also possible.

The physical mechanisms which may be responsible for the thermodynamic and kinetic promotions were hypothesized to be:

1. Thermodynamic promotion may be caused by the ordered adsorption of water molecules on some surface into a structure which is very close to a hydrate lattice, which would ease the formation of the hydrate structure. Therefore, the hydration reaction for systems where adsorption of water molecules is possible, should be rewritten as a two step process:

(1) water + adsorbing compound + gas ⟶ adsorbed water + gas

(2) adsorbed water + gas ⟶ adsorbed hydrate

where, adsorbed hydrate refers to hydrates formed within the adsorbed water structure.

2. Kinetic promotion may be caused by the presence of an external surface which would provide nucleation sites.

The difference between the mechanisms for kinetic promotion and thermodynamic promotion is that kinetic promotion requires only that a surface adsorb water molecules into random clusters which can encourage the formation of hydrate crystal nuclei leading to faster and greater crystal growth. This behavior is referred to as a 'surface nucleation' effect. Thermodynamic promotion, however, requires that the surface adsorb water molecules into ordered layers which are close in structure to that of hydrate cages. Therefore, the water can reorganize into hydrates much easier and at higher temperatures.

Due to the nature of the screening program in which fluids containing many compounds were tested, precise confirmation of these hypotheses was not possible. To solve this dilemma, a program of hydrate formation tests was designed to examine the phenomena of formation enhancement.

The fundamental test program consisted of hydrate formation tests on four fluids. These were:

1. Water + bentonite
2. Water + bentonite/thinner/caustic
3. Water + Polymer B (PHPA)
4. Water + bentonite/thinner/caustic + Polymer B

The first test was designed to investigate the effect of ordered adsorption on hydrate formation. As a clay, the bentonite has the potential to adsorb a large amount of water which we hypothesize will provide a great deal of ordered adsorption. However, since the bentonite particles will layer themselves, a possible gas diffusion problem may exist which might affect the formation kinetics.

The purpose of the second test was to determine the effect of adsorption without surface ordering. The thinner and caustic will partially shield the bentonite (as described in the sample characterization section), which should significantly reduce the ordered adsorption of water onto the clay.

The third test was implemented in order to determine if only adsorption by a clay, like bentonite, will provide thermodynamic promotion or if other types of compounds, such a macromolecule like the PHPA polymer, will also provide enhancement,

The last test was included to determine if the effects of surface nucleation and ordered adsorption are additive. The dispersed bentonite provides a source of external surface while the polymer can provide adsorption.

The results of the fundamental tests shown graphically in Figure 14, seem to confirm the hypotheses regarding the enhancement of hydrate formation. Figure 16, which is patterned after Figure 15, gives an indication of relative kinetic effects for all of the fundamental tests.

The results of tests 1 and 2 indicate that the thermodynamic promotion and the change in formation enthalpies may be due to the ordered adsorption of water molecules. Test 1, which contained only bentonite, shows a large thermodynamic promotion and a change in the enthalpy of formation. However, once the clay was sealed (test 2), virtually eliminating the ordered adsorption, the thermodynamic effects disappeared. Kinetically, test 2 had the most significant promotion, while test 1 seemed inhibited, even though the pressure drops shown in Figure

16 do not seem to indicate any inhibition. The formation rate of test 1 was observed to be extremely slow, taking as long as 70 hours to complete compared to 20-30 hours for a typical experiment.

The kinetic inhibition in test 1 might be due to the difficulty a gas molecule has diffusing through the gel-like structure of a water-bentonite fluid. The kinetic enhancement observed in test 2 probably may be the result of dispersing the clay, which would remove any gas diffusion problems and would promote the initial nucleation of hydrates by providing a great deal of external surface upon which hydrates could form.

The results of test 2 also indicate that some surfaces can enhance the kinetics of formation and not the thermodynamics. Conversely, test 3, which was structured so that an ordered adsorbed phase was present without the diffusion problems of test 1, showed only marginal kinetic enhancement. This seems to indicate that ordered adsorption of water molecules has only a minor effect on the kinetics.

The results of test 2, which indicated that the Bent/thinner/caus group could not promote thermodynamically, seems to contradict the results of the drilling mud study. However, the results for the bentonite group must be kept within the context of the drilling mud study, where independent effects are very hard to observe. Therefore, the promotional powers attributed to the bentonite group may actually have arisen from unidentifiable interactions between bentonite and other compounds.

Test 3 reveals that clays are not the only compounds which can properly order water molecules for thermodynamic promotion of natural gas hydrates. Promotion was also evident in test 3, therefore, certain macromolecules can also sufficiently order water molecules.

The behavior of test 4, which displayed both kinetic and thermodynamic promotion, indicates that the effect of adsorption and surface nucleation are not exclusive of each other but can be complimentary. One effect does not seem to significantly disturb the other.

In summary, the results of the fundamental tests are:

1. Ordered Adsorption can significantly promote the thermodynamics of hydration but does not necessarily affect the kinetics of hydration.

2. Some forms of surface nucleation may not affect the thermodynamics but will greatly enhance formation kinetics.

The results of the fundamental tests are consistent with the results of the drilling mud study. Components such as barite or the drill solids, which provide external surface area for nucleation but cannot provide ordered adsorption like a clay (barite, unlike clays, does not have a smooth surface upon which layers of water molecules can adsorb onto), can only promote the kinetics and not the thermodynamics.

The proposed physical mechanism for thermodynamic promotion seems to be very consistent with the experimental data. However, a serious question is whether or not the model is also consistent with thermodynamic theory.

5.3 Thermodynamic Considerations

In systems where thermodynamic promotion was evident, a change in ΔH, which corresponds to the slope of the three phase line on a ln P vs. 1/T plot (shown on the following page), was observed.

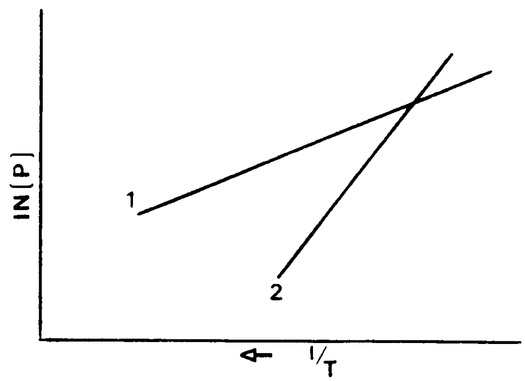

where: system 1 = water + gas

system 2 = water +gas + ordered adsorption agent

The change in enthalpy indicates a change in the amount of heat released during hydrate formation. Specifically, on an absolute basis:

$$\Delta H_2 > \Delta H_1 \tag{1}$$

but numerically, with the appropriate sign convention:

$$\Delta H_2 < \Delta H_1 \tag{2}$$

This indicates that more heat is released upon hydration in system 2 than system 1.

The point where the equilibrium line for system 1 intersects the equilibrium line for system 2 represents a situation where the pressure and the temperature conditions of hydrate formation are identical for both systems. At this point, the change in Gibbs free energy for the phase change can be written for each system as:

$$\Delta G = \Delta H - T\,\Delta S = 0 \qquad (3)$$

which leads to the equality:

$$\Delta H_1 - T\,\Delta S_1 = \Delta H_2 - T\,\Delta S_2 \qquad (4)$$

so that if ΔH_1 is greater than ΔH_2, then ΔS_2 must be less than ΔS_1. However, since hydration is a crystallization process (negative entropy change), the magnitude of S_2 (total entropy change) is greater than the magnitude of S_1. Rewritten:

$$S_1^H - S_1^I > S_2^H - S_2^I \qquad (5)$$

where: S_i^H = entropy of hydrated state

S_i^I = entropy of initial state

Because the temperature and pressure are fixed, either the entropy of initial states or the entropy of the final, hydrated, states must be different for the inequality in equation (5) to be obeyed. If we assume that the initial entropies are similar, for the inequality in equation 5 to hold, the entropy of the hydrated state in system 2 must be less than the hydrated state in system 1.

The initial state in system 1 is gas and water while the initial state of system 2 is gas, water, and adsorption agent. The initial entropies can be written as:

$$S_1^I = S_{gas} + S_{water} \tag{6}$$

$$S_2^I = S_{gas} + S_{water} + S_{adsorber} \tag{7}$$

Since the adsorbing compound is either a clay, such as bentonite, or a macromolecule, such as PHPA polymer, the entropy of system 2 should be similar to that of system 1. It is not unreasonable to assume that the entropy of system 2 may even be less than that of system 1, due to the additional stability from adsorption agent.

If the initial entropies are similar, the final entropies must obey the inequality:

$$S_1^H > S_2^H \tag{8}$$

which suggests that the hydrated structures are different.

The physical mechanism does predict a hydrated structure in system 2 which is different from the hydrated structure of system 1. The mechanism suggests that hydrates in system 2 form in the layers of adsorbed water molecules then remain attached to the adsorbing compound.

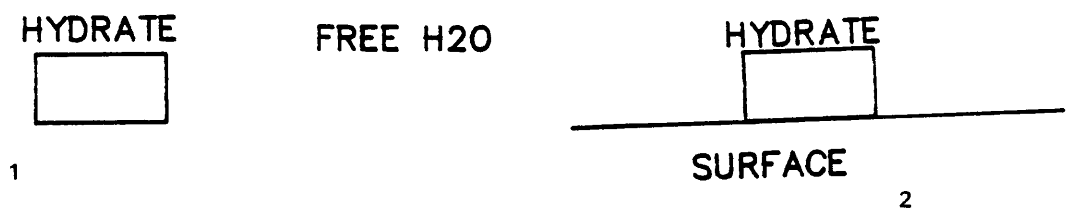

The hydrates in system 2 would have significantly reduced translational and rotational freedom. This would result in a possible reduction of entropy in the adsorbed hydrate which would satisfy the inequality of equation 8. If we extend this analysis further, a possible mechanism for the enthalpy change also arises. Because the hydrates in system 2 are forming from the adsorbed water, the creation of this transitional species should also be included as a reaction step.

Consider the hydration reaction for system 1:

$$\text{water} + \text{gas} \longrightarrow \text{hydrate}$$

now consider the hydration reaction for system 2:

$$\text{water} + \text{gas} + \underset{\text{compound}}{\text{adsorbing}} \longrightarrow \underset{\text{water}}{\text{adsorbed}} + \text{gas} \longrightarrow \underset{\text{hydrate}}{\text{adsorbed}}$$

so that now ΔH_2 is a combination of the heat of adsorption and the heat of hydration. Because both the heat of adsorption and the heat of hydration are always negative, ΔH_2 should always be greater in magnitude than the enthalpy for just hydration, ΔH_1. This was observed experimentally.

This analysis indicates that the proposed physical mechanism for thermodynamic promotion of natural gas hydrates is consistent with both the experimental observations and the laws of thermodynamics.

An interesting result which arises from the existence of thermodynamically promoted gas hydrates is the possibility of promoting the formation point of ice. Gas hydrates are similar in nature to ice, both representing solid states of water, therefore, both ice and gas hydrates may respond similarly to compounds which disrupt the phase equilibria of water. For example, the effect an inhibitor, such as NaCl, has on the formation point of hydrates will be very similar to the effect it will have on the freezing point of water. If this relationship is to hold, then compounds which increase the formation temperature of gas hydrates should also increase the freezing point of water, a phenomena of extremely important consequences which has never been observed. Future work should examine this possibility. If future work determines that the relationship between hydrates and ice is very strong, it may be possible to determine how a compound will affect hydrate equilibria by examining how the compound affects the freezing point of water, a much easier experimental study.

In summary, this work identified the effect of certain water-based drilling mud compounds on hydrate formation in drilling muds. The results were somewhat relative and may not be applicable to systems dissimilar to the one studied by this work. The results cannot give absolute quantification of the hydrate/drilling mud/gas equilibrium conditions. For this type of result, a more realistic drilling mud should be examined. A physical model of hydrate formation in systems where significant water adsorption is present was also proposed. The model seemed consistent with experimental results and the laws of thermodynamics.

Chapter 6

CONCLUSIONS AND RECOMMENDATIONS

6.1 Conclusions

The experimental results along with both the statistical and conventional analysis have led to the following conclusions:

1. Major thermodynamic promoters are:
   - (a) Bent/thinner/caustic
   - (b) Polymer B
   - (c) Polymer B + Bentonite or Barite

2. Major thermodynamic inhibitors are:
   - (a) NaCl
   - (b) MEOH
   - (c) Polymer A
   - (d) LVT Oil
   - (e) Polymer A + Oil
   - (f) Polymer A + Oil + Barite

3. Major kinetic promoters are:
   - (a) Bentonite/thinner/caustic
   - (b) Barite
   - (c) Drill Solids
   - (d) Bentonite/thinner/caustic + Polymer B

4. Major kinetic inhibitors are:

   (a) NaCl

   (b) Polymer A + Oil + Barite

5. Within the experimental conditions, hydrates could not be formed with fluids which contained Polymer A + Oil + Barite

6. Mixture effects are present and seem to be more important at low pressures.

7. The limitation of the statistical model is that the model neglects the presence of mixture effects.

8. The screening procedure identified water, Bent /thinner/caustic, and NaCl as only statistically significant components.

9. The results are valid only within experimental pressure, (200-1500 psi) and should not be extrapolated to higher pressures.

10. The physical mechanism of thermodynamic promotion was hypothesized to be the result of ordered adsorption of water molecules

10. (cont.) onto some surface. This hypothesis was found be consistent with experimental data and the laws of thermodynamics.

11. Kinetic promotion was hypothesized to be caused by surface nucleation effects. Surface nulceation was found to have no affect on the thermodynamics of hydrate formation. The presence of ordered adsorption was found to have little affect on the kinetics of formation.

6.2 RECOMMENDATIONS

Future studies into this area should deal mainly with:

1. Investigation of freezing point promotion.

2. Extending the results to higher pressures.

3. Closer examination of important components and mixtures.

4. Experimentation with more realistic test fluids.

5. Experimentation with different adsorbing compounds

Reference Cited

Barker, J.W., Gomez, R.K., "Formation of Hydrates During Deepwater Drilling Operations," SPE/IADC Drilling Conference, New Orleans LA., (1987).

Bechtold, I.C., Chem. & Met. Eng, 49-5, 136, (1942).

Bily, C., Dick, J.W., "Naturally Occurring Gas Hydrates in the McKenzie Delta, N.W.T.",Bulletin of Canadian Petroleum Geology, 22, 340-352, (1974).

Carson, D.B., Katz, D., Trans. AIME, 146, 150, (1942).

Claussen, W.F., "Suggested Structures of Water in Inert Gas Hydrates," J. Physical Chem., 19, 259-260, (1951)

Claussen, W.F., "A Second Water Structure for Inert Gas Hydrates," J.Physical Chem., 19, 1425-1426, (1951)

Davidson, D.W., "C;athrate Hydrates," in Water: A Comprehensive Treatise, Vol. 2, ed. F. Franks, Plenum Press, New York, (1973).

Davidson, D.W., Handa, Y.P., Ratcliffe, C.I., Tse, J.S., and Powell, B.M., "The Ability of Small Molecules to Form Clathrate Hydrate Structures of Structure II," NRCC No. 23110, NRC of Canada, Ottawa, Canada, (1984).

De Forcrand, Compt. Rend., 133, 1304, (1902)

De Forcrand, Compt. Rend., 181, 15, (1925)

Deaton, W.M., Frost, E.M., "Gas Hydrates and Their Relation to the Operation of Natural Gas Pipelines," U.S. Bureau of Mines Monograph 8, (1946)

Gray, G., Darcy, H.C., Composition and Properties of Oil Well Drilling Fluids, Gulf Publishing, Houston, TX., (1980)

Giussani, A., "Inhibition of Natural Gas Hydrates," M.S. Thesis, Colorado School of Mines, (1981).

Hammerschmidt, E.G., "Formation of Gas Hydrates in Natural Gas Transmission Lines," Ind. and Eng. Chem., 26, 851-855, (1934).

Holder, G.D., Grigoriou, G.C., "Hydrate Dissociation Pressure of Methane/Ethane/Water," J. Chem. Thermo., 12, 1093, (1980)

Holder, G.D., Sloan, E.D., Malekar, S.T., "Determination of Hydrate Thermodynamic Reference Properties from Experimental Hydrate Decomposition Data," Ind. Chem. Eng. Fund., 23, 123, (1984).

Hess, J., Personal Communication to Author, (1987).

Jefferey, G.A., McMullen, R.R., Progr. Inorg. Chem., 8, 43, (1967).

Jones, R.D., Sherman, J., "Controlling Hydrates in Deep Water," Offshore, 6, 27, (1986).

Kamath, V.A., Holder G.D., "The Hydrates of Propane/ n-Butane, Propane/Trans-2-Butene, Propane/Isobutane, cis-2-Butene, and trans-2-Butene Below the Ice Point," AICHE National Meeting, Los Angeles, Ca., (1982).

Katz, D.L., Trans. AIME, 160,140, (1945).

Katz, D., "Depths to Which Frozen Gas Fields (Gas Hydrates) May Be Expected," J. Petroleum Tech., 419-423, (1971).

Katz, D., "Depths to Which Frozen Gas Fields May Be Expected-Footnotes," J. Petroleum Tech., 557-558 (1972).

Kobayashi, R., Saito, S., Marshall, D.R., AICHE J., 10, 202, (1964).

Kobayashi, R., Ind. Eng. Chem. Fund., 5, 346, (1966).

Makogon, Y., Hydrates of Natural Gas, Penwell Publishing Comp., Tulsa, Ok., (1981)

Malachosky, E., "Status Report: Oil Field Copolymers, " Pet. Eng., 5, 48, (1987).

Malachosky, E., Personal Communication to Dr. E.D. Sloan, (1988).

Marshall, D.R., Saito, S., Kobayashi, R., "Hydrates at High Pressures: Part 1. Methane/Water, Argon/Water/ and Nitrogen/Water Systems," J. AICHE, 10, 202-205, (1964).

Menten, P., Parrish, W., Sloan, E.D., "Effects of Inhibitors on Hydrate Formation," Ind. Chem. Eng., 20, 399-401, (1981).

McKoy, V., Sinanoglu, O., "Theory of Dissociation Pressure of Some Gas Hydrates," J. Chem. Physics, 38, 2946-2955, (1963).

Mitchell, T.J., "An Algorithm for the Construction of D-optimal Experimental Designs," Technometrics, 16-2, 203-211, (1974)

Ng., H.J., Robinson, D.B., "The Measurement and Prediction of Hydrate Formation in Liquid Hydrocarbon-Water Systems," Ind. Emg. Chem Fund., 15-4, 293-298, (1976).

Ng, H.J., Robinson, D.B., "The Prediction of Hydrate Formation in Condensed Systems," J. AICHE, 22-4, 477-482, (1977).

Ng, H.J., Robinson, D.B., "The Measurement and Predicition of the Formation and Inhibition of Hydrates in Hydrocarbon Systems," GPA Convention, Denver, CO., (1981).

Parrish, W., Prausnitz, J.M., "Dissociation Pressures of Gas Hydrates Formed by Gas Mixtures," Ind. Eng. Chem., 11, 26-34, (1972).

Ripmeester, J., Tse, J., Ratcliffe, C., Powell, B., "A New Clathrate Hydrate Structure," Nature, 325, 135-136, (1987).

Robinson, D.B., "Vapor Liquid Equilibrium and Condensing Curves in the Vinicity of the Critical Point for a Typical Gas Condensate," GPA Report RR-96, (1986).

Selim, M.S., Sloan, E.D., "Modeling of the Dissociation of an In-situ Hydrate," SPE Regional Meeting, Bakersfield, CA., (1985).

Stoll, R.D., Bryan, G.M., "Physical Properties of Sediments Containing Gas Hydrates," J. Geoph. Res., 84, 1629-1634, (1979).

van der Waals, J.H., Platteeuw, J.C., "Clathrate Solutions," Adv. in Chem. Phys., 2, 1-57, (1959).

van Oplhen, H., Clay Colloid Chemistry: For Clay Technologists, Geologists, and Soil Scientist, John Wily & Sons, New York, N.Y., (1974).

Villard, Compt. Rend., 106, 1602, (1887).

Villard, Compt. Rend., 107, 395, (1888)

Villard, Compt. Rend., 111, 302-305, (1890)

Von Stackelberg, M., Muller, H.R., "On the Structure of Gas Hydrates," J. Phys. Chem., 19, 1319-1320, (1951).

Von Stackelberg, M., Muller, H.R., "Feste Gas Hydrate II. Struktur und Raumchemie," Z. Elektrochem., 58, 25, (1954).

Wheeler, R.E., "Efficient Experimental Design," Annual Meeting, ASA, (1972).

Wheeler, R.E., ECHIP Course Text, Expert In A Chip Inc., Hockessin, DE, (1986).

Wilcox, W.I., Carson, D.B., Katz, D.L., "Natural Gas Hydrates," Ind. Eng. Chem., 33, 662-665, (1941).

Wynn, H.P., "The Sequential Generation of D-Optimum Experimental Designs," Ann. Math. Statist., 1655-1664, (1970).

Appendix A

STATISTICAL SCREENING PROGRAM

A1. Background

The major goal of this research was to determine how the components of a water-based drilling mud can effect the formation of natural gas hydrates. Because of the number of components (9), an extremely large number of tests were possible. A method was needed to determine which tests, or group of tests, would provide the most information while minimizing any experimental bias which may be induced when certain experiments are chosen over others. The approach chosen for this work was a statistical screening program.

The statistical screening program belongs to an experimental philosophy known as systematic experimentation. The focus of systematic experimentation is to provide the most efficient path between experimental limitations and goals. An efficient path is a collection of tests which will satisfy the experimental limitations and goals while maintaining an unbiased atmosphere so that results will not be tainted with any preconceived ideas of the investigator. For this investigation, the main limitation was the number of tests, which had to be kept to a minimum.

The statistical screening program consists a 5 step cycle shown in Figure A1.

In such an analysis, the first step is to decide which variables and responses best characterize the experimental system. That is, if the system could be thought of as an equation, Y=F(x's), what would be the Y, the dependent variable and what would be the X's, the independent variables. For this investigation, the variables are the individual water-based mud components while the response is the temperature that hydrates will form within the system.

Independent Variables (X's)	Dependent Variable (Y)
X1 = Bentonite/thinner/caustic	Y1 = Hydrate Formation Temperature
X2 = Barite	
X3 = NaCl	
X4 = Polymer A	
X5 = Polymer B	
X6 = LVT Oil	
X7 = Drill Solids	
X8 = MEOH	
X9 = Water	

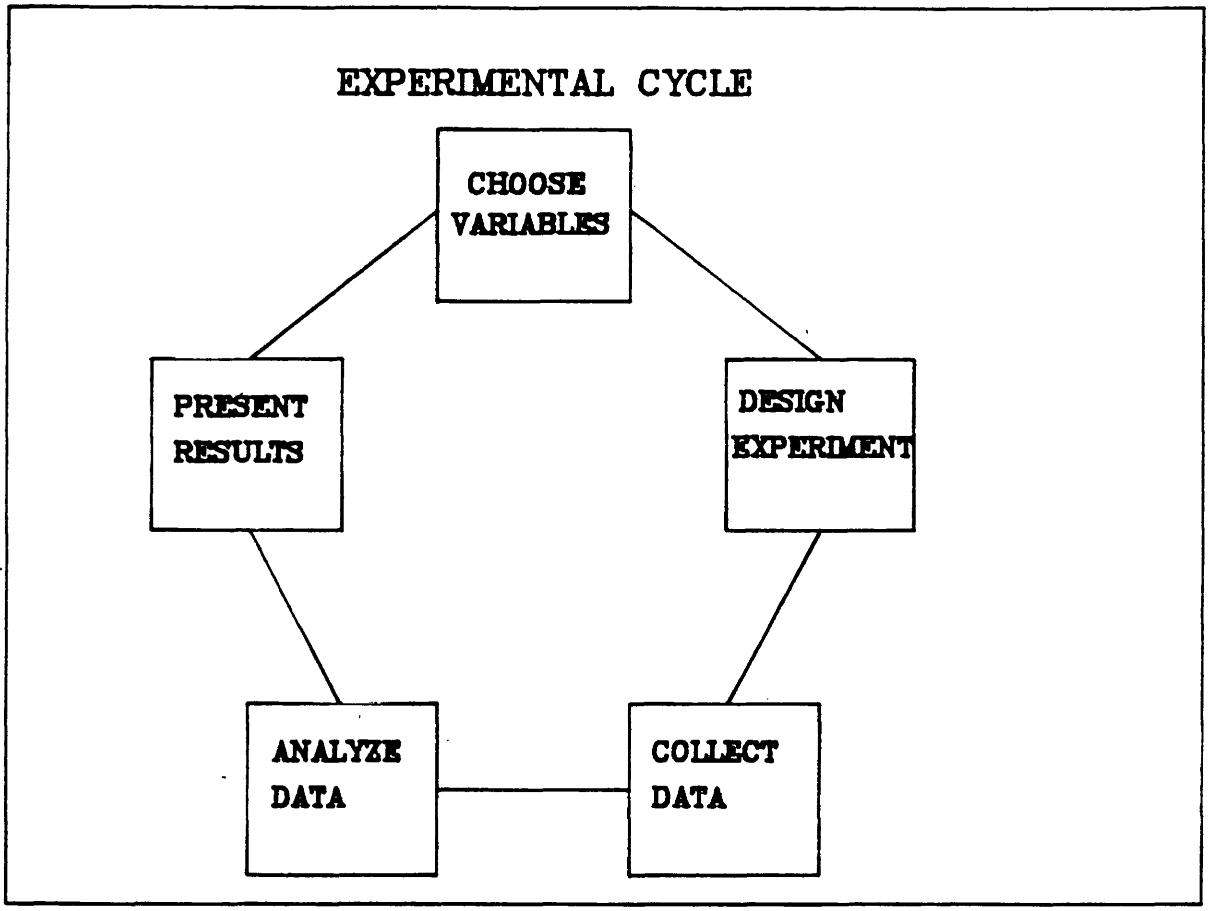

FIGURE A1 STATISTICAL EXPERIMENTATION CYCLE

The system is modeled as:

$$\frac{\text{Hydrate Formation}}{\text{Temperature}} = F(\text{ X1, X2, X3, ...X9})$$

The range of each component is measured in volume percent and varies from zero (except water), up to the concentration of each component in the mock drilling fluid. These values are shown in Table 5.

The next step is to design a batch of tests which will provide the maximum knowledge for the fewest number of tests. This requires that two important decisions be made:

1. How should the system be modeled ?

2. How many tests can be done ?

Since the purpose of this work was to determine the effect of <u>individual</u> components, a linear model was chosen for the test scheme. A linear model is of the form:

$$Y = C1\ X1 + C2\ X2 + \ldots..C9\ X9$$

Where C_i = constant

A linear model assumes that the behavior of each compound is independent of all other compounds and that there are no interactive, or mixture, effects present. The model will provide some indication of the importance of mixture effects, but cannot identify specific interactions. Therefore, this test scheme will 'screen' individual components for their independent effects.

The next decision regards the size of the system. As a general rule, the more experiments performed, the better the results. However, in the real world, there are limits, both time-wise and financial, which limit the amount of work that can be done. A balance must be struck between the number of tests necessary to obtain reasonably accurate results and the number of tests realistically possible. For a linear model with 9 variables. at least 9 tests are required and 3N+1, or 28 tests most desirable (Hess, 1987). However, the number of desirable tests can be pared by increasing the boldness of the scheme. Boldness refers to the degree to which variable is changed, or 'tweaked', during the experimentation. The greater the boldness of the experiments, the less subtle the responses, and therefore, the fewer the tests necessary. Since this investigation was an initial screening effort, the decision was made to be as bold as possible. That is, the value of the variable will be either the maximum possible or the minimum possible, which would be zero for all components except water. The concentration of water was adjusted so that regardless of the concentration of all other variables, the total volume percent would always add up to 100%. As a result, 17 tests, including one with just water, were decided upon as reasonable.

Once the model type and number of tests were fixed, the actual experimental design was computer generated, using a program called 'ECHIP'. The program follows a four step process:

1. Initial design
2. Efficiency check
3. Application of the Wynn algorithm
4. Application of the Exchange algorithm.

Each step is explained and discussed below.

Initial Design: An initial design is generated by ECHIP using the nullification (Wheeler, 1972) algorithm but will give priority to trials from an old design if one exists. The initial design must have at least k trials for a k term model.

Efficiency Check: Next, all trials of an old design are incorporated into the design and the G-efficiency of the resulting design is evaluated over all candidate trials. The G-efficiency is defined as the ratio of k, the number of terms in the model, to the largest variance, or standard deviation, of a given design. The list of candidate trials comprises all trials in the grid generated for all levels of all variables.

Application of the Wynn Algorithm: The Wynn algorithm is used to add trials up to n, the number specified. The idea behind the Wynn algorithm is to create candidate trials, calculate the standard deviation of the value predicted by the model for each trial, and pick the trials with the largest standard deviation as the trials to include in the design (Wynn, 1970).

Application of the Exchange Algorithm: Once the number of desired tests is reached, an exchange algorithm is used to exchange trials in the initial design with those outside it (from the Wynn algorithm). The algorithm first exchanges single trials until the G-efficiency no longer increases, then exchanges pairs of trials, etc. up to the maximum exchange length (Mitchell, 1974).

The experimental design was optimized by checking the resulting design for undesirable tests then redesigning the program with only the desired tests. This may give the indication that the test program was biased since certain tests were eliminated, however, this is not the case. Each time an old design was edited, the resulting new design was an unbiased collection of tests which happen to include the desired ones. The final design is shown in Table A1.

After the data has been collected, linear regression is used to analyze the data. This procedure is discussed in the statistical results section.

TABLE A1

RESULTING TEST FLUIDS
FOR SCREENING PROGRAM IN VOL%

TRIAL NO.	BENT/THIN/CAUS	BARTIE	SALT	POLYMER A	POLYMER B	OIL	DRILL SOLID	MEOH	WATER
1	0	0	0	0	0	0	0	0	100.0
7	1.6	10.2	0	0	0	0	2.3	10.0	75.9
15	1.6	10.2	0	0	0	10.0	2.3	10.0	65.9
4	0	10.2	5.0	0.2	0.2	0	2.3	0	82.1
14	0	0	0	0.2	0.2	10.0	0	10.0	79.6
2	1.6	0	5.0	0.2	0.2	0	2.3	10.0	80.7
5	1.6	10.2	5.0	0.2	0	10.0	0	0	73.0
6	1.6	10.2	5.0	0	0.2	10.0	0	0	73.2
12	0	10.2	5.0	0	0.2	10.0	0	10.0	64.6
10	1.6	0	5.0	0.2	0	0	0	10.0	83.2
13	1.6	0	0	0	0.2	0	2.3	0	95.9
16	0	0	5.0	0	0	0	0	0	95.0
8	0	10.2	0	0.2	0.2	0	0	10.0	79.4
11	0	10.2	0	0.2	0	10.0	2.3	0	77.3
3	1.6	0	0	0.2	0.2	10.0	0	0	88.0
7	1.6	0	5.0	0.2	0.2	10.0	2.3	0	80.7
9	0	0	5.0	0	0	10.0	2.3	10.0	72.7

Compositions given in volume %

A2. STATISTICAL RESULTS

The statistical analysis was done by linear regression of the data shown in Table A2. Table A2 represents the hydrate equilibrium temperature deviation from pure water equilibrium temperatures at 400, 600, 800, 1000, and 1200 psia. The values were obtained by subtracting the test fluid equilibrium temperature from a water baseline value, resulting in a positive sign (+) for inhibition and a negative sign (-) for promotion of formation temperatures. This in turn will affect the coefficients of the linear regression resulting in a positive (+) coefficient for an inhibitor and a negative (-) coefficient for a promoter.

The deviations were not calculated from raw experimental values but from best fit expressions of the experimental values. The best fit isobaric values are shown in Table A3 and the best fit expression are shown in Table A4. The best fit procedure was done so that data along isobars could be used which would eliminate pressure as a variable. Table A5 provides a comparison of the raw experimental data against fitted values, along with a percent difference.

The response data (temperature deviations) were correlated and the model analyzed using MINITAB statistical

TABLE A2

EQUILIBRIUM TEMPERATURE DEVIATIONS FROM A WATER BASELINE

MUD	400 PSI	600 PSI	800 PSI	1000 PSI	1200 PSI
7	1.08	1.61	2.01	2.32	2.58
15	4.87	6.60	7.88	8.89	9.73
14	3.11	3.47	3.73	3.94	4.11
2	20.04	19.62	19.31	19.06	18.85
6	8.00	10.32	12.01	13.35	14.70
10	13.06	13.65	14.08	14.42	14.70
13	-6.03	-3.33	-1.36	0.20	1.50
16	9.02	8.63	8.35	8.12	7.92
8	-1.52	1.29	3.34	4.97	6.32
3	1.36	0.72	0.25	-0.12	-0.44
17	9.05	10.93	12.30	13.39	14.30
9	>30	>30	>30	>30	31.07
4	>30	>30	>30	>30	>30
5	>30	>30	>30	>30	>30
12	>30	>30	>30	>30	>30
11	>30	>30	>30	>30	>30

TABLE A3

BEST FIT FORMATION TEMPERATURES

MUD	400 PSI	600 PSI	800 PSI	1000 PSI	1200 PSI
7	57.10	62.32	66.09	69.05	71.49
15	57.31	57.33	60.22	62.48	64.35
14	55.07	60.47	64.36	67.43	69.96
2	38.14	44.31	48.79	52.61	55.23
6	50.18	53.62	56.09	58.02	59.60
10	45.126	50.29	54.02	56.95	59.37
13	64.21	67.27	69.46	71.17	72.57
16	49.16	55.30	59.75	63.25	66.15
8	59.71	62.65	64.75	66.40	67.75
3	56.82	63.21	67.84	71.49	74.51
17	49.14	53.01	55.79	57.97	59.77
9	DNF	DNF	DNF	DNF	43.00
4	DNF	DNF	DNF	DNF	DNF
5	DNF	DNF	DNF	DNF	DNF
12	DNF	DNF	DNF	DNF	DNF
11	DNF	DNF	DNF	DNF	DNF

TABLE A4

BEST FIT EXPRESSIONS

TEST	C1	C2
7	-20.249	46.57
15	-26.795	58.19
14	-20.134	45.08
2	-16.503	39.12
6	-30.896	66.55
10	-20.230	46.04
13	-36.683	75.97
16	-17.325	40.01
8	-37.457	78.06
3	-17.157	39.19
17	-27.344	59.70

DATA WAS BEST FIT TO THE EXPRESSION:

1/TEMPERATURE = C1*EXP (C2*PRESSURE)
(1/RANKINE) (PSI)

TABLE A5

COMPARISON OF BEST FIT AND
ACTUAL FORMATION TEMPERATURES

MUD	PRESS(PSI)	FORMATION TEMPERATURE (F) ACTUAL	BEST FIT	% DIFFERENCE
7	318	50.00	53.20	6.40
	492	58.00	58.76	1.31
	785	62.00	64.84	4.58
	1160	68.00	71.04	4.47
15	404	53.00	53.41	0.77
	880	61.00	61.18	0.30
	770	60.00	59.83	0.28
	1100	63.00	63.46	0.72
14	292	51.00	50.95	0.09
	592	60.00	60.29	0.48
	885	66.00	65.75	0.38
	1148	69.00	69.34	0.50
2	588	45.00	44.00	2.22
	904	49.00	50.71	3.49
	1112	54.00	54.00	0.01
6	596	54.00	53.56	0.82
	884	57.00	56.95	0.09
	1006	59.00	58.07	1.58
10	600	51.00	50.29	1.39
	880	54.00	55.27	2.35
	1060	58.00	57.72	0.48
13	394	64.00	64.10	0.15
	600	68.00	67.27	1.08
	800	69.00	69.46	0.66
	1030	71.00	71.39	0.55
16	385	49.00	48.59	0.84
	584	56.00	54.89	1.99
	800	58.00	59.75	3.02
	1048	65.00	63.99	1.55
8	410	60.00	59.88	0.19
	590	62.00	62.52	0.84
	790	65.00	66.29	0.43
	985	66.00	66.29	0.43
3	390	56.00	56.43	0.75
	596	63.00	63.11	0.17
	925	71.00	70.21	1.11
17	400	48.00	49.14	2.37
	644	54.00	53.69	0.57
	1000	58.00	57.97	0.04
	1310	61.00	60.64	0.59

software. A summary of model coefficients and statistics, including the standard deviation and values of the square of the correlation coefficient (R^2), at each pressure, are listed in Table A6. A good fit is indicated by a small standard deviation and a R^2 value close to 100.

Figures A2-A6 plot the actual response versus predicted values for each pressure. Response plots give some indication of how well the model fits the actual response data, with a perfect fit indicated by a 45^o line

Figures A7-A11 give an indication of the significance of each component's effect on the system by plotting the model's response at the maximum and minimum values of components range. The end points on the X-axis of Figures A7-A11 represent either the maximum or minimum concentration value. The Y-axis represents the temperature deviation response.

Compositional effects on the temperature deviation are calculated as the difference between the predicted response at the maximum value of a components range and the predicted value at the minimum value. The volume percent of

TABLE A6

LINEAR MODEL SUMMARY

	MODEL COEFFICIENTS									STATISTICS	
PRESS (PSI)	X1	X2	X3	X4	X5	X6	X7	X8	X9	S	R^2
400	-6.00	.617	3.32	36.3	-32.2	.667	3.13	.007	-.0196	7.5	67
600	-5.58	.672	3.22	33.4	-27.7	.647	3.16	.012	-.0172	6.72	71
800	-5.28	.712	3.15	31.3	-24.4	.633	3.19	.016	-.0155	6.26	74
1000	-5.04	.743	3.09	29.7	-21.8	.622	3.21	.019	-.0141	5.97	75
1200	-4.95	.752	3.07	27.7	-2.01	.632	3.30	.035	-.0126	5.85	76

WHERE: X1 = BENT/THINNER/CAUSTIC
X2 = BARITE
X3 = NaCL
X4 = POLYMER A
X5 = POLYMER B
X6 = OIL
X8 = MEOH

S = STANDARD DEVIATION

R^2 = SQUARE OF CORRELATION COEFFICIENT

X7 = DRILL SOLIDS
X9 = H2O

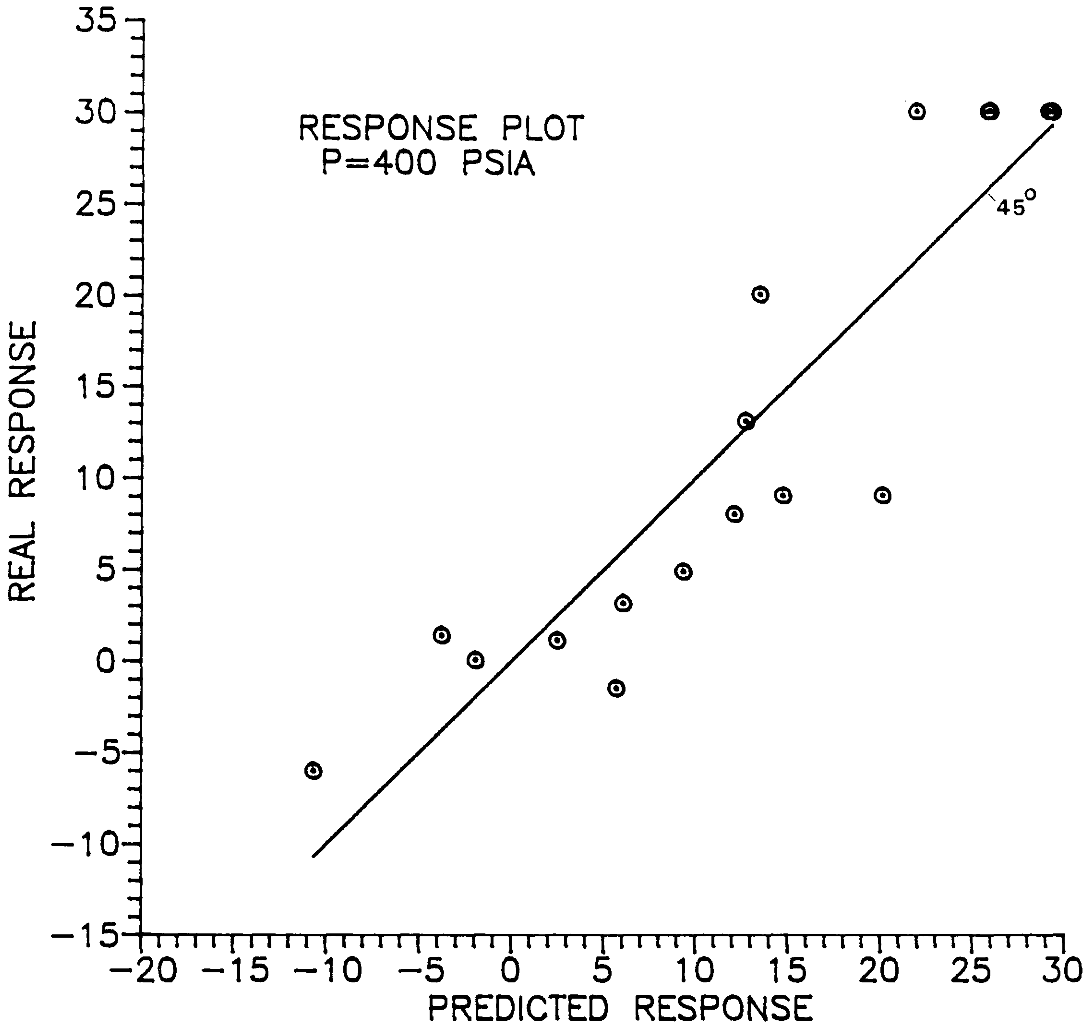

FIGURE A2 RESPONSE PLOT FOR P=400 PSIA

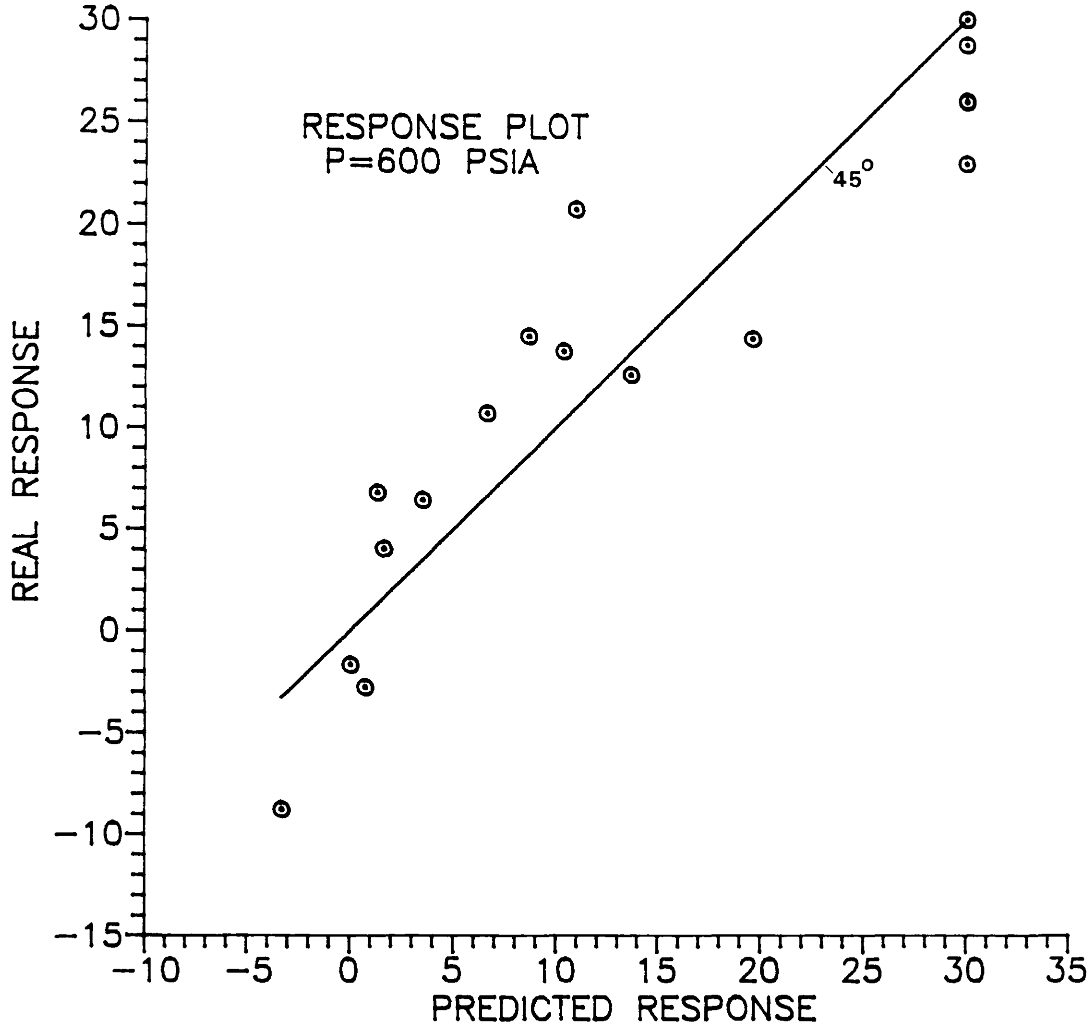

FIGURE A3 RESPONSE PLOT FOR P=600 PSIA

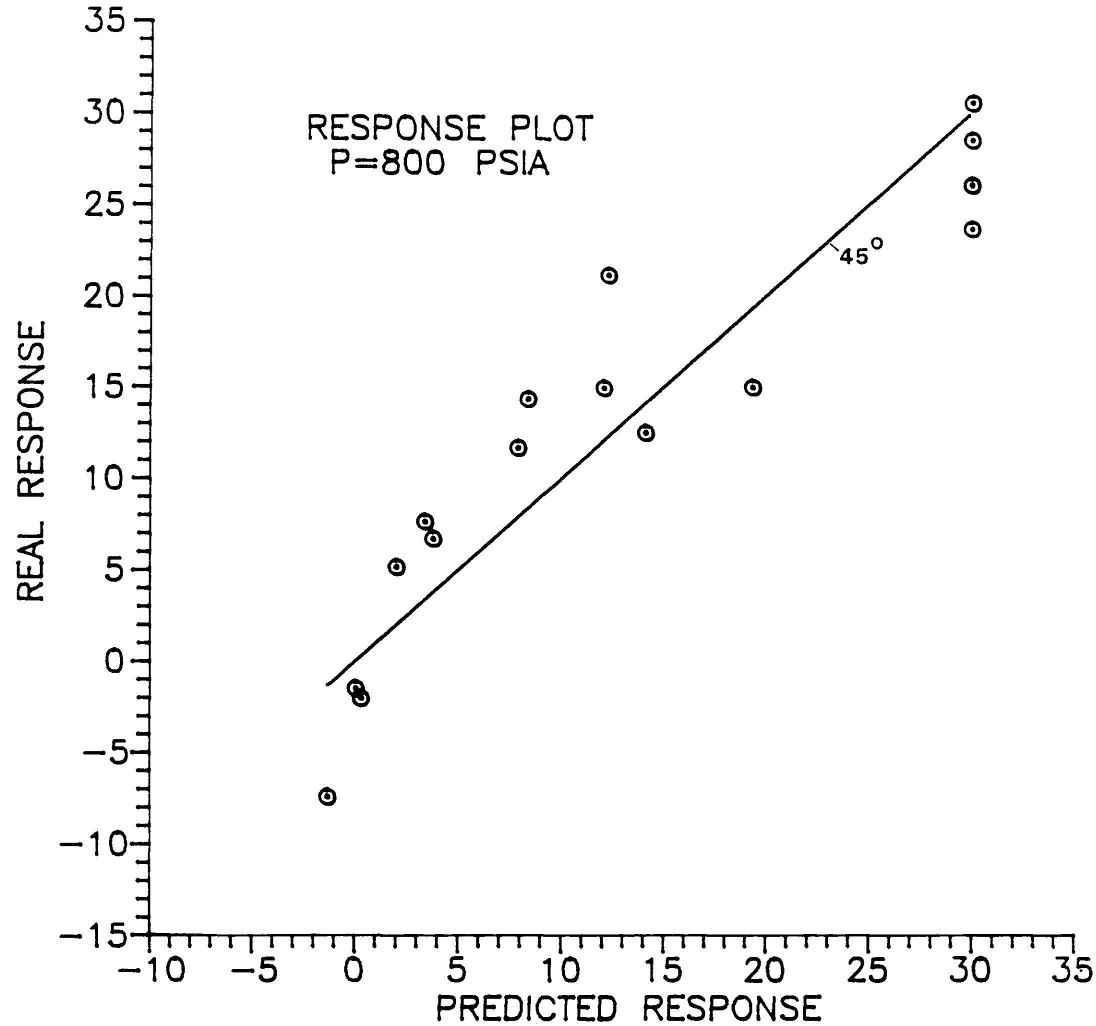

FIGURE A4 RESPONSE PLOT FOR P=800 PSIA

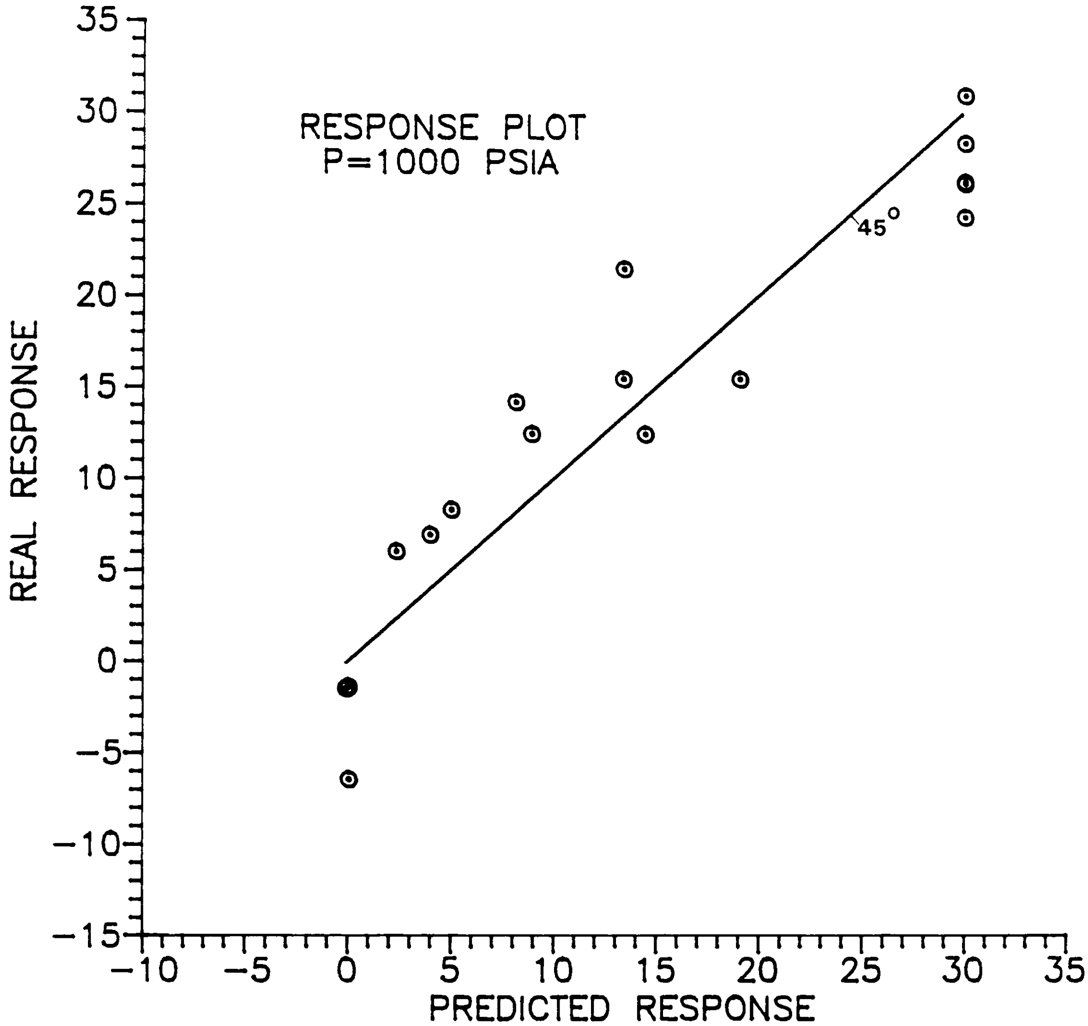

FIGURE A5 RESPONSE PLOT FOR P=1000 PSIA

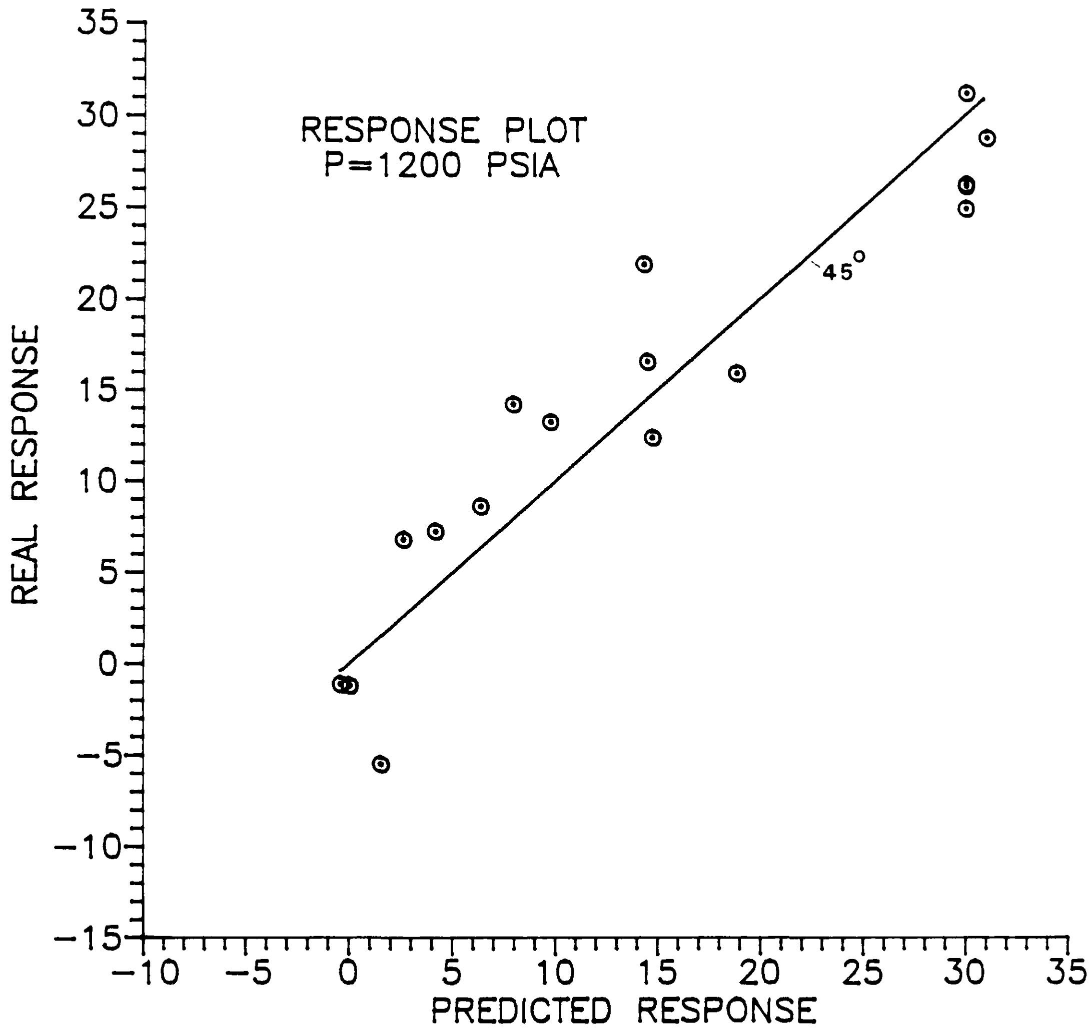

FIGURE A6 RESPONSE PLOT FOR P=1200 PSIA

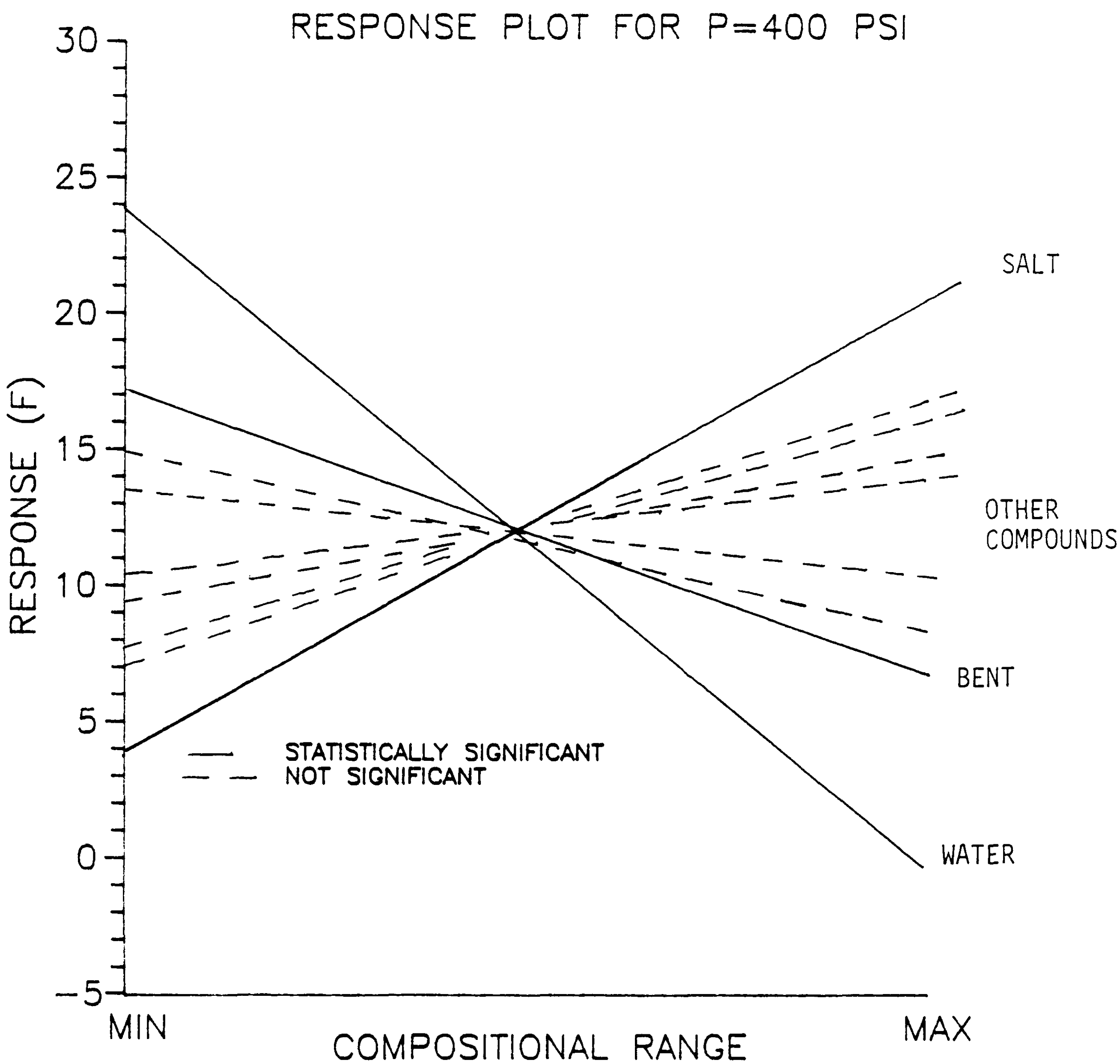

FIGURE A7 PLOT OF COMPONENT EFFECTS
P=400 PSIA

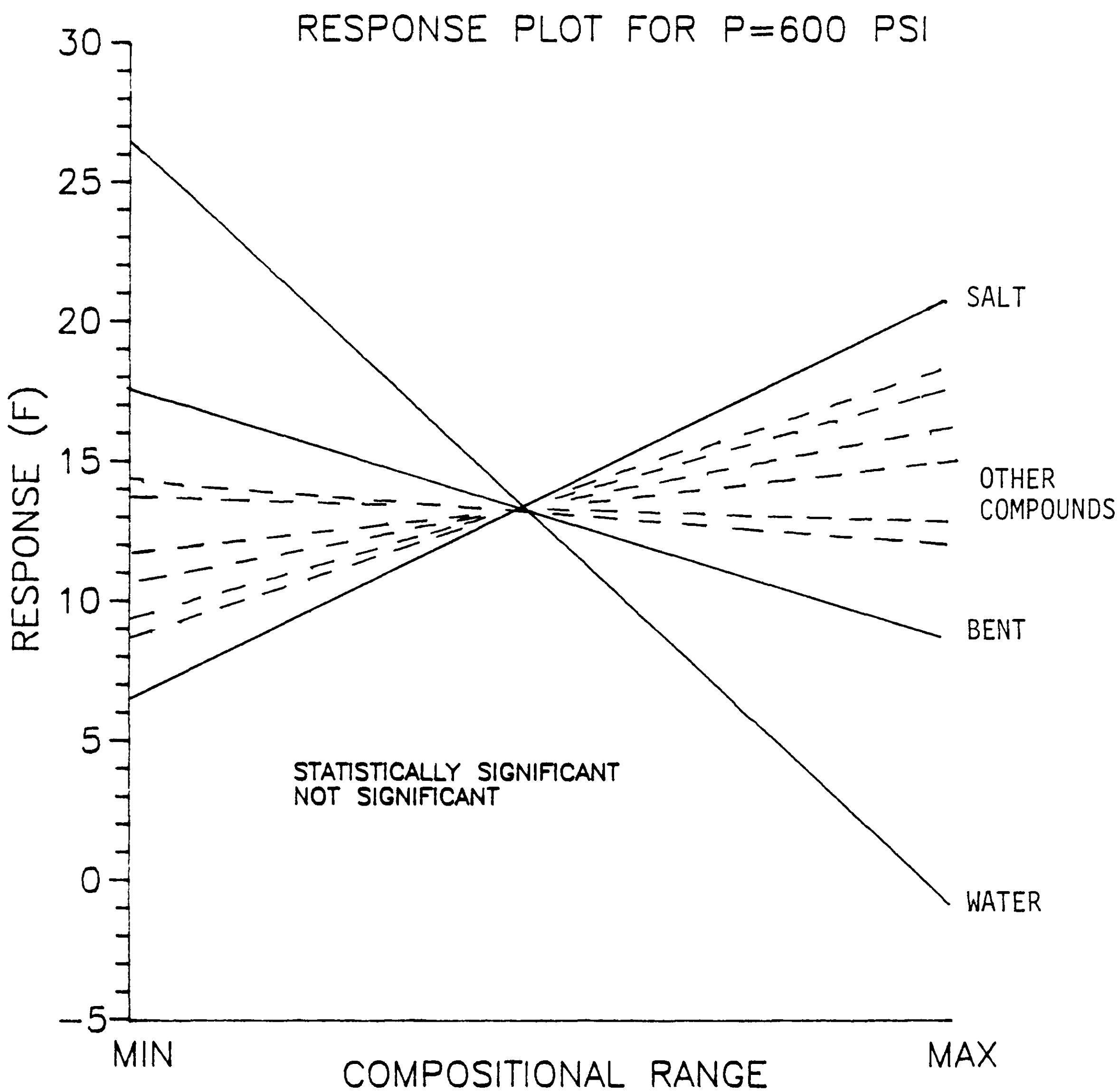

FIGURE A8 PLOT OF COMPONENT EFFECTS
P=600 PSIA

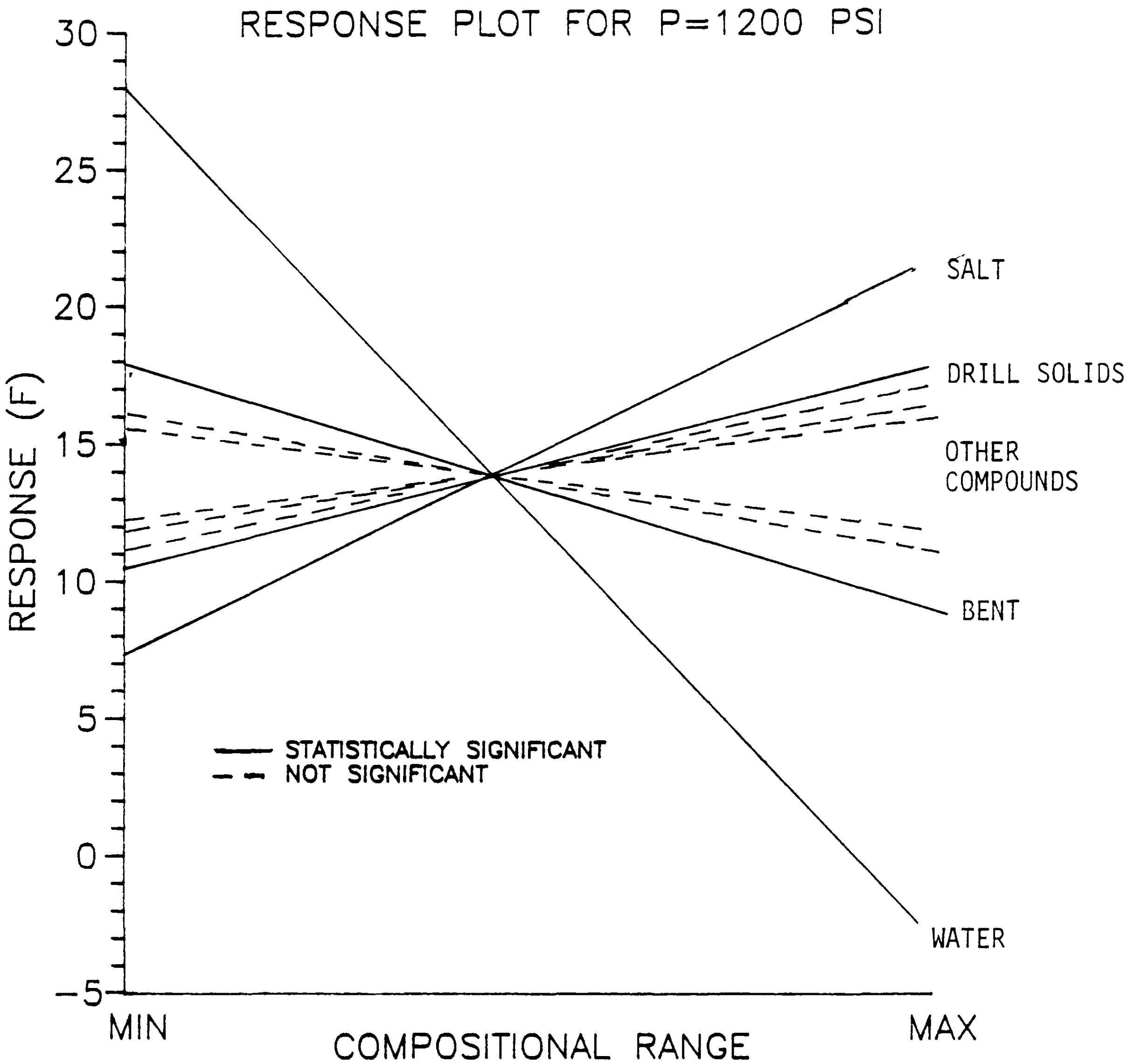

FIGURE A11 PLOT OF COMPONENT EFFECTS P=1200 PSIA

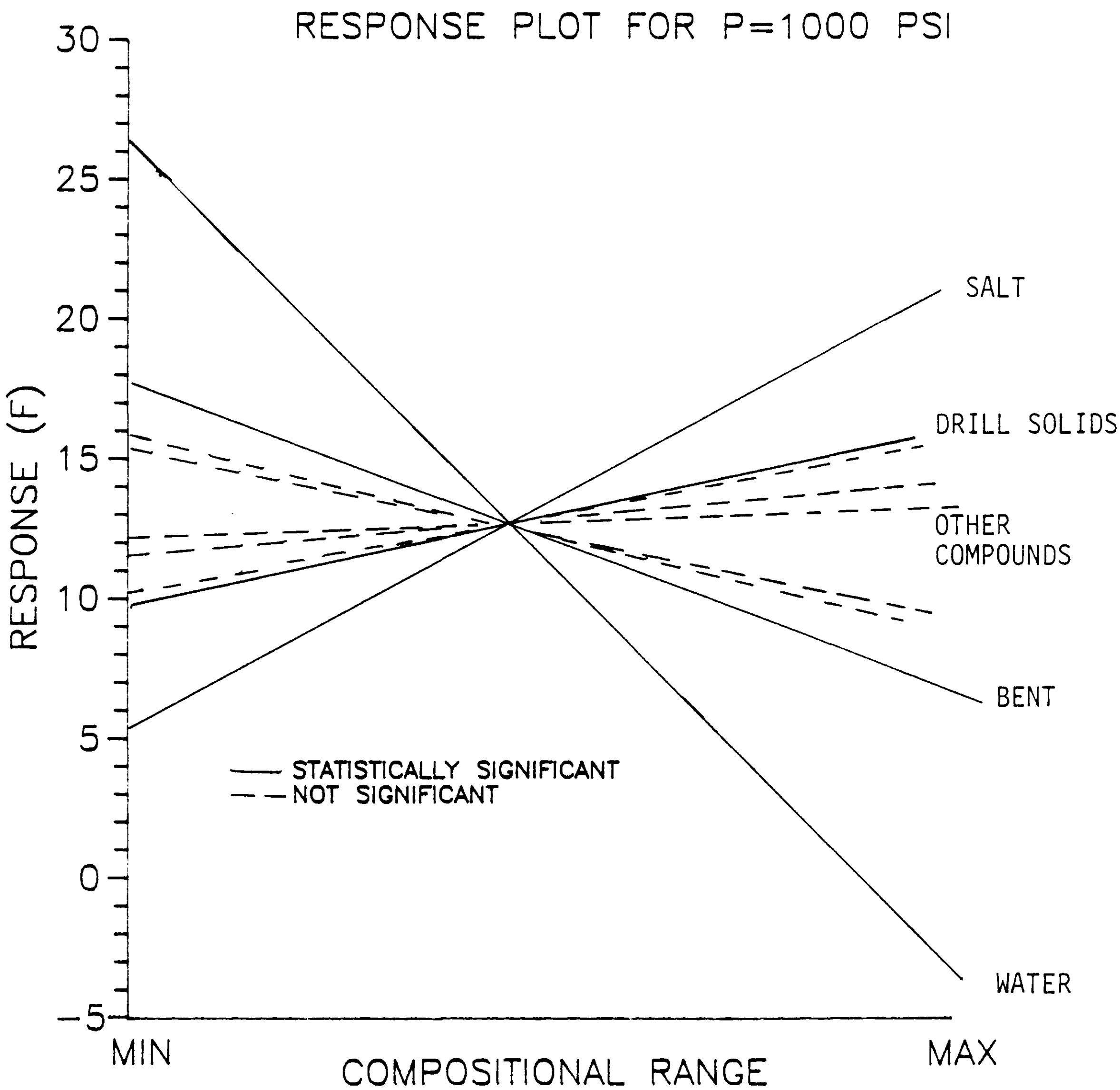

FIGURE A10 PLOT OF COMPONENT EFFECTS
P=1000 PSIA

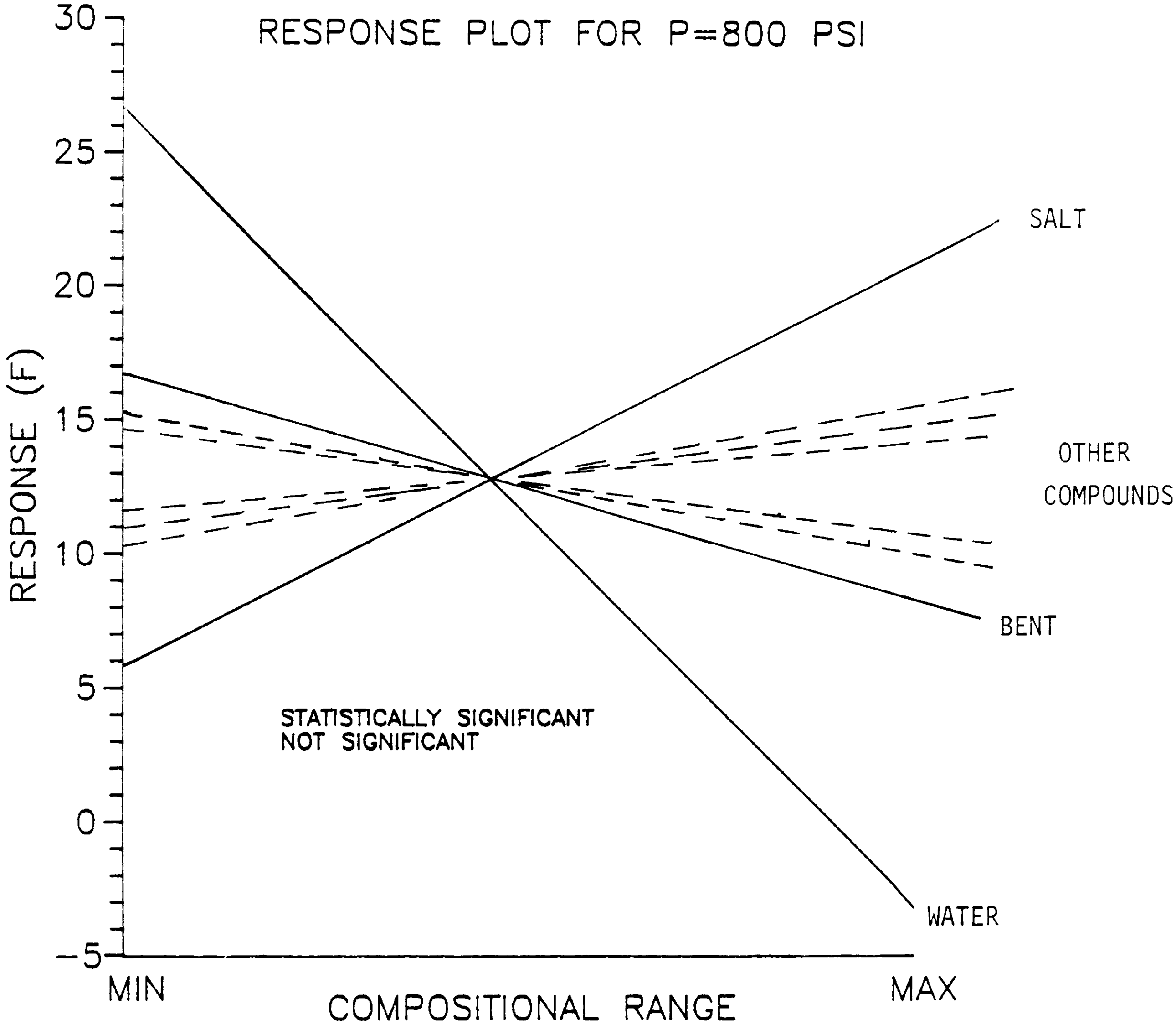

FIGURE A9 PLOT OF COMPONENT EFFECTS
P=800 PSIA

the remaining components are adjusted within their concentration range so that sum of components will still equal 100. Statistically significant effects (95% confidence) are reported and listed in Table A7. A positive effect indicates that the temperature deviation from the baseline value increases as the component increases (inhibitor), a negative effect indicates that the response decreases as the component increases (promoter).

TABLE A7

SUMMARY OF SIGNIFICANT EFFECTS

COMPONENT EFFECTS ON TEMPERATURE DEVIATION (F)

COMPONENT	400 PSI	600 PSI	800 PSI	1000 PSI	1200 PSI
H2O	-25.83	-26.63	-27.22	-27.68	-28.12
NaCL	15.81	15.21	14.77	14.42	14.27
BENT	-10.41	-9.75	-9.28	-8.89	-8.76
DRILL SOLIDS	-----	-----	-----	6.66	6.86

A3. ANALYSIS OF STATISTICAL RESULTS

The results of the statistical analysis were based upon data which consisted of deviations of formation temperatures from a baseline of pure water formation temperatures. This approach enables relative comparisons between components and minimizes systematic error from the analysis. However, the results are only valid for this system of components, and cannot be treated as absolute values.

The statistical analysis assumes a linear model of nine variables (X's) with temperature deviation as the response term.

$$\text{temp. dev.} = C1\ X1 + C2\ X2 + \ldots\ldots\ldots C9\ X9$$

The major assumption of a linear model is that there is absolutely no interaction between variables. It treats each variable as independent, so that, within an experiment, a component's effect is not dependent on the presence of other components. The model constants are fitted to the response data by means of linear regression, and the model is analyzed.

The regression analysis indicates good consistency of the response data, evident by the lack of outlier in the residuals, which are listed in the appendix . However R^2 values, which represent the square of the correlation coefficient (listed in Table A6), are somewhat low, suggesting that a linear model may not be the best. This can also be seen in the response plots, figures A2-A6, which plot actual response versus predicted response. The closer the points fall to a straight 45^o line, the better the model fit. The scatter of the data points, especially at low pressures, indicates a lack of fit. The deviations from the model are probably due to mixture effects which are ignored by the model. In a system as complex as the one for this investigation, the presence of mixture effects is not unreasonable.

The effects analysis, shown graphically in Figures A7-A11, suggests that only three components are statistically significant over the whole range of pressures. These are water, bentonite/thinner/caustic, and NaCl. Water and the bentonite group are promoters, while the NaCl is an inhibitor. Further, one component, drill solids, becomes significant at the two highest pressures. We question the statistical significance of the drill solids. Since the model does not fit well, components close to the confidence limits, like drill solids, should be suspect.

This emphasizes the major weakness of the statistical analysis. The analysis of effects are only as good as the model on which the analysis is based. If the model fits well, then the analysis is good. However, if the model does not fit well, as in this case, then confidence in the analysis is decreased.

It is important to note that there are other significant single additive effects, which are identified in the discussion of results, that the model cannot detect because of the built-in limitations.

Appendix B

COMPUTERIZED DATA ACQUISITION SYSTEM

B1. Introduction

A personal computer based data acquisition unit was designed and built. The objective of the design was to built a system capable of automatically monitoring the temperature and pressure inside the equilibrium cell at constant intervals of time. The system was also designed to store the readings into data files in order to ease data analysis.

The major constraints on the design were that it:

1. Be operational within 3 months, as project deadlines for experimental results had to be met.

2. Provide accurate results, reliable service and be easy to maintain, as the system must be able to endure continuous operation up to two weeks at a time.

3. Be cost effective, as the cost had to be held within the project limits.

The resulting design, shown in Figure B1, which satisfies these constraints consisted of: an IBM XT personal computer, a Keithly Series 500 data acquisition system, an Omega pressure transducer, and a thermistor to monitor temperature, also from Omega.

The design was built and operational less than two months after all the equipment had been obtained. The system has provided reasonable accuracy and has been quite reliable. There have not been any major break downs during nine months of heavy use.

B2. INTERFACE HARDWARE

IBM XT PC: The IBM XT personal computer is the heart of the system. It is widely used and operational information is easy to obtain. The computer has a Kaypro monochrome monitor along with a 20 MB hard disk and an Intel 8087 math coprocessor chip. The computer is also equipped with a communications card for printer interface.

Keithly Series 500: The Keithly Series 500 is a completely integrated hardware and software package. The series 500 consists of three main parts, a base system, modular additions, and a software package for easy access

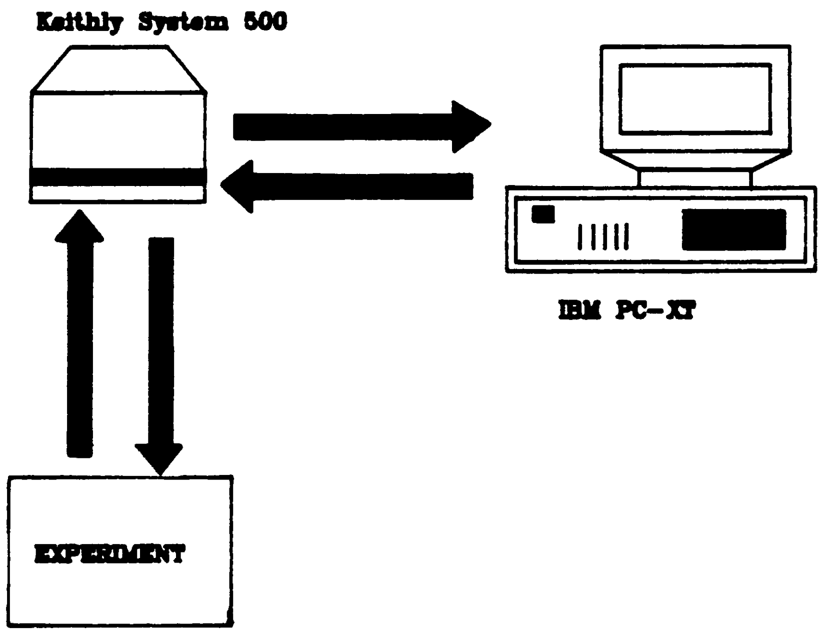

Figure B1 OVERALL SYSTEM DESIGN

to the system from a BASIC program.

The base system, shown in Figure B2, consists of a aluminum-cased card cage with a built in non-switching DC power supply and ten slots for installation of modular additions. In addition, there is an interface card which is inserted into the computer, as shown in Figure B3, which allows the personal computer to access the conditioned signals from the base system.

There are three modular additions to the base system. These are: an analog input board, an analog-to-digital board, and a digital-to-analog board.

The analog input board is an AIM 1 board, shown schematically in Figure B4. The analog input module has two important functions in the Series 500 system. It provides signal selection and conditioning for local input (from screw terminals located on the module board) and provides higher level selection and conditioning for all analog signals received by the Series 500, including signals arriving through the AIM 1 itself. Thus, all incoming analog signals must pass through two sets of signal selection and conditioning circuitry: preliminary circuitry on the card of origin and secondary circuitry on the AIM1.

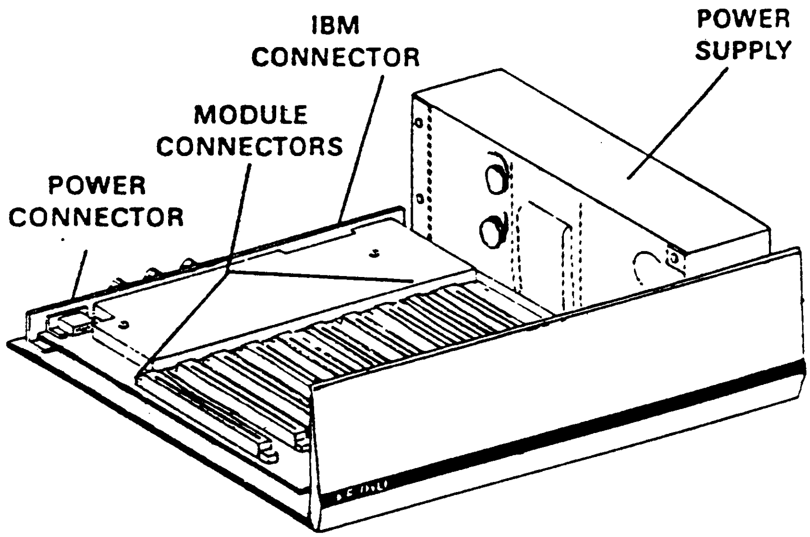

SERIES 500 Mainframe

Figure B2 S500 BASE UNIT

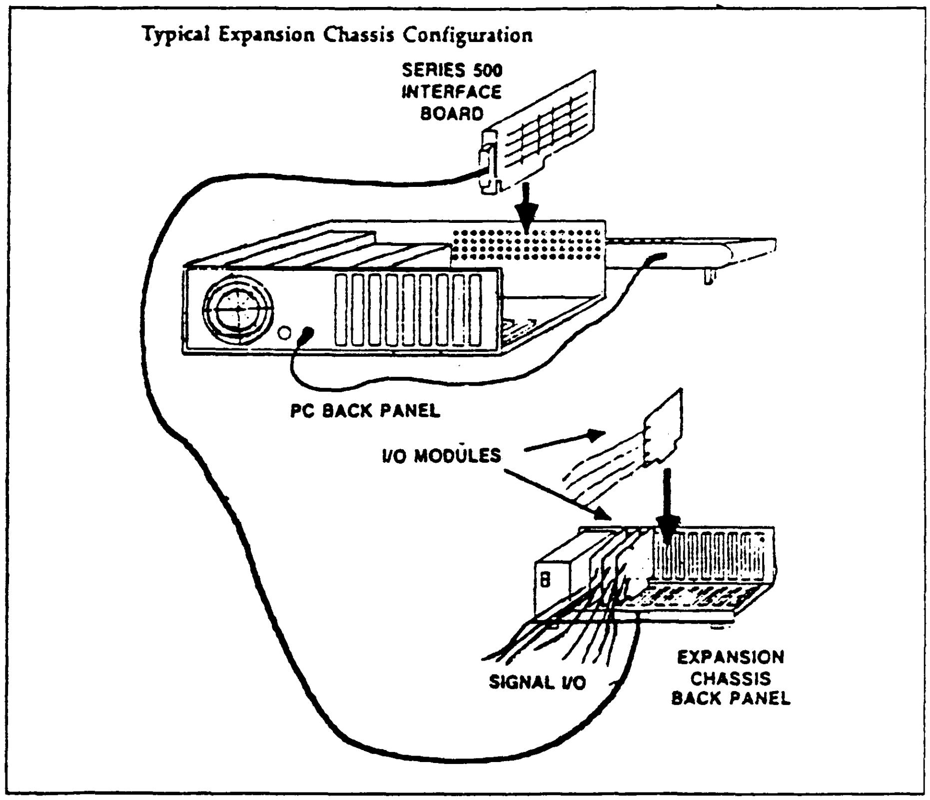

Figure B3 S500 INTERFACE CARD

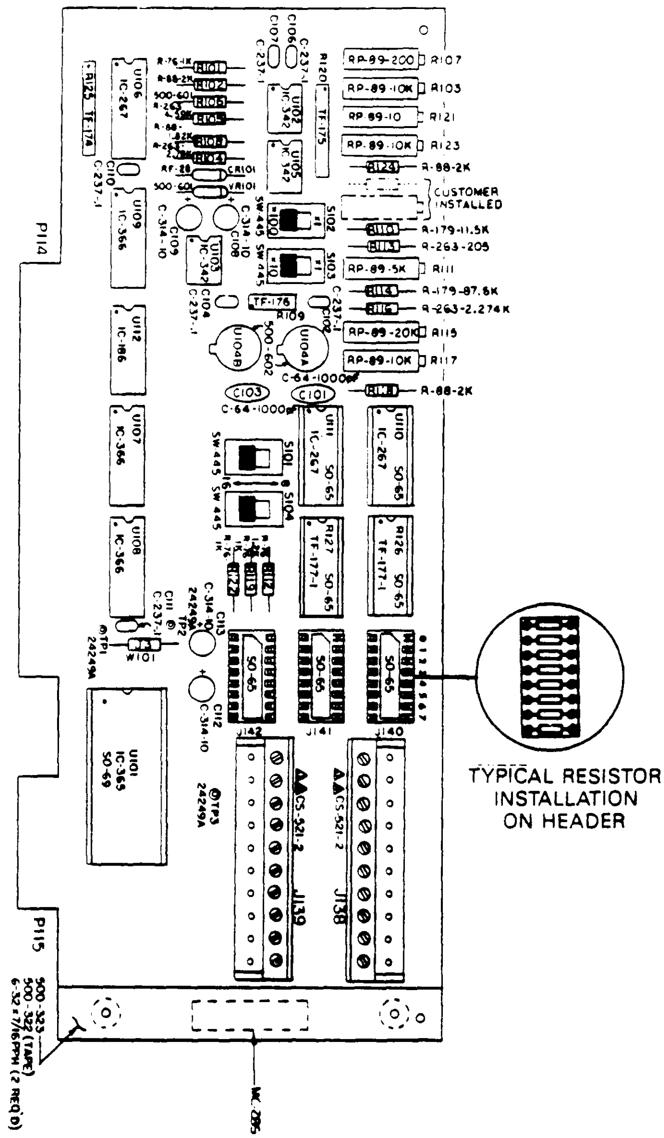

AIM1 Module Layout

Figure B4 AIM 1 DIAGRAM

The AIM1 offers 16 local channels of single-ended input or 8 channels of differential input, with switch selectable gains of x1, x10, or x100 volts/volt for the direct connection of low level analog signals. Global signal conditioning is provided by a high-speed programmable gain amplifier. The amplifier offers four software controlled gains, x1, x2, x5, and x10. All local channels are connected directly on to the on-card screw terminals. The AIM1 is necessary for all systems requiring analog input.

The analog-to-digital board is the ADM2 module, shown in Figure B5, and offers high resolution A/D conversion by means of a 14-bit successive approximation convertor designed for applications requiring high resolution. It offers a conversion time of 35 microseconds and sample-and-hold time of 4 microseconds. Analog signals are resolved across a full scale of 16,384 steps. To maximize A/D resolution, four input ranges (0 to +5 V, 0 to +10 V, +/- 5 V, and +/- 10 V) can be selected on-card by dip switch settings. Range selection supplements the signal conditioning available on the AIM1 board and provides flexibility in connecting various signal types.

The AOM1, shown in Figure B6, is a digital-to-analog convertor. The purpose of this board is to take a digital

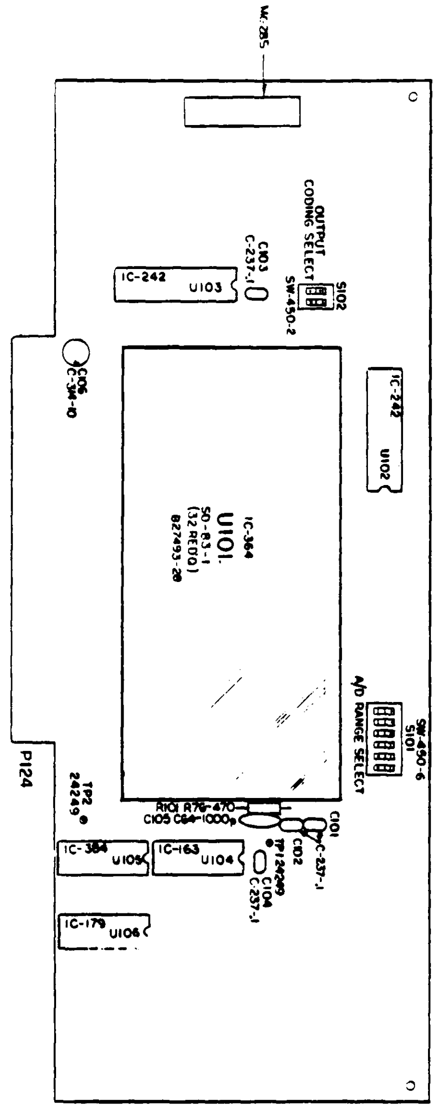

Figure 1. ADM2 Module

Figure B5 ADM2 DIAGRAM

AOM1 COMPONENT LAYOUT

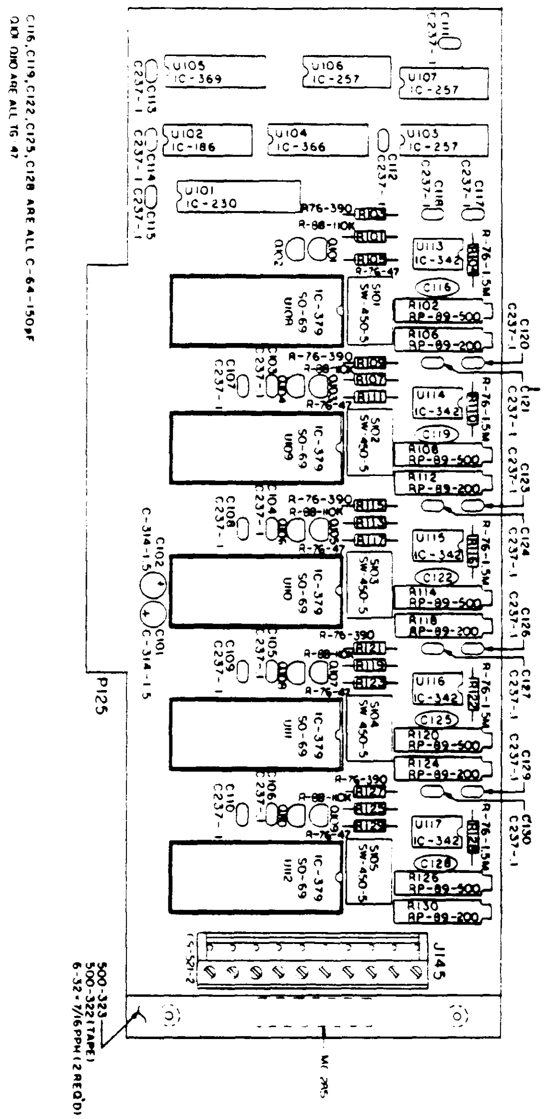

Figure B6 AOM 1 DIAGRAM

signal from the Series 500 baseboard, then converts it to an analog signal which is capable of supplying power to various devices, such as thermistors. The minimum load resistance must be 5000 ohms. The AOM1 offers 12 bit accuracy with a minimum nonlinearity of +/- .012%. Five switch set output ranges are available: 0 to 5 V, 0 to 10 V, +/- 5 V, +/- 10 V, and +/- 2.5 V.

A software package, called Soft500, is supplied with the Series 500. Soft500 is an extension of BASICA which allows the Series 500 to be accessed and controlled by BASICA commands, which trigger Soft500 subroutines. The subroutines are machine language routines that can access data, write to ports, trigger devices, and many other tasks, depending on the routine. This allows the full utilization of the Series 500 from within a BASIC program, which greatly simplifies the the task of running a data acquisition system. A detailed description of Soft500 and its capabilities cannot be presented within the limits of this thesis. For complete documentation of Soft500, the reader is referred to manuals written by Keithly INC. (1987).

Pressure Transducer: The pressure transducer was built by Omega, model PX621-3KG. The transducer is designed to convert a pressure reading inside the equilibrium cell into an analog signal that can be interpreted by the data acquisition system. This model of transducer incorporates an optical means of detecting the effective pressure, so there is no contact between the strained member and the portion of the gauge that produces the electrical signal. This type of device offers extreme accuracy and repeatability. Full range of the transducer is 0-3000 psi. Characteristics of this device are available from Omega, with the most important being:

1. Output: 4-20 mA
2. Sensitivity: better than 0.005% of span
3. Accuracy: +/- 0.15% of span, including linearity, repeatability, and hysteresis at 73 ^{o}F.

The transducer is powered by an external power supply, also from Omega, model PST-28, that will supply the transducer with 28 V at 150 A. The power supply is run by 110 V from a wall socket.

Thermistor: The thermistor was made by Omega, model ON-905-44006, with an internal resistance of 10,000 ohms. This model of thermistor is made for liquid immersion and consists of a thermistor sensor mounted in a closed-end stainless steel tube with vinyl shielded cable. The thermistor is accurate to +/- 0.1 ^{o}C and has a maximum temperature limit of 100 ^{o}C.

B2. <u>INTERFACE SCHEME</u>

A diagram of the overall interfacing scheme is shown in Figure B1 and a wiring diagram is shown in Figure B7. The system consists of the equilibrium cell where the experiment takes places, a pressure transducer that is connected to the cell by a pressure line, a thermistor placed in the bath, the Keithly Series 500, and the IBM XT computer.

Both the transducer and the thermistor generate analog signals that are fed into the AIM1 board. Once there, the signal is passed onto the ADM2 where it is converted into a digital value then passed onto the Series 500 base system which passes the signal to the computer where it can be processed and interpreted.

The thermistor and transducer both require external power for operation. The transducer is supplied by the

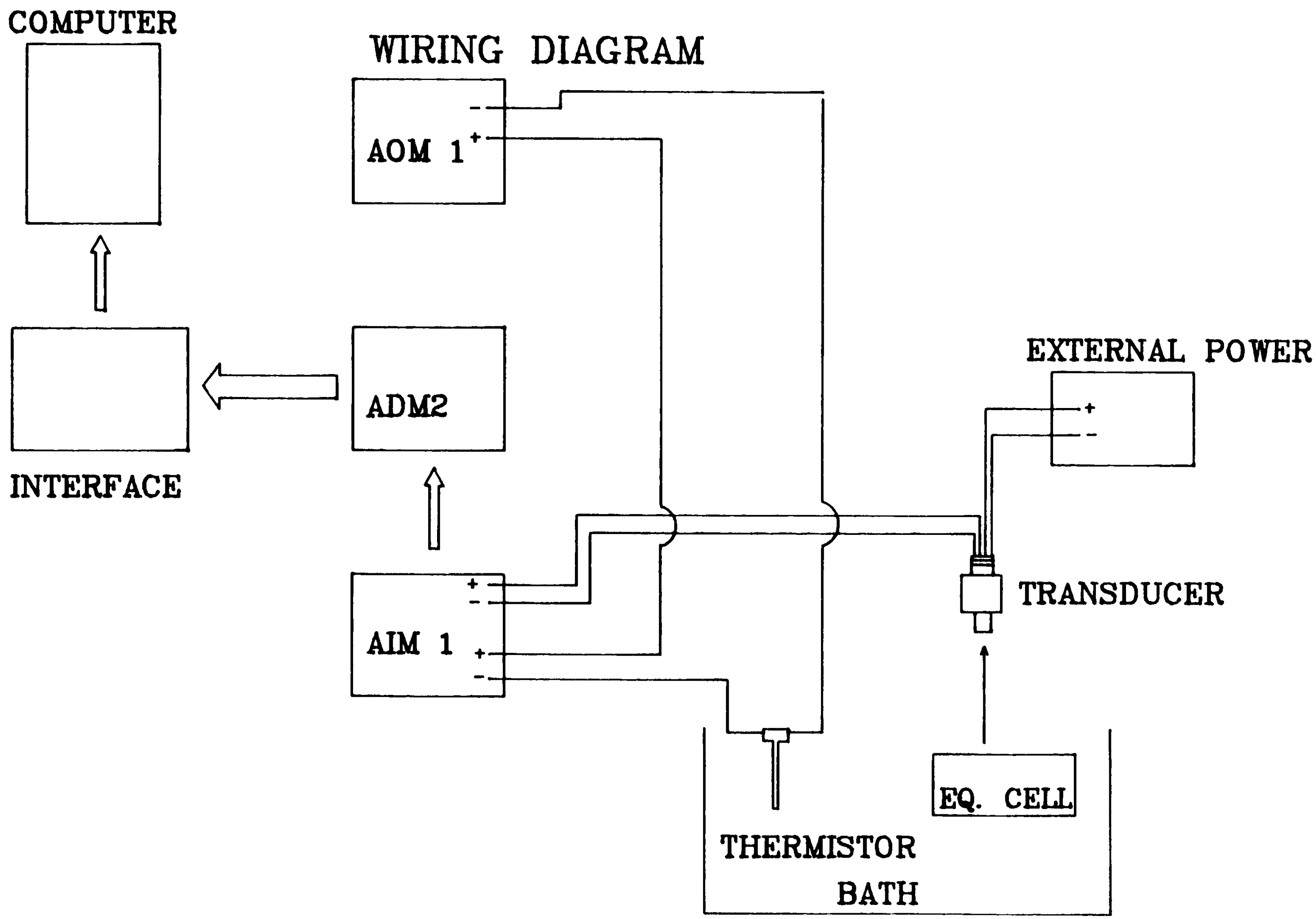

Figure B7 OVERALL SYSTEM WIRING DIAGRAM

PST-28 unit while the thermistor is run by a signal from the AOM1 board. The value of the signal from the AOM1 board is determined and triggered by the computer.

Pressure readings are generated by the transducer which will send an analog signal that is proportional to the pressure inside the cell. The value of the signal is determined by the relationship:

Volts = Pressure x 1/300 (Volts/Pressure)

The leads from the transducer are connected as differential inputs to screw terminals on the AIM1 board, channel 4. The AIM1 board takes the raw signal and passes it on to the ADM2 board where it is processed into a digital value. This digital value is then passed onto the computer via the baseboard, and accessed by a Soft500 subroutine. The value is then converted back to a voltage by the same subroutine that accesses the reading. Once in terms of voltage, the inverse of the previous equation is used to convert the value into a pressure reading. A diagram of this process is shown in Figure B8.

The temperature reading of the cell is arrived at in a secondary manner. Rather than place a thermistor inside the

TRANSDUCER SET-UP

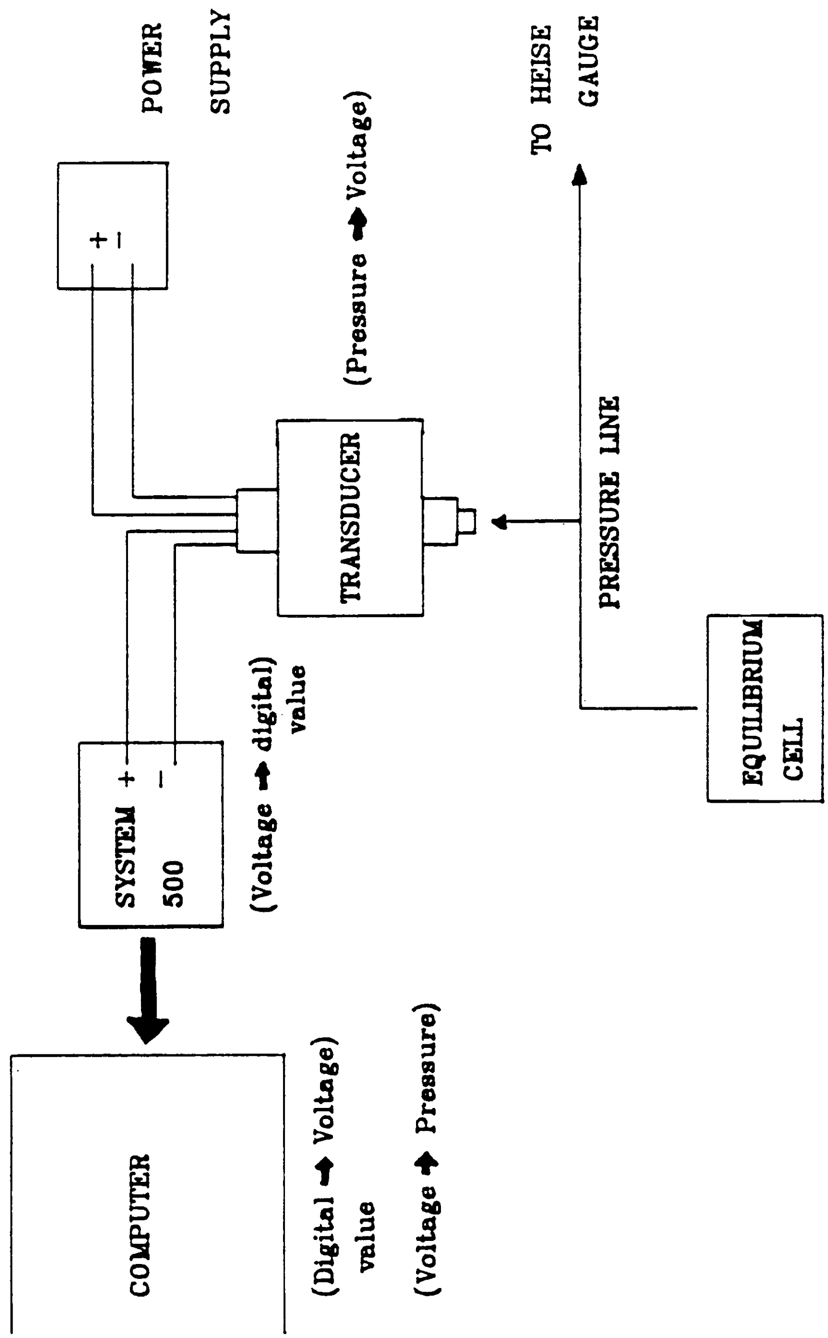

Figure B8 TRANSDUCER SET-UP

cell itself, the thermistor is placed in the water/glycol bath to measure the temperature of the bath instead, as shown in Figure B9. By either cooling or heating at very slow rate, the temperature of the bath is very close to the temperature in the cell.

A thermistor operates by relating temperature to the electrical resistance of the thermistor material. In order to determine the temperature that the thermistor is reading, the resistance of the thermistor material must first be found. To do this, a voltage divider circuit (Figure B10) is set up using the thermistor, the AIM1 board, the AOM1, and a resister of known value. The circuitry is set up so that the AIM1 board will read the voltage drop across the known resistor and the thermistor. The resistance in the thermistor is then given by the voltage divide rule:

$$R = R_{known} \times V_{ther}/V_{resis}$$

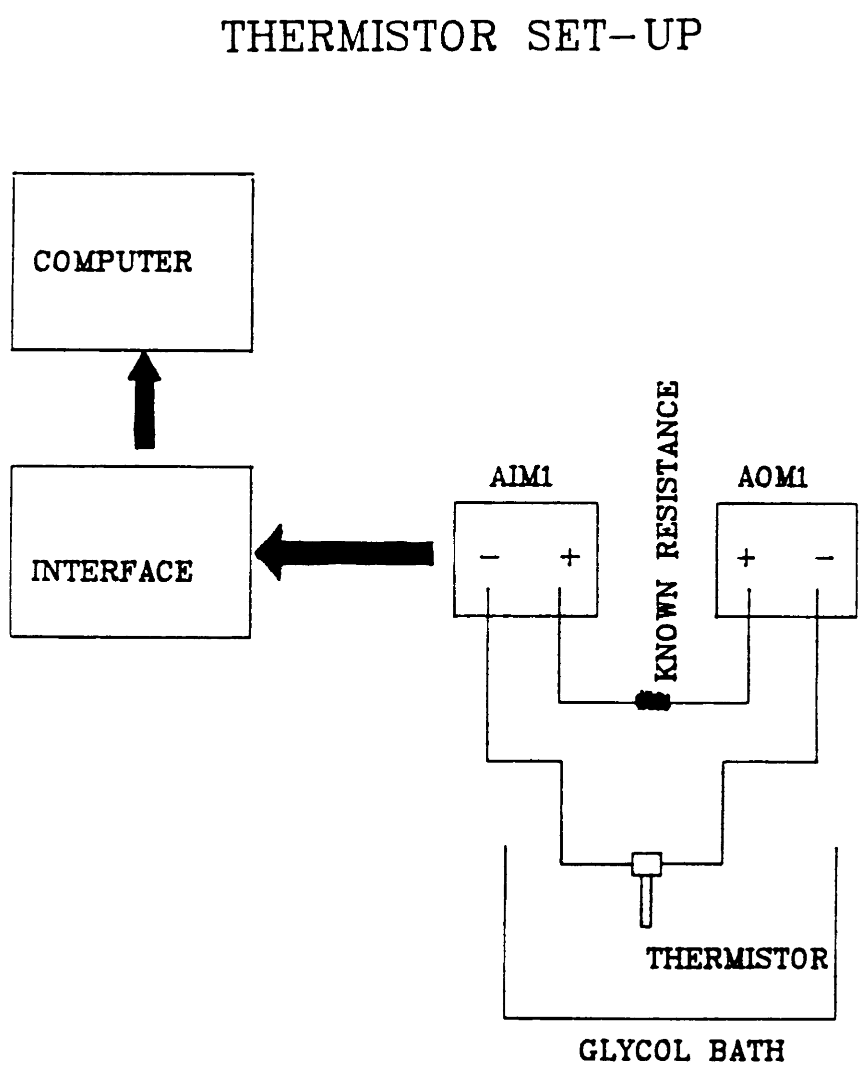

Figure B9 THERMISTOR SET-UP

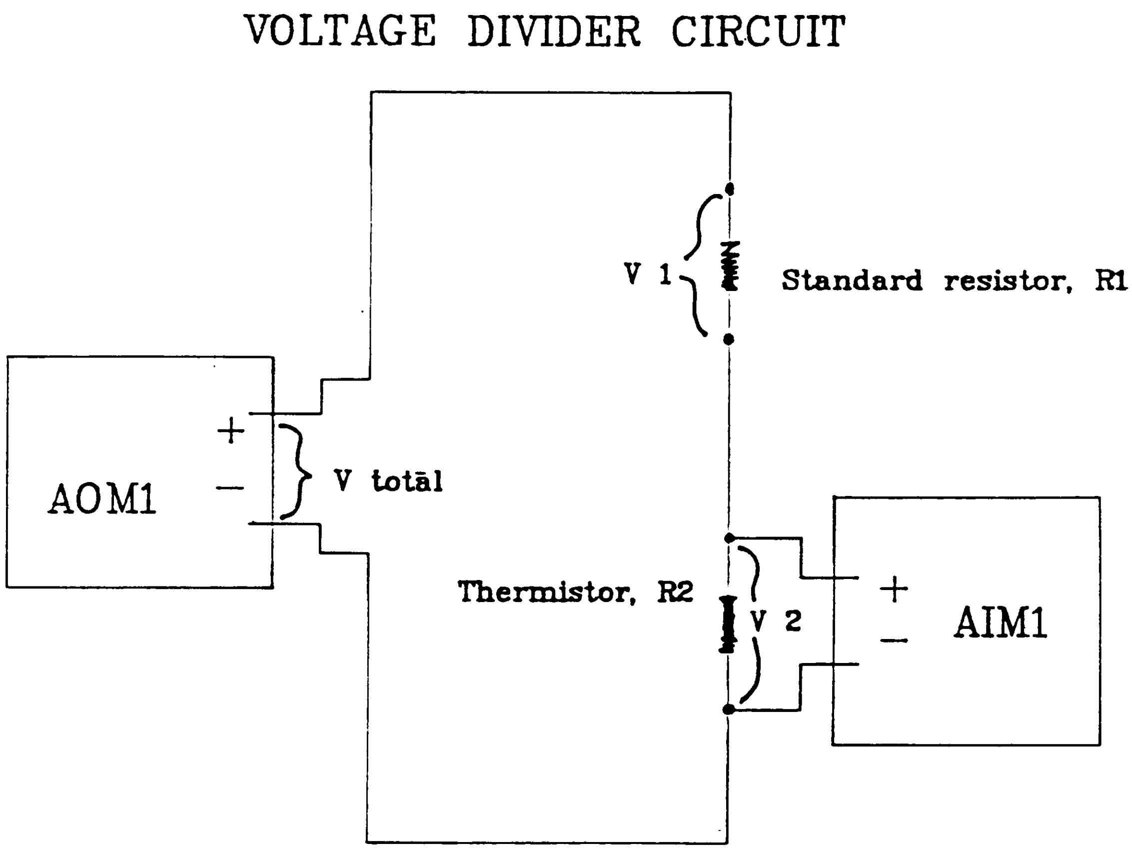

Figure B10 THERMISTOR VOLTAGE DIVIDER DIAGRAM

The temperature can then be backed out of a calibration equation:

$$1/T = A + B \times LOG(R) + C \times (LOG(R))^3$$

where,

A,B,C = experimentally fitted constants

R = resistance (ohms)

T = temperature, ^{o}K

All measurement readings are triggered through Soft500 commands contained within a BASIC computer program. The program also processes the data, displaying it on screen then storing it in a data file.

B3. COMPUTER PROGRAM

The computer program that runs the data acquisition system is written in BASIC and run in the Soft500 environment. The objective of the program is to access the Keithly Series 500 for data points at regular intervals, then display and store the information. A listing of the program is located in Appendix C.

The major portions of the program include:

1. An input section, where initial data about the experiment are input.

2. A screen setup section, where the a display of relevant information is setup.

3. The data acquisition portion, where Soft500 commands are used to obtain readings.

4. A conversion section, where the raw data is converted into either a temperature or pressure value.

5. A data management section, where the data is plotted on screen then stored in a data file.

Data Input Section: The purpose of this section is to obtain initial identification data about the experiment, such as the experimental number, the particular run number, and the pressure at which the experiment is being run. This information is used to label a data file where the experimental data can be placed. The name of the file begins with the experimental run followed by an 'R' then the run number followed by a 'P" then the pressure. For example, experiment 1, run 2b, at 300 psi, would be labeled 1R2bP300.

The input section also asks for data to set the scales of the on-screen graph. It will ask for the the anticipated maximum and minimum temperatures and pressures of the experiment, then uses these values as the extreme limits of the X-axis (temperature) and the Y-axis (pressure).

The program is also geared to resume an experiment in case of a power failure or some other interruption. It will ask if the is a new experiment, if the answer is no, the computer will proceed with the identification input, then look for the old data file. Once the file is opened, the old data is plotted on-screen before new points are obtained. The new data is then placed at the end of the old file.

Screen Setup: Once the input section is complete, the computer program will set up an on screen display of relevant data and a plot of all data points. A diagram of the setup is shown in Figure B11. The display includes information on the experiment number, the run number, and the time the experiment was started. The setup also

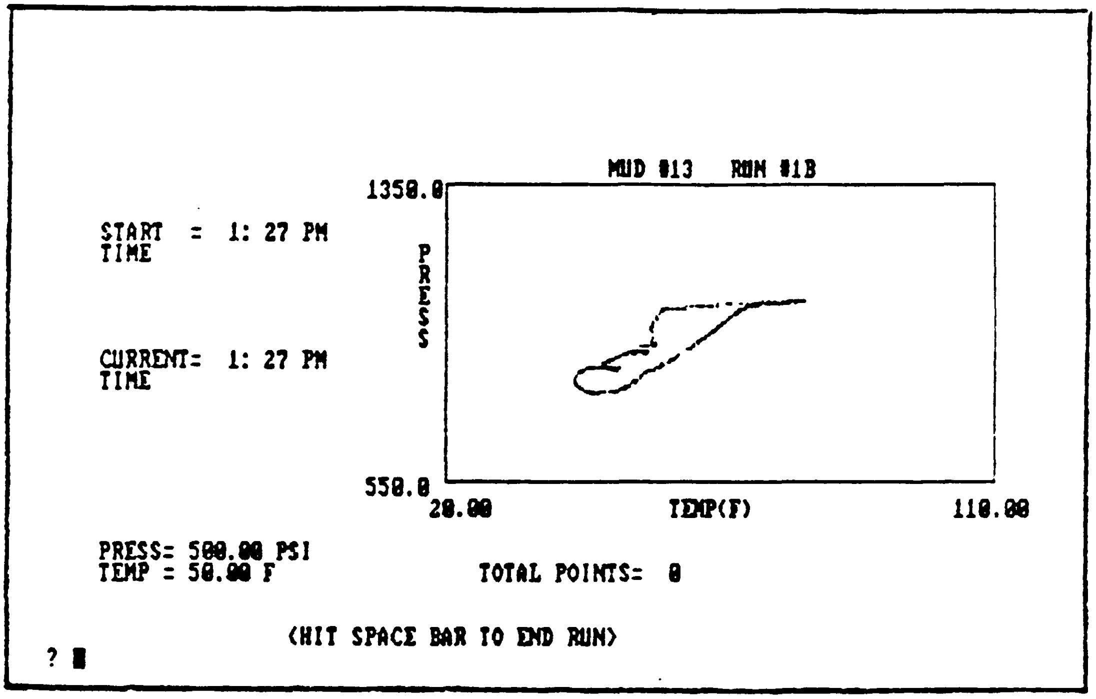

Figure B11 COMPUTER DISPLAY

displays the present temperature and pressure inside cell along with the current time.

An on-screen graph is setup to show a plot of how the experiment is proceeding. Temperature is plotted on the X-axis while pressure is plotted on the Y-axis.

Data Acquisition Routine: Once the screen has been setup, the program proceeds to collect experimental data. This involves using a variety of BASIC commands and Soft500 routines.

The first step is to clear and initialize the Series 500 apparatus. This is done within the program by calling the Soft500 routine INIT. In any Soft500 program, the first command must be INIT. The INIT command initializes the Soft500 environment, setting up memory management and other system functions. If INIT is not called, the program does not start off with a 'clean slate' and errors may result.

Once the system has been initialized, the program will proceed to create arrays for data input and output. There is one input array, call 'OUT%', and one output array, called 'TEMP%'. The input array is where all data collect from the Series 500 is initially stored, while the output array is where output data, in this case the voltage value put out by the AOM1, is stored for processing. The arrays are created by calling the Soft500 command ARMAKE. Every array has two dimensions: width and depth. The width of the array is related to the specific channels to be accessed by the program and the depth of the array is where the data is stored. The Series 500 is setup for for eight input channels, each one a differential input on the AIM1 board, and 5 output channels, each one an output lead on the AOM1 board. For example, if an array is needed that would access channels 0,1,4,and 5 of the input board for 20 data points, ARMAKE would create an array where the first place across is reserved for all data from channel 0, the second place for channel 1, etc. Each place would then have a depth of 20 places deep.

After all the arrays are created, the output array is loaded with the desired output value. This is done using the ARPUT command. ARPUT will put the desired value, which can be either in binary or straight voltage, into the appropriate place of the array.

The next step is the actual collection of the data. Two commands are initially called. The first is ANIN, a routine that uses the input array to determine which channels are to be accessed for how many data points, then reads the appropriate channels and places the data inside the array. The next command is ANOUT, which uses the output array to determine which output channel is to be activated and at what voltage value. Both commands do not commence operation unless triggered by the INTON command. This command signals the Series 500 to begin data acquisition and activates both ANIN and ANOUT.

The ARLASTP command is used to check the depth of the input arrays. When the array is filled, the ARLASTP command will send a flag, which triggers the INTOFF command, which halts data acquisition and turns the Series 500 off. After, the input array is filled, the ARGETVAL command is used to retrieve the data. The program is written so that 20 data points are taken, then averaged to give a single data point. The arrays are setup so that one channel reads the signal from the pressure transducer, while two channels are dedicated to the thermistor. This is necessary because of the voltage divider setup employed to determine the resistance of the thermistor.

Once a set of data points is obtained, the system processes the data, plots it on-screen, then stores it in a data file. After this is complete, the program runs into a delay cycle, where it will wait three minutes before the next point is taken.

Before another data point can be taken, the input array must be emptied. This is done using the ARDEL command, which completely deletes the array. It is then necessary to recreate the array every time a point is taken. The output array need be created only once since the output value to the thermistor does not change.

Once the input array is recreates, the sequence restarts with the calling of the INTON routine.

Data Conversion: The raw data from the acquisition sequence consists of voltage readings which must be converted to either pressure or temperature readings. To convert to pressure, a simple expression is used:

$$\text{Pressure (psi)} = \text{Voltage (V)} \times 300$$

For temperature, a more complex approach is necessary The voltage must be first converted to a resistance (previously discussed), then the resistance converted into a temperature reading (also previously discussed). The temperature is obtained in units of Kelvin and is converted to Fahrenheit.

Data Management: Once the raw data has been processed, it is graphed on screen using the basic command PSET. The data is then stored in the appropriate data file, in the order temperature, pressure, and time the point was taken.

A complete listing of the program is located in the Appendix. For detailed information concerning the Soft500 commands and their use, the reader is referenced to the SOft500 manual by Keithly Inc. (1987)

Appendix C

DATA ACQUISITION COMPUTER PROGRAM

The computer program used by the data acquisition system is listed below. A detailed description of the commands and logic used for the program is located in Appendix B.

```
10 CLEAR:TPOINT=0:GOSUB 630:GOSUB 310
15 GOSUB 450:GOSUB 465
20 CLS:SCREEN 2:VIEW(250,10)-(600,120),,1:WINDOW(TMIN,PMIN
7,30:PRINT USING"###.##";TMIN:LOCATE 17,50:PRINT"TEMP(F)"
NG"###.##";TMAX:LOCATE 2,26:PRINT USING"####.#";PMAX:LOC
#.#";PMIN
30 LOCATE 5,30:PRINT"P":LOCATE 6,30:PRINT"R":LOCATE 7
INT"S":LOCATE 9,30:PRINT"S":LOCATE 1,45:PRINT "MUD #";
";B$:GOSUB 510:LOCATE 4,5:PRINT "START  = ";COUNT$:LOCAT
35 PRINT "TIME":CRO=MIN%
37 IF RUNC=1 THEN GOSUB 710
40 GOSUB 100:GOSUB 260:PSET(LL,PP),1:LOCATE 10,5:PRINT"CURRENT
11.5:PRINT"TIME"
50 LOCATE 19,5:PRINT USING"PRESS=####.## PSI";PP:LOCATE 20,5:PRINT
###.## F";LL:LOCATE 20,35:PRINT "TOTAL POINTS= "TPOINT:GOSUB 290
60 LOCATE 23,20:PRINT"<HIT SPACE BAR TO END RUN>":
70 CB$=INKEY$:IF CB$=" " GOTO 90
80 GOSUB 550:GOTO 40
90 CALL INIT
95 GOTO 600
100 R1=10.001:CALL INIT
110 CALL ARMAKE'("OUT%",20.,"AO0")
120 FOR D=1 TO 20:VAO=5!:CALL ARPUTVAL'("OUT%",D,"AO0",VAO,0)
130 VA=0:CALL ARGETVAL'("OUT%",D,"AO0",VA,0)
140 NEXT D
145 CALL ANIN'("TEMP%",20.,"ANI1,ANI0,ANI4",1)
150 CALL ANOUT'("OUT%","AO0",1,-1)
160 CALL INTON'(500,"MIL")
165 LP=0
170 CALL ARLASTP'("TEMP%",LP)
180 IF LP<20 THEN GOTO 170
190 T1=0:T2=0:PP=0:PT=0:T1T=0:T2T=0:FOR I=1 TO 20:CALL ARGETVAL'("TEMP%",I,"ANI0
",T1,0)
200 CALL ARGETVAL'("TEMP%",I,"ANI1",T2,0)
210 CALL ARGETVAL'("TEMP%",I,"ANI4",PP,0)
220 T1T=T1T+T1:T2T=T2T+T2:PT=PT+PP:NEXT I:T1=T1T/20:T2=T2T/20:PP=PT/20
230 LOCATE 20,5:R2=R1*T2/T1:LL=R2:PP=PP*300:PP=ABS(PP)
240 CALL INTOFF
247 GOSUB 510
250 TPOINT=TPOINT+1
255 RETURN
```

```
260 TK=A+B*LOG(LL)+C*((LOG(LL))^3)
270 TK=1!/TK:TC=TK-273!:TF=TC*9/5+32!:LL=TF
280 RETURN
290 OPEN FILE$ FOR APPEND AS 1:PRINT#1,LL,PP,SCOUNT$
295 LPRINT LL,PP,SCOUNT$:CLOSE
300 RETURN
310 CLS:VIEW(10,10)-(600,120),,1:LOCATE 17,10:PRINT"MUD# = ":LOCATE 18,10:PRINT"
RUN# = ":LOCATE 19,10:PRINT"PRESS= ":LOCATE 17,50:PRINT"START TEMP= ":LOCATE 18,
50:PRINT"START PRESS=":LOCATE 19,50:PRINT"MIN TEMP =":LOCATE 20,50:PRINT"MIN PRE
SS ="
320 LOCATE 6,15:A1$="M":B1$="R":C1$="P":PRINT"ENTER MUD SAMPLE NUMBER:"
330 LOCATE 8,15:PRINT"ENTER RUN #":LOCATE 10,15:PRINT"ENTER TEST PRESSURE IN HUN
DRED PSI"
340 LOCATE 6,40:INPUT;A$:LOCATE 17,18:PRINT A$
350 LOCATE 8,27:INPUT;B$:LOCATE 18,18:PRINT B$:LOCATE 10,50:INPUT;C$:LOCATE 19,1
8:PRINT C$:FILE$=A$+B1$+B$+C1$+C$
360 CLS:LOCATE 6,15:PRINT"ENTER THE STARTING TEMP(F) AND PRESSURE(PSI)":LOCATE 8
,15:PRINT"ENTER THE MINUMUM TEMP(F) AND PRESSURE(PSI)"
370 LOCATE 6,60:INPUT;TMAX,PMAX:LOCATE 17,63:PRINT USING "####.## F";TMAX:LOCATE
 18,63:PRINT USING "####.## psi";PMAX:LOCATE 8,60:INPUT;TMIN,PMIN:LOCATE 19,63:P
RINT USING "####.## F";TMIN:LOCATE 20,63:PRINT USING"####.## psi";PMIN
380 CLS:LOCATE 7,10:PRINT"IS EVERYTHING RIGHT CORRECT "
390 Y$=INKEY$:IF Y$="" THEN GOTO 390
400 IF Y$="Y" THEN GOTO 430
410 IF Y$="N" THEN GOTO 310
420 LOCATE 9,10:PRINT"ENTER Y FOR YES:AND N FOR NO":BEEP:GOTO 390
430 TMAX=TMAX+10:PMAX=PMAX+50:TMIN=TMIN-10:PMIN=PMIN-50
440 VIEW:RETURN
450 OPEN "I",#2,"CALIB.DAT"
460 RETURN
465 DEF SEG=20
480 R1=10.001
490 INPUT #2,A,B,C
495 HR%=0:MIN%=0:SEC%=0:MON%=0:DAY%=0:YR%=0
500 RETURN
510 CALL CLOCKREAD'(HR%,MIN%,SEC%,DAY%,MON%,YR%)
515 DT$=STR$(DAY%)+"/"+STR$(MON%)+"/"+STR$(YR%)
517 MMM$=STR$(MIN%):IF MIN%<10 THEN MMM$="0"+RIGHT$(MMM$,1)
520 COUNT$=STR$(HR%)+":"+MMM$+" AM"
530 IF HR%>12 THEN HR%=HR%-12:COUNT$=STR$(HR%)+":"+MMM$+" PM"
535 SCOUNT$=STR$(HR%)+":"+STR$(MIN%)+":"+STR$(SEC%)
540 RETURN
550 I=0
551 ST=TIMER
555 V=TIMER:IF V<ST THEN V=V+86400!
560 DELTA=V-ST:IF DELTA<40 THEN GOTO 555
565 I=I+1:GOSUB 510:LOCATE 10,5:PRINT "CURRENT= ";COUNT$:IF I<4 THEN GOTO 551
570 RETURN
600 END
630 CLS:SCREEN 2:VIEW(10,10)-(600,120),,1:LOCATE 6,15:PRINT "IS THIS A NEW RUN ?
"
640 CB$=INKEY$:IF CB$="" THEN GOTO 640
650 IF CB$="N" THEN 670
660 RUNC=0:GOTO 700
670 RUNC=1
700 VIEW:RETURN
710 CLOSE:OPEN "I",#1,FILE$
720 INPUT #1,T,P,JUNK$:PSET(T,P)
730 V=EOF(1):IF V<0 THEN GOTO 750
740 GOTO 720
750 CLOSE:RETURN
```

Appendix D

PRIMARY EXPERIMENTAL DATA

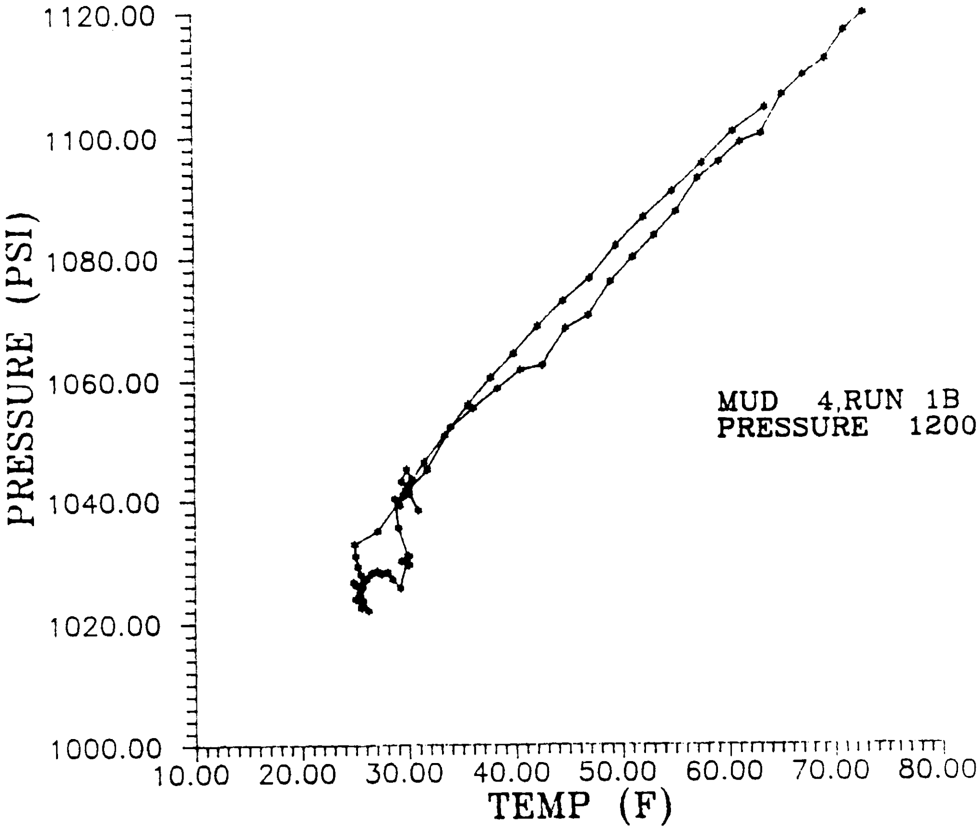
1120.00
1100.00
1080.00
1060.00
1040.00
1020.00
1000.00
PRESSURE (PSI)
10.00
20.00
30.00
40.00
50.00
60.00
70.00
80.00
TEMP (F)
MUD 4,RUN 1B
PRESSURE 1200

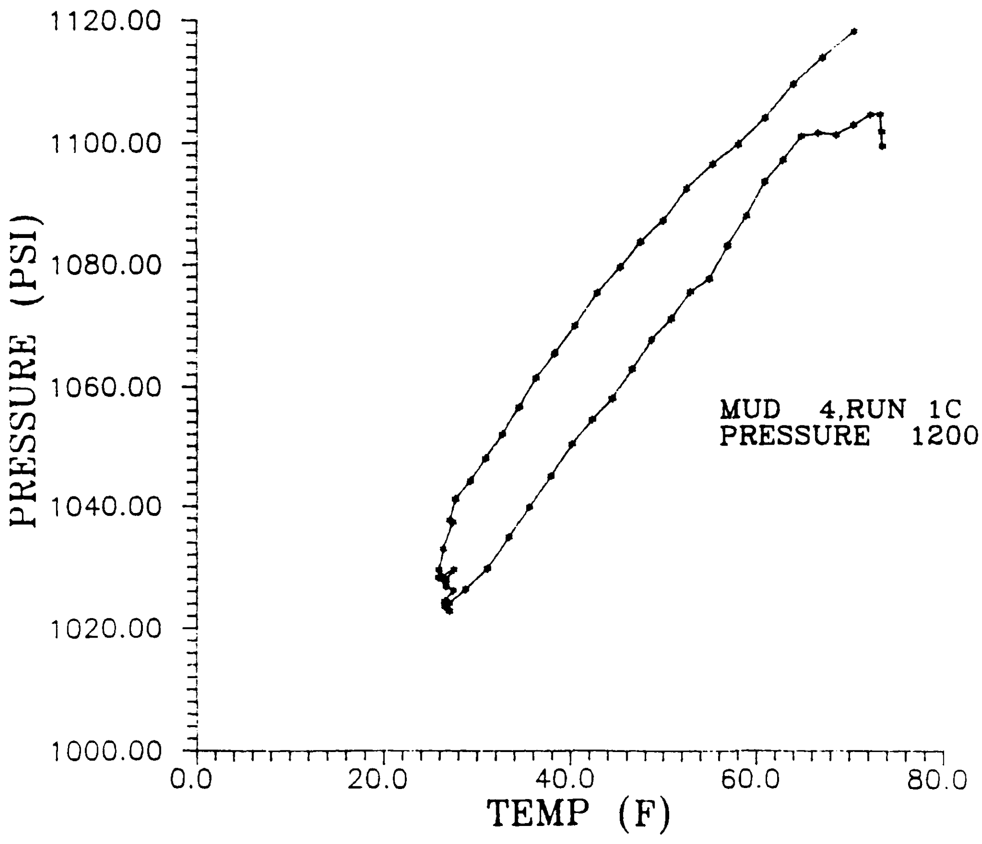
1120.00
1100.00
1080.00
1060.00
1040.00
1020.00
1000.00
PRESSURE (PSI)
0.0
20.0
40.0
60.0
80.0
TEMP (F)
MUD 4,RUN 1C
PRESSURE 1200

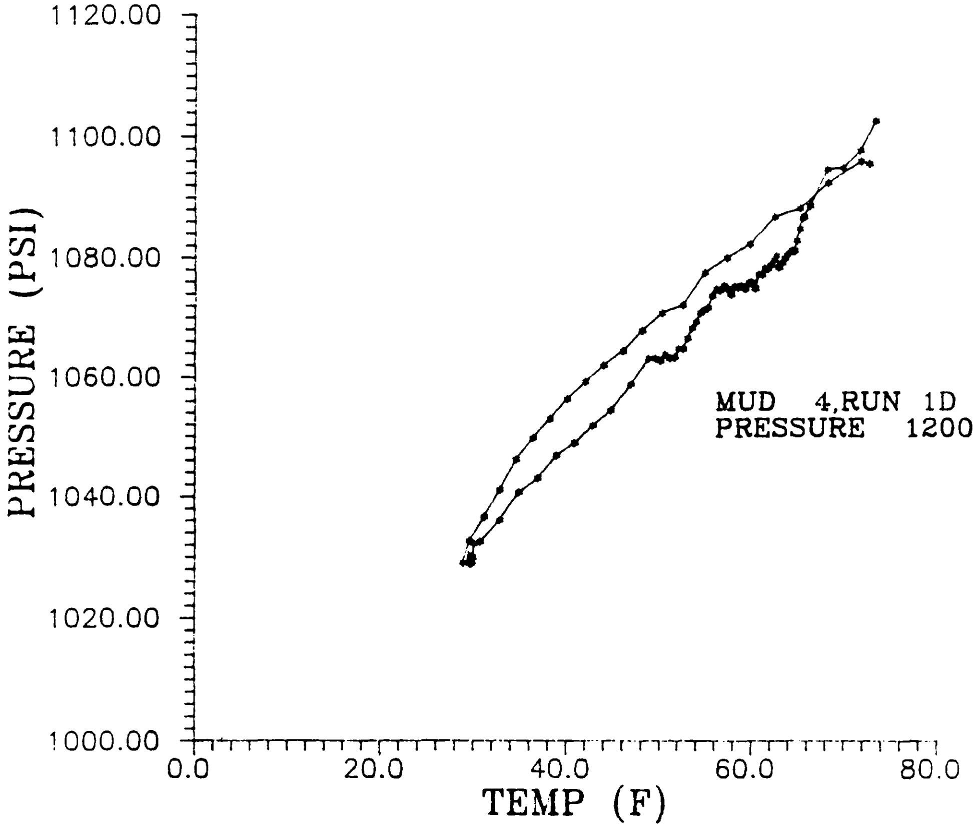

1120.00
1100.00
1080.00
1060.00
1040.00
1020.00
1000.00
PRESSURE (PSI)
0.0
20.0
40.0
60.0
80.0
TEMP (F)
MUD 4,RUN 1D
PRESSURE 1200

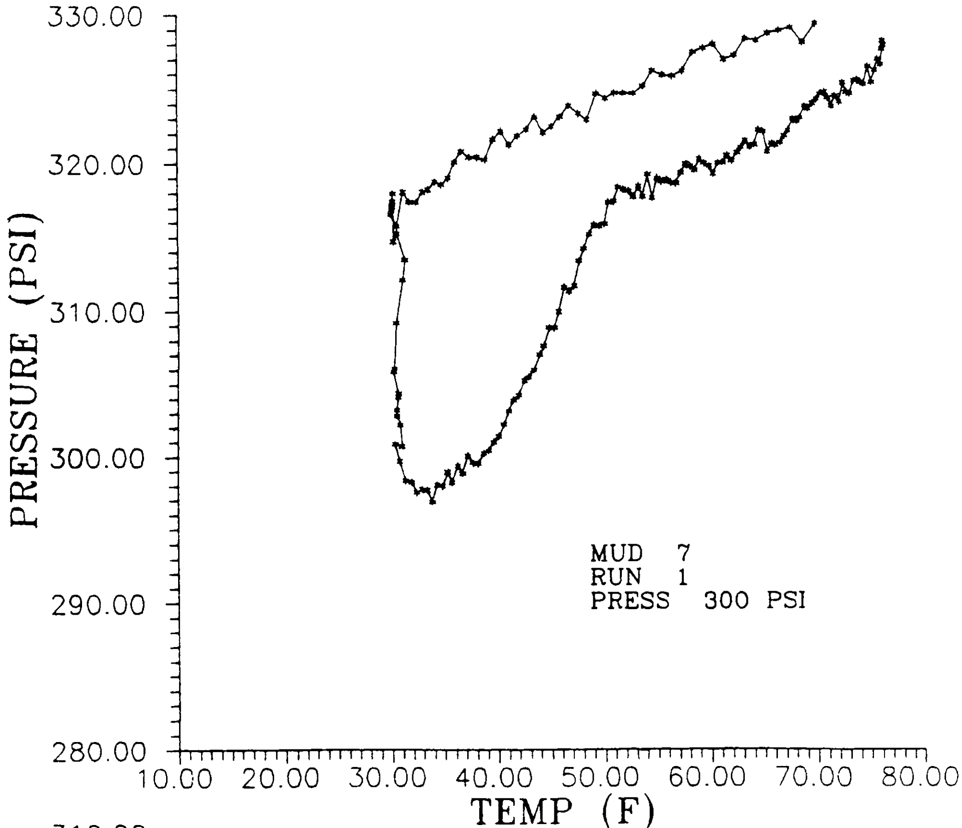
330.00
320.00
310.00
300.00
290.00
280.00
PRESSURE (PSI)
MUD 7
RUN 1
PRESS 300 PSI
10.00 20.00 30.00 40.00 50.00 60.00 70.00 80.00
TEMP (F)

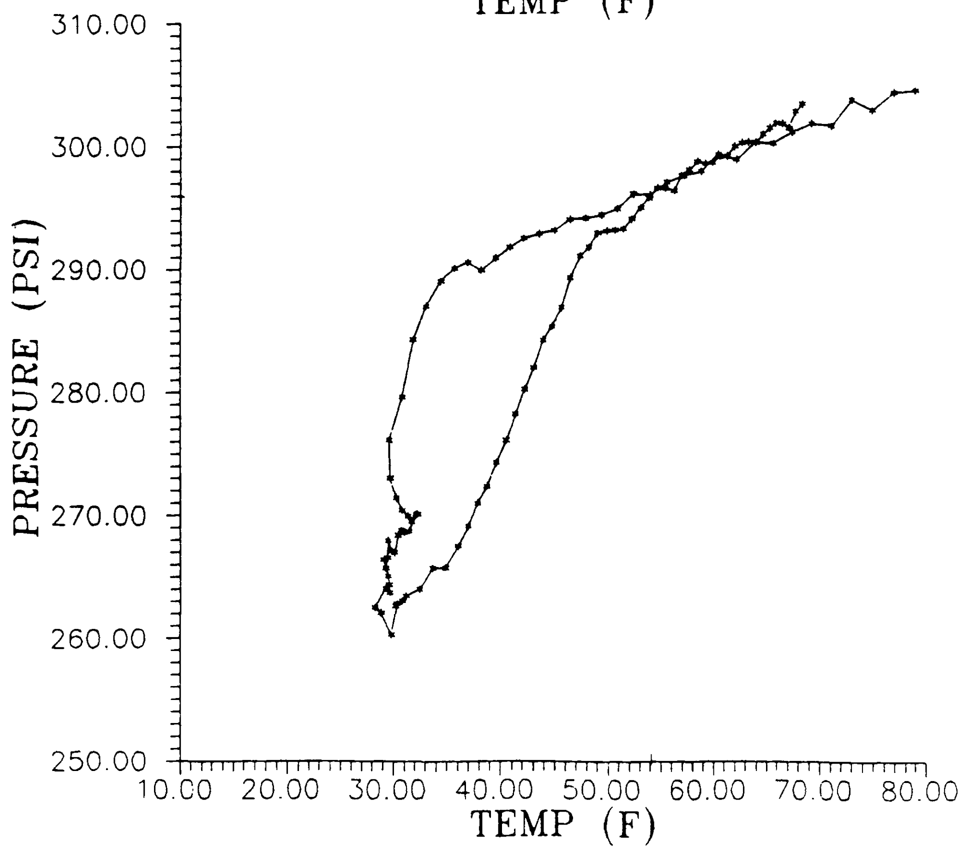
310.00
300.00
290.00
280.00
270.00
260.00
250.00
PRESSURE (PSI)
10.00 20.00 30.00 40.00 50.00 60.00 70.00 80.00
TEMP (F)

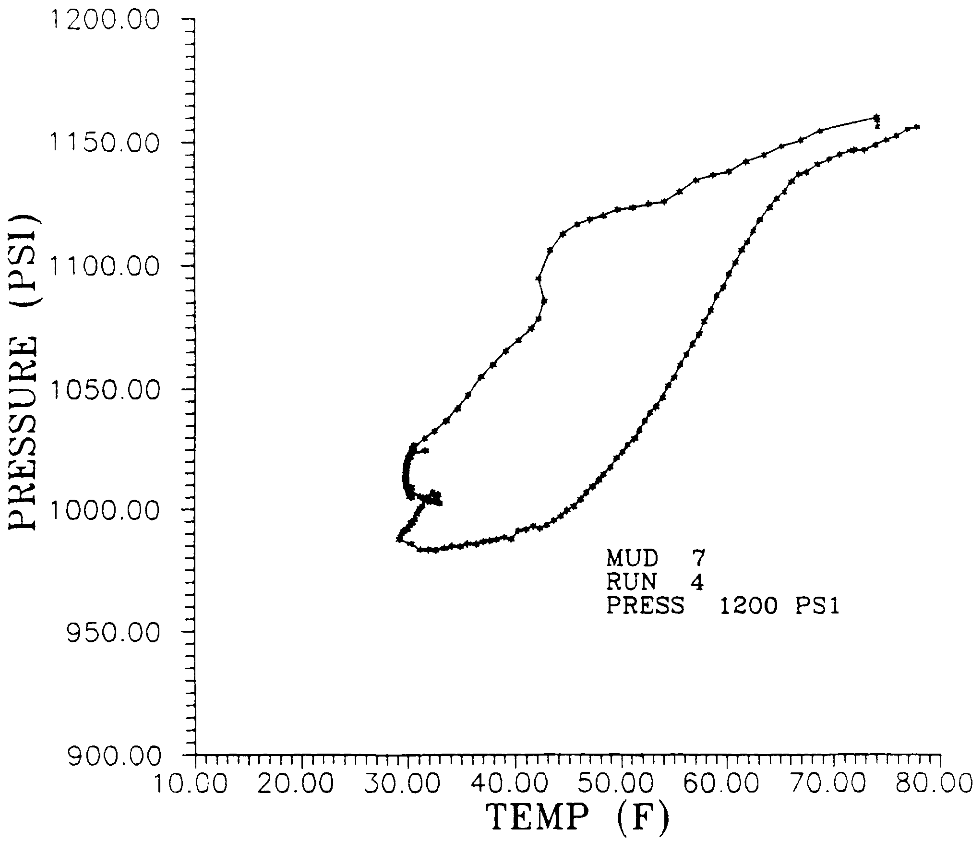
1200.00
1150.00
1100.00
1050.00
1000.00
950.00
900.00
PRESSURE (PSI)
10.00
20.00
30.00
40.00
50.00
60.00
70.00
80.00
TEMP (F)
MUD 7
RUN 4
PRESS 1200 PS1

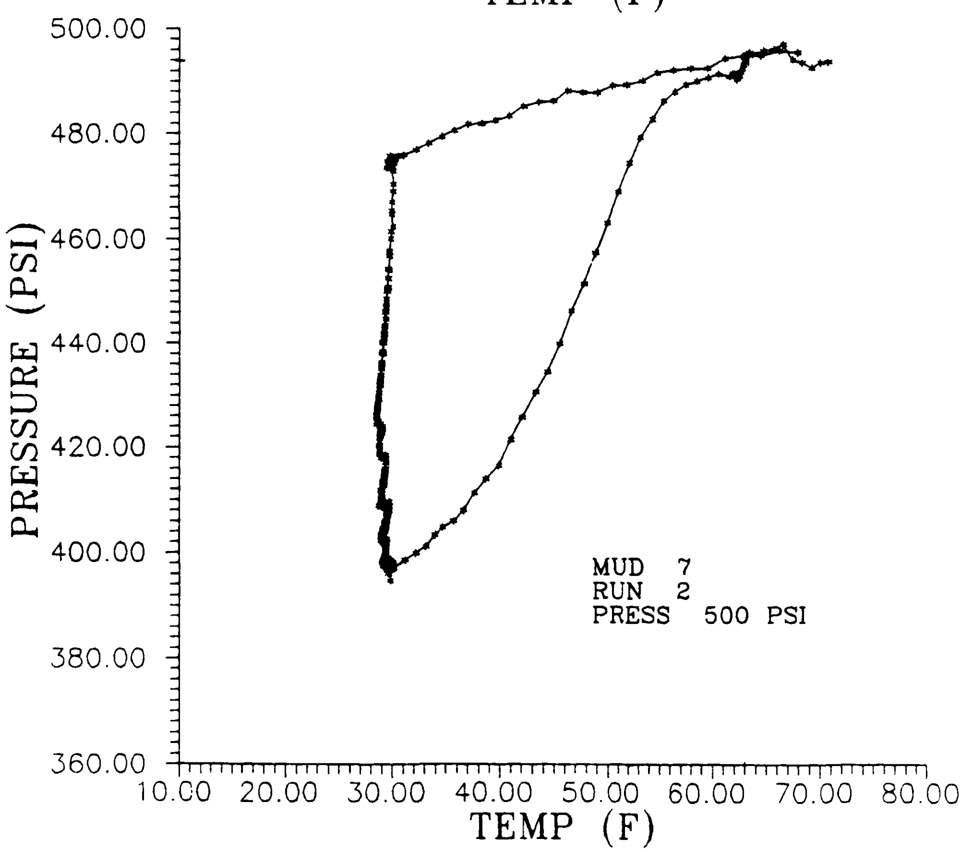
500.00
480.00
460.00
440.00
420.00
400.00
380.00
360.00
PRESSURE (PSI)
10.00
20.00
30.00
40.00
50.00
60.00
70.00
80.00
TEMP (F)
MUD 7
RUN 2
PRESS 500 PSI

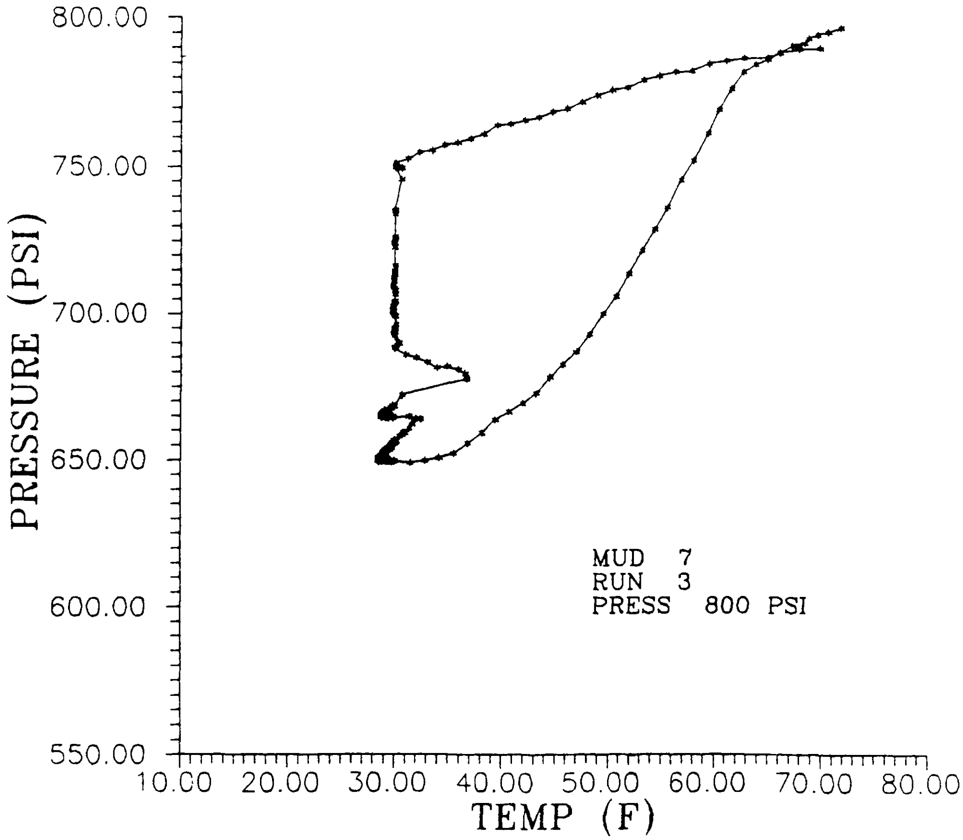
800.00
750.00
700.00
650.00
600.00
550.00
PRESSURE (PSI)
10.00 20.00 30.00 40.00 50.00 60.00 70.00 80.00
TEMP (F)
MUD 7
RUN 3
PRESS 800 PSI

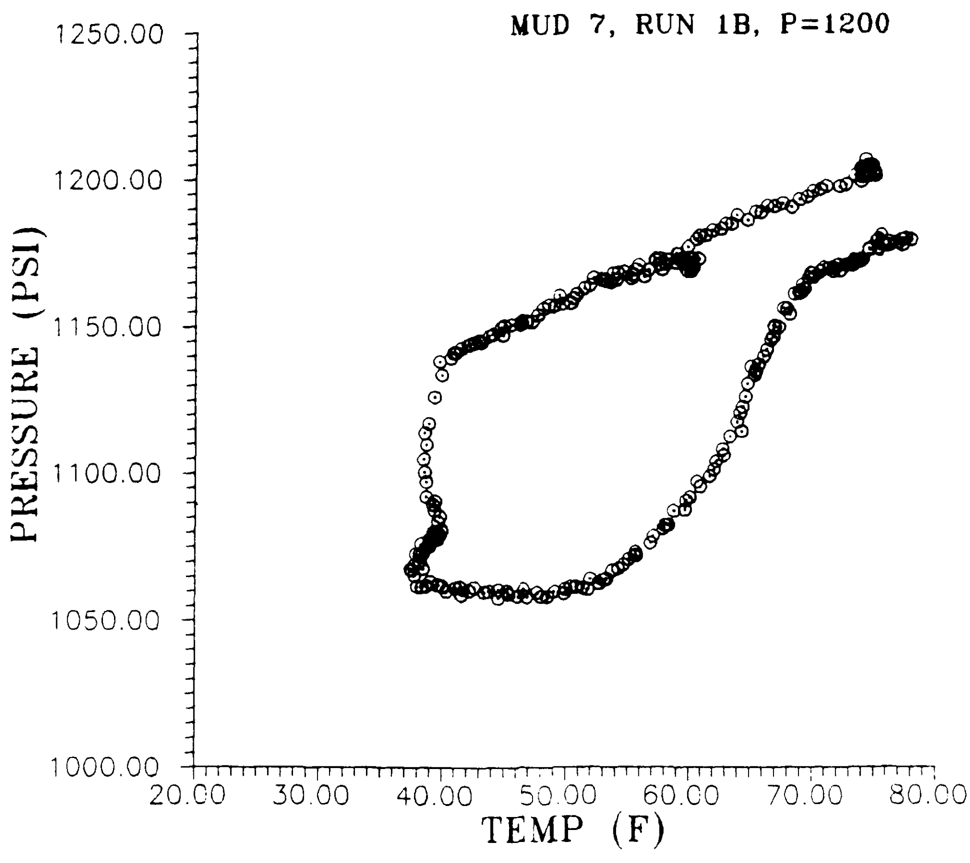
MUD 7, RUN 1B, P=1200
1250.00
1200.00
1150.00
1100.00
1050.00
1000.00
PRESSURE (PSI)
20.00 30.00 40.00 50.00 60.00 70.00 80.00
TEMP (F)

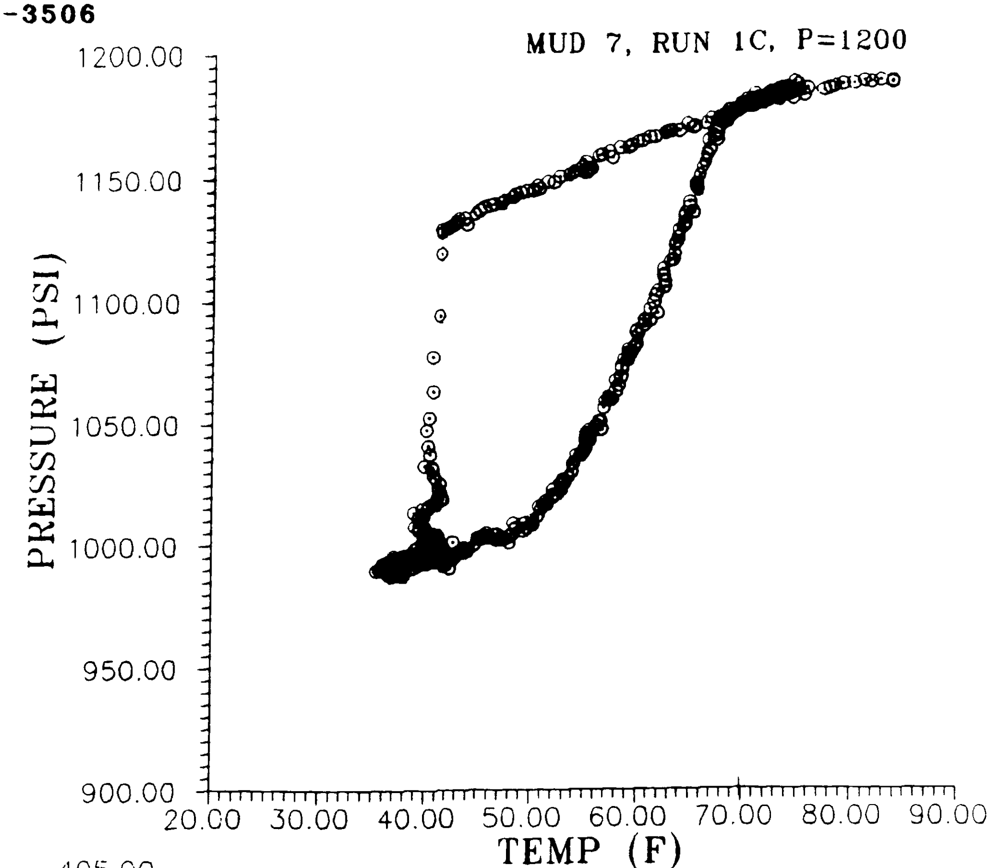
MUD 7, RUN 1C, P=1200
PRESSURE (PSI)
1200.00
1150.00
1100.00
1050.00
1000.00
950.00
900.00
20.00 30.00 40.00 50.00 60.00 70.00 80.00 90.00
TEMP (F)

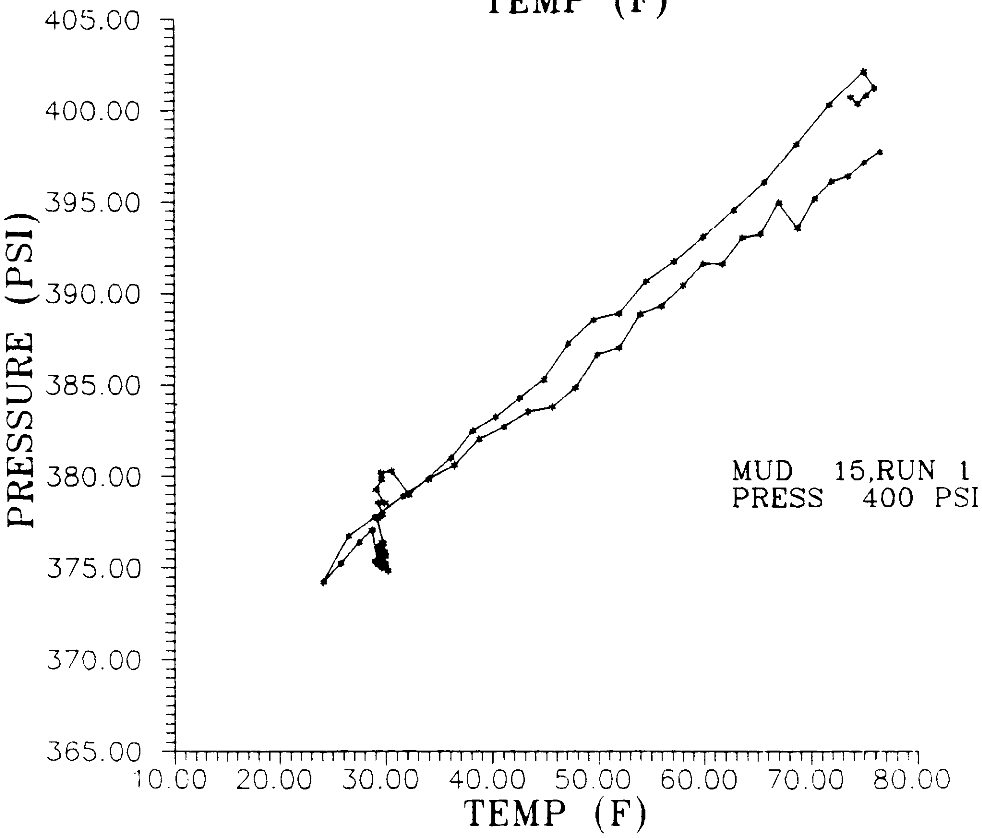
PRESSURE (PSI)
405.00
400.00
395.00
390.00
385.00
380.00
375.00
370.00
365.00
MUD 15,RUN 1
PRESS 400 PSI
10.00 20.00 30.00 40.00 50.00 60.00 70.00 80.00
TEMP (F)

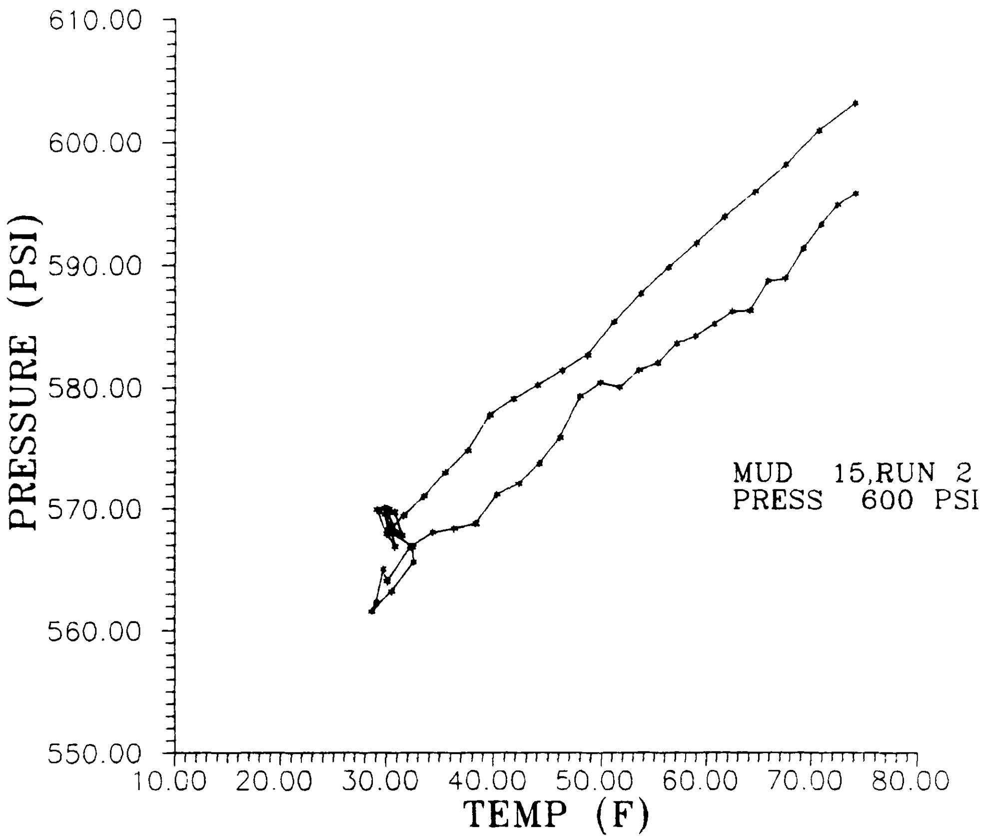
610.00
600.00
590.00
580.00
570.00
560.00
550.00
PRESSURE (PSI)
10.00
20.00
30.00
40.00
50.00
60.00
70.00
80.00
TEMP (F)
MUD 15,RUN 2
PRESS 600 PSI

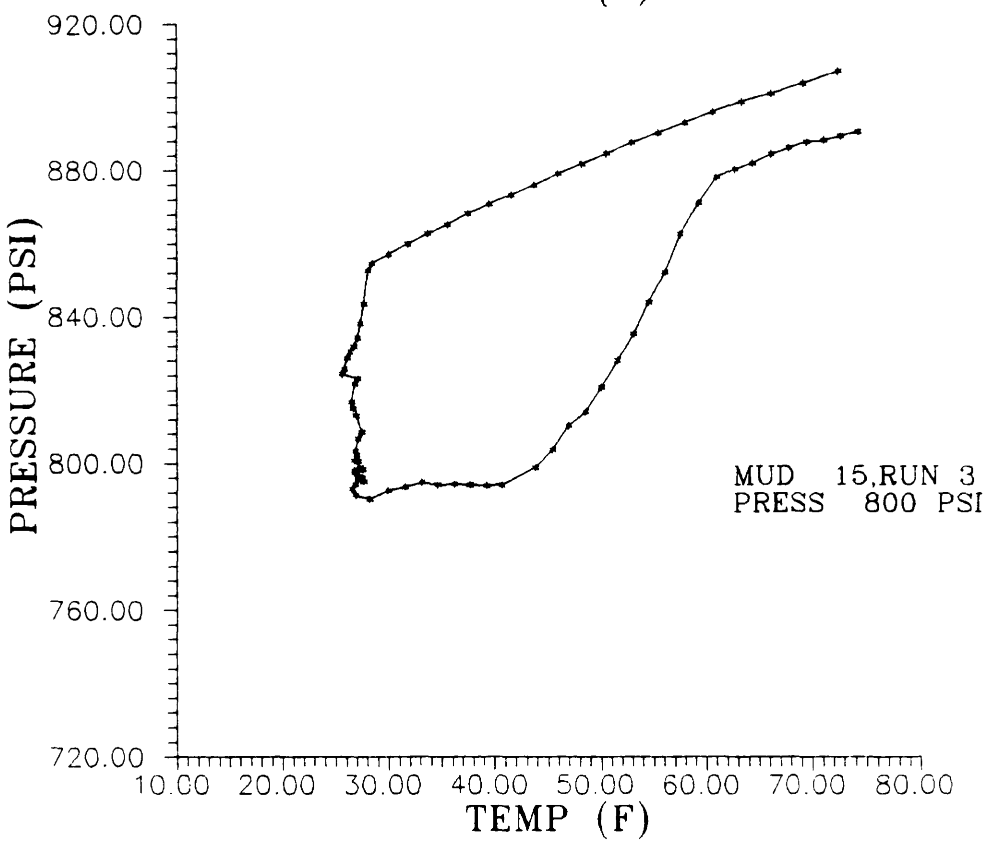
920.00
880.00
840.00
800.00
760.00
720.00
PRESSURE (PSI)
10.00
20.00
30.00
40.00
50.00
60.00
70.00
80.00
TEMP (F)
MUD 15,RUN 3
PRESS 800 PSI

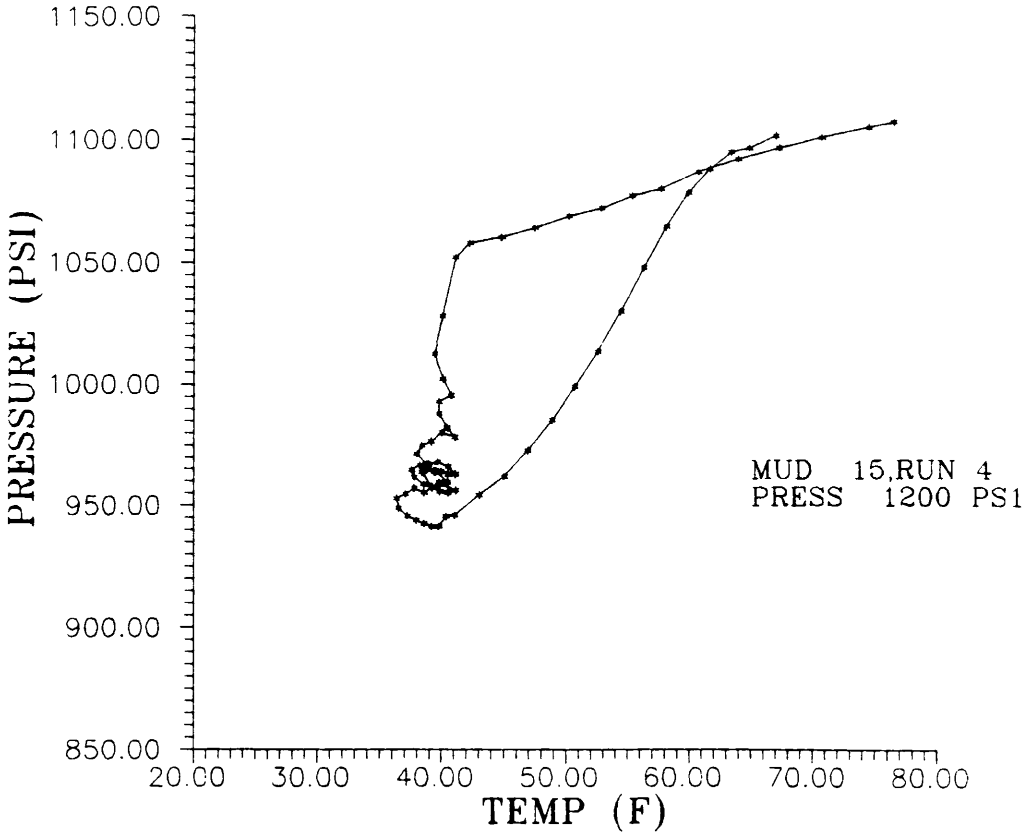
1150.00
1100.00
1050.00
1000.00
950.00
900.00
850.00
PRESSURE (PSI)
20.00 30.00 40.00 50.00 60.00 70.00 80.00
TEMP (F)
MUD 15,RUN 4
PRESS 1200 PS1

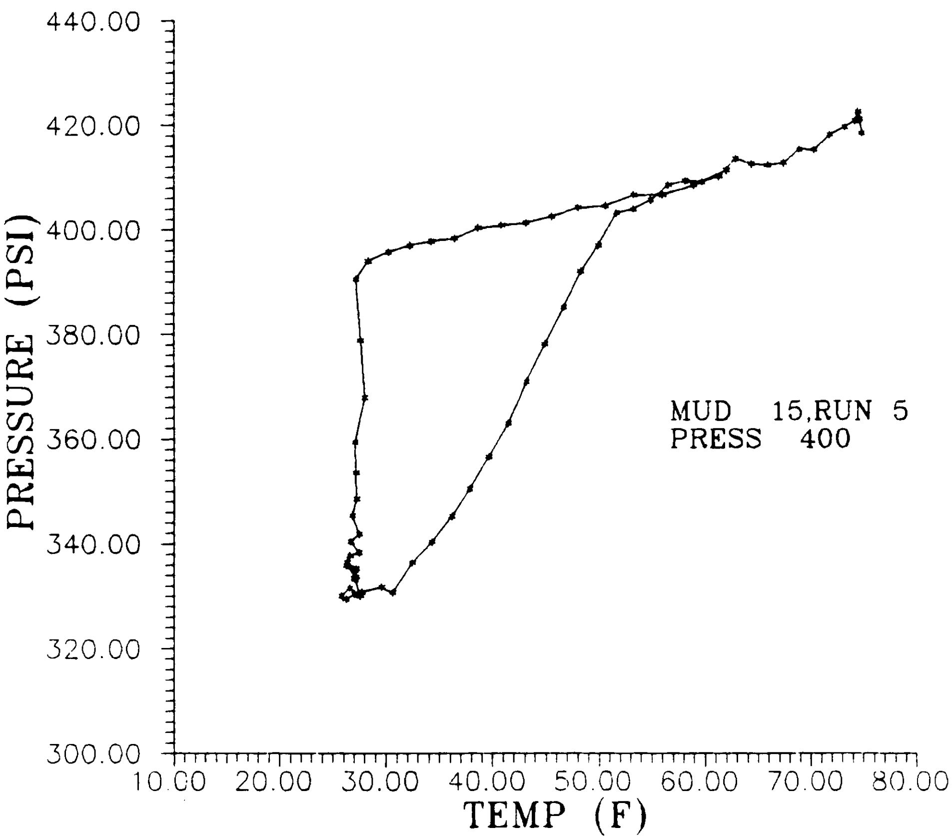
440.00
420.00
400.00
380.00
360.00
340.00
320.00
300.00
PRESSURE (PSI)
10.00 20.00 30.00 40.00 50.00 60.00 70.00 80.00
TEMP (F)
MUD 15,RUN 5
PRESS 400

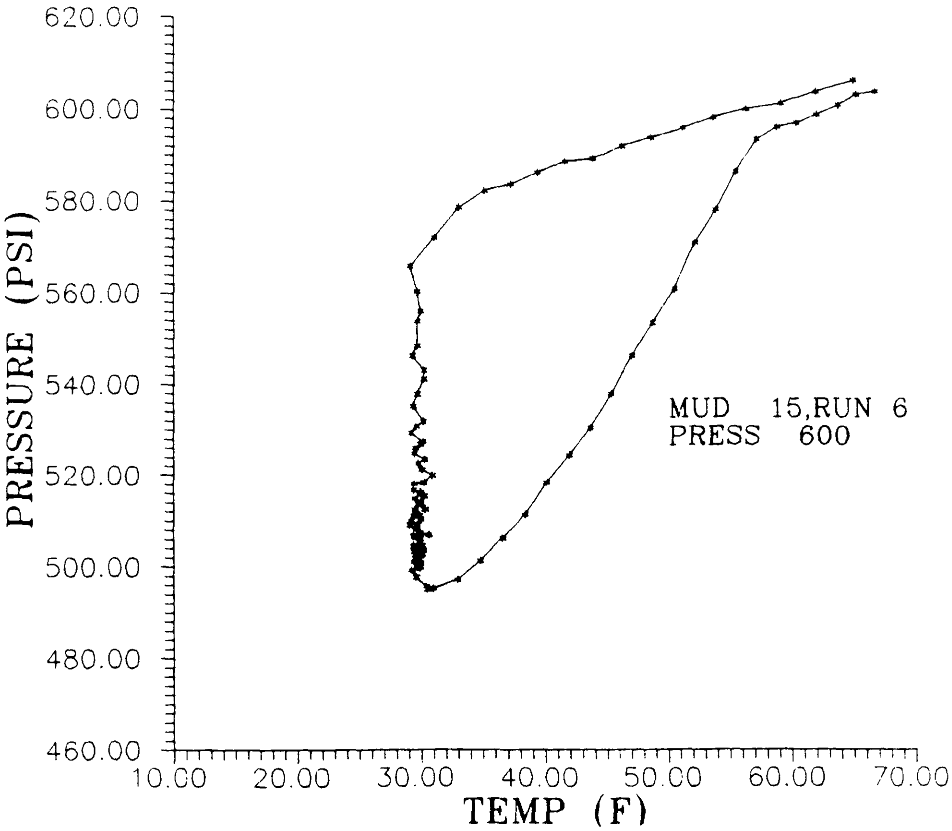

MUD 15, RUN 3D, P=800

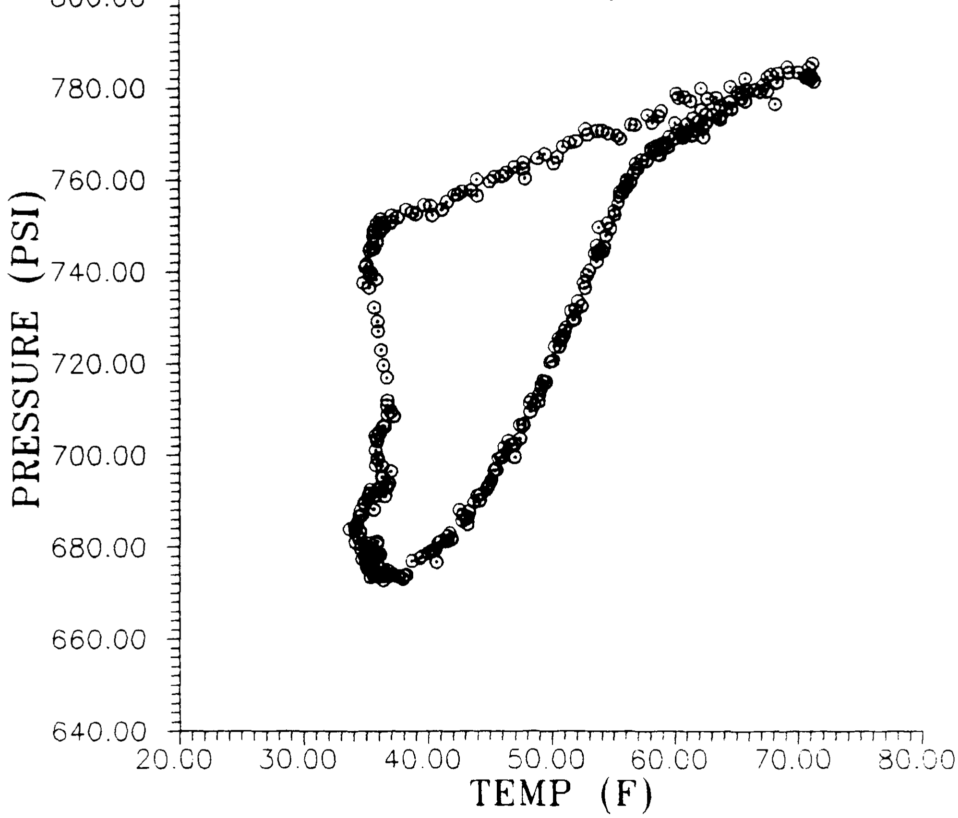

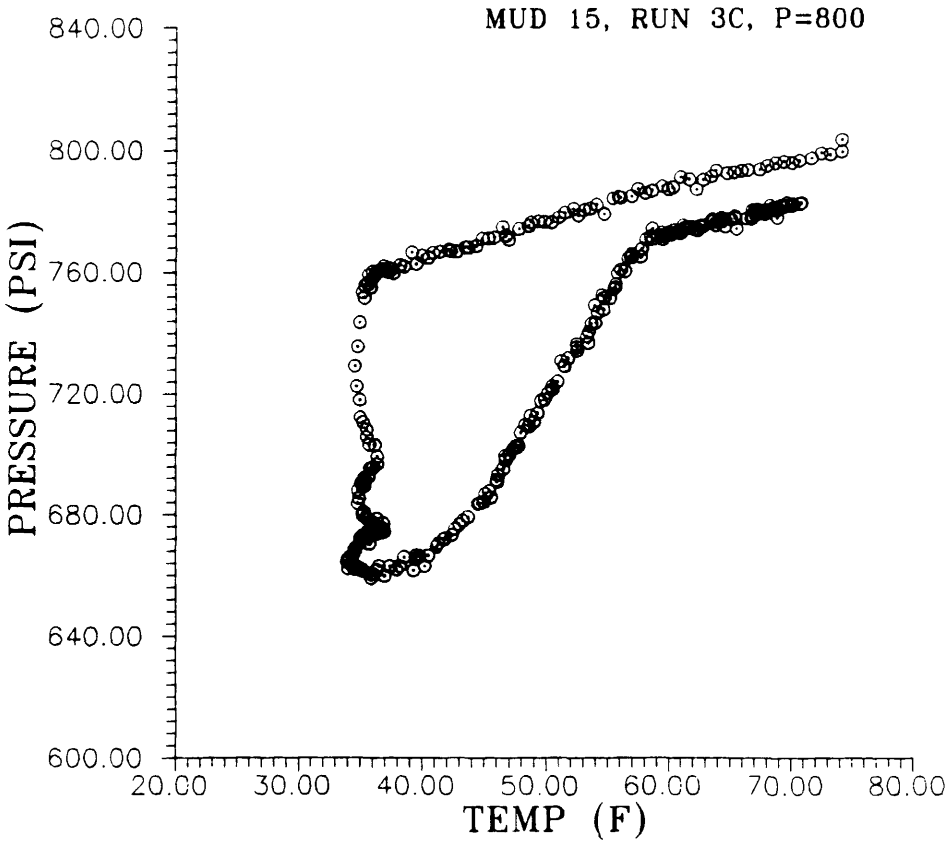
MUD 15, RUN 3C, P=800
840.00
800.00
760.00
720.00
680.00
640.00
600.00
PRESSURE (PSI)
20.00
30.00
40.00
50.00
60.00
70.00
80.00
TEMP (F)

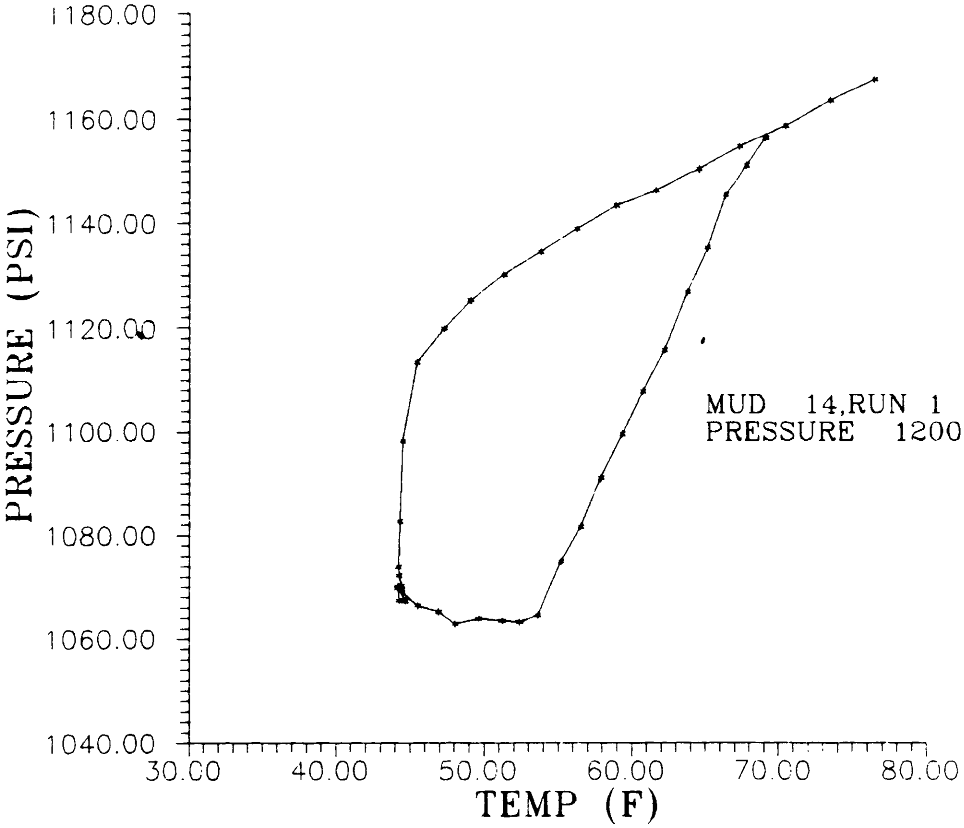
1180.00
1160.00
1140.00
1120.00
1100.00
1080.00
1060.00
1040.00
PRESSURE (PSI)
30.00
40.00
50.00
60.00
70.00
80.00
TEMP (F)
MUD 14,RUN 1
PRESSURE 1200

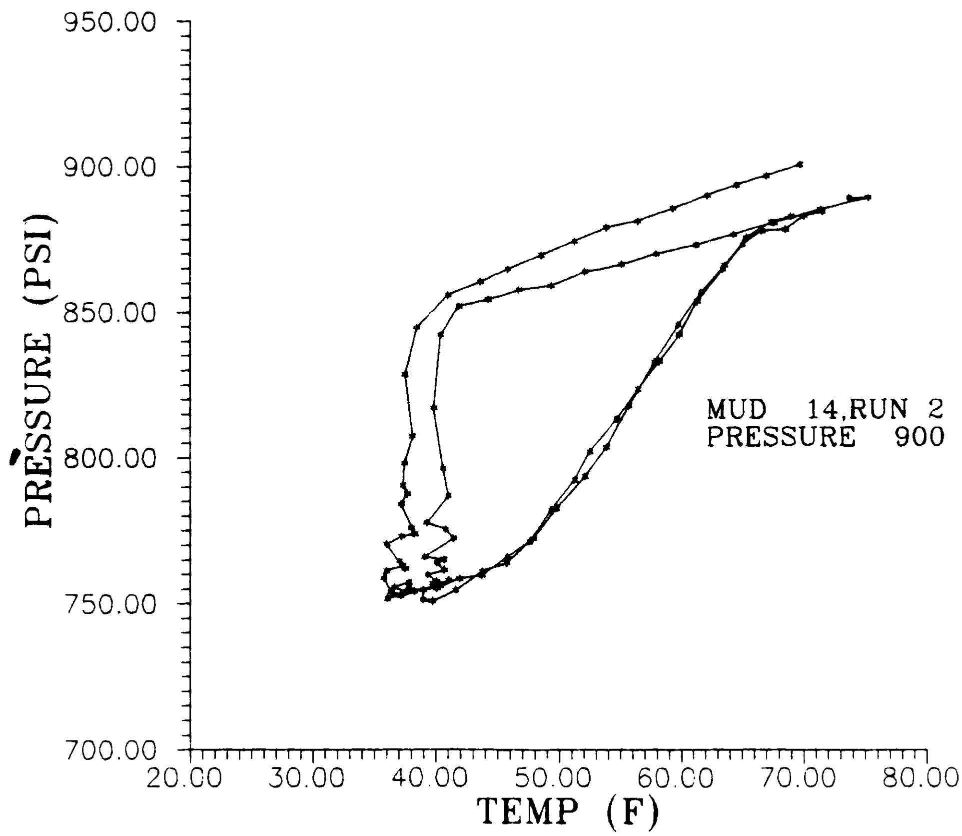
950.00
900.00
850.00
800.00
750.00
700.00
PRESSURE (PSI)
20.00
30.00
40.00
50.00
60.00
70.00
80.00
TEMP (F)
MUD 14,RUN 2
PRESSURE 900

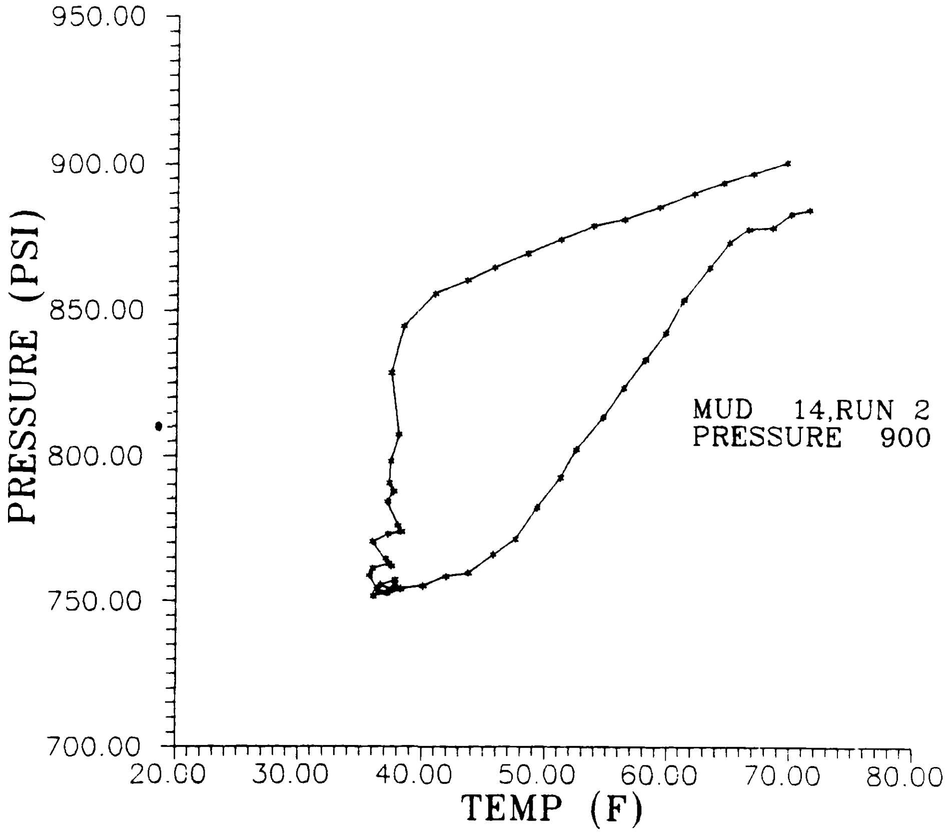
950.00
900.00
850.00
800.00
750.00
700.00
PRESSURE (PSI)
20.00
30.00
40.00
50.00
60.00
70.00
80.00
TEMP (F)
MUD 14,RUN 2
PRESSURE 900

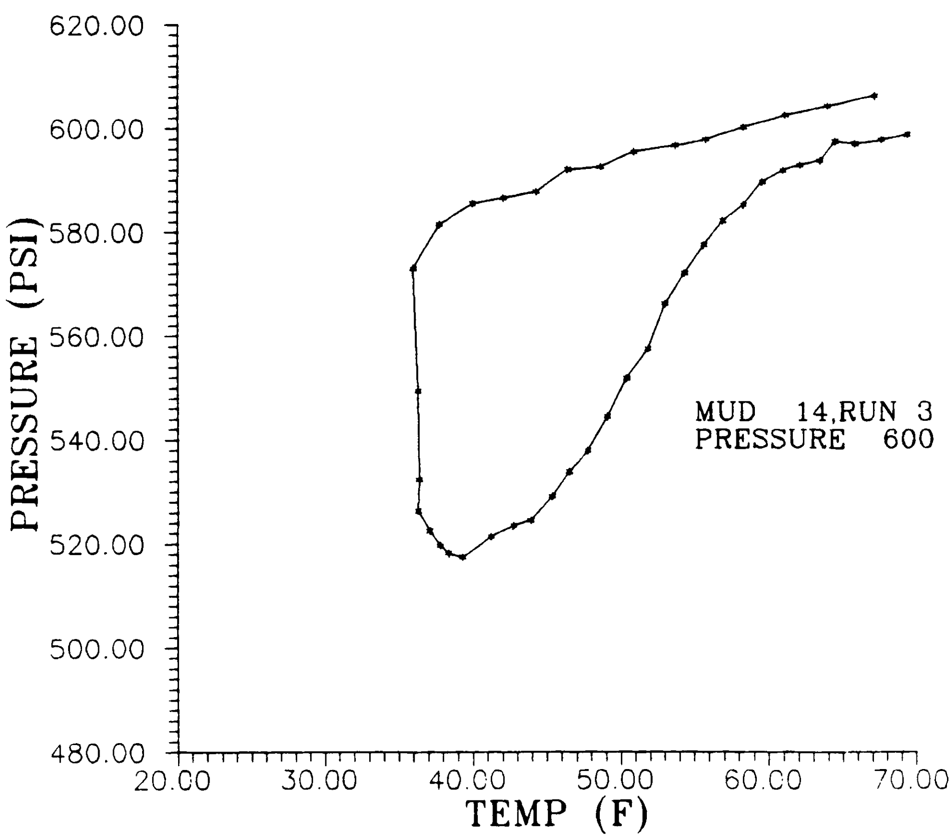
620.00
600.00
580.00
560.00
540.00
520.00
500.00
480.00
PRESSURE (PSI)
20.00
30.00
40.00
50.00
60.00
70.00
TEMP (F)
MUD 14,RUN 3
PRESSURE 600

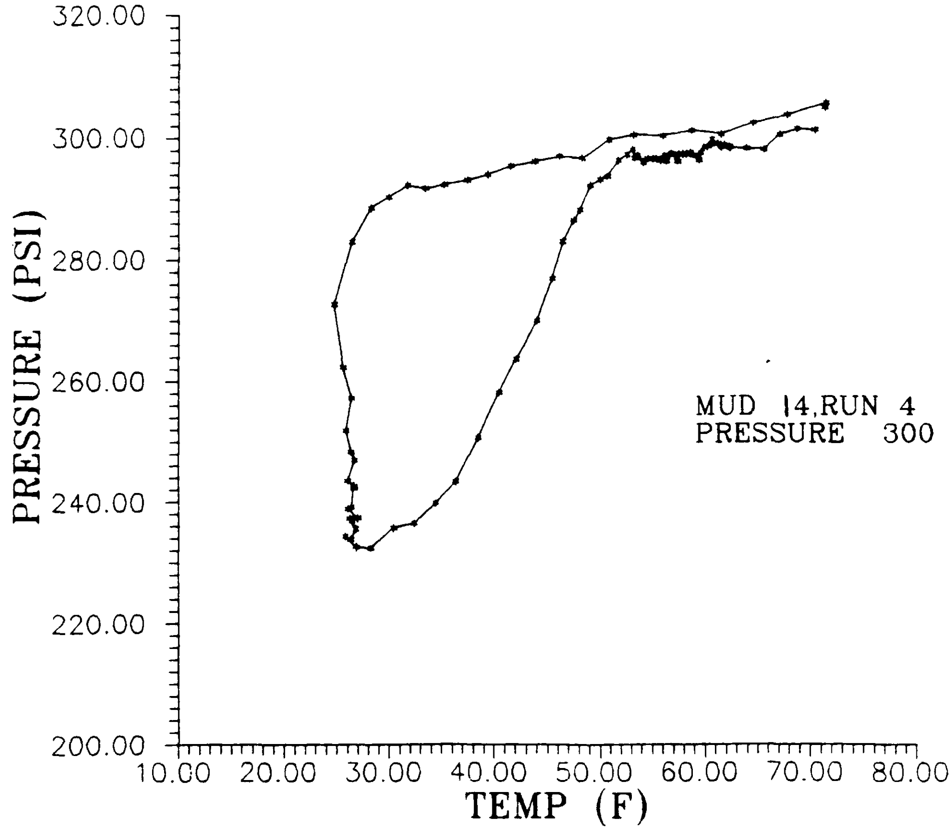
320.00
300.00
280.00
260.00
240.00
220.00
200.00
PRESSURE (PSI)
10.00 20.00 30.00 40.00 50.00 60.00 70.00 80.00
TEMP (F)
MUD 14,RUN 4
PRESSURE 300

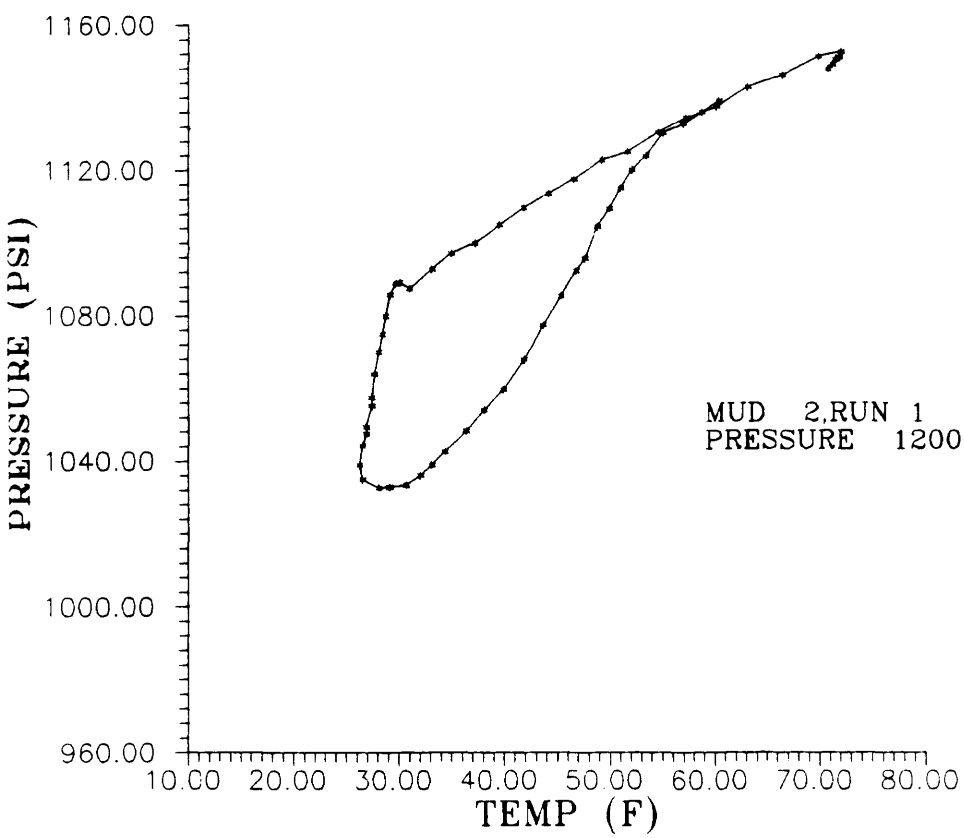
1160.00
1120.00
1080.00
1040.00
1000.00
960.00
PRESSURE (PSI)
10.00 20.00 30.00 40.00 50.00 60.00 70.00 80.00
TEMP (F)
MUD 2,RUN 1
PRESSURE 1200

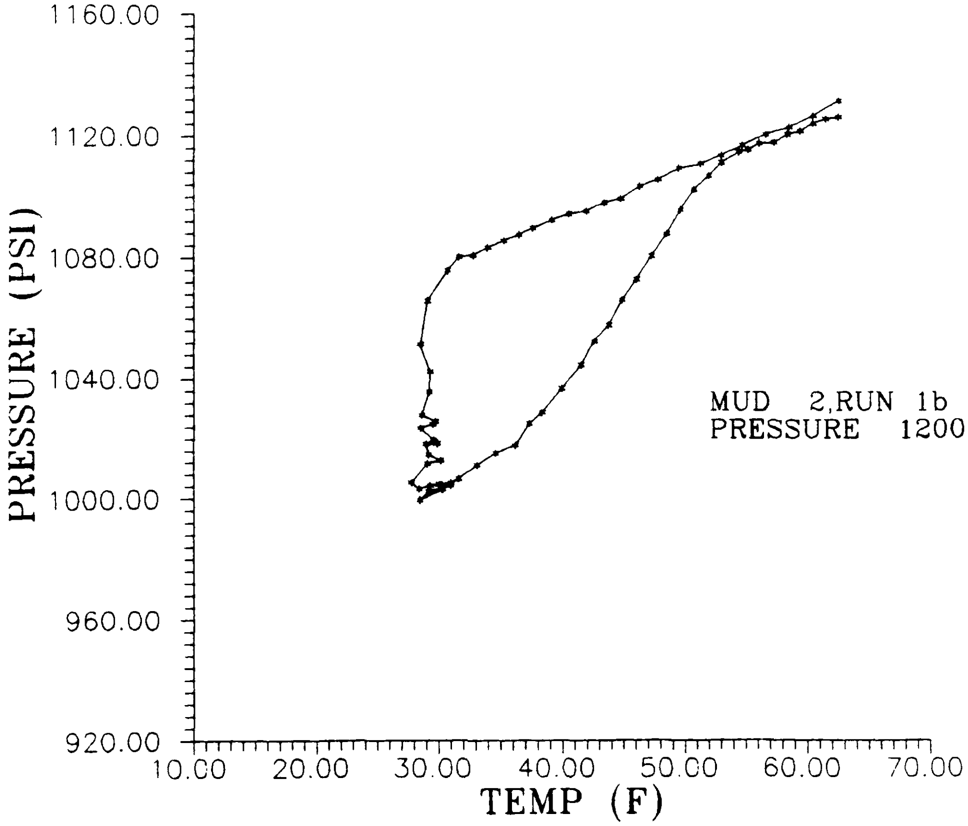
1160.00
1120.00
1080.00
1040.00
1000.00
960.00
920.00
PRESSURE (PSI)
10.00
20.00
30.00
40.00
50.00
60.00
70.00
TEMP (F)
MUD 2,RUN 1b
PRESSURE 1200

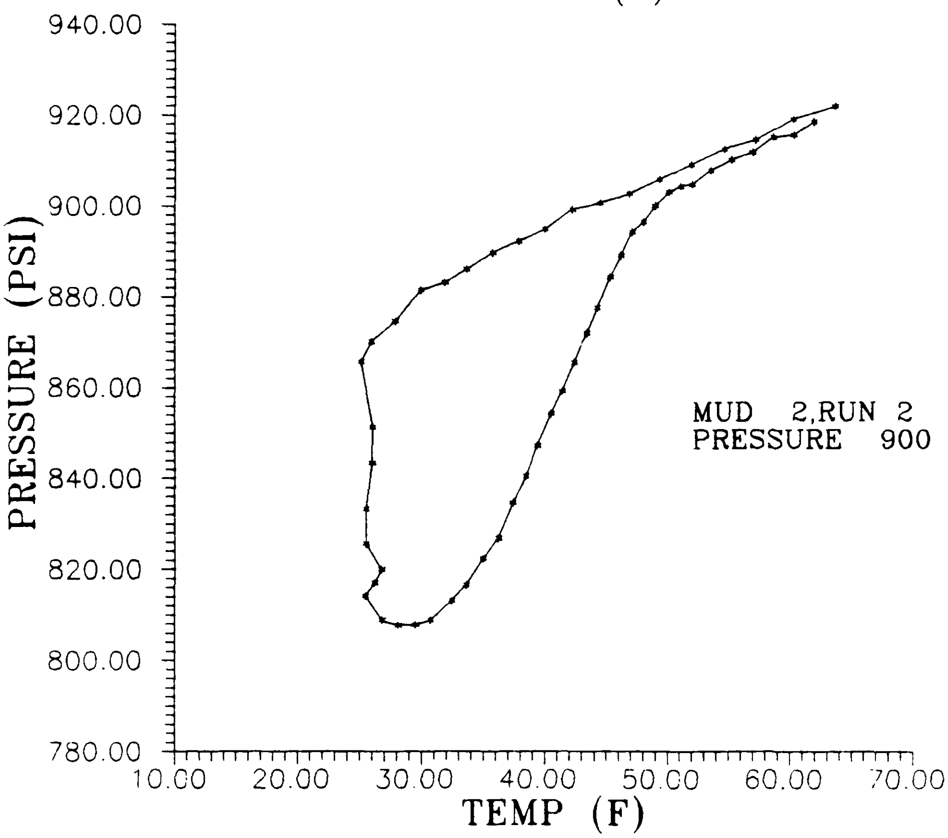
940.00
920.00
900.00
880.00
860.00
840.00
820.00
800.00
780.00
PRESSURE (PSI)
10.00
20.00
30.00
40.00
50.00
60.00
70.00
TEMP (F)
MUD 2,RUN 2
PRESSURE 900

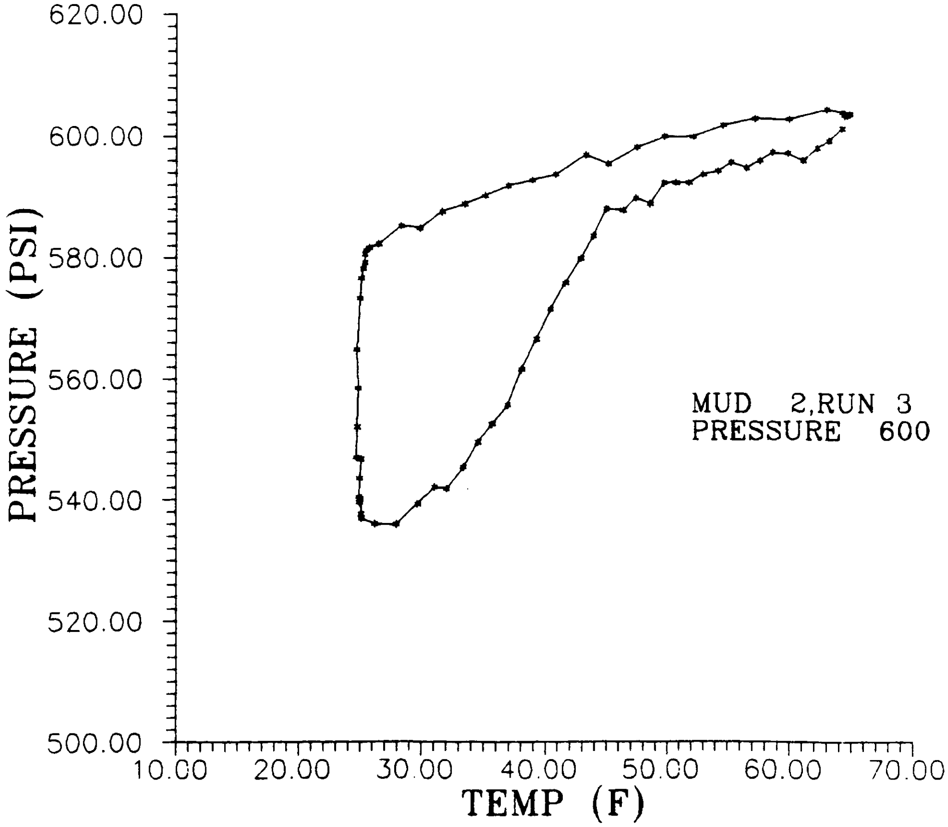
620.00
600.00
580.00
560.00
540.00
520.00
500.00
PRESSURE (PSI)
MUD 2,RUN 3
PRESSURE 600
10.00
20.00
30.00
40.00
50.00
60.00
70.00
TEMP (F)

MUD 5, RUN 1

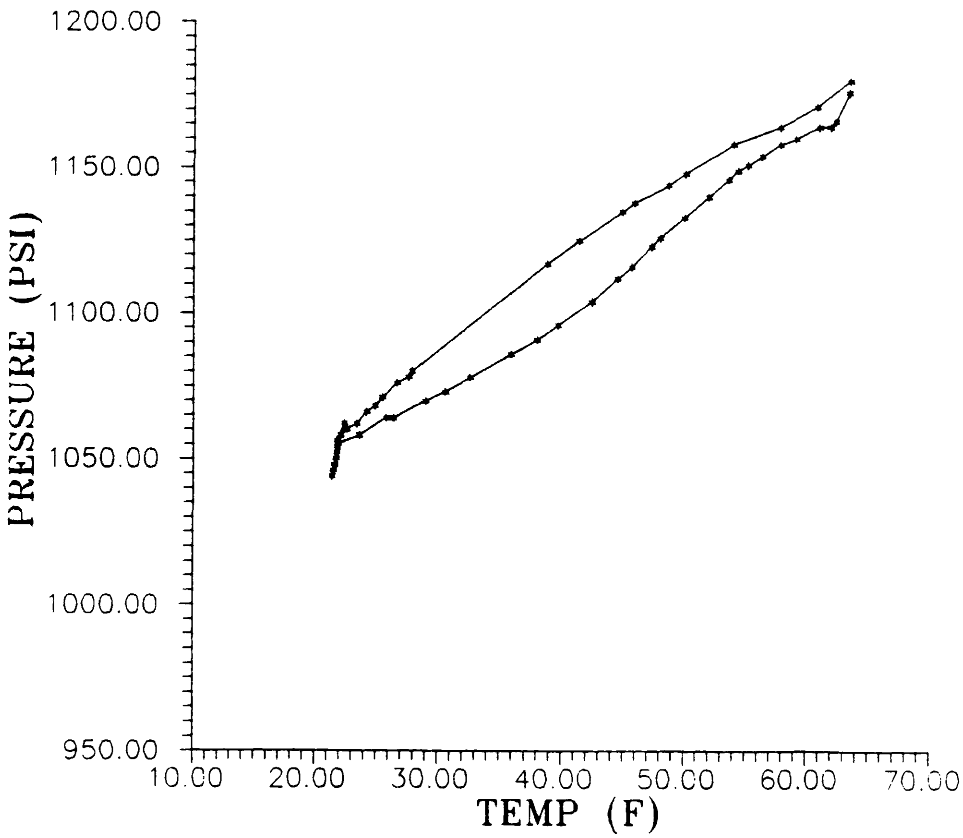
1200.00
1150.00
1100.00
1050.00
1000.00
950.00
PRESSURE (PSI)
10.00
20.00
30.00
40.00
50.00
60.00
70.00
TEMP (F)

MUD 5,RUN 2

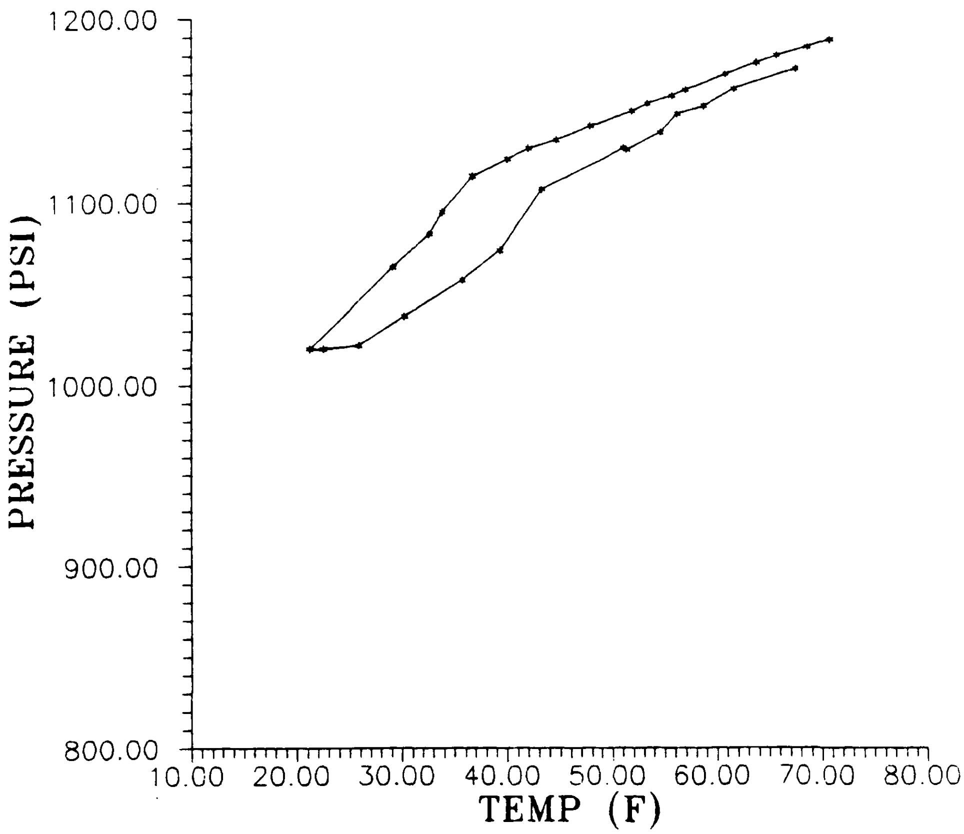

MUD 5

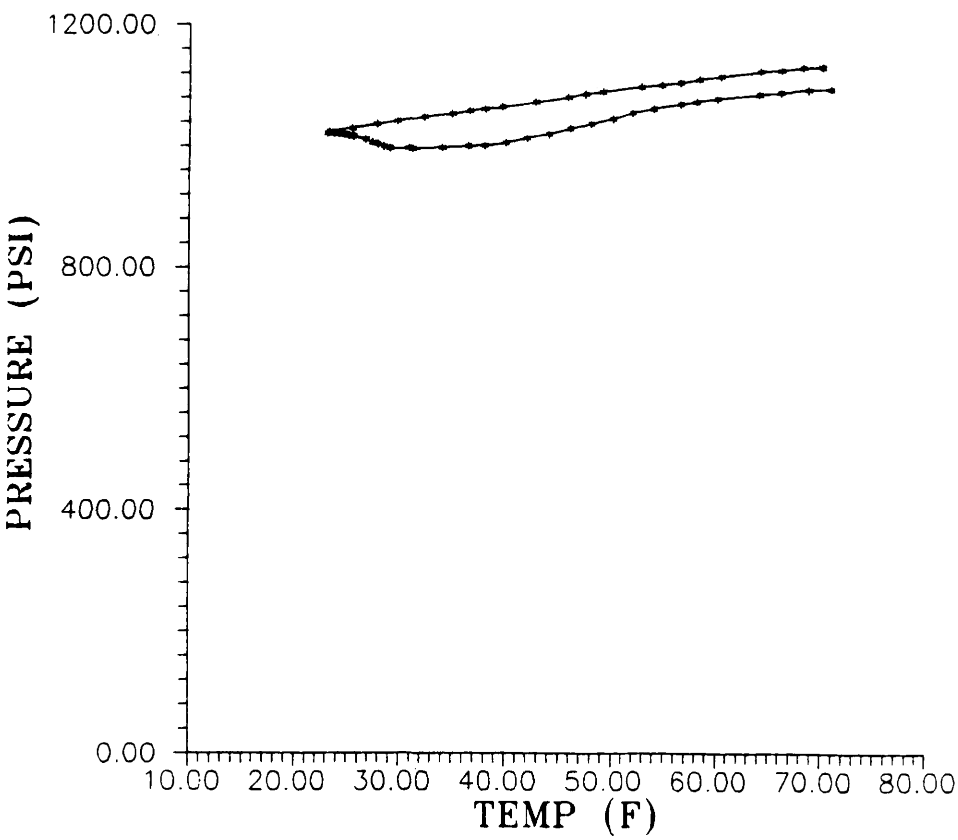

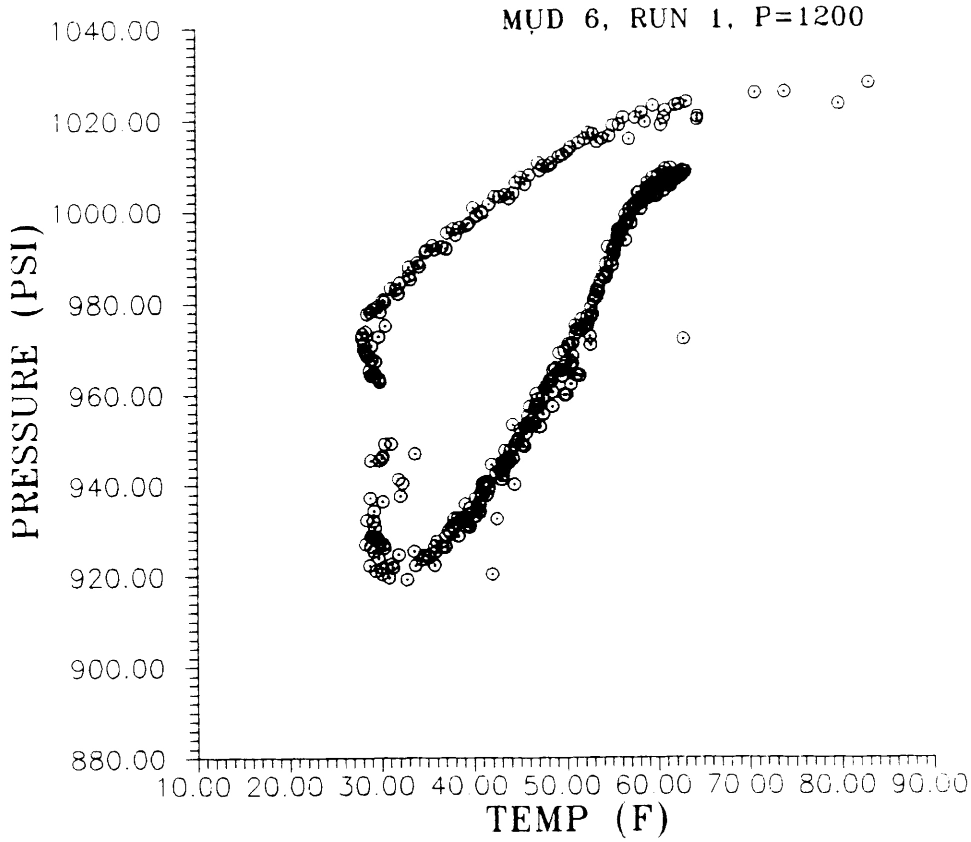
MUD 6, RUN 1, P=1200
PRESSURE (PSI)
1040.00
1020.00
1000.00
980.00
960.00
940.00
920.00
900.00
880.00
10.00 20.00 30.00 40.00 50.00 60.00 70.00 80.00 90.00
TEMP (F)

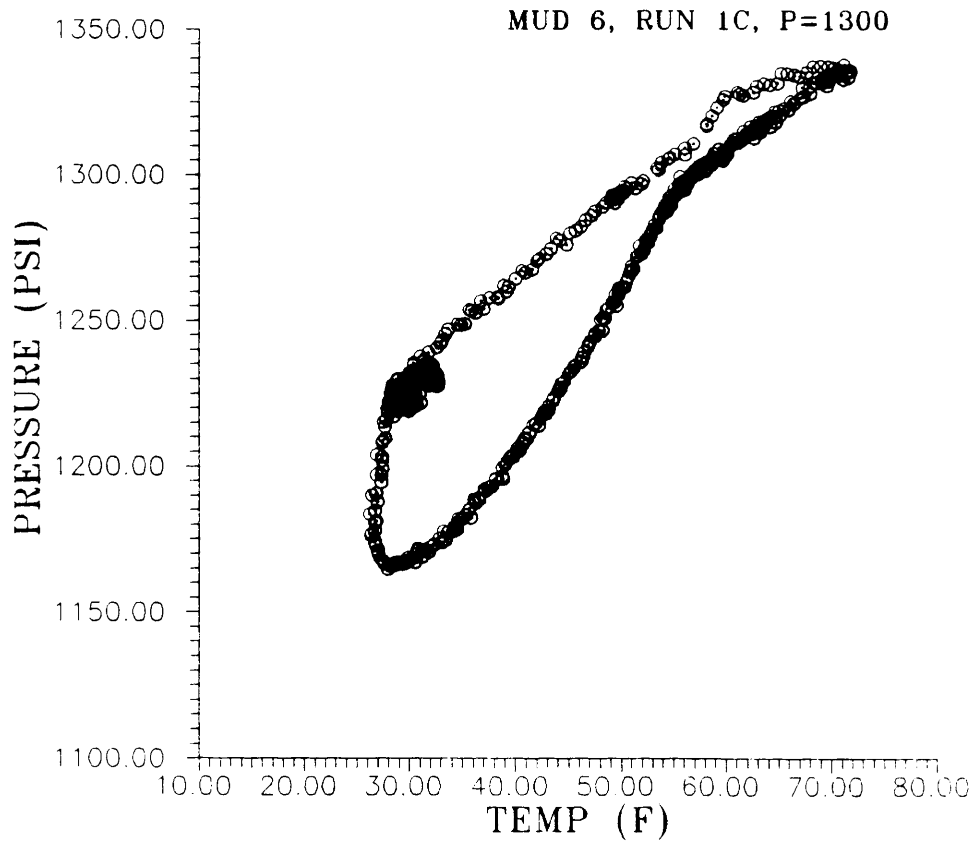
MUD 6, RUN 1C, P=1300
PRESSURE (PSI)
1350.00
1300.00
1250.00
1200.00
1150.00
1100.00
10.00 20.00 30.00 40.00 50.00 60.00 70.00 80.00
TEMP (F)

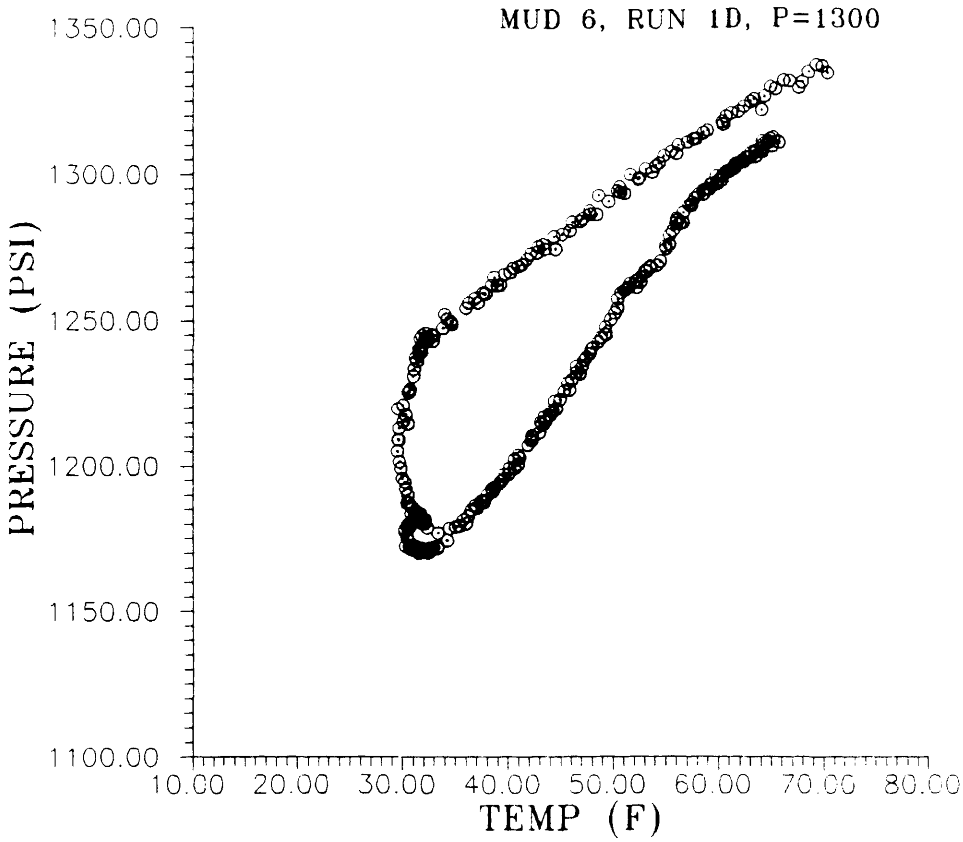
MUD 6, RUN 1D, P=1300
PRESSURE (PSI)
1350.00
1300.00
1250.00
1200.00
1150.00
1100.00
10.00
20.00
30.00
40.00
50.00
60.00
70.00
80.00
TEMP (F)

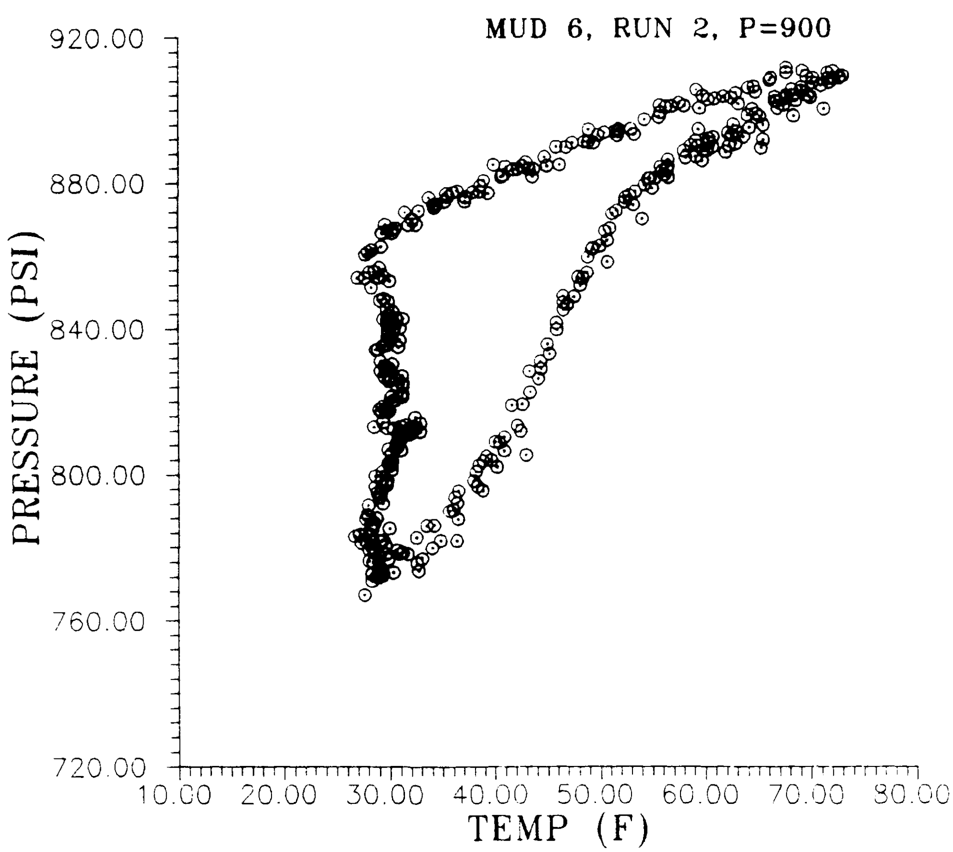
MUD 6, RUN 2, P=900
PRESSURE (PSI)
920.00
880.00
840.00
800.00
760.00
720.00
10.00
20.00
30.00
40.00
50.00
60.00
70.00
80.00
TEMP (F)

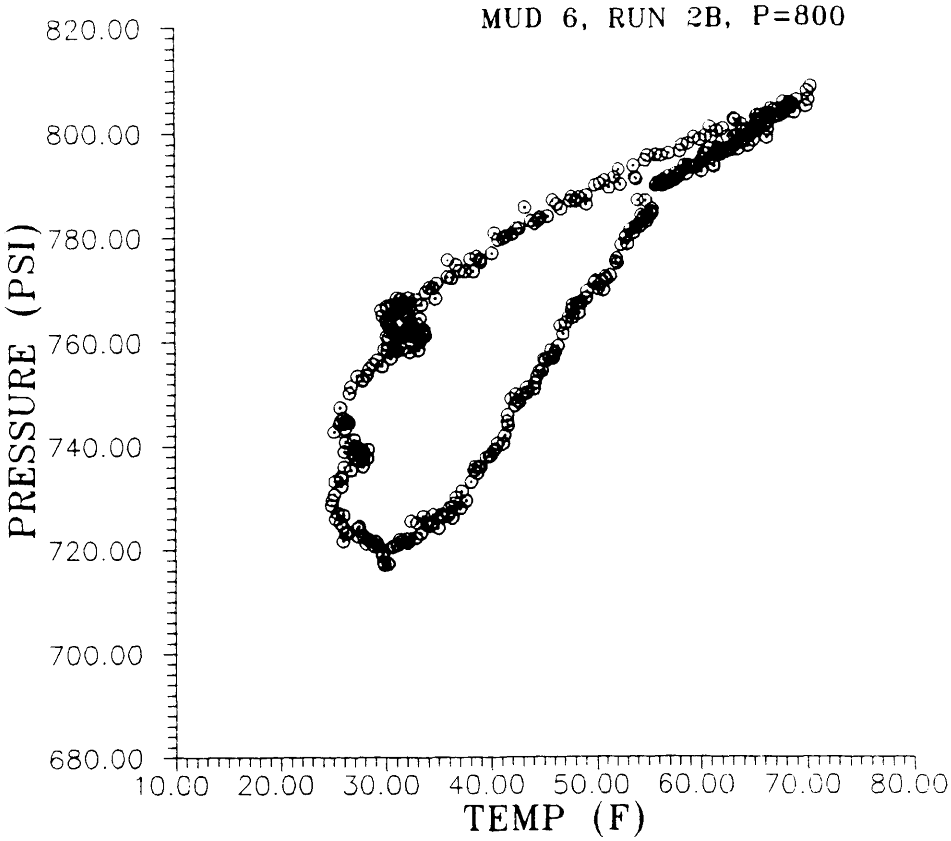
MUD 6, RUN 2B, P=800
PRESSURE (PSI)
820.00
800.00
780.00
760.00
740.00
720.00
700.00
680.00
10.00 20.00 30.00 40.00 50.00 60.00 70.00 80.00
TEMP (F)

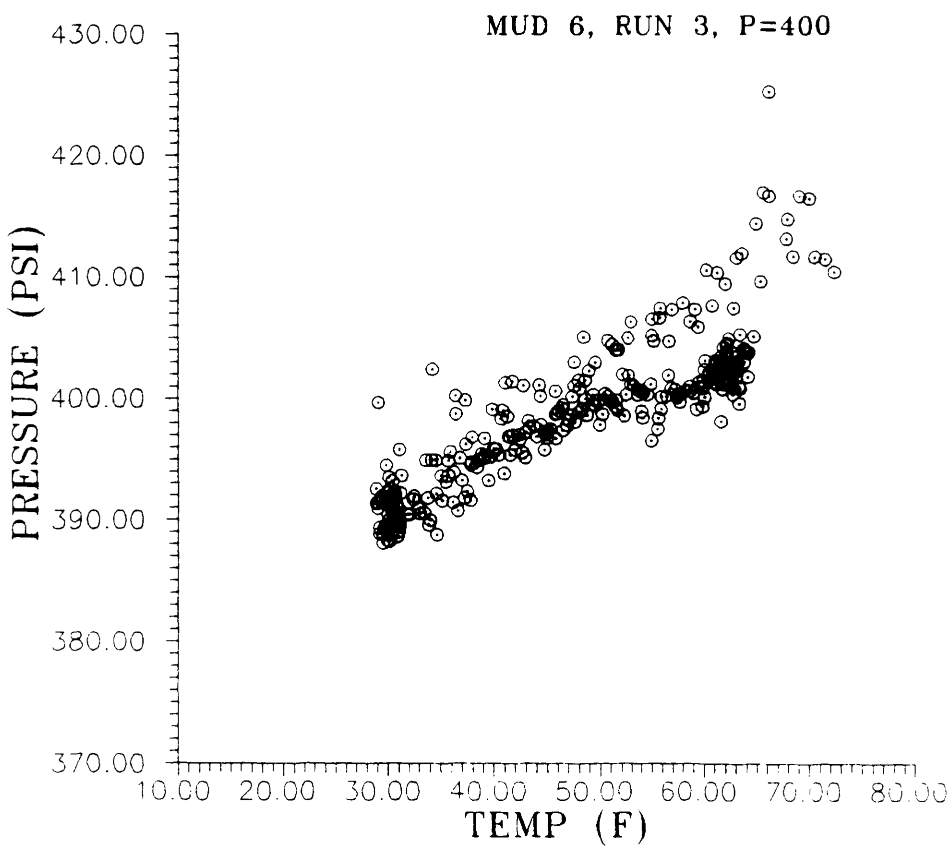
MUD 6, RUN 3, P=400
PRESSURE (PSI)
430.00
420.00
410.00
400.00
390.00
380.00
370.00
10.00 20.00 30.00 40.00 50.00 60.00 70.00 80.00
TEMP (F)

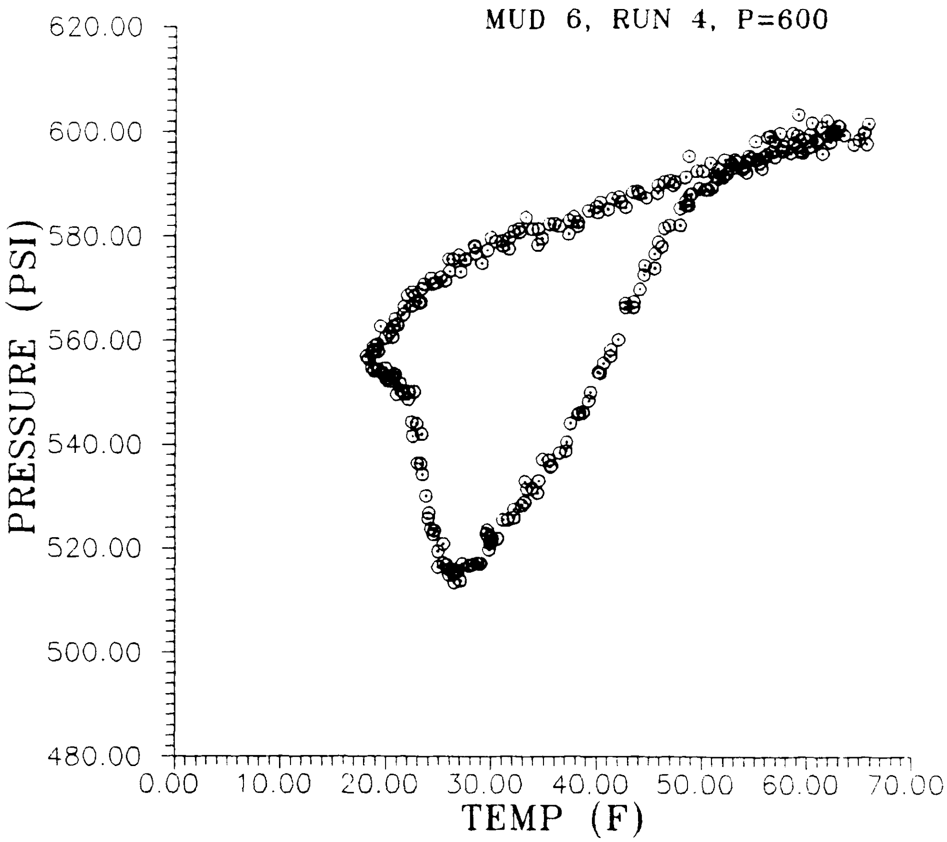
MUD 6, RUN 4, P=600
PRESSURE (PSI)
620.00
600.00
580.00
560.00
540.00
520.00
500.00
480.00
0.00
10.00
20.00
30.00
40.00
50.00
60.00
70.00
TEMP (F)

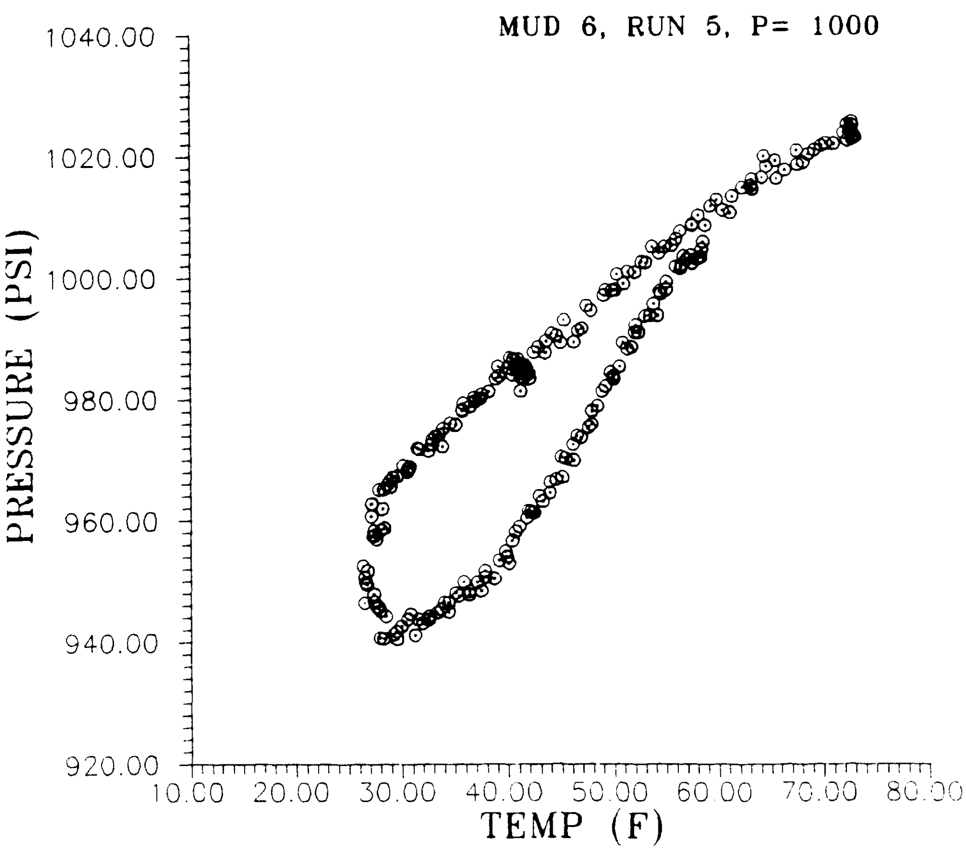
MUD 6, RUN 5, P= 1000
PRESSURE (PSI)
1040.00
1020.00
1000.00
980.00
960.00
940.00
920.00
10.00
20.00
30.00
40.00
50.00
60.00
70.00
80.00
TEMP (F)

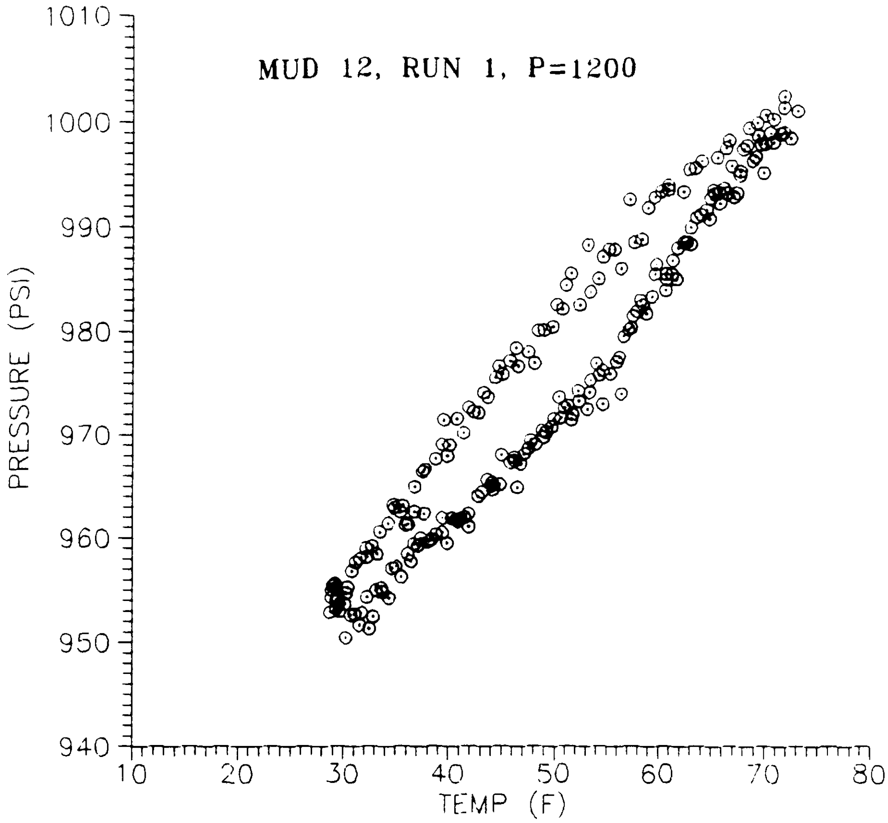
MUD 12, RUN 1, P=1200
PRESSURE (PSI)
1010
1000
990
980
970
960
950
940
10
20
30
40
50
60
70
80
TEMP (F)

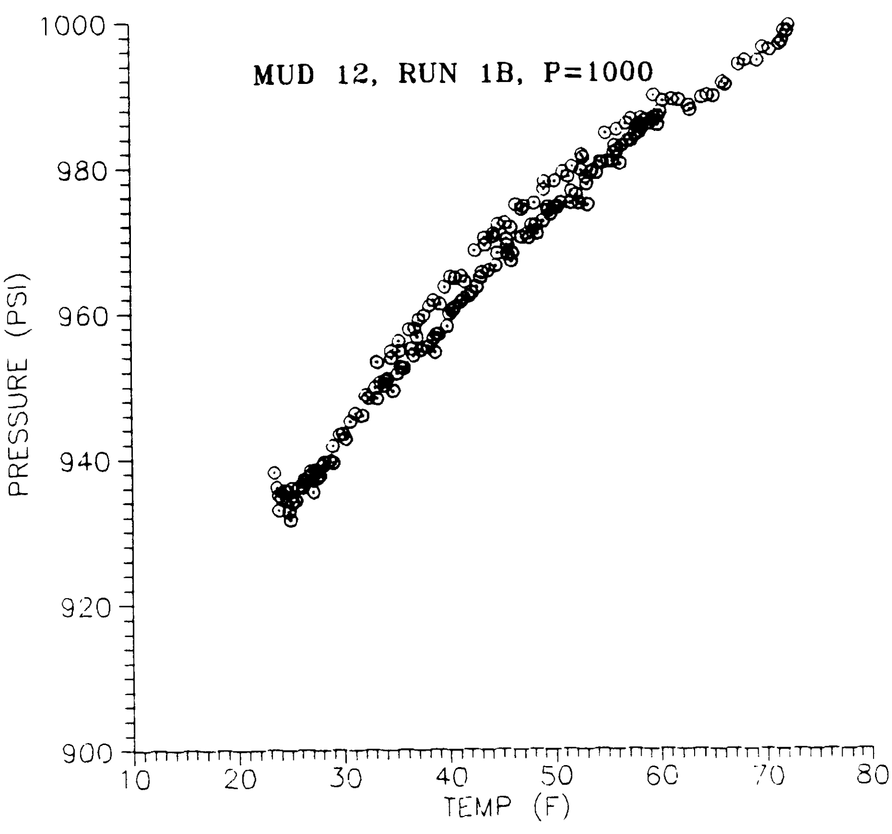
MUD 12, RUN 1B, P=1000
PRESSURE (PSI)
1000
980
960
940
920
900
10
20
30
40
50
60
70
80
TEMP (F)

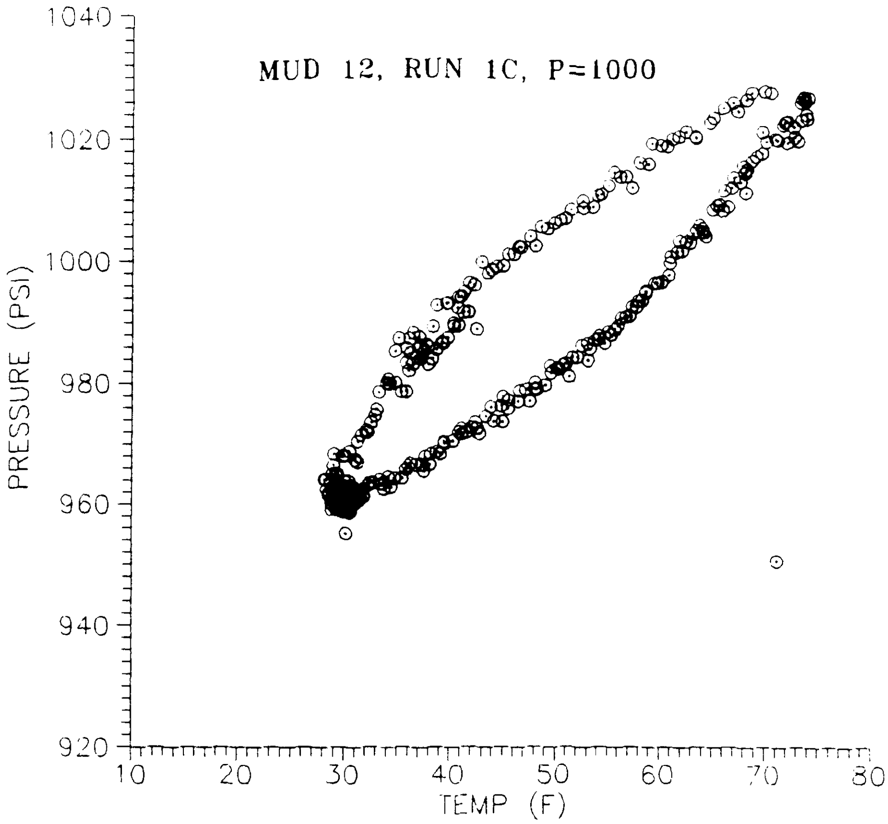
MUD 12, RUN 1C, P=1000
PRESSURE (PSI)
TEMP (F)
1040
1020
1000
980
960
940
920
10
20
30
40
50
60
70
80

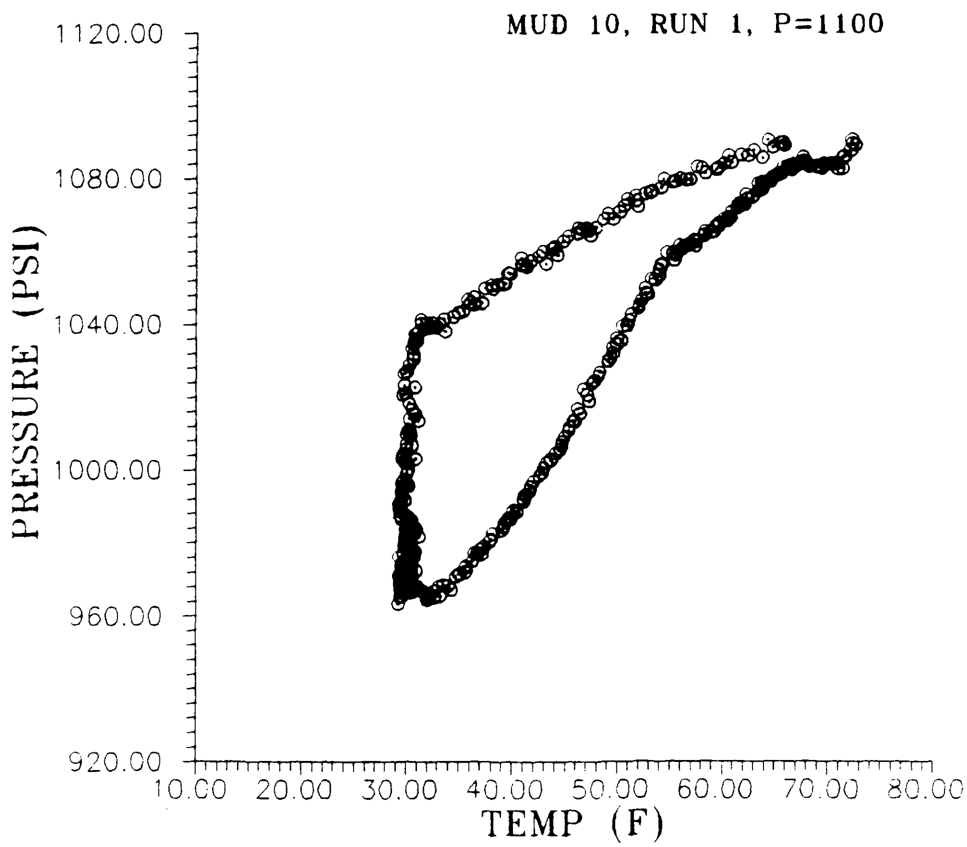
MUD 10, RUN 1, P=1100
PRESSURE (PSI)
TEMP (F)
1120.00
1080.00
1040.00
1000.00
960.00
920.00
10.00
20.00
30.00
40.00
50.00
60.00
70.00
80.00

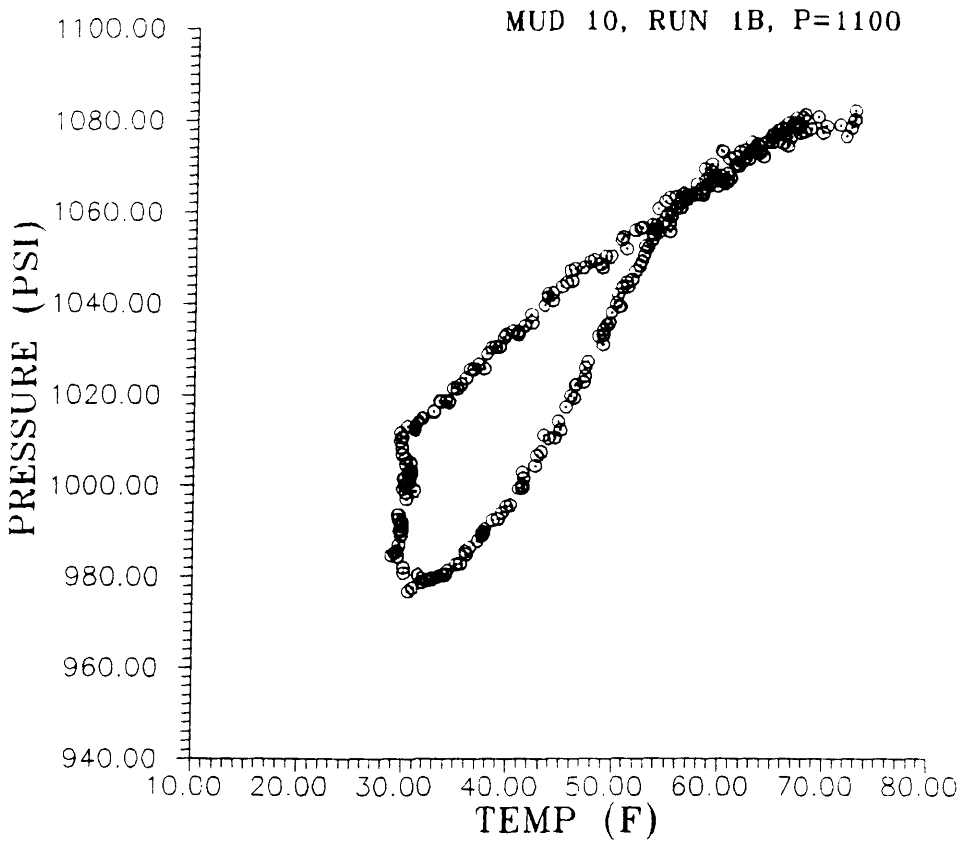
MUD 10, RUN 1B, P=1100
PRESSURE (PSI)
1100.00
1080.00
1060.00
1040.00
1020.00
1000.00
980.00
960.00
940.00
10.00 20.00 30.00 40.00 50.00 60.00 70.00 80.00
TEMP (F)

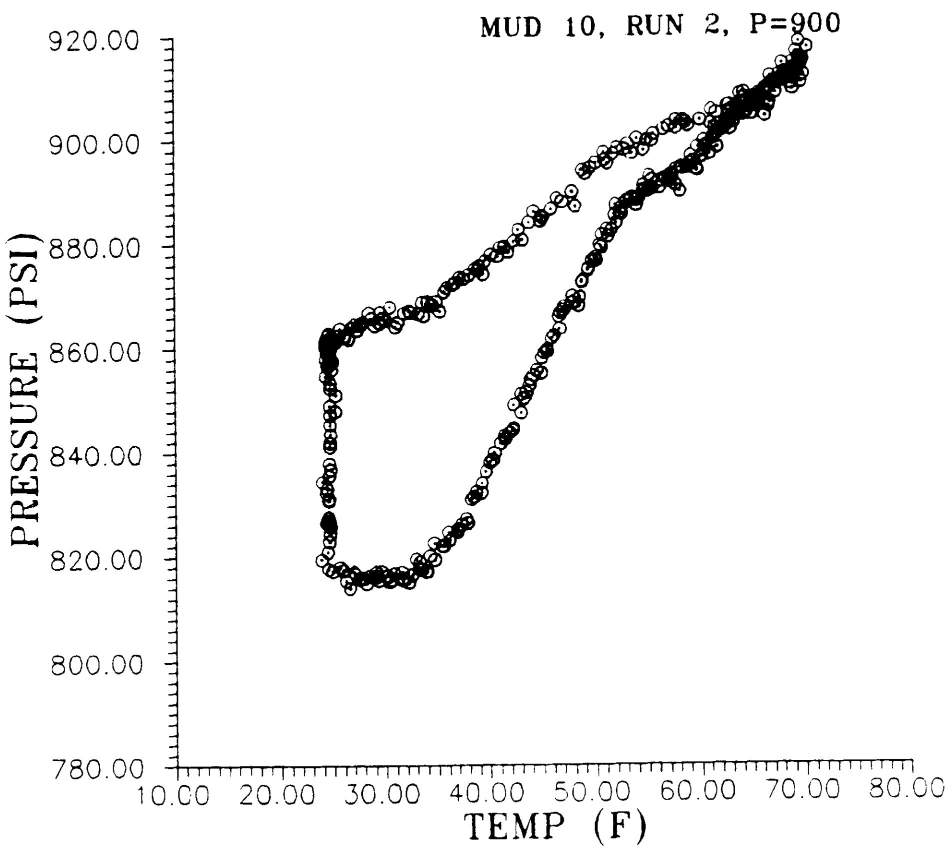
MUD 10, RUN 2, P=900
PRESSURE (PSI)
920.00
900.00
880.00
860.00
840.00
820.00
800.00
780.00
10.00 20.00 30.00 40.00 50.00 60.00 70.00 80.00
TEMP (F)

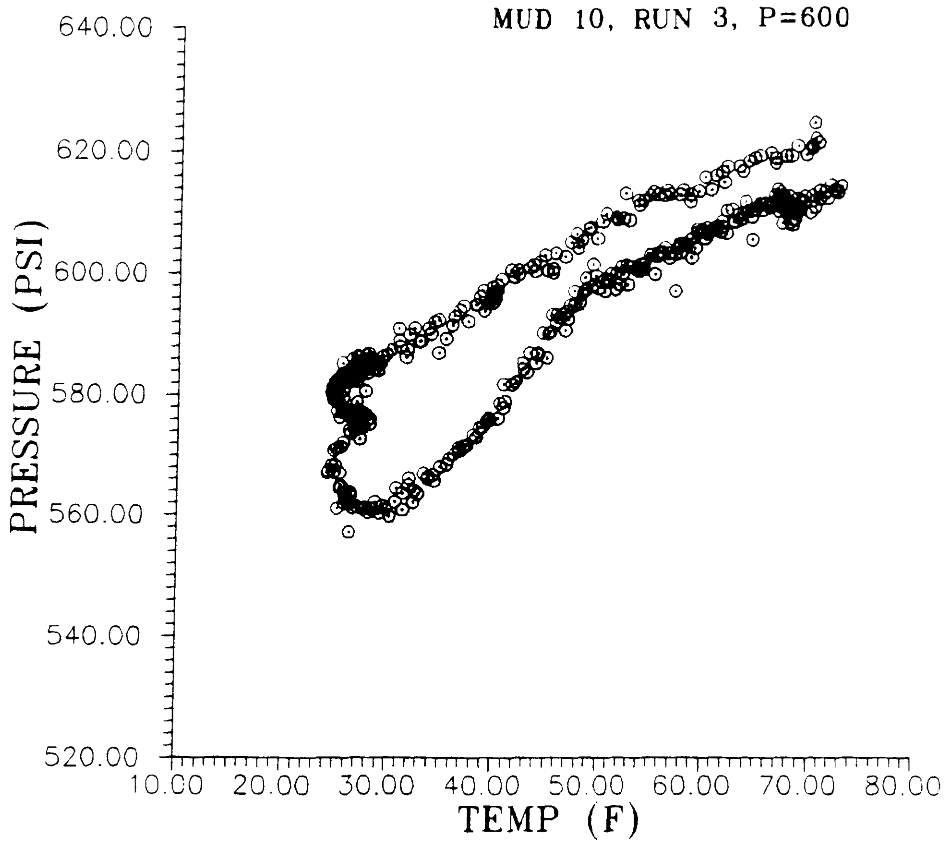
MUD 10, RUN 3, P=600
PRESSURE (PSI)
640.00
620.00
600.00
580.00
560.00
540.00
520.00
10.00
20.00
30.00
40.00
50.00
60.00
70.00
80.00
TEMP (F)

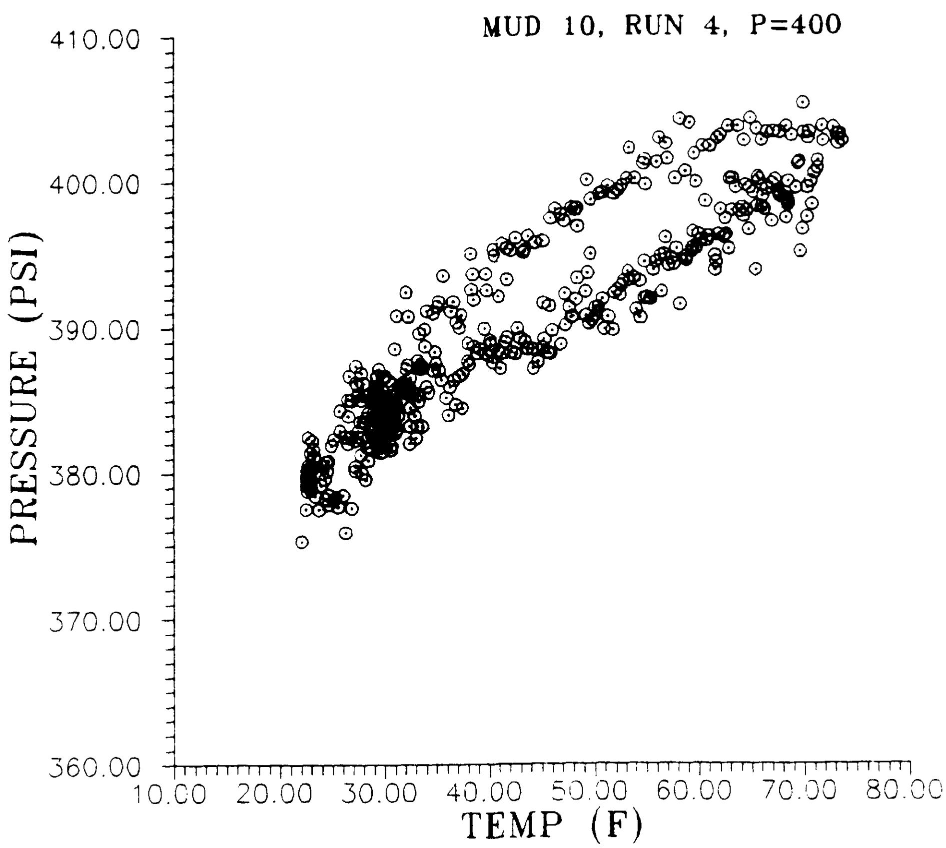
MUD 10, RUN 4, P=400
PRESSURE (PSI)
410.00
400.00
390.00
380.00
370.00
360.00
10.00
20.00
30.00
40.00
50.00
60.00
70.00
80.00
TEMP (F)

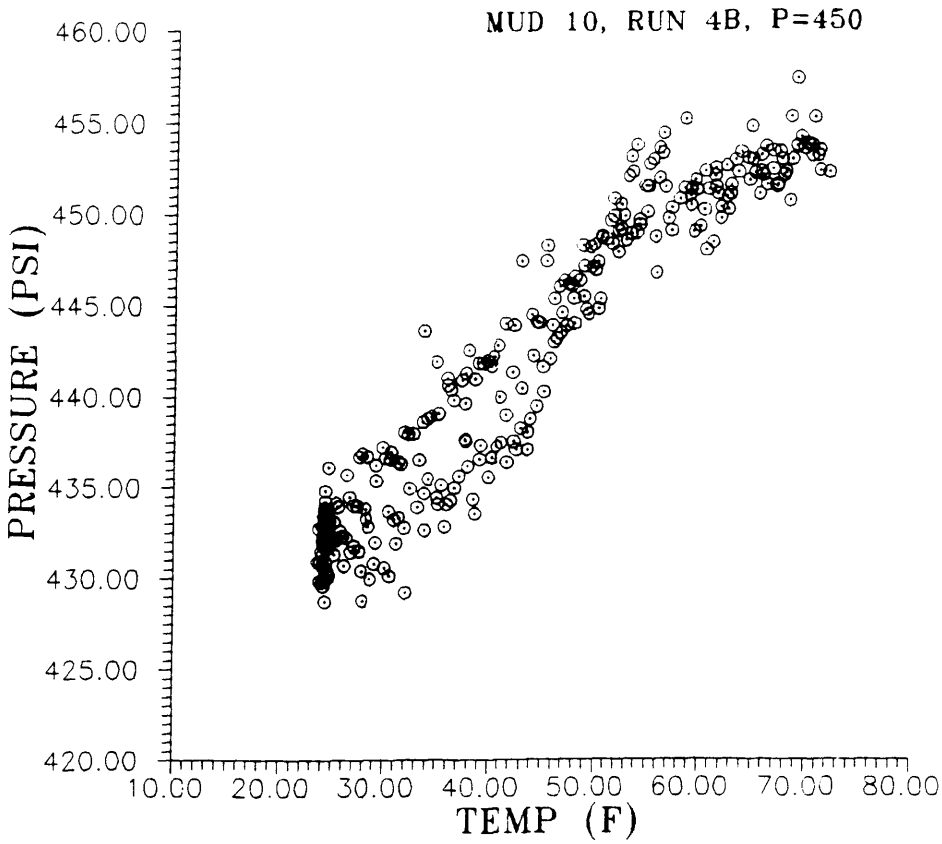
MUD 10, RUN 4B, P=450
PRESSURE (PSI)
TEMP (F)
460.00
455.00
450.00
445.00
440.00
435.00
430.00
425.00
420.00
10.00
20.00
30.00
40.00
50.00
60.00
70.00
80.00

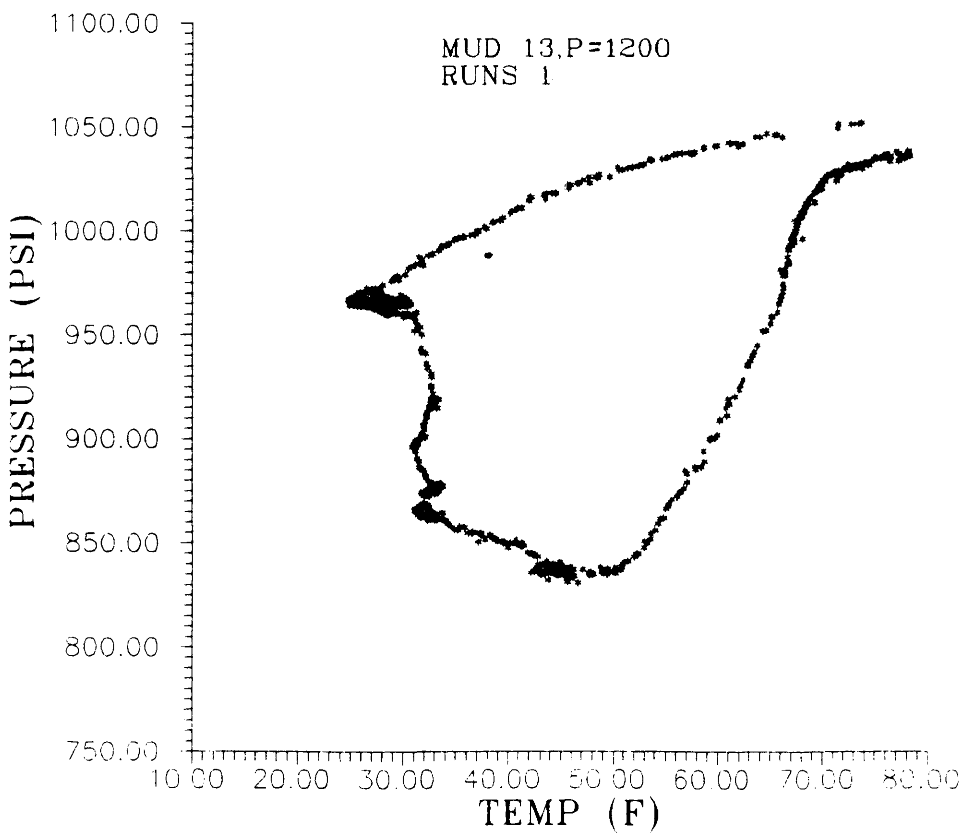
MUD 13,P=1200
RUNS 1
PRESSURE (PSI)
TEMP (F)
1100.00
1050.00
1000.00
950.00
900.00
850.00
800.00
750.00
10.00
20.00
30.00
40.00
50.00
60.00
70.00
80.00

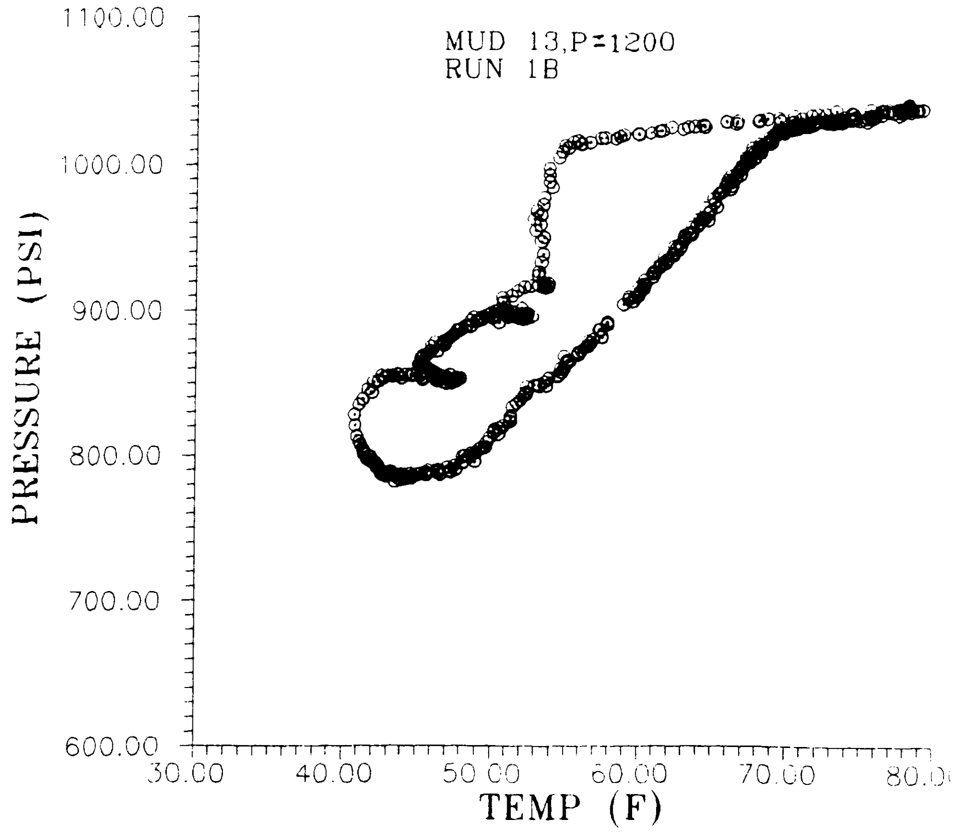
MUD 13,P=1200
RUN 1B
1100.00
1000.00
900.00
800.00
700.00
600.00
PRESSURE (PSI)
30.00
40.00
50.00
60.00
70.00
80.00
TEMP (F)

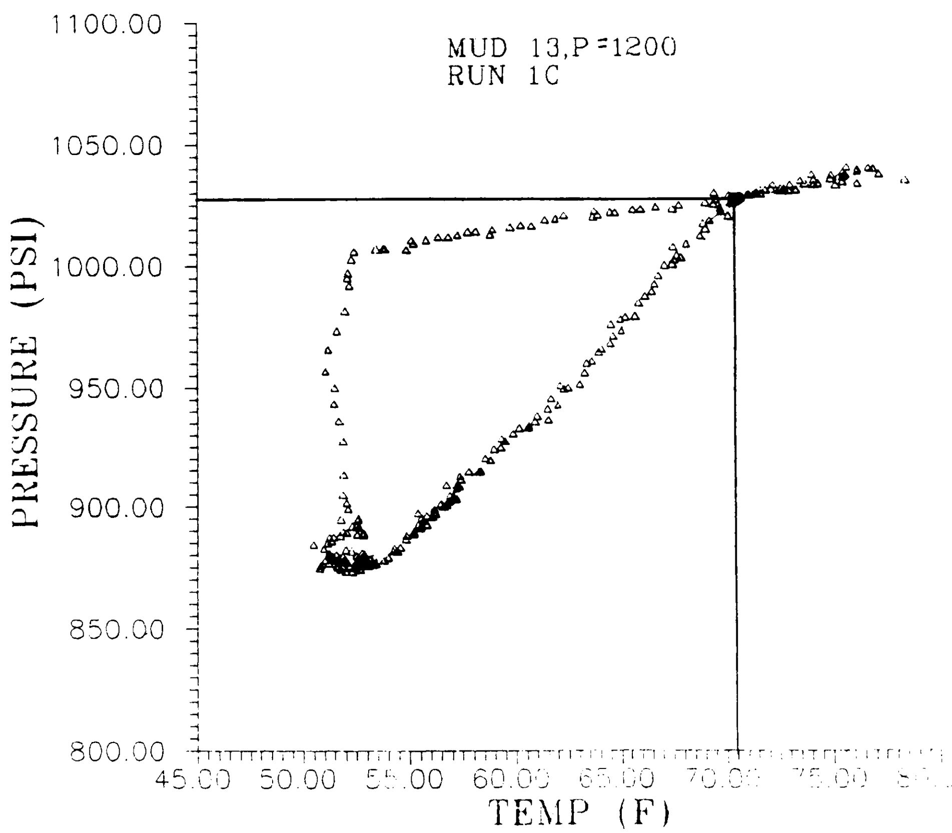
MUD 13,P=1200
RUN 1C
1100.00
1050.00
1000.00
950.00
900.00
850.00
800.00
PRESSURE (PSI)
45.00
50.00
55.00
60.00
65.00
70.00
75.00
TEMP (F)

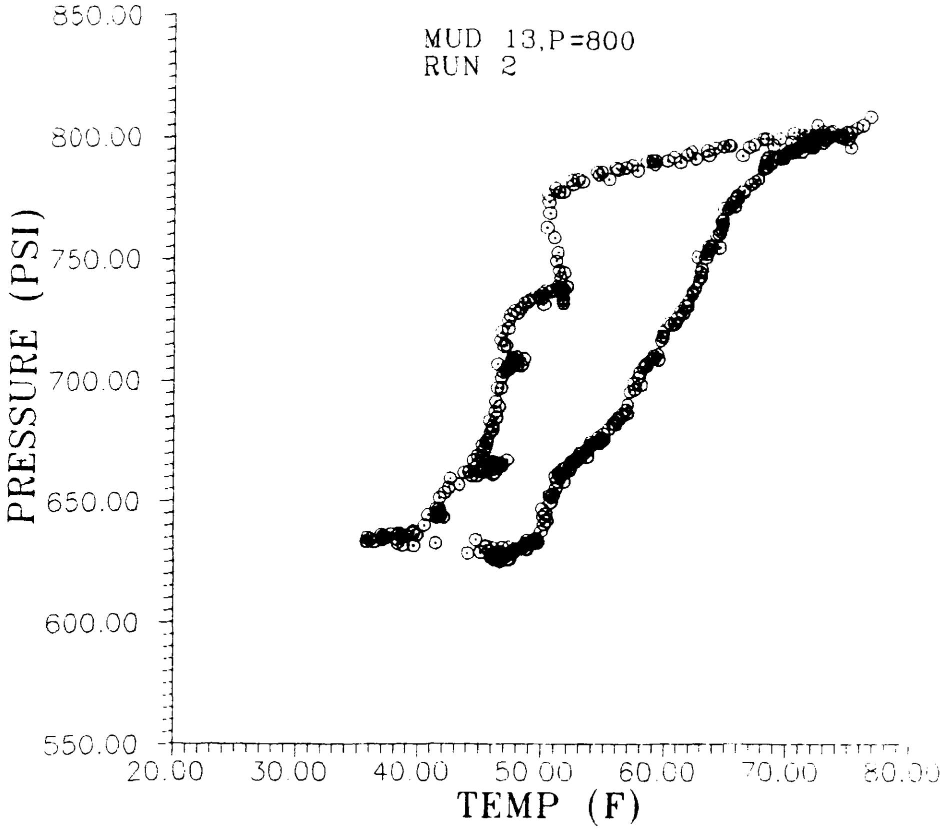
MUD 13,P=800
RUN 2
PRESSURE (PSI)
TEMP (F)
850.00
800.00
750.00
700.00
650.00
600.00
550.00
20.00
30.00
40.00
50.00
60.00
70.00
80.00

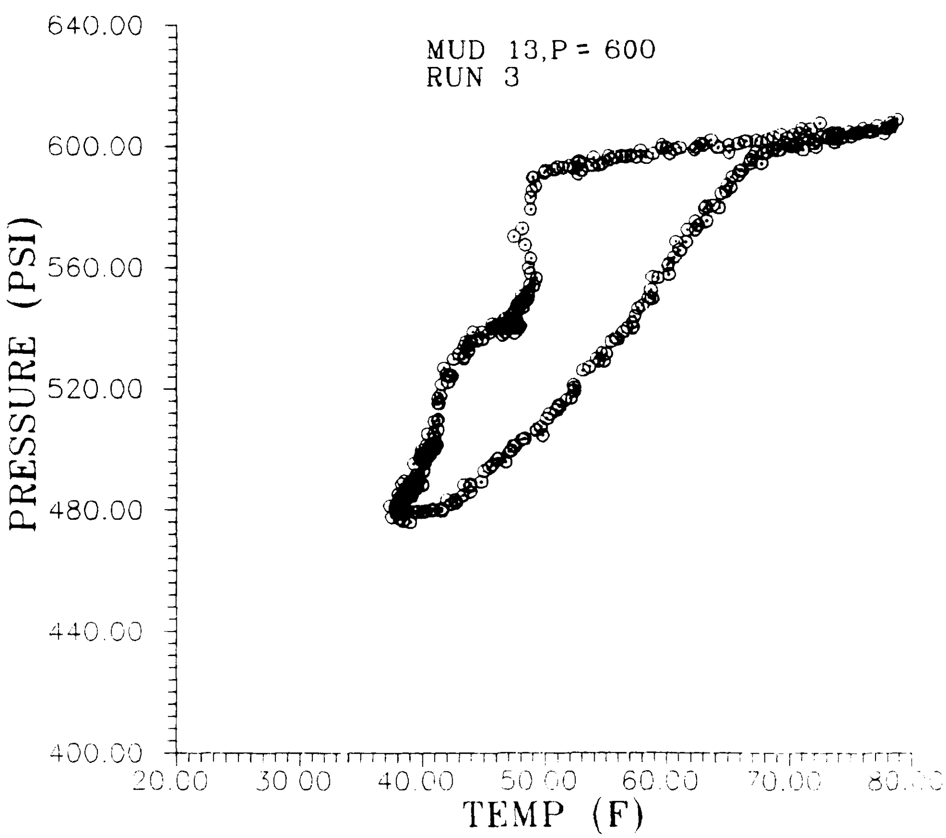
MUD 13,P = 600
RUN 3
PRESSURE (PSI)
TEMP (F)
640.00
600.00
560.00
520.00
480.00
440.00
400.00
20.00
30.00
40.00
50.00
60.00
70.00
80.00

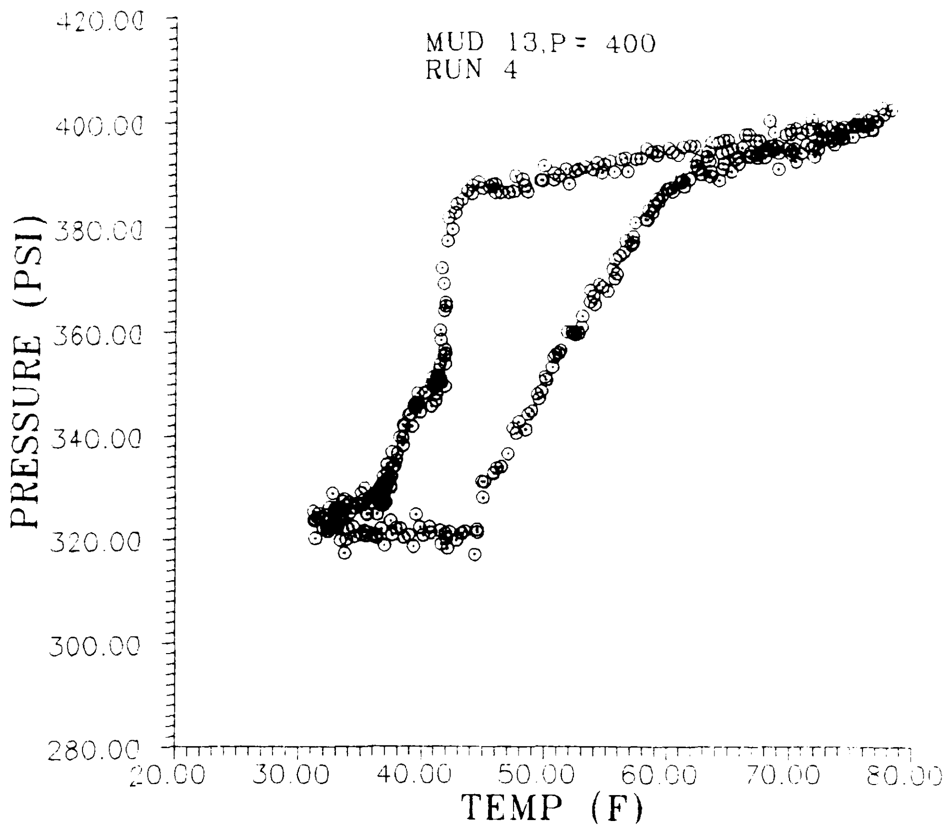
MUD 13,P = 400
RUN 4
PRESSURE (PSI)
TEMP (F)
420.00
400.00
380.00
360.00
340.00
320.00
300.00
280.00
20.00
30.00
40.00
50.00
60.00
70.00
80.00

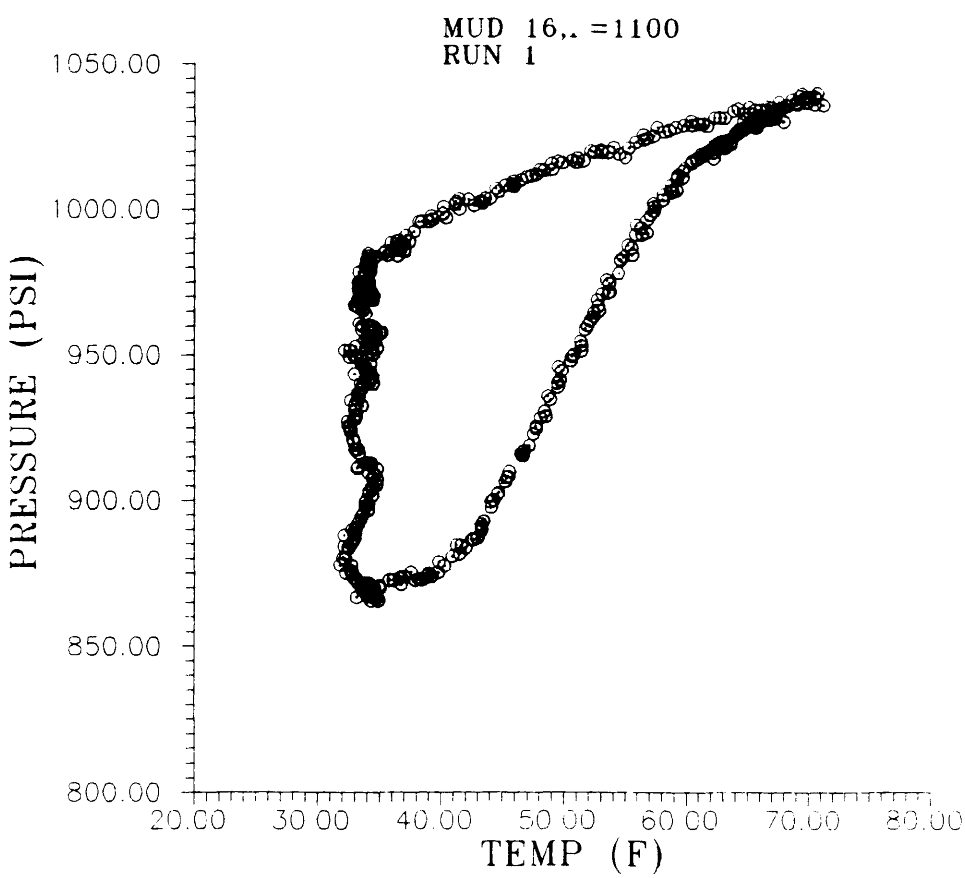
MUD 16,. =1100
RUN 1
PRESSURE (PSI)
TEMP (F)
1050.00
1000.00
950.00
900.00
850.00
800.00
20.00
30.00
40.00
50.00
60.00
70.00
80.00

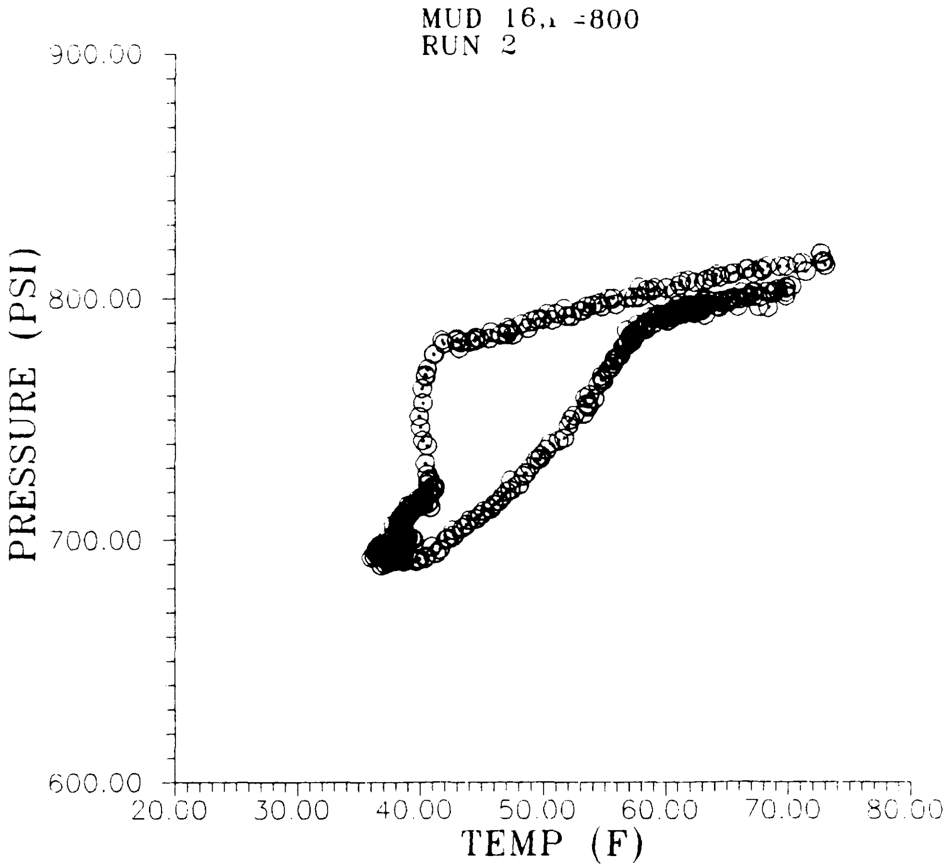
MUD 16,ι =800
RUN 2
900.00
800.00
700.00
600.00
PRESSURE (PSI)
20.00
30.00
40.00
50.00
60.00
70.00
80.00
TEMP (F)

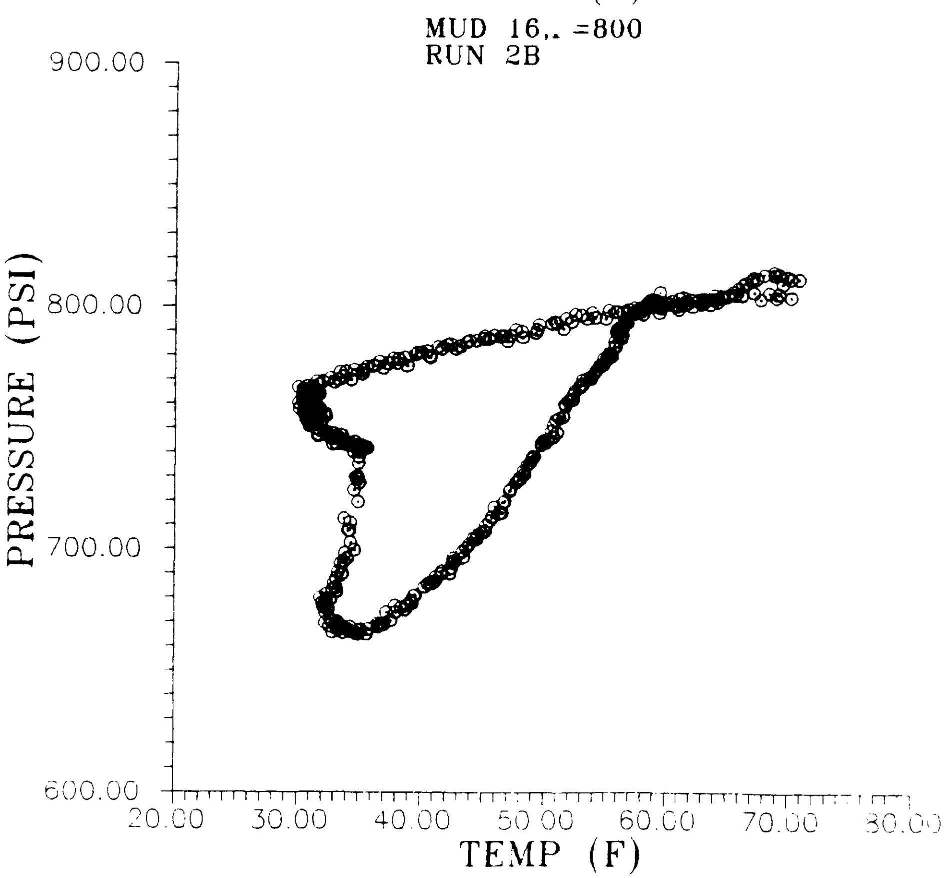
MUD 16,. =800
RUN 2B
900.00
800.00
700.00
600.00
PRESSURE (PSI)
20.00
30.00
40.00
50.00
60.00
70.00
80.00
TEMP (F)

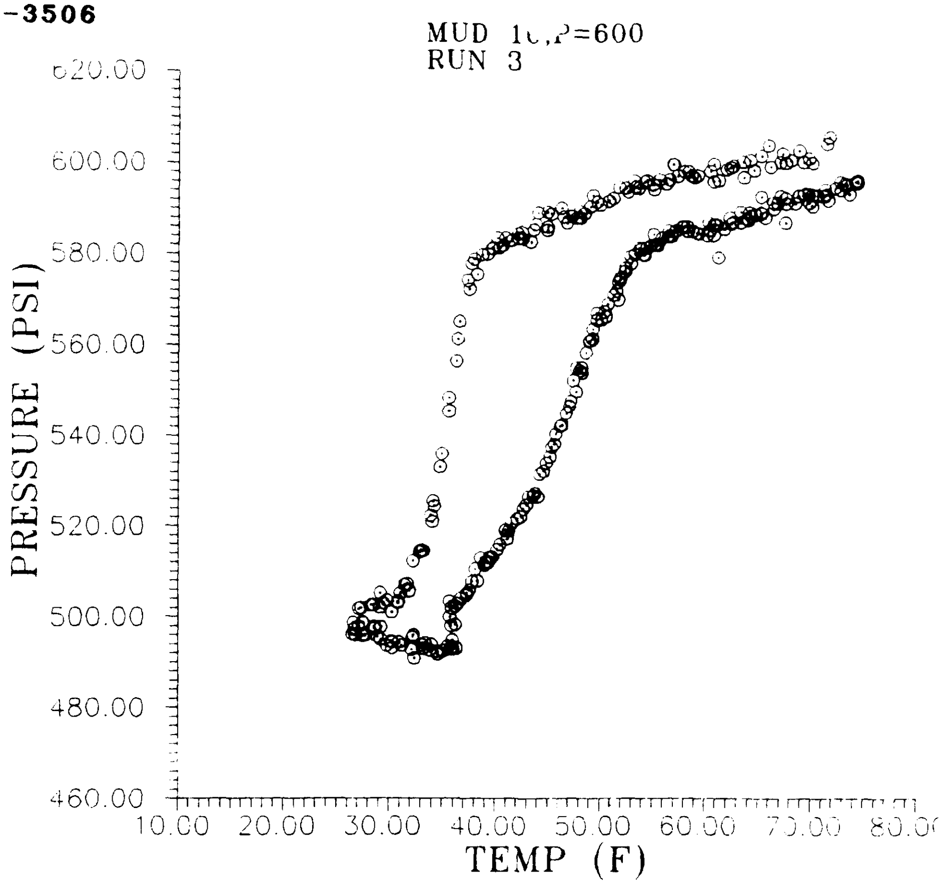
MUD 1ᴗ,P=600
RUN 3
PRESSURE (PSI)
TEMP (F)
620.00
600.00
580.00
560.00
540.00
520.00
500.00
480.00
460.00
10.00
20.00
30.00
40.00
50.00
60.00
70.00
80.00

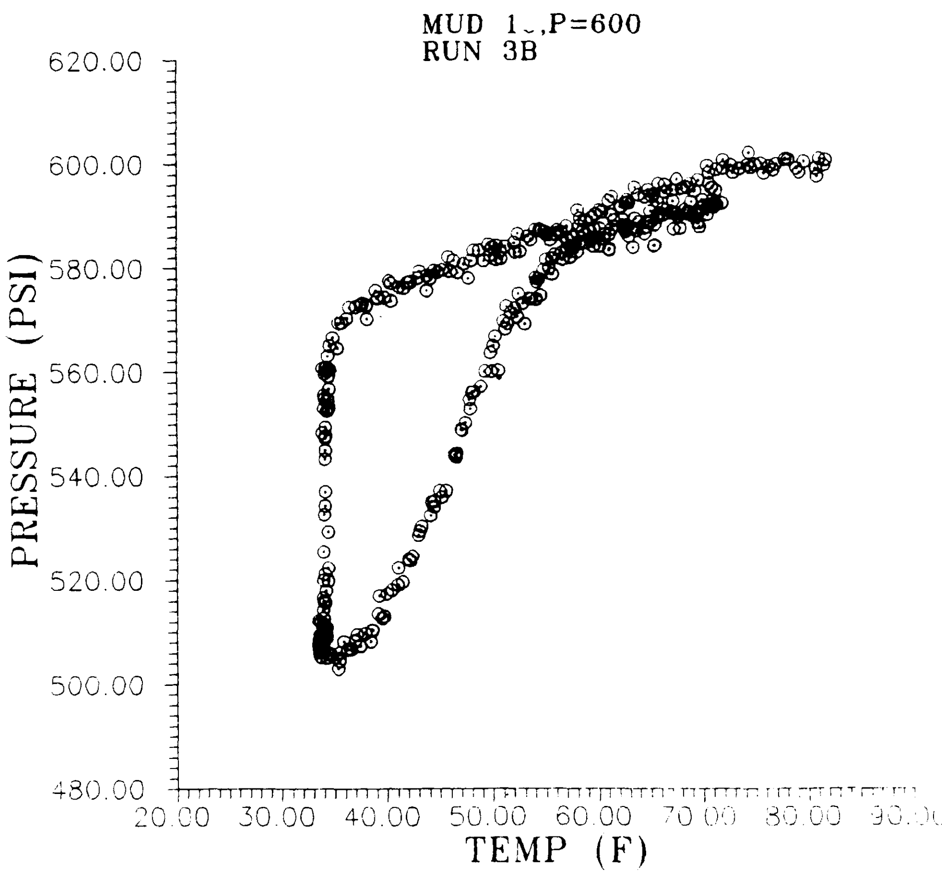
MUD 1ᴗ,P=600
RUN 3B
PRESSURE (PSI)
TEMP (F)
620.00
600.00
580.00
560.00
540.00
520.00
500.00
480.00
20.00
30.00
40.00
50.00
60.00
70.00
80.00
90.00

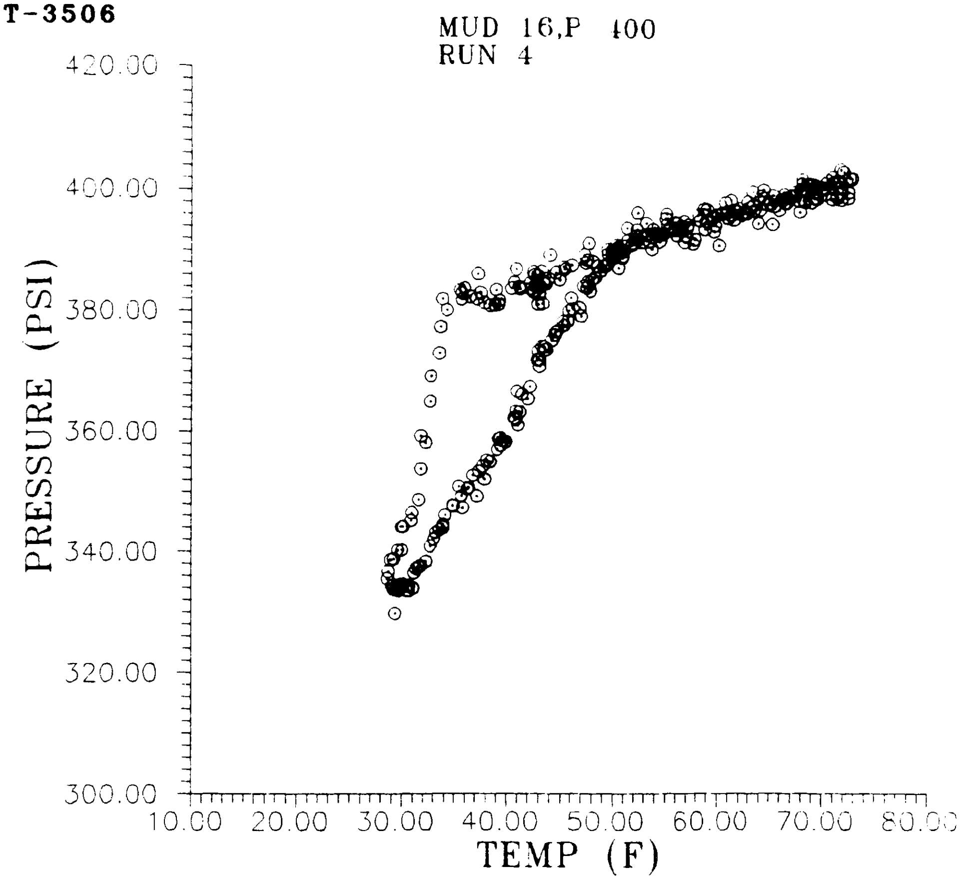
MUD 16,P 400
RUN 4
PRESSURE (PSI)
420.00
400.00
380.00
360.00
340.00
320.00
300.00
10.00
20.00
30.00
40.00
50.00
60.00
70.00
80.00
TEMP (F)

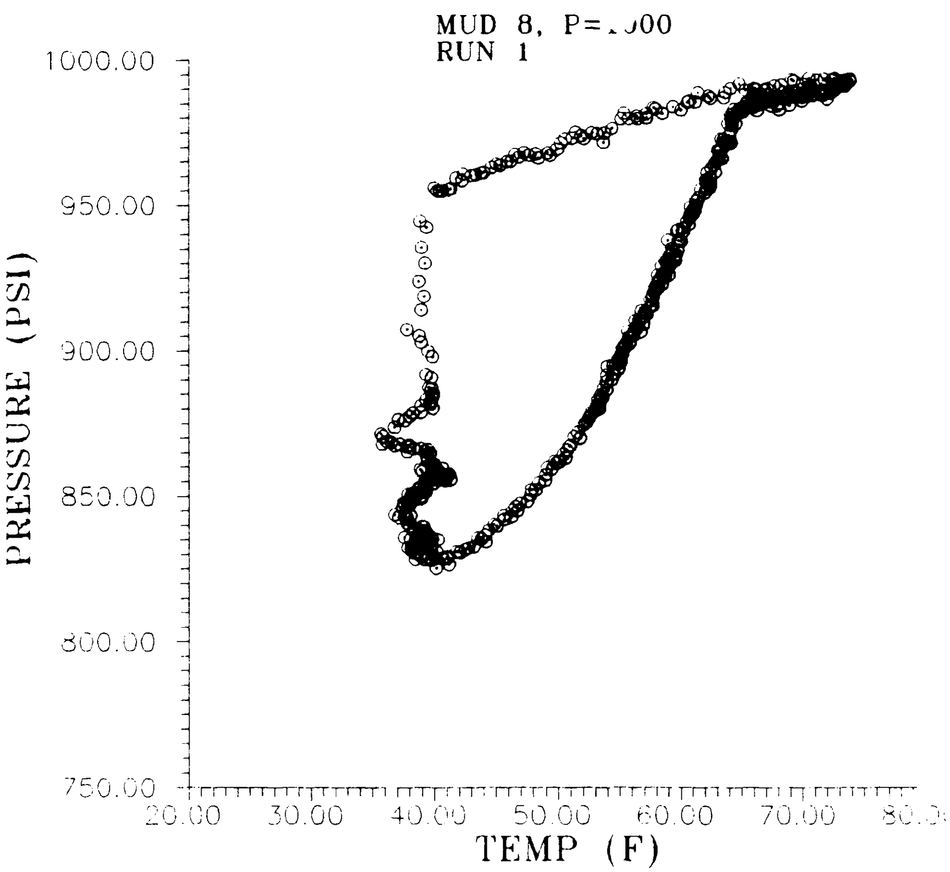
MUD 8, P=.,00
RUN 1
PRESSURE (PSI)
1000.00
950.00
900.00
850.00
800.00
750.00
20.00
30.00
40.00
50.00
60.00
70.00
80.00
TEMP (F)

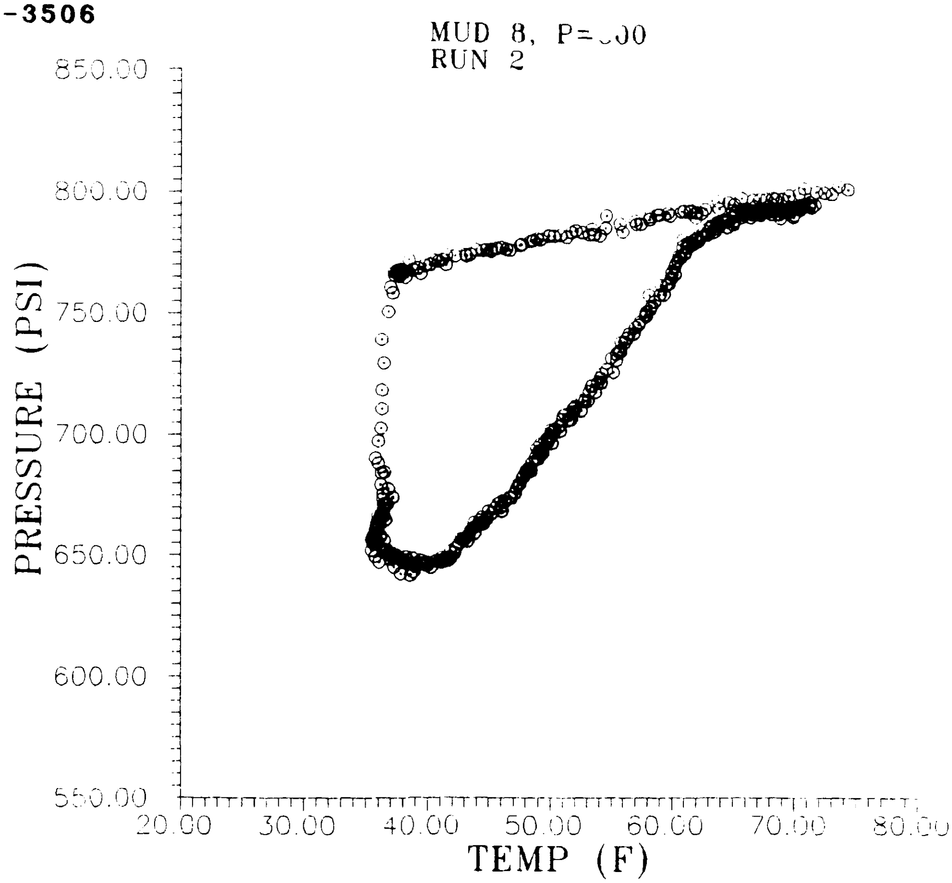
MUD 8, P=.00
RUN 2
PRESSURE (PSI)
850.00
800.00
750.00
700.00
650.00
600.00
550.00
20.00
30.00
40.00
50.00
60.00
70.00
80.00
TEMP (F)

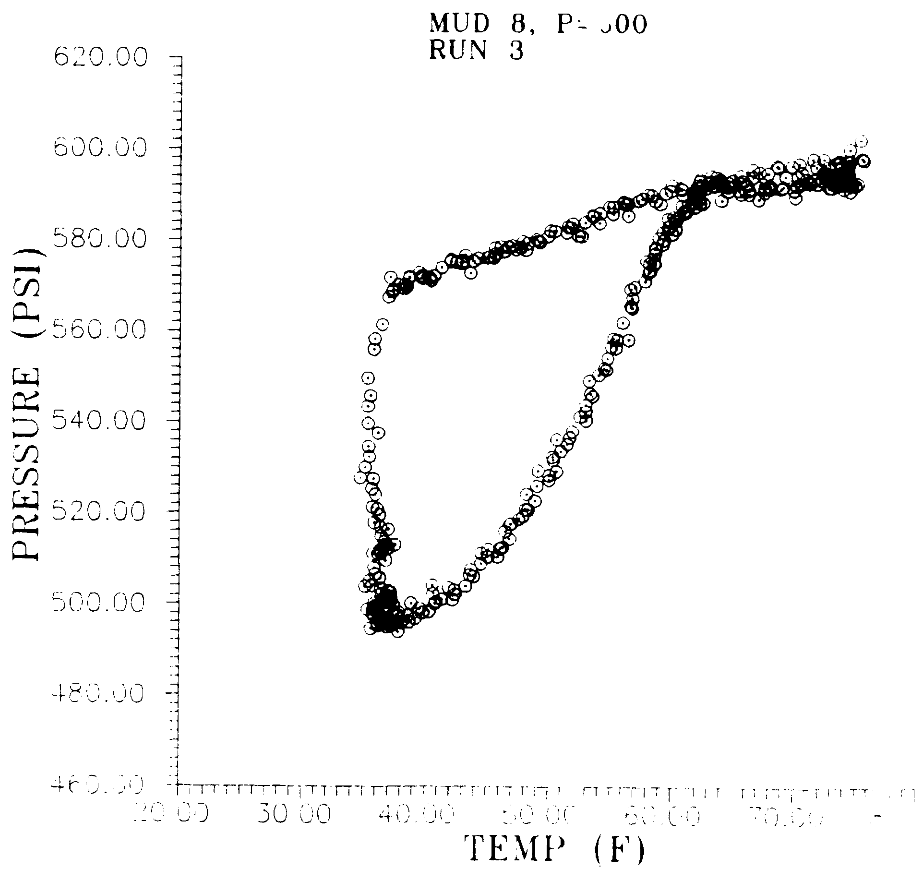
MUD 8, P=.00
RUN 3
PRESSURE (PSI)
620.00
600.00
580.00
560.00
540.00
520.00
500.00
480.00
460.00
20.00
30.00
40.00
50.00
60.00
70.00
TEMP (F)

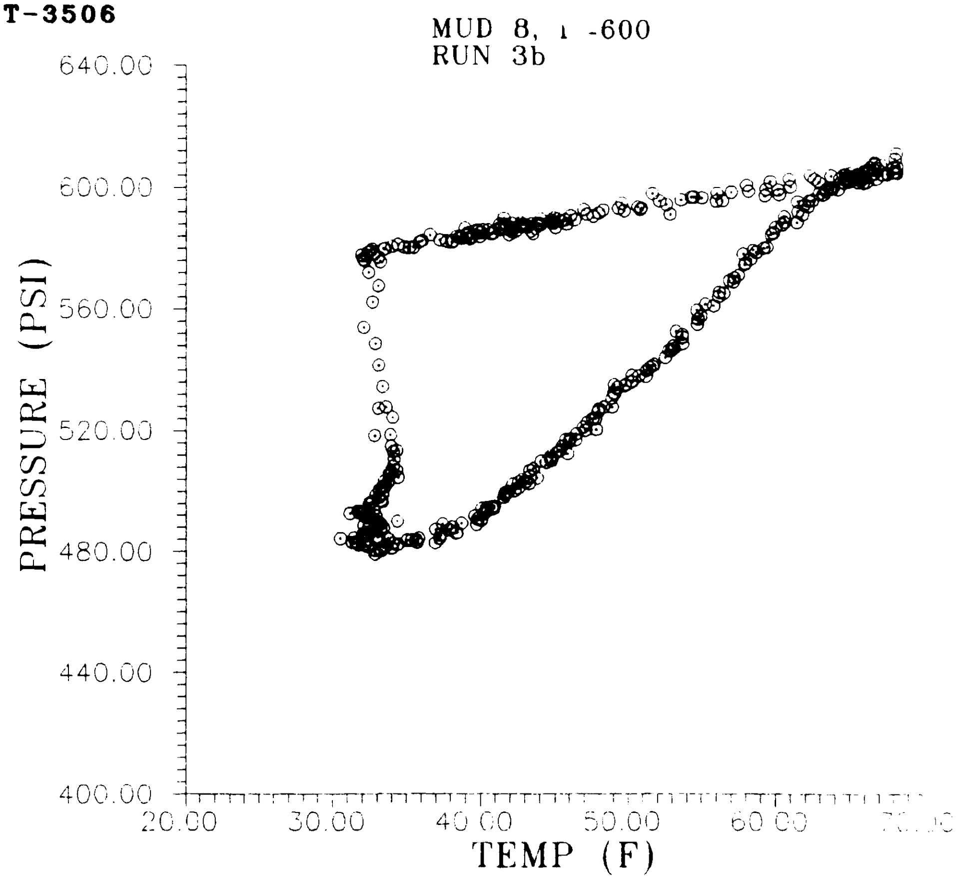
MUD 8, ı -600
RUN 3b
PRESSURE (PSI)
640.00
600.00
560.00
520.00
480.00
440.00
400.00
20.00
30.00
40.00
50.00
60.00
TEMP (F)

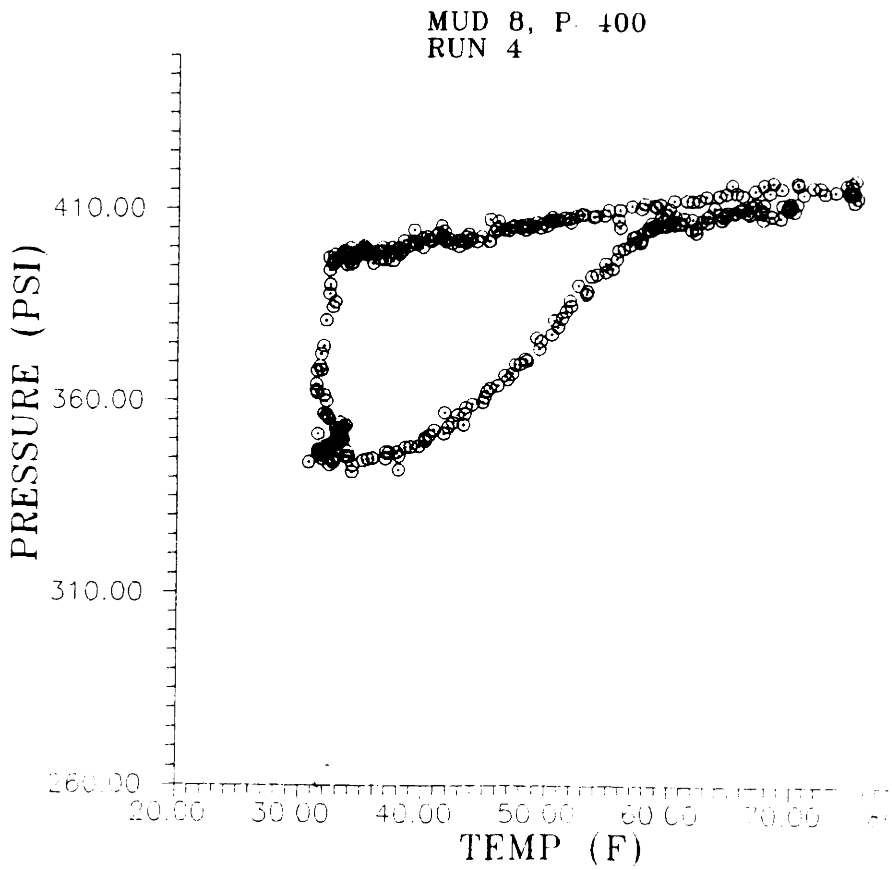
MUD 8, P 400
RUN 4
PRESSURE (PSI)
410.00
360.00
310.00
20.00
30.00
40.00
50.00
TEMP (F)

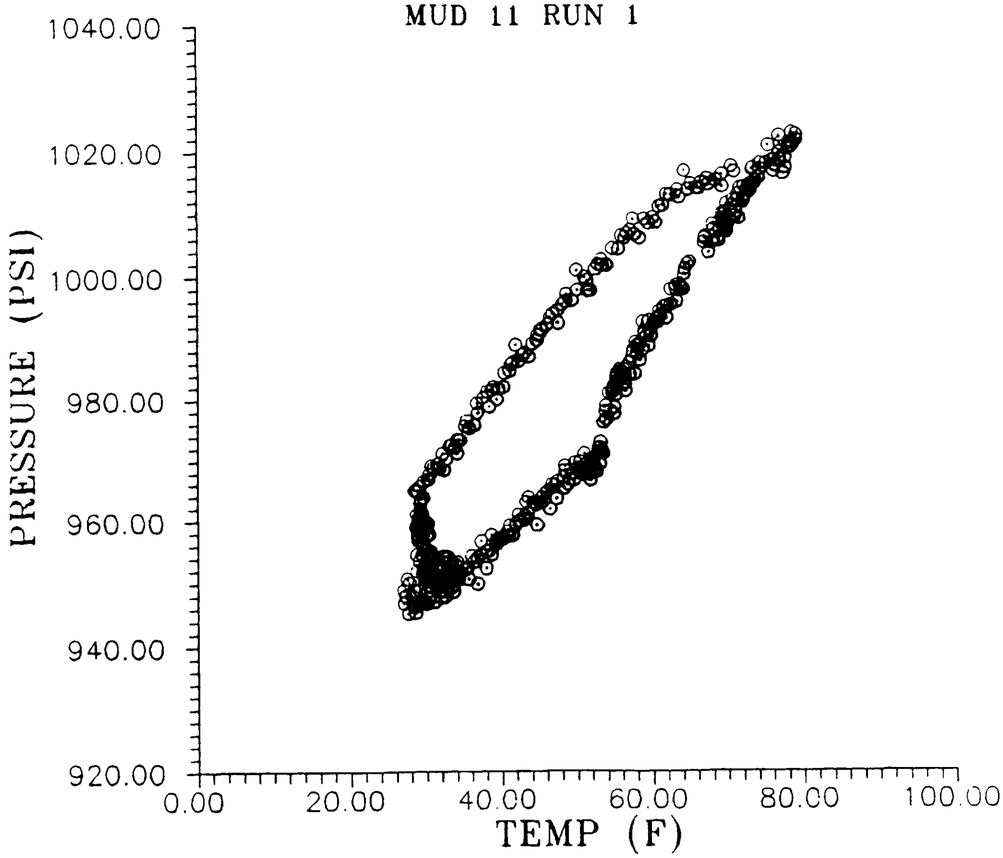
MUD 11 RUN 1
PRESSURE (PSI)
1040.00
1020.00
1000.00
980.00
960.00
940.00
920.00
0.00
20.00
40.00
60.00
80.00
100.00
TEMP (F)

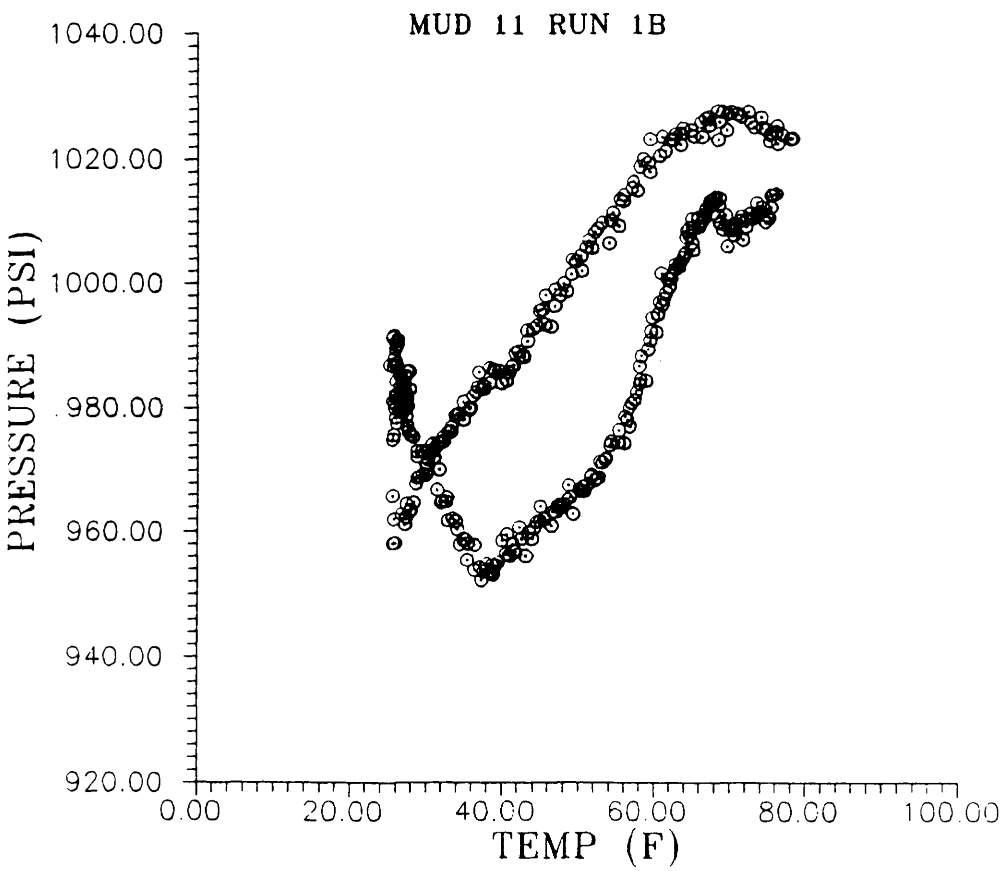
MUD 11 RUN 1B
PRESSURE (PSI)
1040.00
1020.00
1000.00
980.00
960.00
940.00
920.00
0.00
20.00
40.00
60.00
80.00
100.00
TEMP (F)

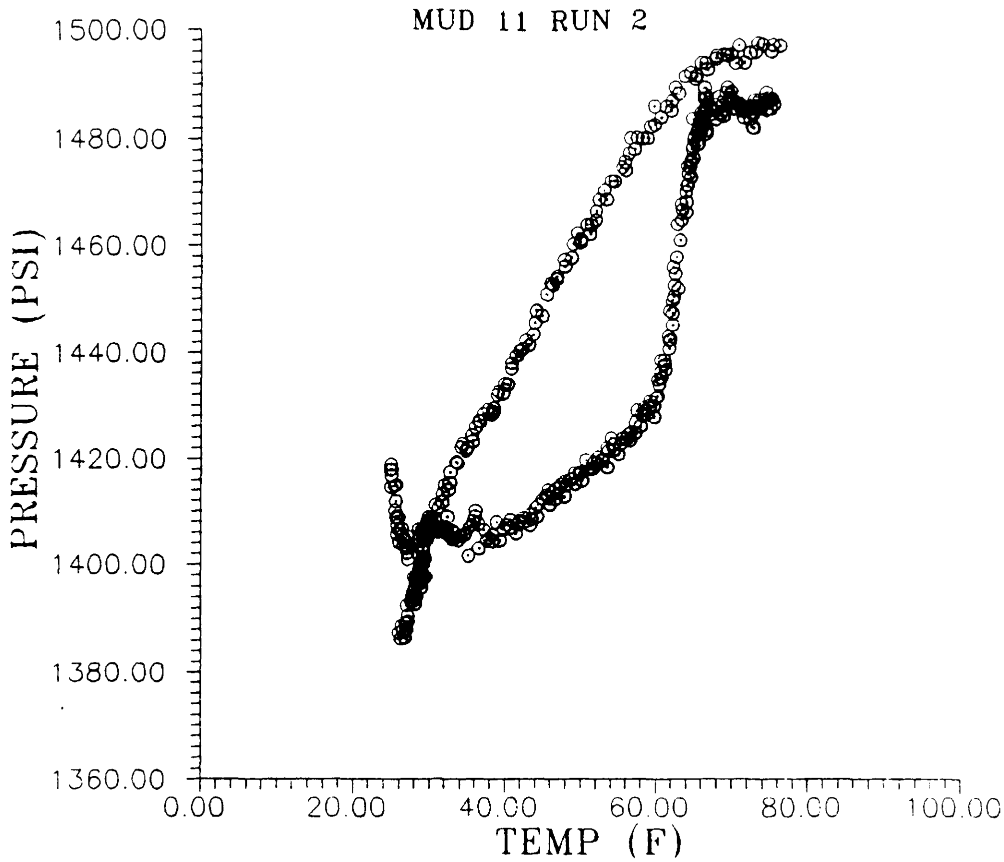
MUD 11 RUN 2
PRESSURE (PSI)
1500.00
1480.00
1460.00
1440.00
1420.00
1400.00
1380.00
1360.00
0.00
20.00
40.00
60.00
80.00
100.00
TEMP (F)

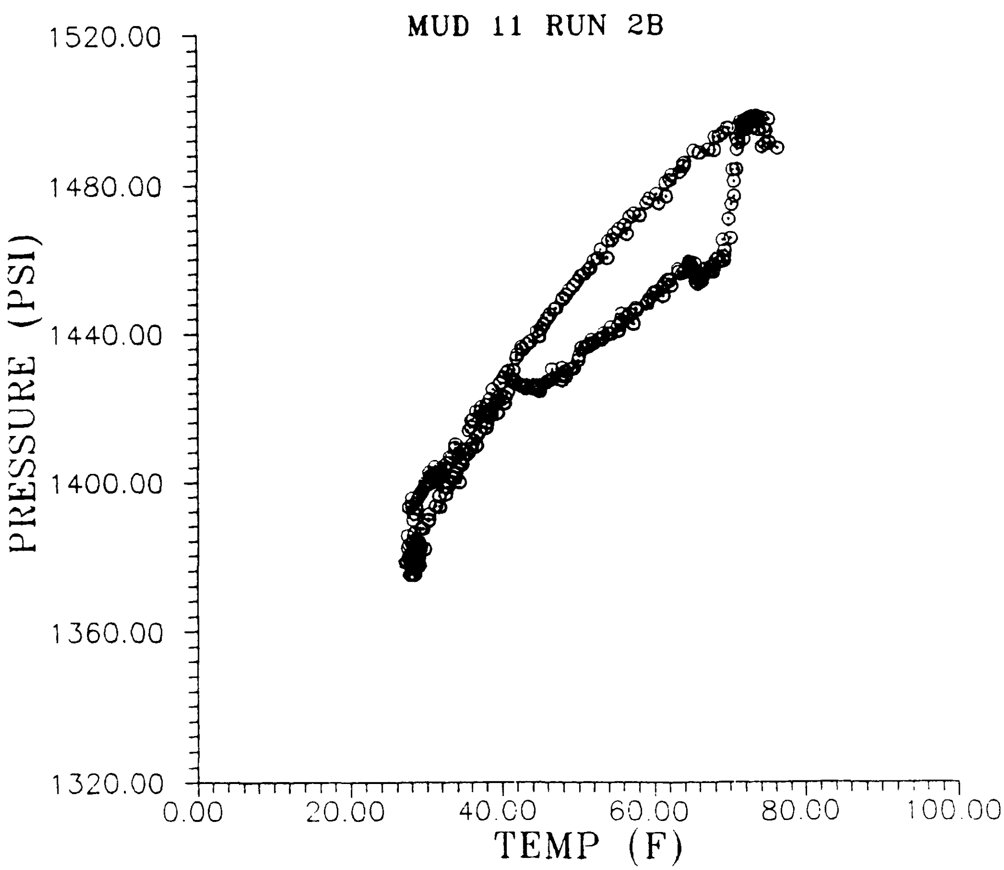
MUD 11 RUN 2B
PRESSURE (PSI)
1520.00
1480.00
1440.00
1400.00
1360.00
1320.00
0.00
20.00
40.00
60.00
80.00
100.00
TEMP (F)

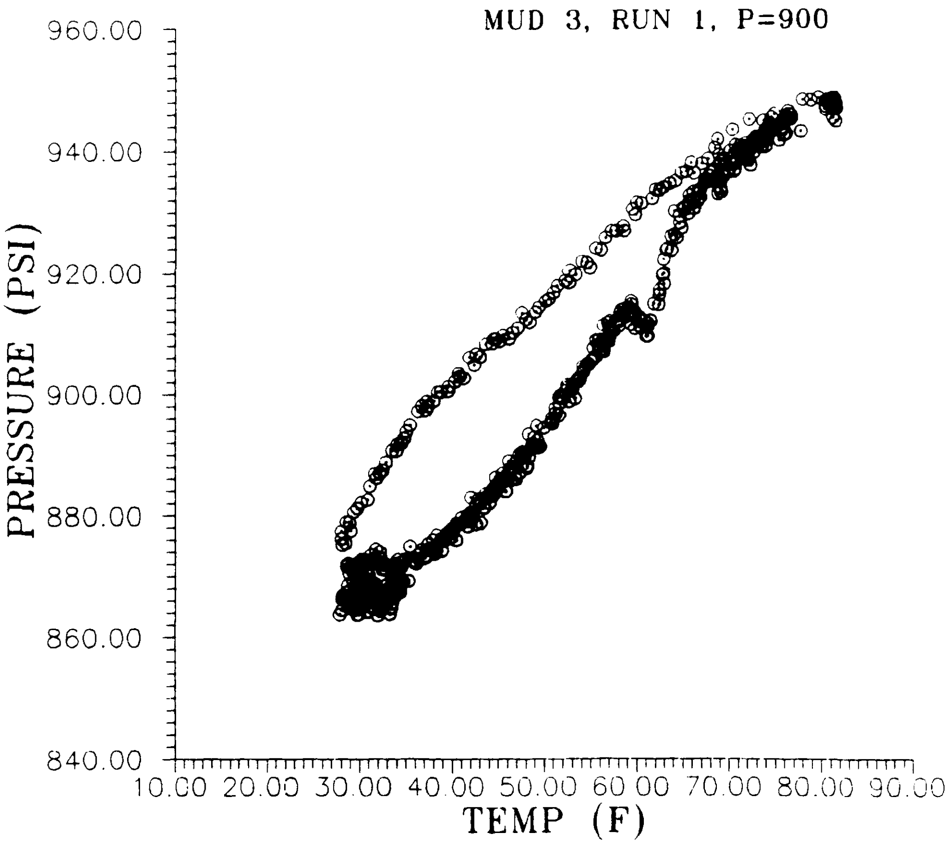
MUD 3, RUN 1, P=900
PRESSURE (PSI)
960.00
940.00
920.00
900.00
880.00
860.00
840.00
10.00 20.00 30.00 40.00 50.00 60.00 70.00 80.00 90.00
TEMP (F)

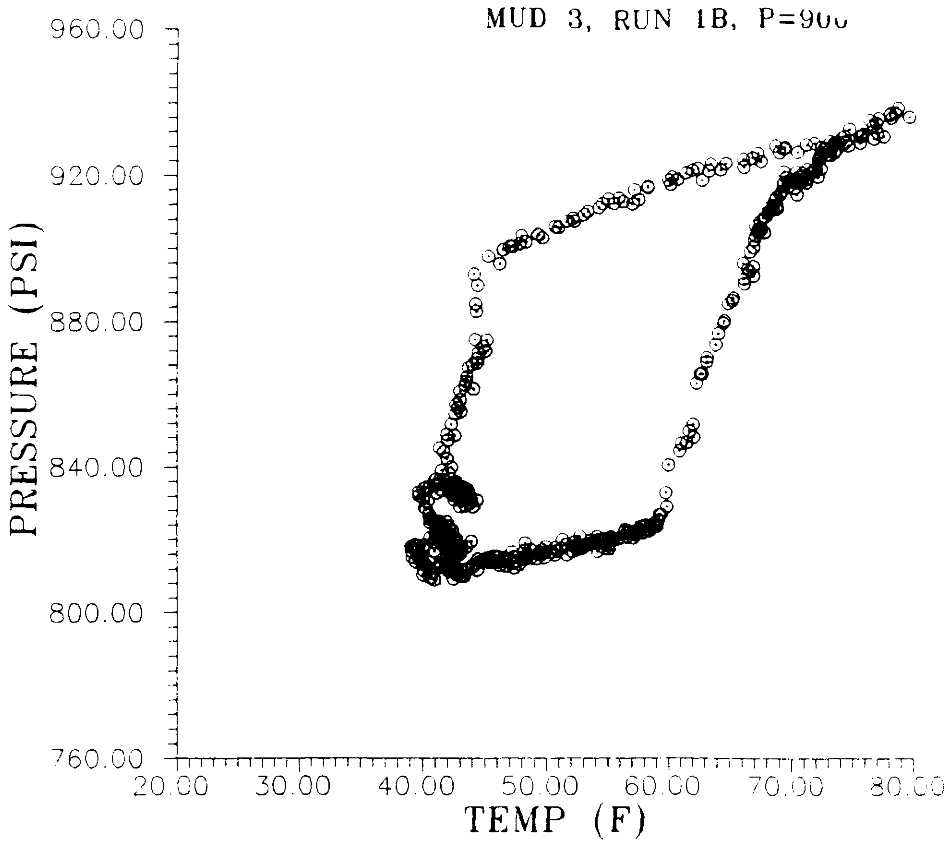
MUD 3, RUN 1B, P=900
PRESSURE (PSI)
960.00
920.00
880.00
840.00
800.00
760.00
20.00
30.00
40.00
50.00
60.00
70.00
80.00
TEMP (F)

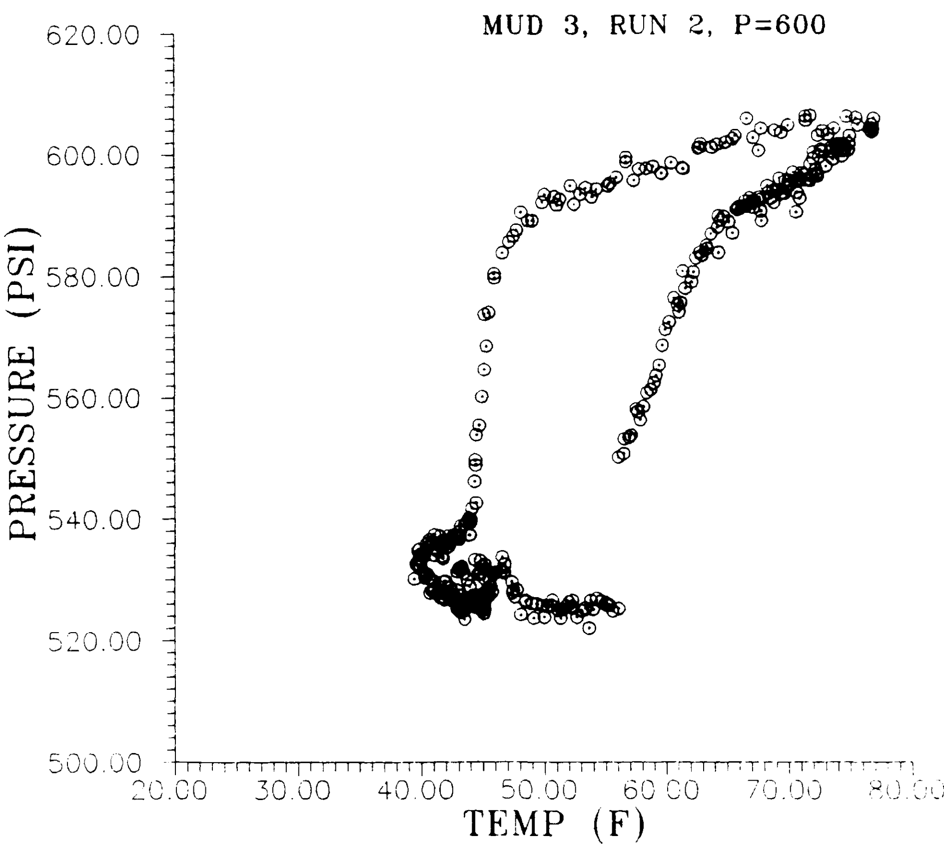
MUD 3, RUN 2, P=600
PRESSURE (PSI)
620.00
600.00
580.00
560.00
540.00
520.00
500.00
20.00
30.00
40.00
50.00
60.00
70.00
80.00
TEMP (F)

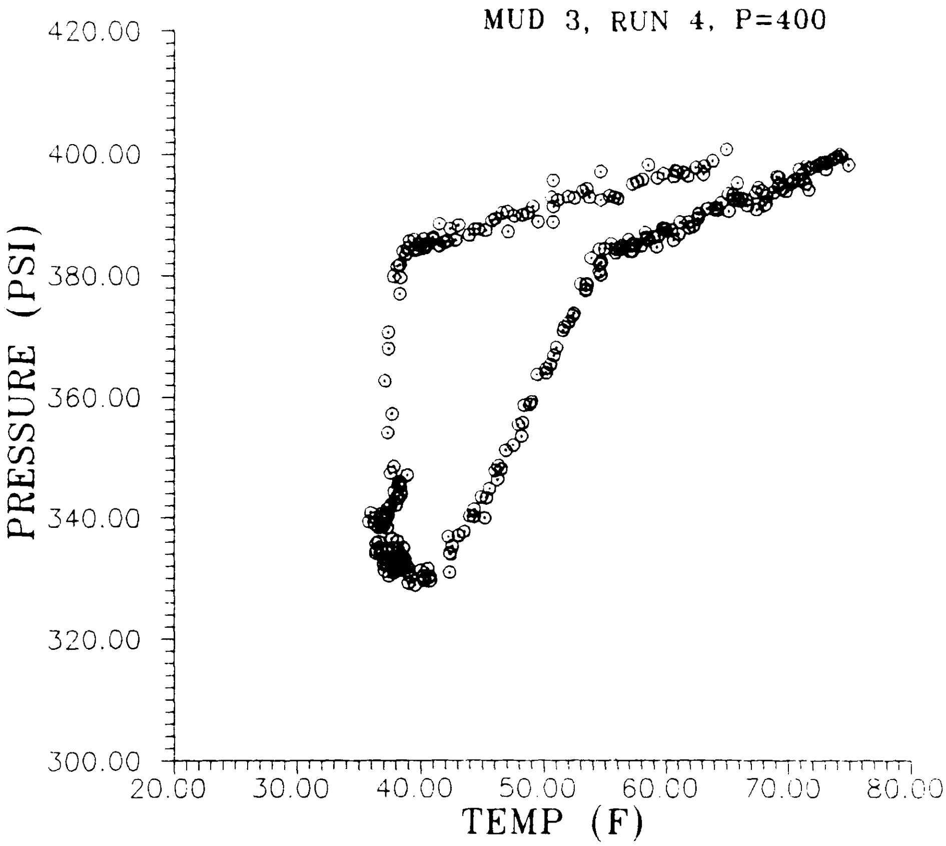
MUD 3, RUN 4, P=400
PRESSURE (PSI)
TEMP (F)
420.00
400.00
380.00
360.00
340.00
320.00
300.00
20.00
30.00
40.00
50.00
60.00
70.00
80.00

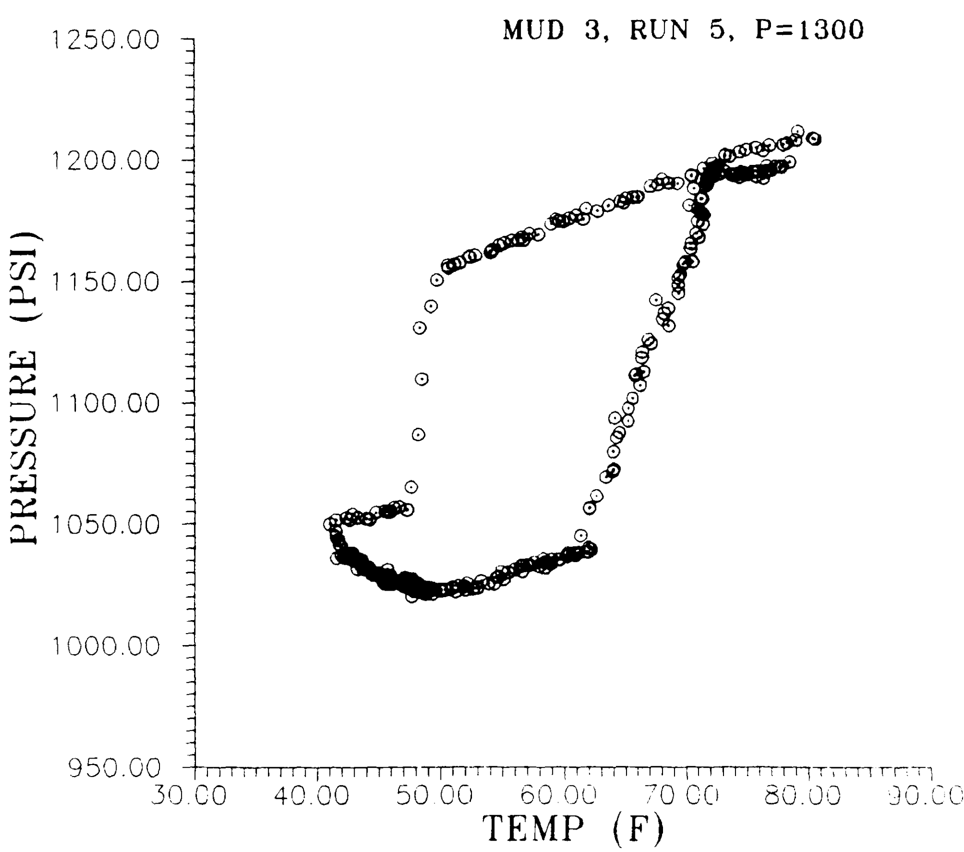
MUD 3, RUN 5, P=1300
PRESSURE (PSI)
TEMP (F)
1250.00
1200.00
1150.00
1100.00
1050.00
1000.00
950.00
30.00
40.00
50.00
60.00
70.00
80.00
90.00

MUD 17, RUN 1, P=1300

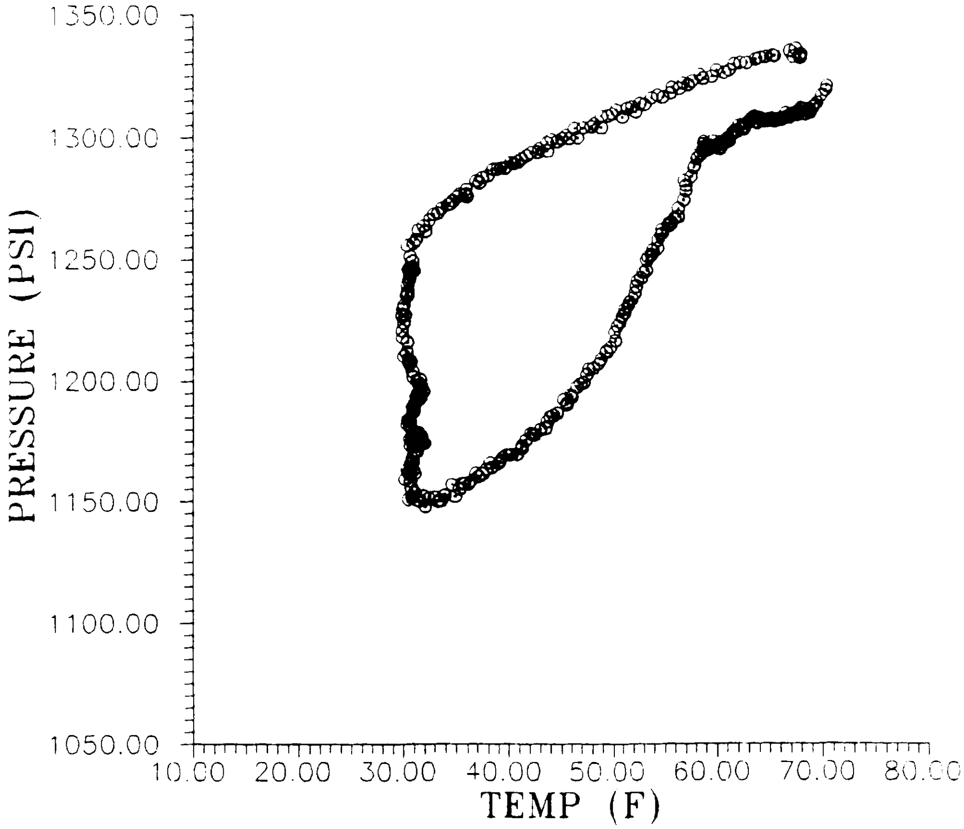

MUD 17, RUN 1B, P=1300

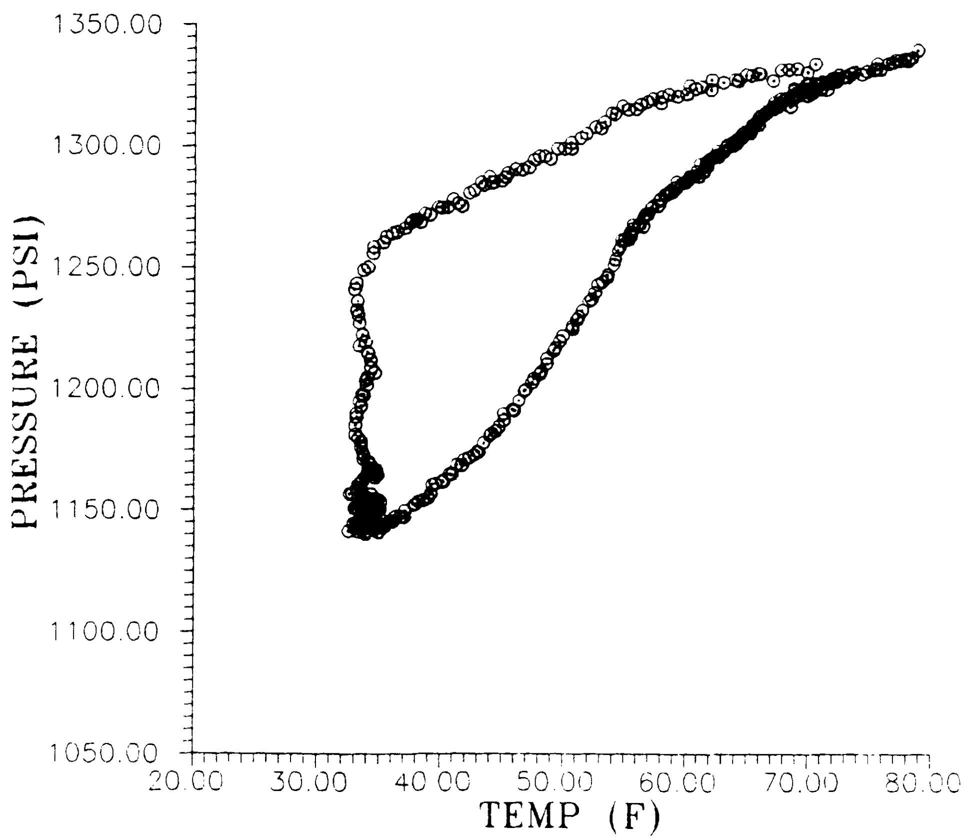

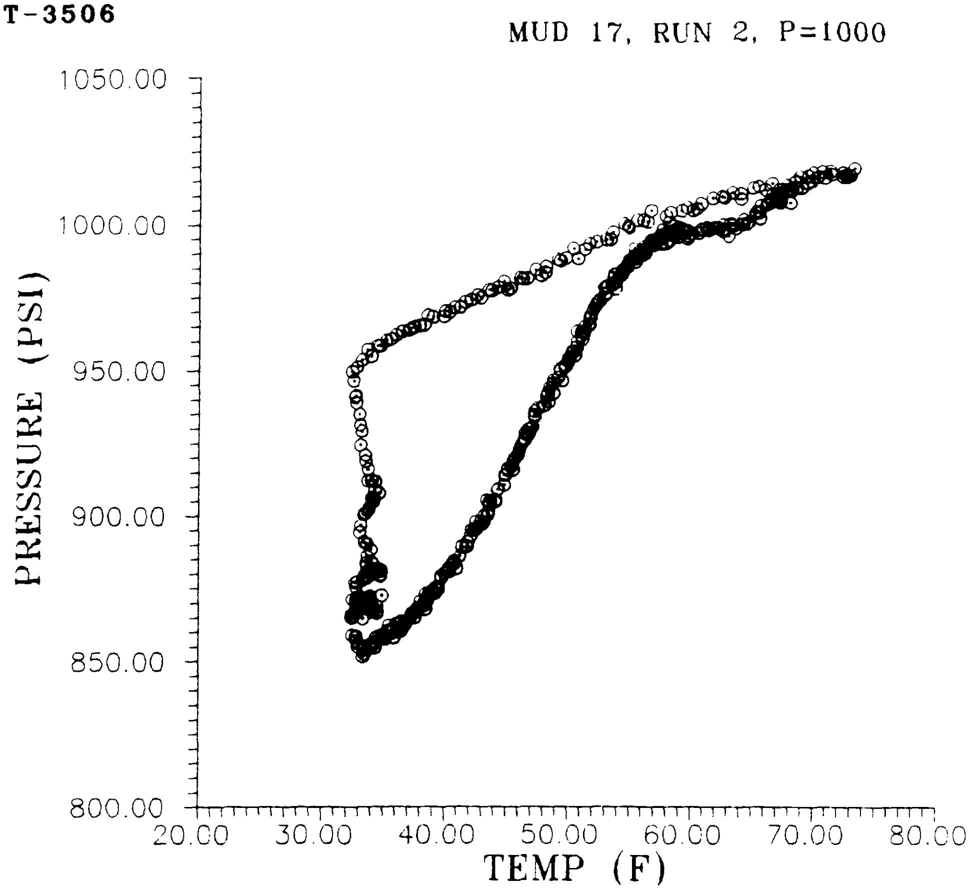
MUD 17, RUN 2, P=1000
PRESSURE (PSI)
1050.00
1000.00
950.00
900.00
850.00
800.00
20.00
30.00
40.00
50.00
60.00
70.00
80.00
TEMP (F)

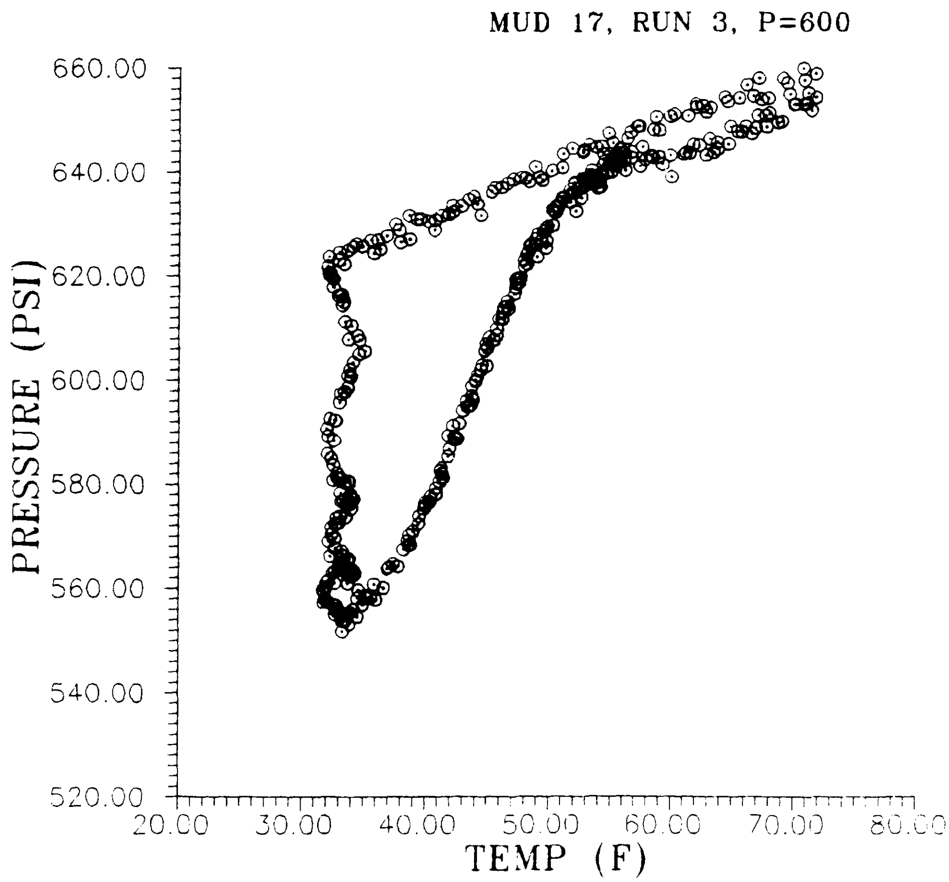
MUD 17, RUN 3, P=600
PRESSURE (PSI)
660.00
640.00
620.00
600.00
580.00
560.00
540.00
520.00
20.00
30.00
40.00
50.00
60.00
70.00
80.00
TEMP (F)

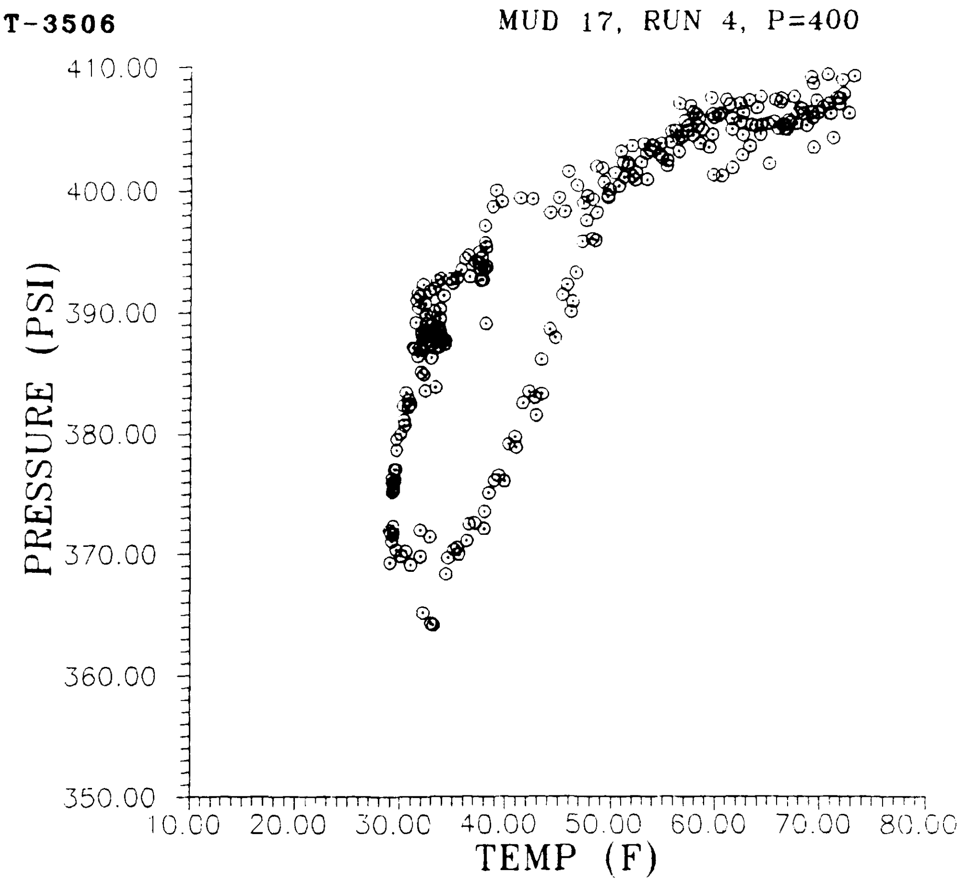
MUD 17, RUN 4, P=400
PRESSURE (PSI)
410.00
400.00
390.00
380.00
370.00
360.00
350.00
10.00
20.00
30.00
40.00
50.00
60.00
70.00
80.00
TEMP (F)

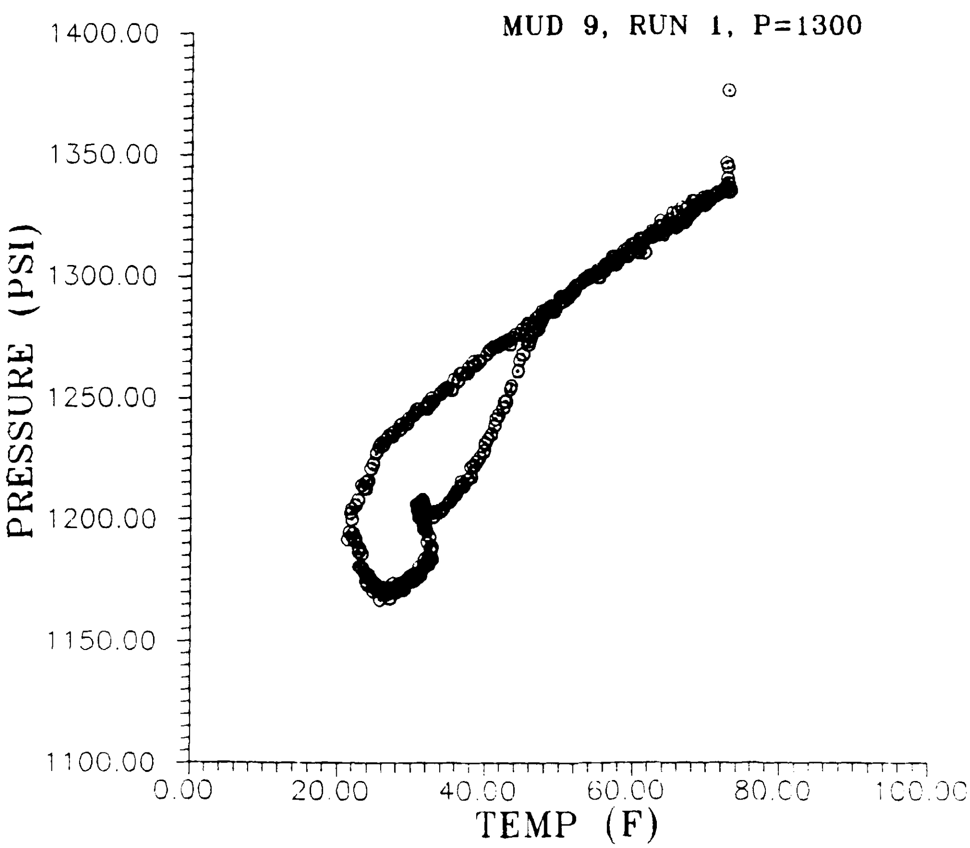
MUD 9, RUN 1, P=1300
PRESSURE (PSI)
1400.00
1350.00
1300.00
1250.00
1200.00
1150.00
1100.00
0.00
20.00
40.00
60.00
80.00
100.00
TEMP (F)

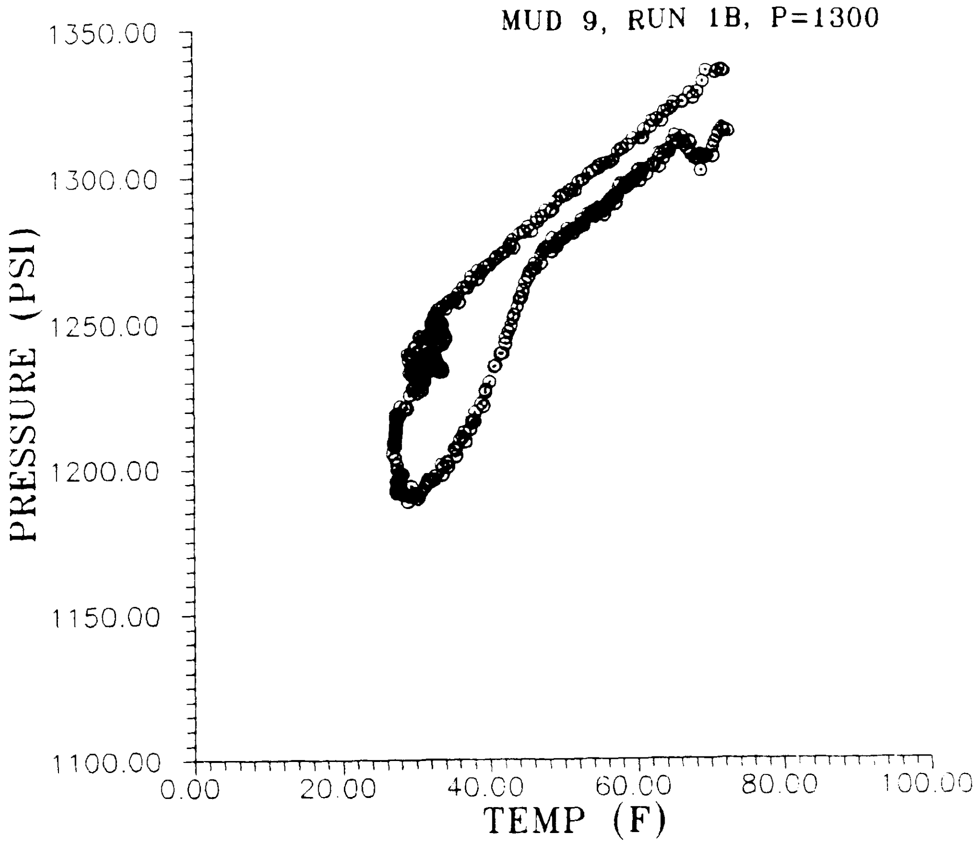
MUD 9, RUN 1B, P=1300
1350.00
1300.00
1250.00
1200.00
1150.00
1100.00
PRESSURE (PSI)
0.00
20.00
40.00
60.00
80.00
100.00
TEMP (F)

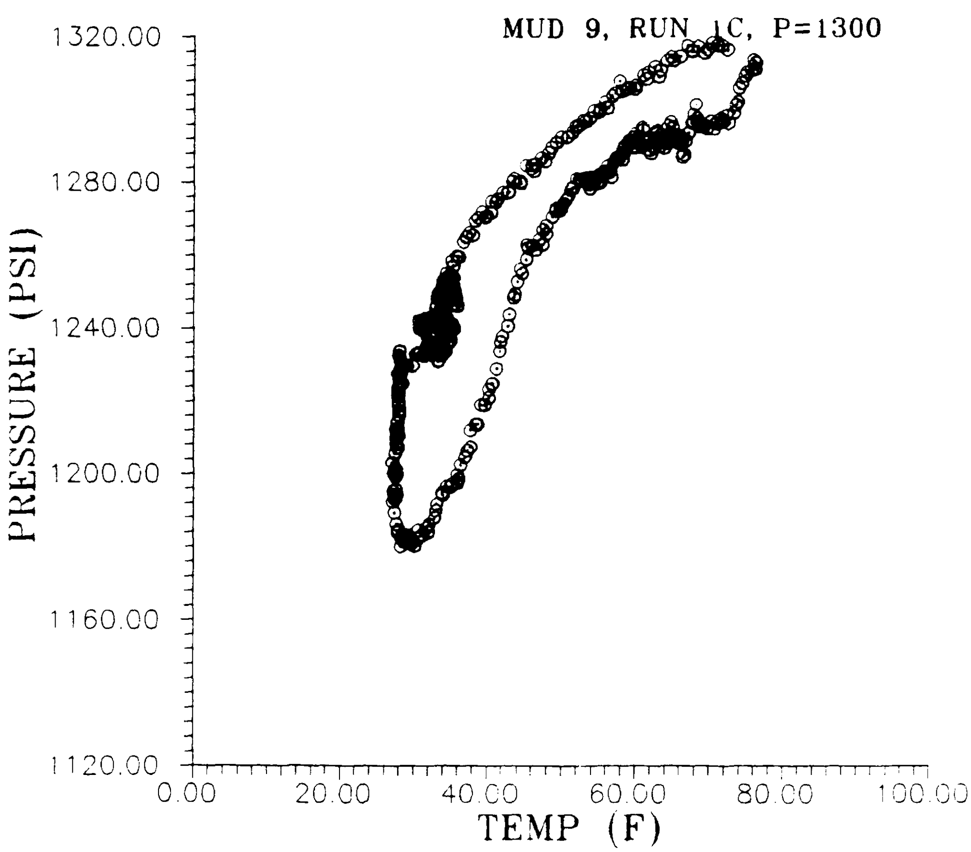
MUD 9, RUN 1C, P=1300
1320.00
1280.00
1240.00
1200.00
1160.00
1120.00
PRESSURE (PSI)
0.00
20.00
40.00
60.00
80.00
100.00
TEMP (F)

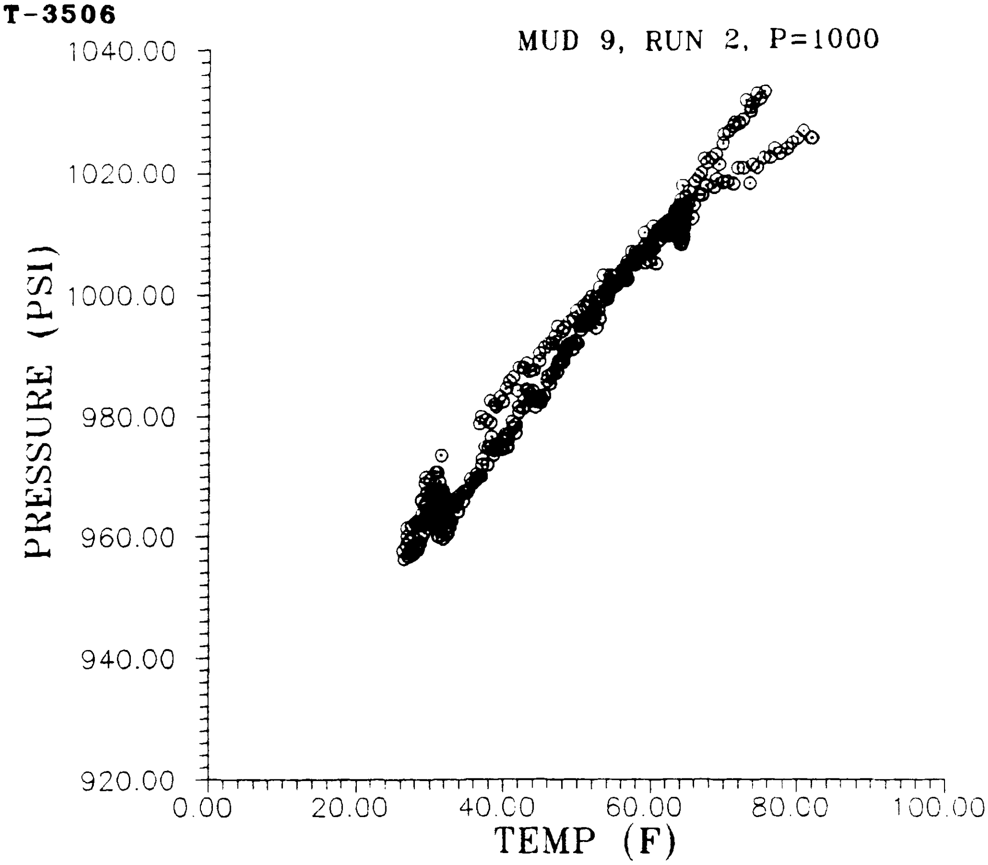
MUD 9, RUN 2, P=1000
PRESSURE (PSI)
1040.00
1020.00
1000.00
980.00
960.00
940.00
920.00
0.00
20.00
40.00
60.00
80.00
100.00
TEMP (F)

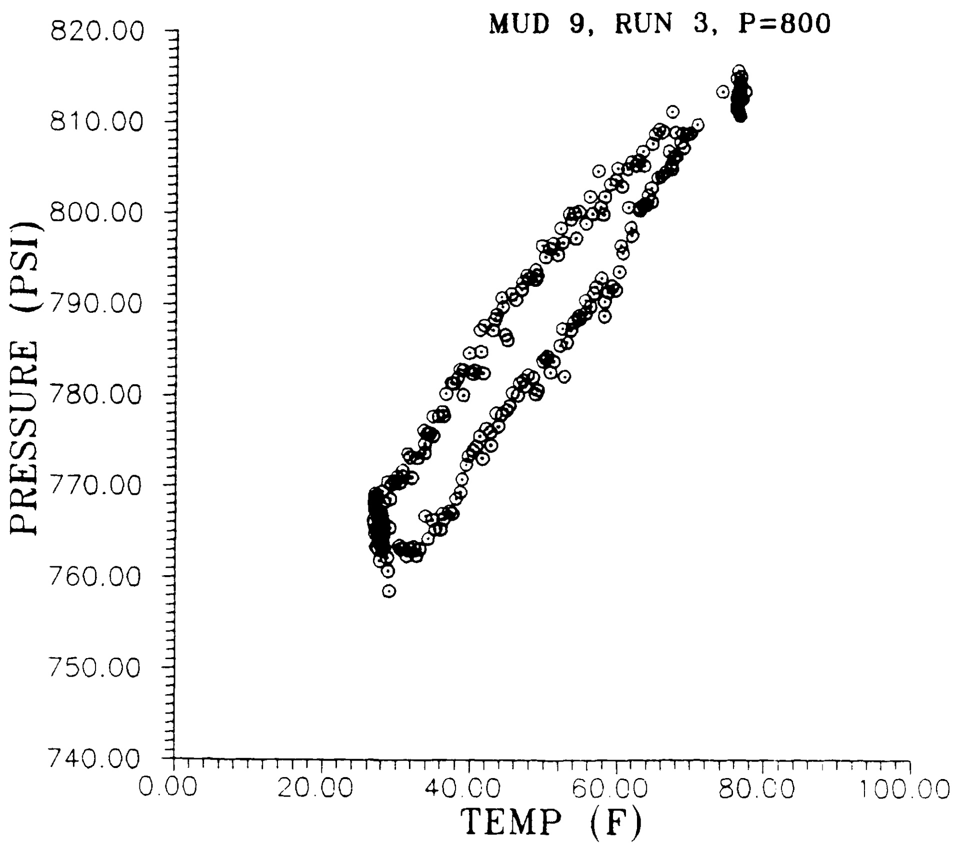
MUD 9, RUN 3, P=800
PRESSURE (PSI)
820.00
810.00
800.00
790.00
780.00
770.00
760.00
750.00
740.00
0.00
20.00
40.00
60.00
80.00
100.00
TEMP (F)

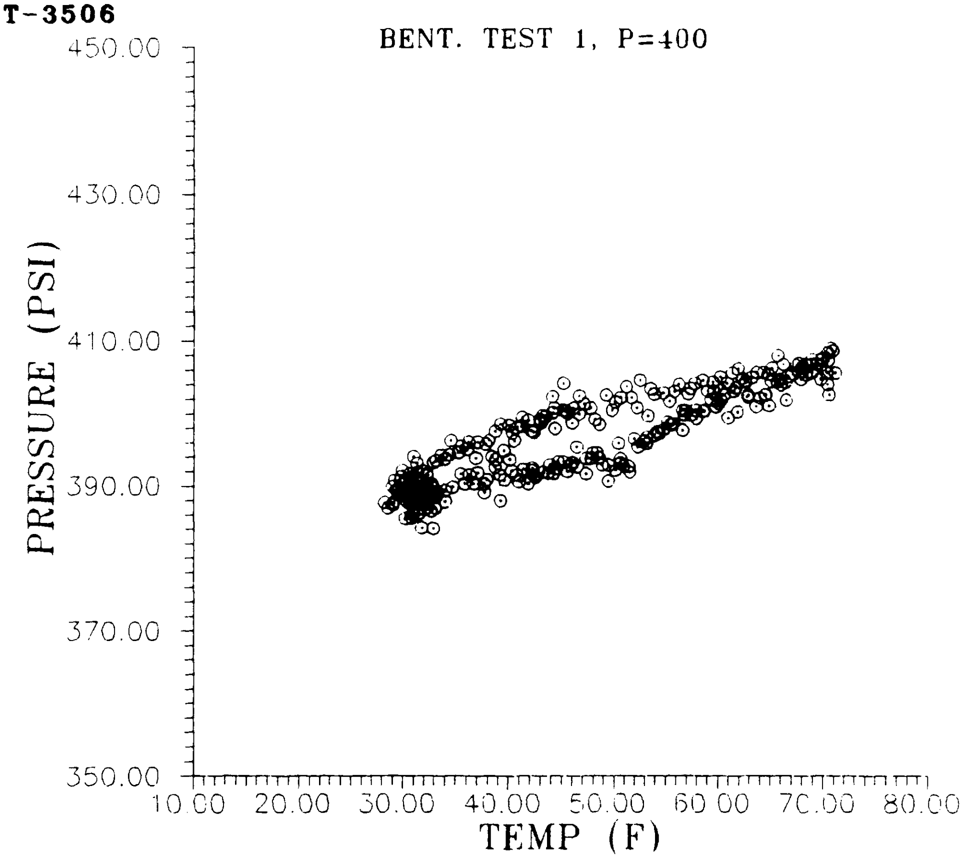
BENT. TEST 1, P=400
PRESSURE (PSI)
450.00
430.00
410.00
390.00
370.00
350.00
10.00 20.00 30.00 40.00 50.00 60.00 70.00 80.00
TEMP (F)

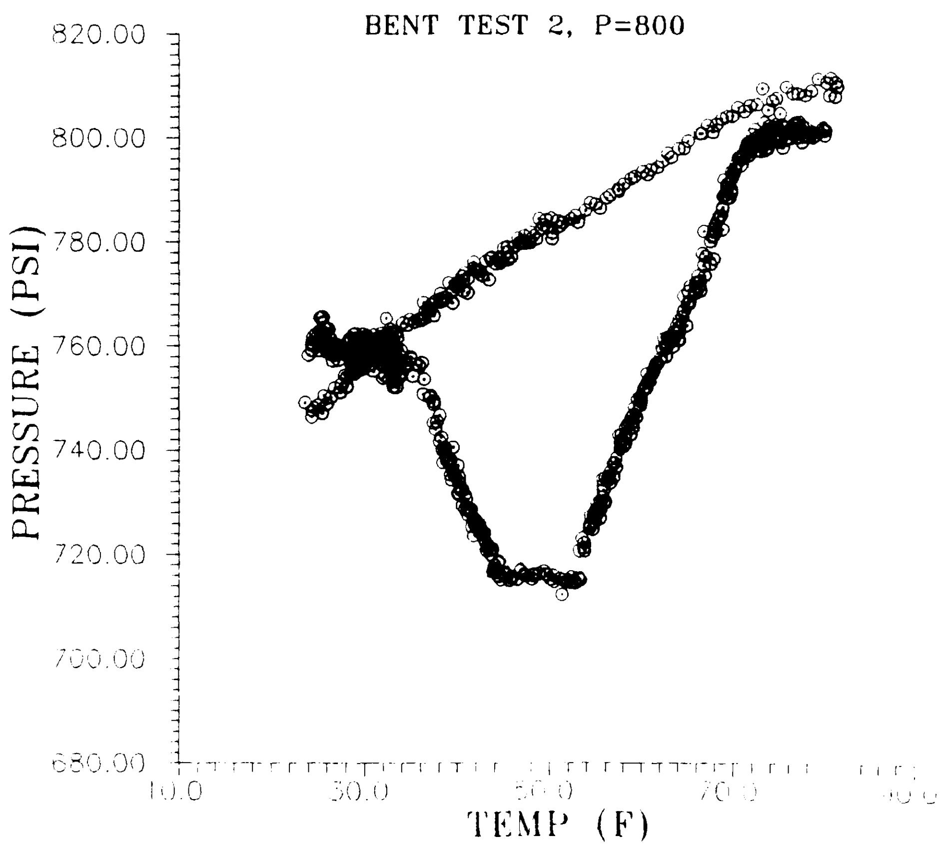
BENT TEST 2, P=800
PRESSURE (PSI)
820.00
800.00
780.00
760.00
740.00
720.00
700.00
680.00
10.0 30.0 70.0
TEMP (F)

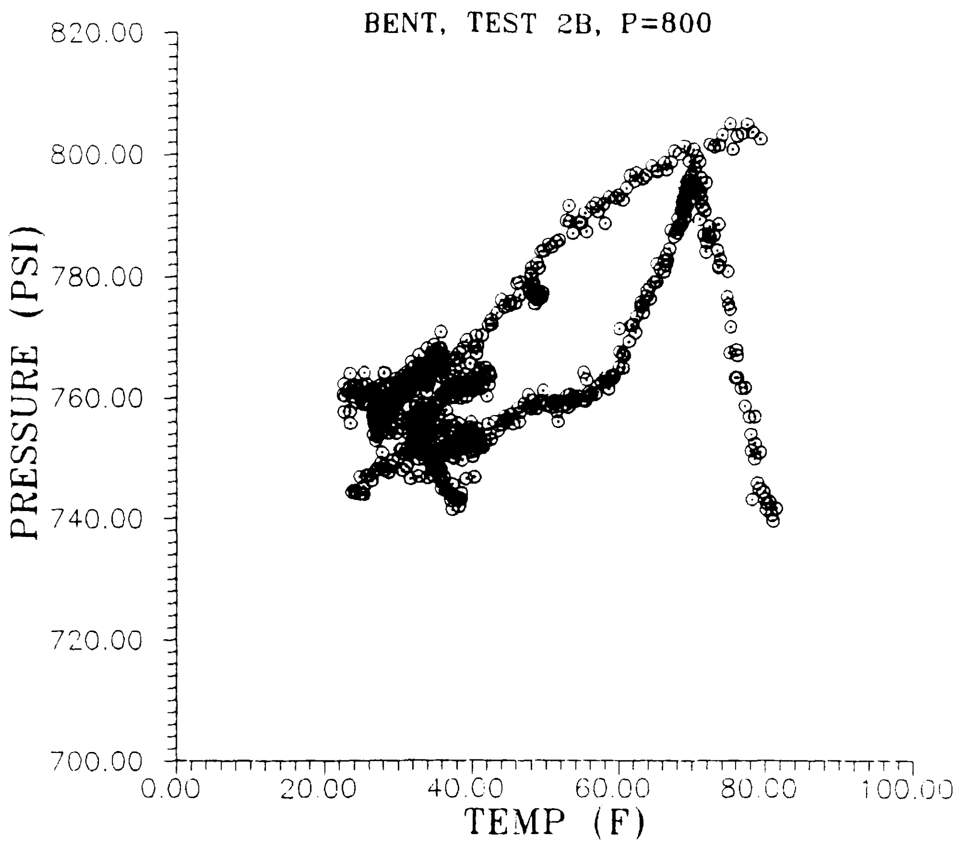
BENT, TEST 2B, P=800
820.00
800.00
780.00
760.00
740.00
720.00
700.00
PRESSURE (PSI)
0.00
20.00
40.00
60.00
80.00
100.00
TEMP (F)

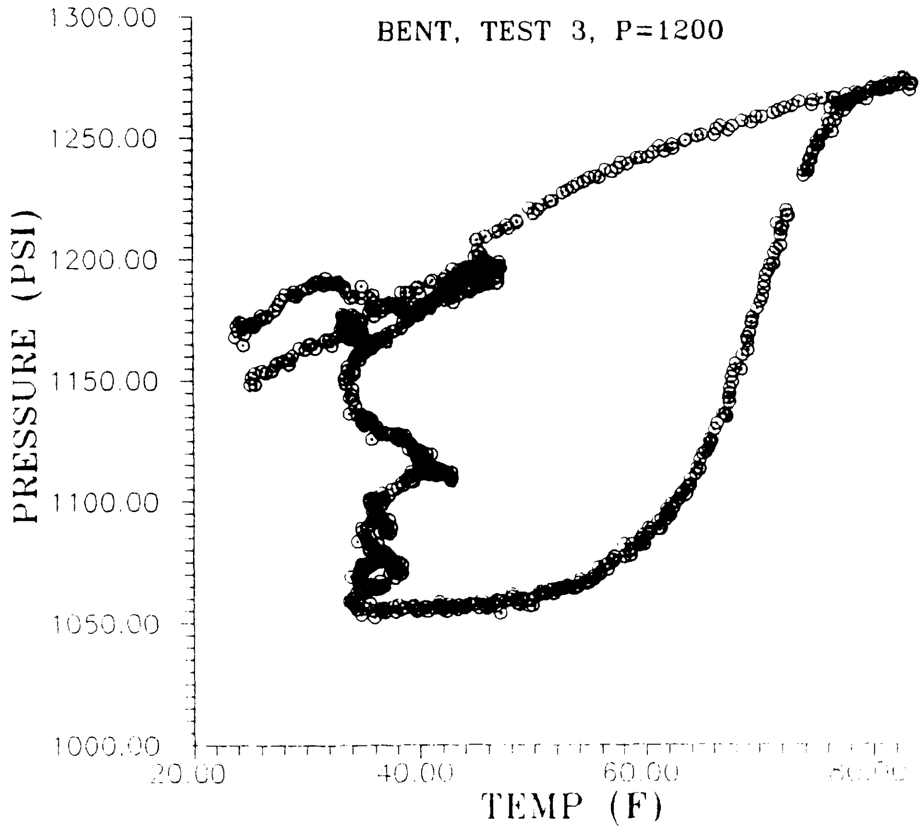
BENT, TEST 3, P=1200
1300.00
1250.00
1200.00
1150.00
1100.00
1050.00
1000.00
PRESSURE (PSI)
20.00
40.00
60.00
TEMP (F)

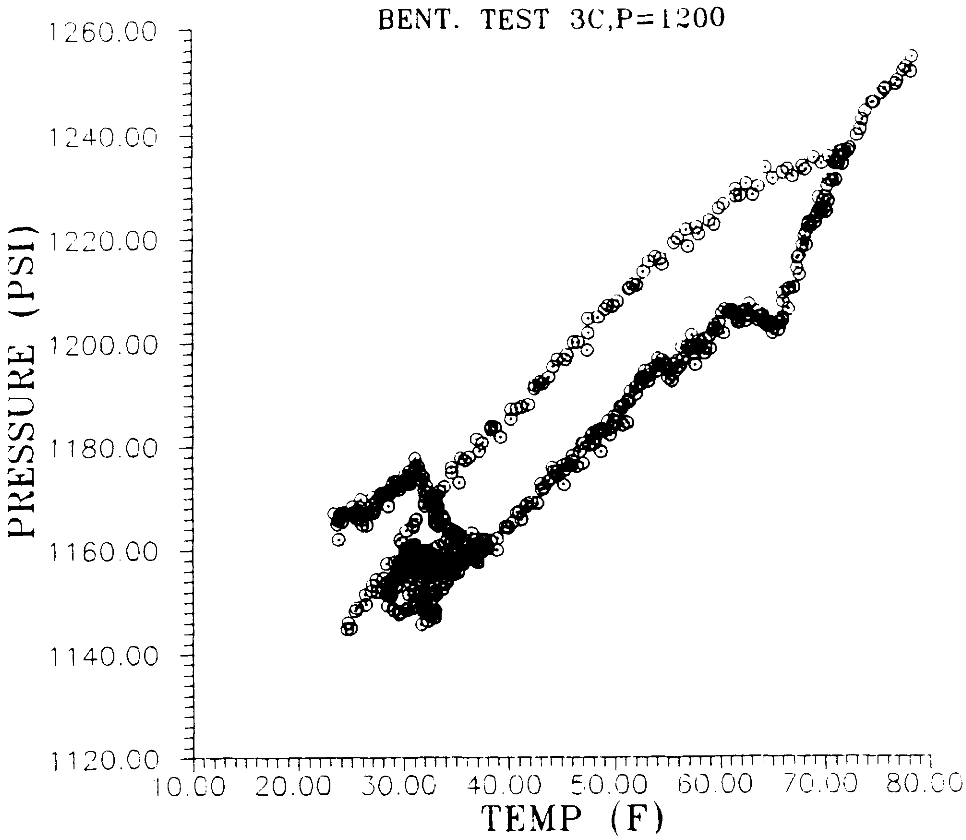
BENT. TEST 3C,P=1200
PRESSURE (PSI)
1260.00
1240.00
1220.00
1200.00
1180.00
1160.00
1140.00
1120.00
10.00 20.00 30.00 40.00 50.00 60.00 70.00 80.00
TEMP (F)

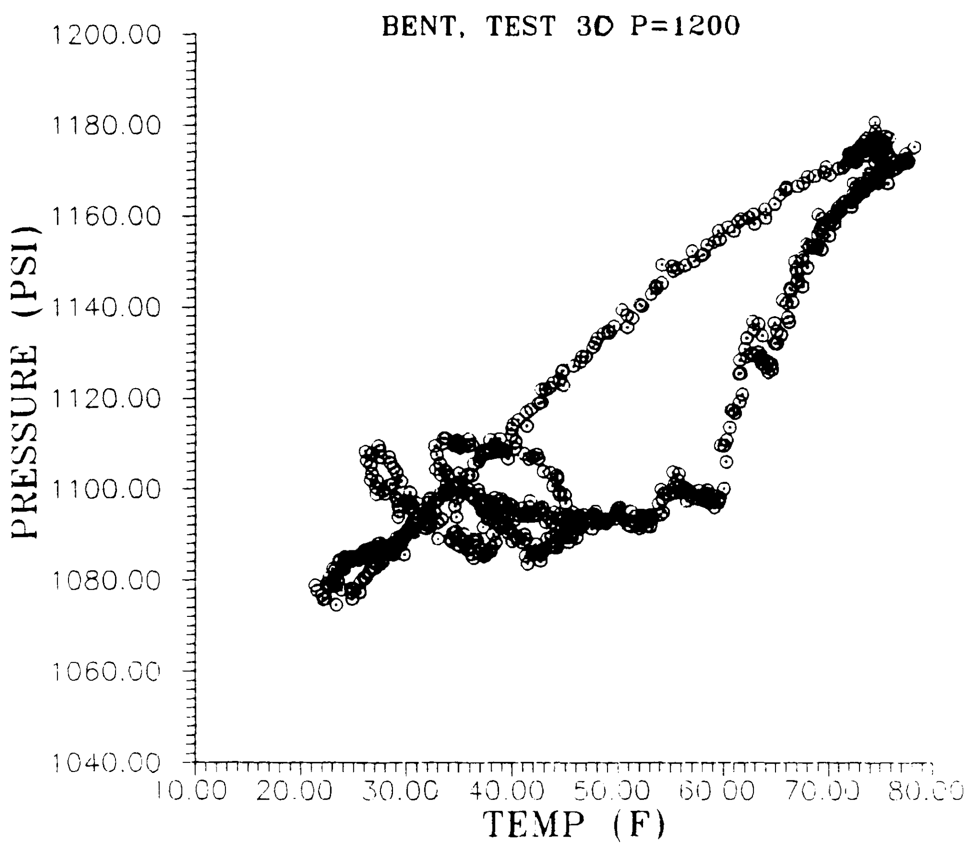
BENT. TEST 3D P=1200
PRESSURE (PSI)
1200.00
1180.00
1160.00
1140.00
1120.00
1100.00
1080.00
1060.00
1040.00
10.00 20.00 30.00 40.00 50.00 60.00 70.00 80.00
TEMP (F)

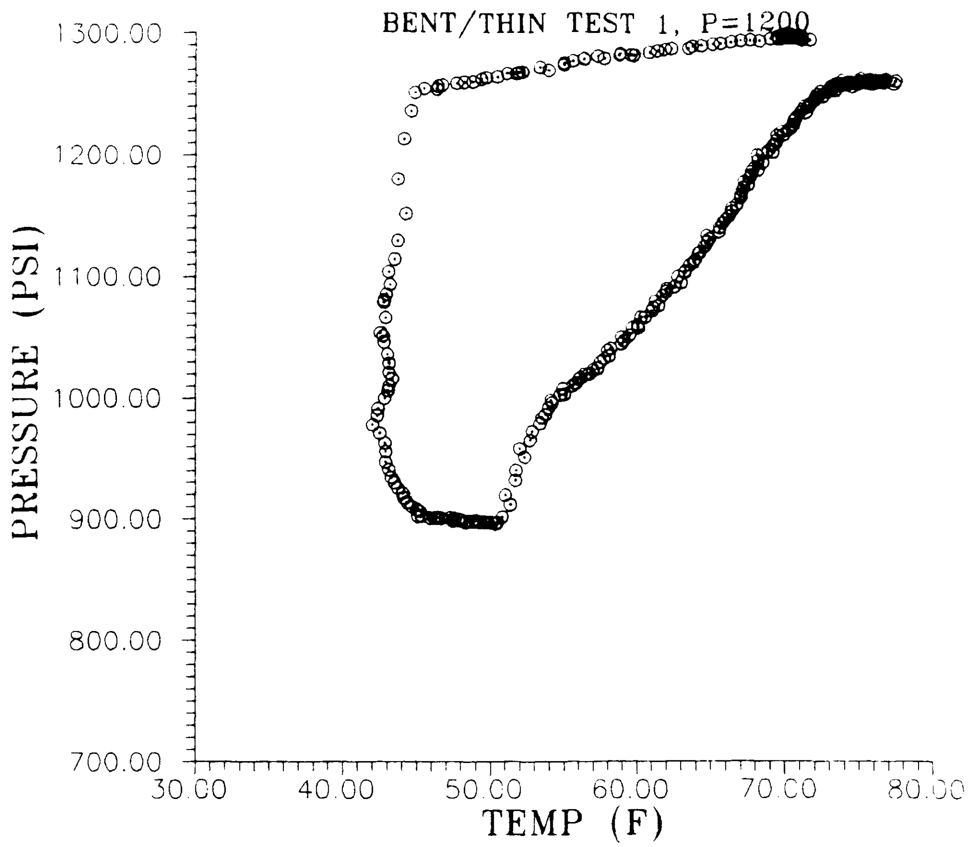
BENT/THIN TEST 1, P=1200
PRESSURE (PSI)
1300.00
1200.00
1100.00
1000.00
900.00
800.00
700.00
30.00
40.00
50.00
60.00
70.00
80.00
TEMP (F)

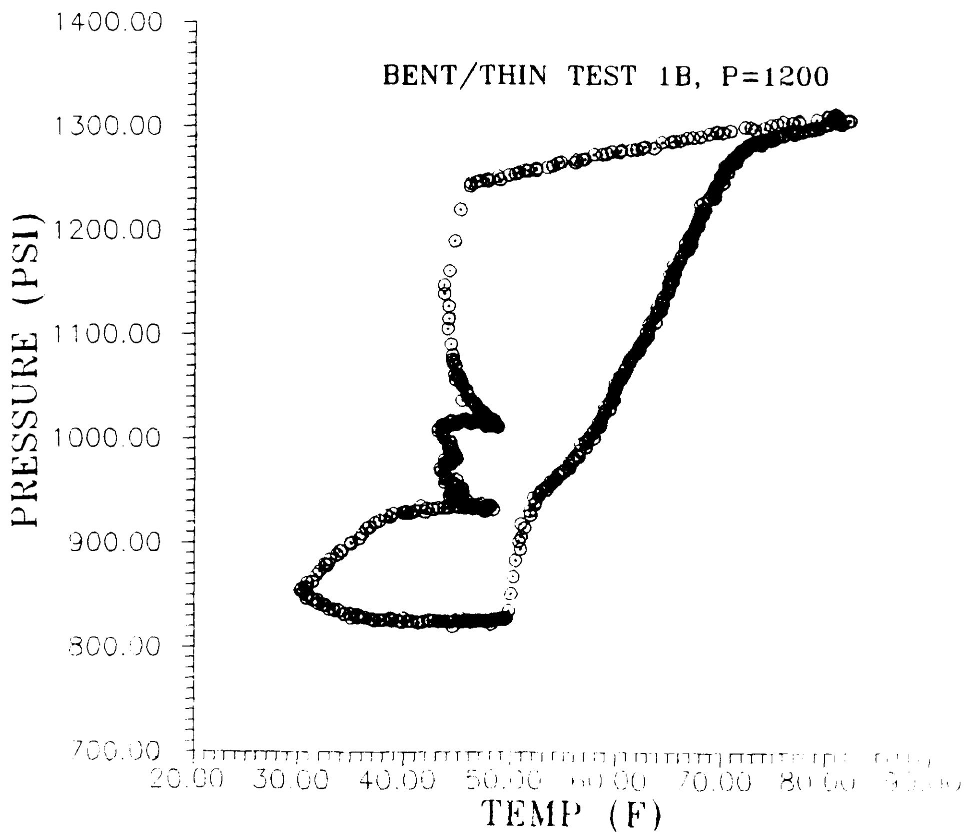
BENT/THIN TEST 1B, P=1200
PRESSURE (PSI)
1400.00
1300.00
1200.00
1100.00
1000.00
900.00
800.00
700.00
20.00
30.00
40.00
50.00
60.00
70.00
80.00
TEMP (F)

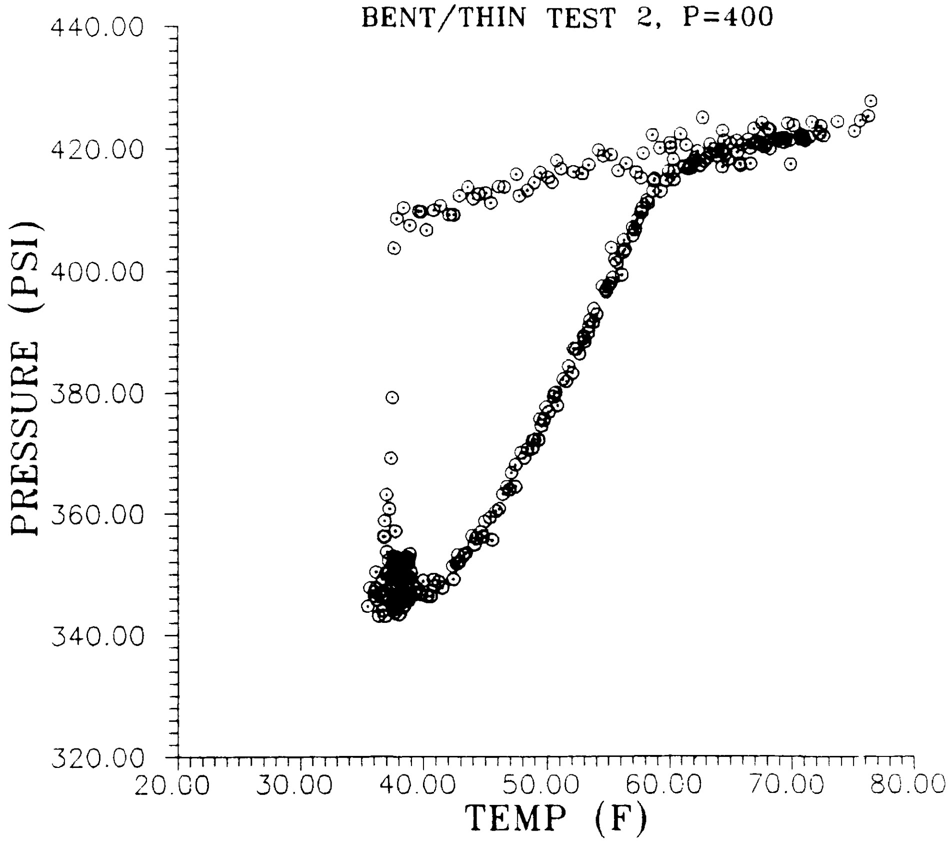
BENT/THIN TEST 2, P=400
PRESSURE (PSI)
TEMP (F)
440.00
420.00
400.00
380.00
360.00
340.00
320.00
20.00
30.00
40.00
50.00
60.00
70.00
80.00

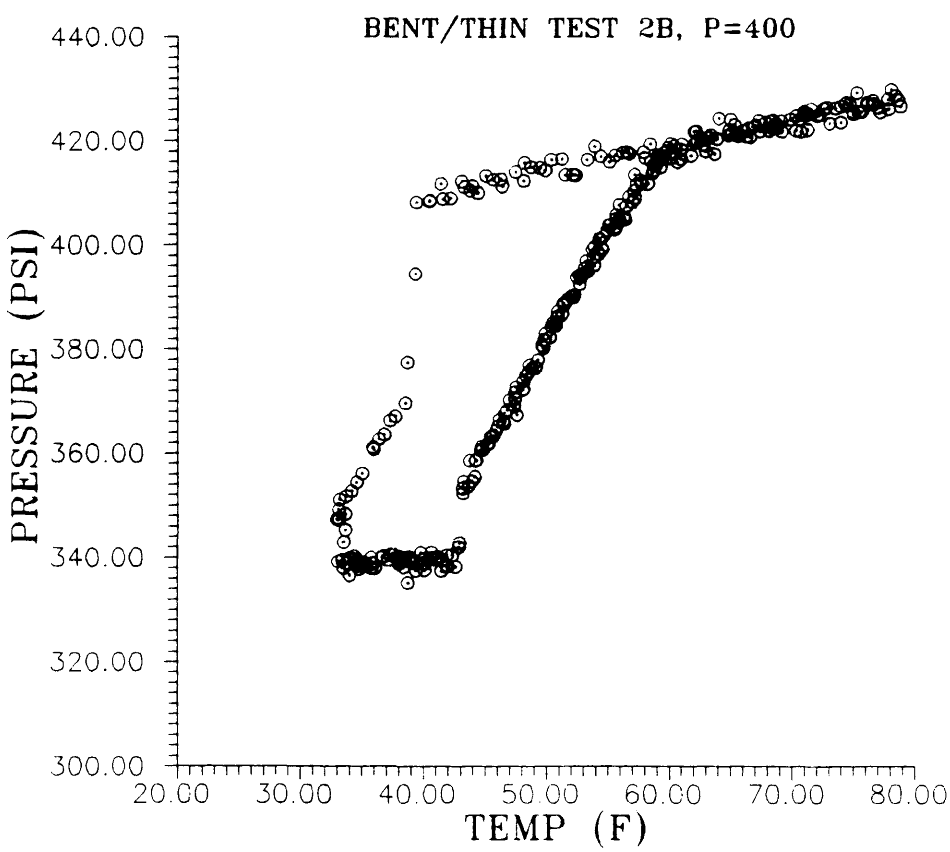
BENT/THIN TEST 2B, P=400
PRESSURE (PSI)
TEMP (F)
440.00
420.00
400.00
380.00
360.00
340.00
320.00
300.00
20.00
30.00
40.00
50.00
60.00
70.00
80.00

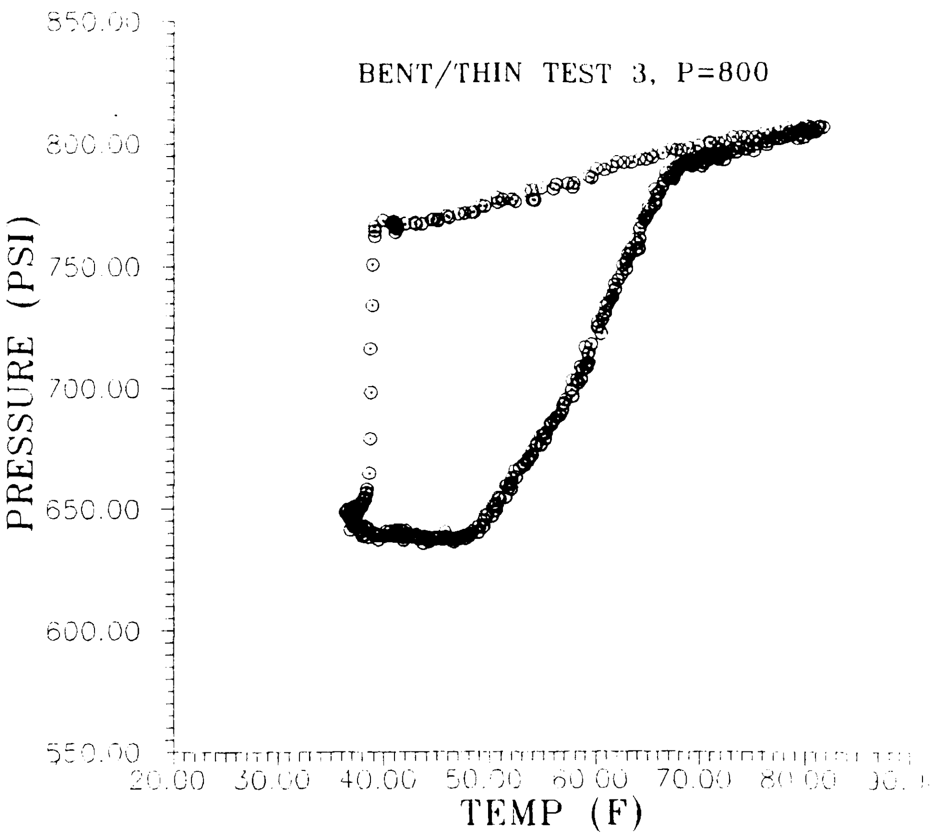
BENT/THIN TEST 3, P=800
PRESSURE (PSI)
850.00
800.00
750.00
700.00
650.00
600.00
550.00
20.00
30.00
40.00
50.00
60.00
70.00
80.00
TEMP (F)

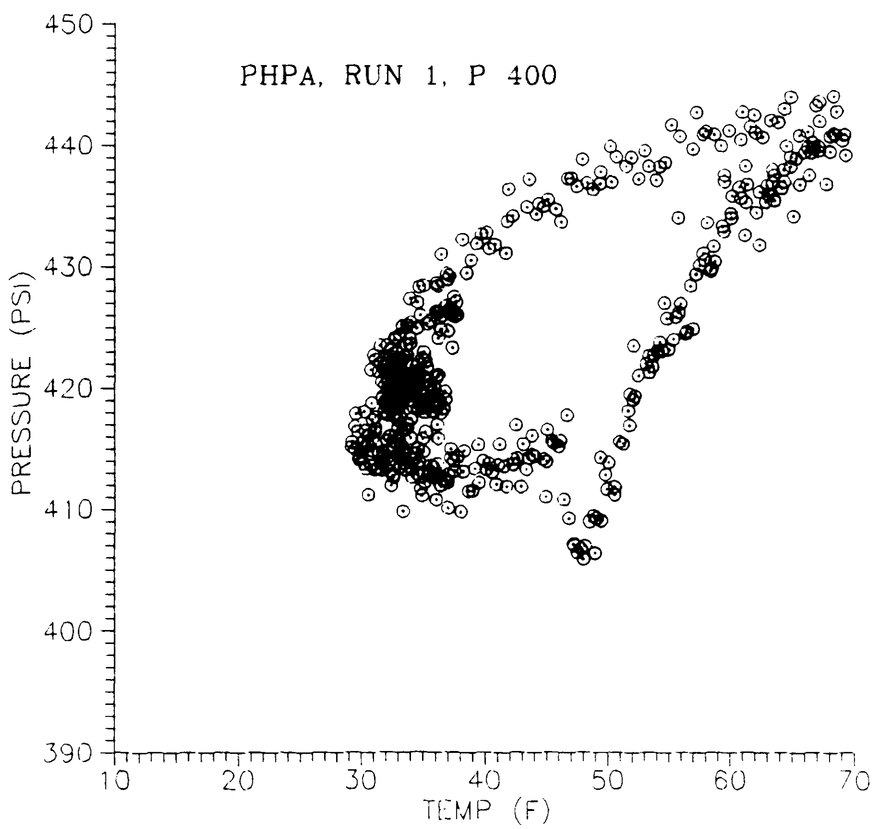
PHPA, RUN 1, P 400
PRESSURE (PSI)
450
440
430
420
410
400
390
10
20
30
40
50
60
70
TEMP (F)

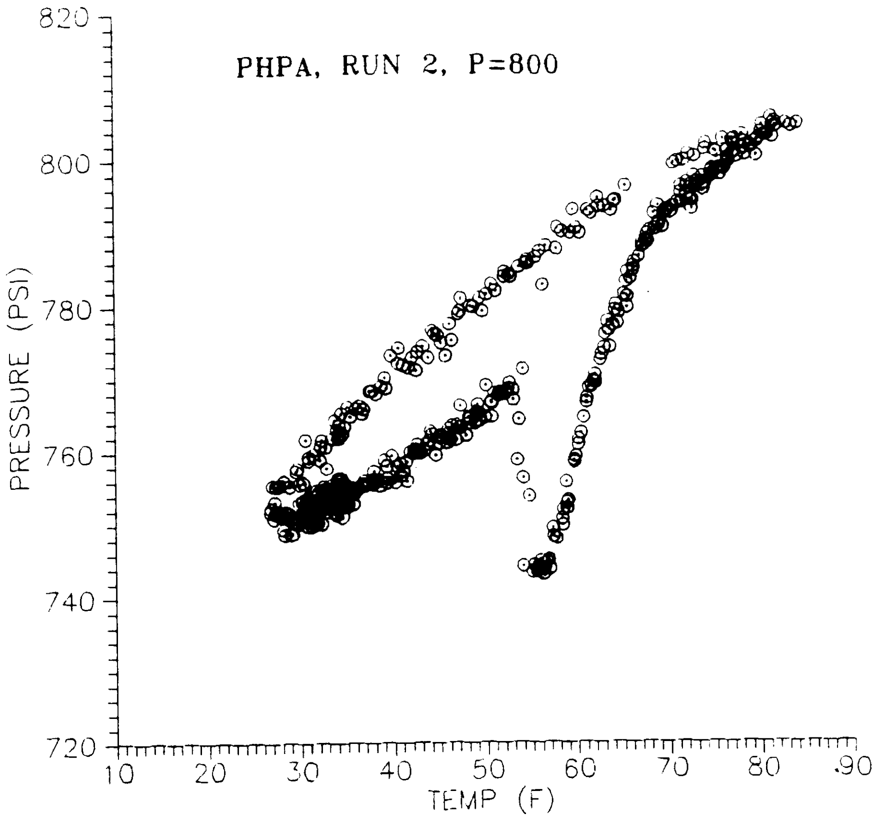
PHPA, RUN 2, P=800
PRESSURE (PSI)
TEMP (F)
820
800
780
760
740
720
10
20
30
40
50
60
70
80
90

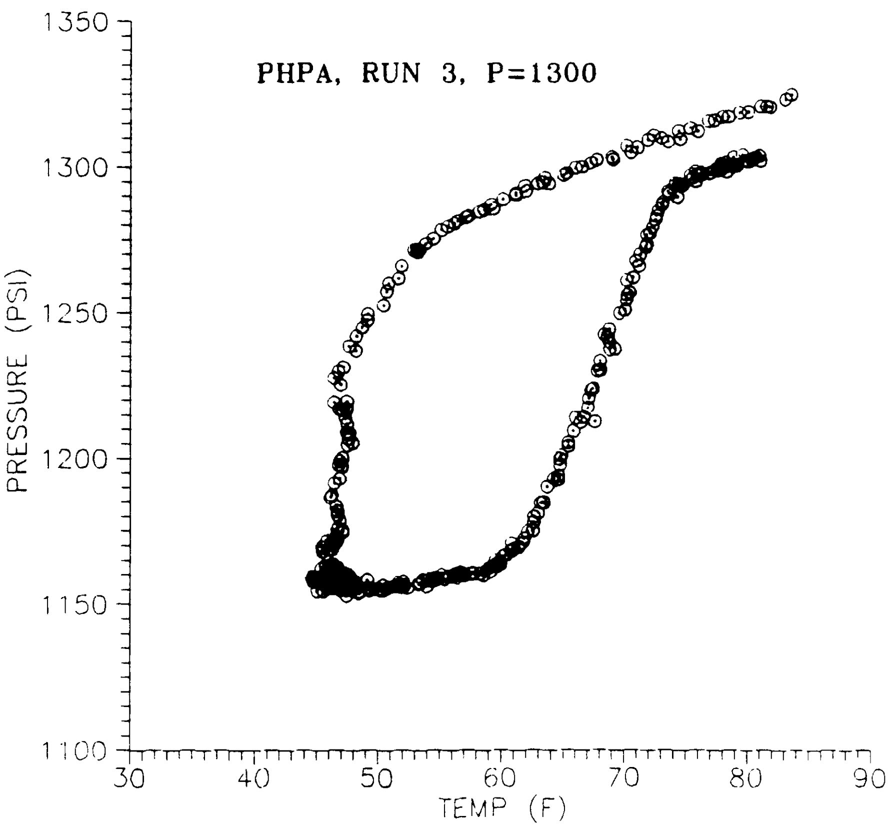
PHPA, RUN 3, P=1300
PRESSURE (PSI)
TEMP (F)
1350
1300
1250
1200
1150
1100
30
40
50
60
70
80
90

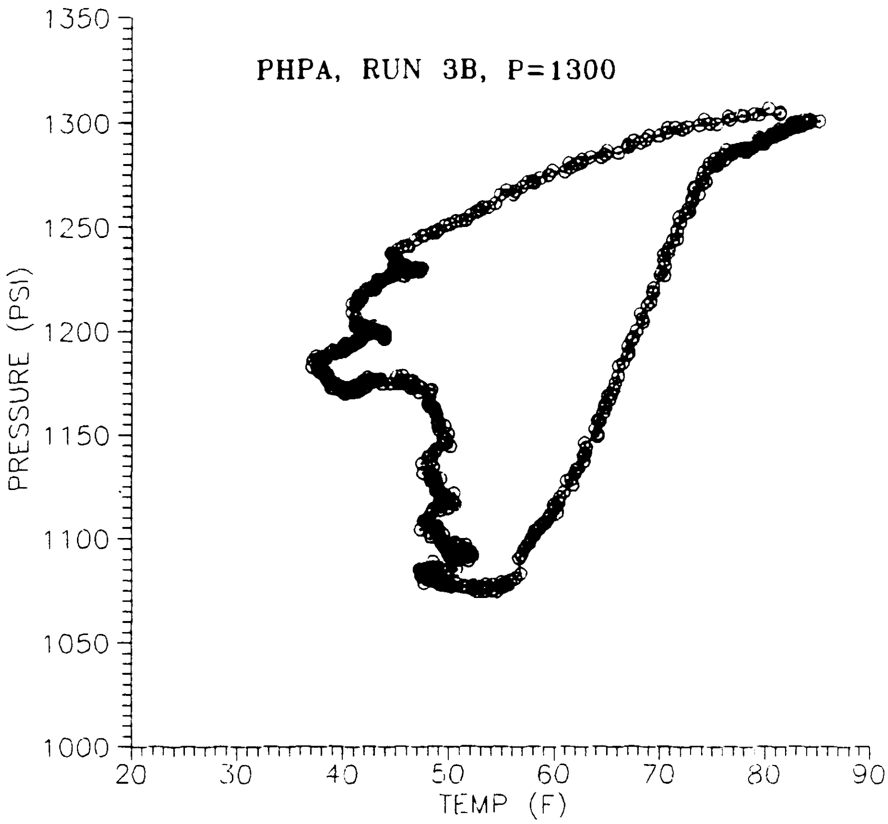
PHPA, RUN 3B, P=1300
PRESSURE (PSI)
TEMP (F)
1350
1300
1250
1200
1150
1100
1050
1000
20
30
40
50
60
70
80
90

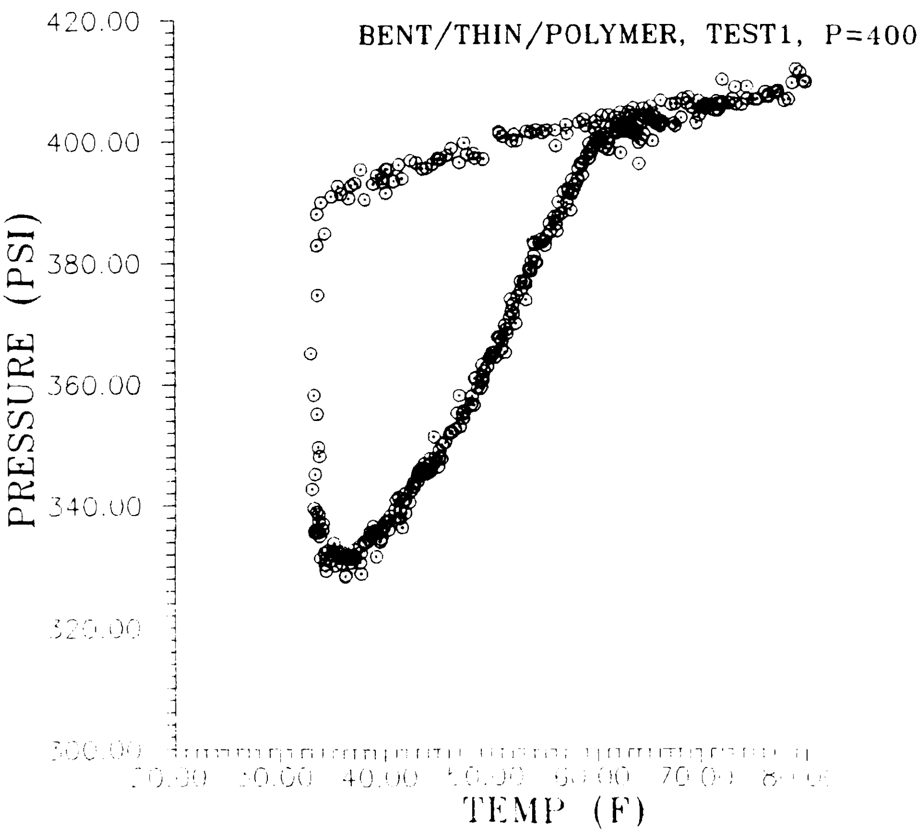
BENT/THIN/POLYMER, TEST1, P=400
PRESSURE (PSI)
TEMP (F)
420.00
400.00
380.00
360.00
340.00

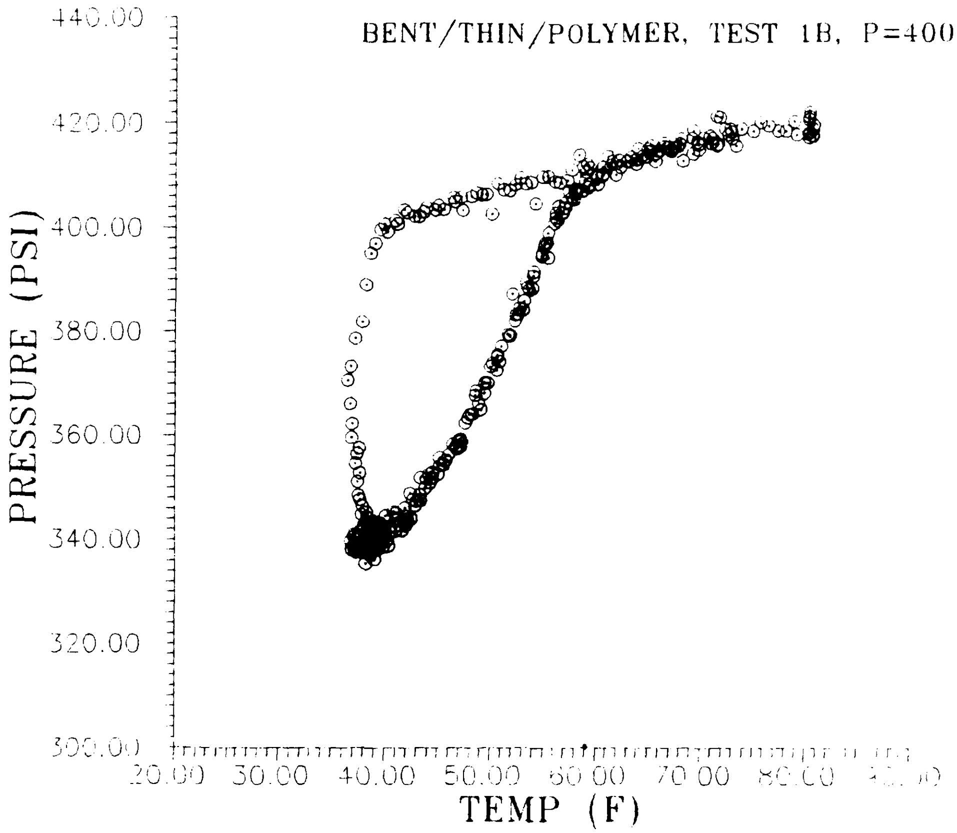
BENT/THIN/POLYMER, TEST 1B, P=400
PRESSURE (PSI)
440.00
420.00
400.00
380.00
360.00
340.00
320.00
300.00
20.00
30.00
40.00
50.00
60.00
70.00
80.00
TEMP (F)

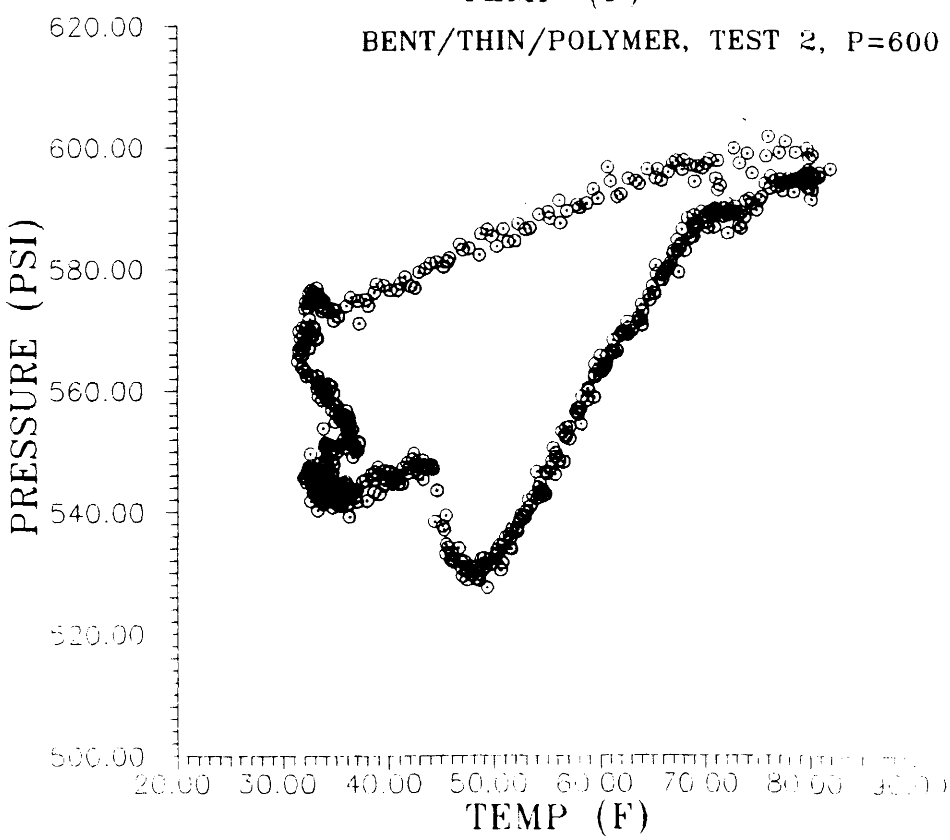
BENT/THIN/POLYMER, TEST 2, P=600
PRESSURE (PSI)
620.00
600.00
580.00
560.00
540.00
520.00
500.00
20.00
30.00
40.00
50.00
60.00
70.00
80.00
TEMP (F)

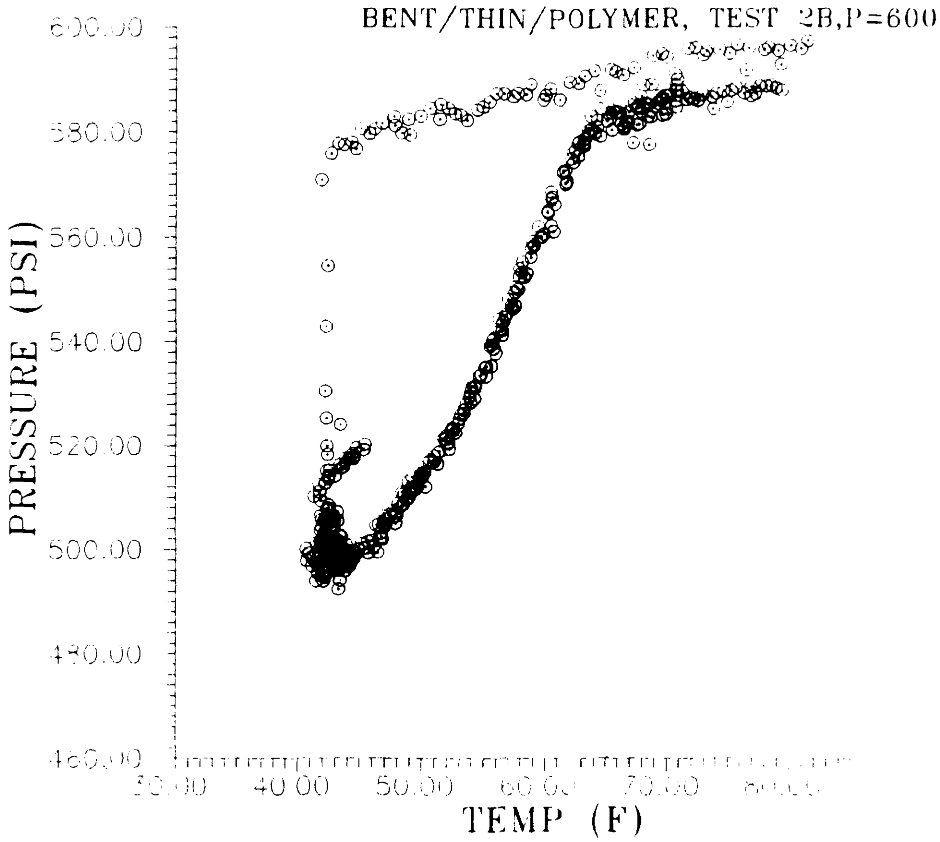
BENT/THIN/POLYMER, TEST 2B,P=600
PRESSURE (PSI)
580.00
560.00
540.00
520.00
500.00
480.00
40.00
50.00
70.00
TEMP (F)

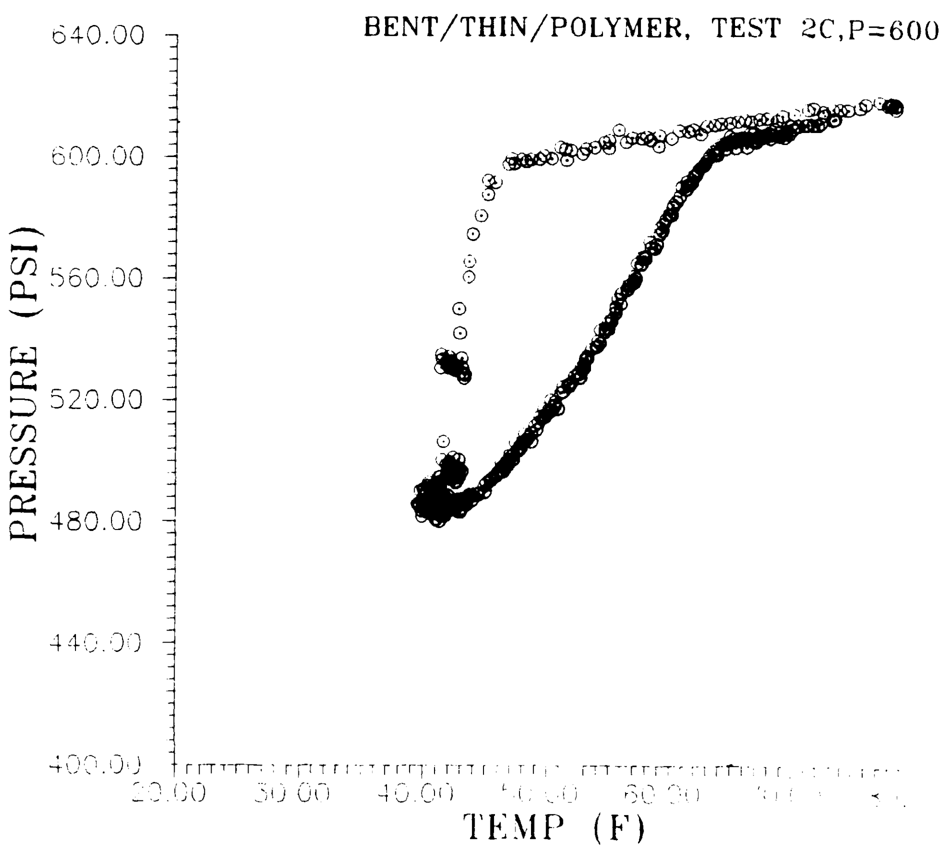
BENT/THIN/POLYMER, TEST 2C,P=600
PRESSURE (PSI)
640.00
600.00
560.00
520.00
480.00
440.00
20.00
30.00
40.00
60.00
TEMP (F)

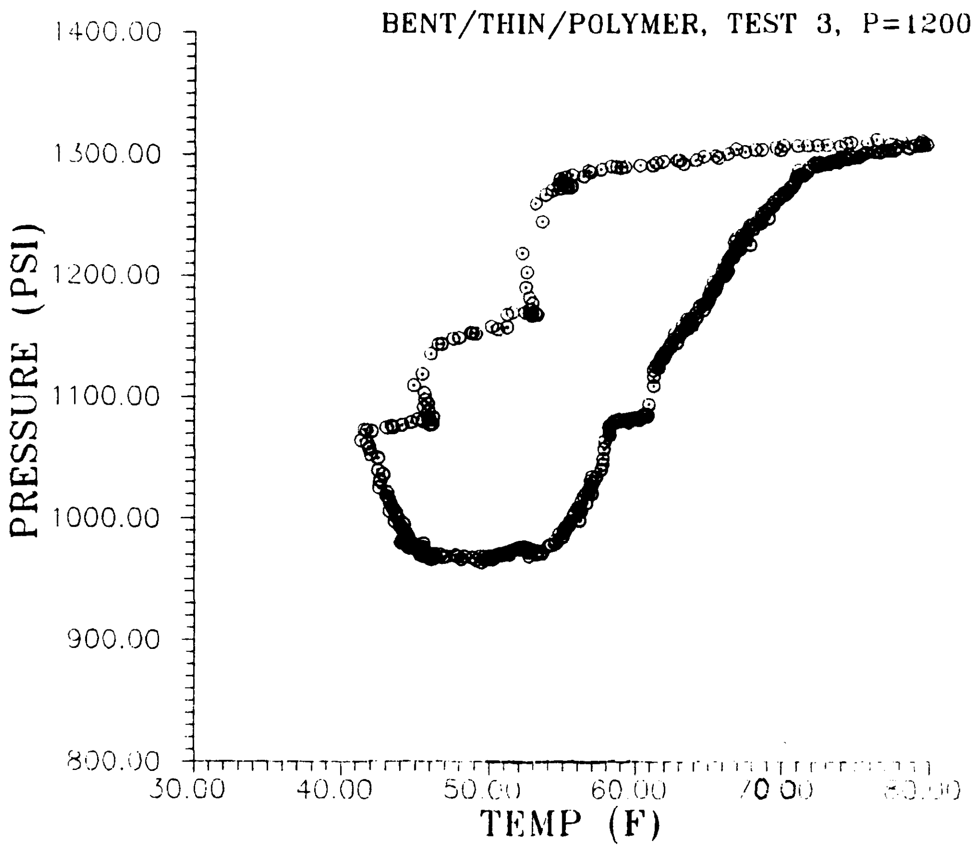
BENT/THIN/POLYMER, TEST 3, P=1200
PRESSURE (PSI)
1400.00
1300.00
1200.00
1100.00
1000.00
900.00
800.00
30.00
40.00
50.00
60.00
70.00
80.00
TEMP (F)